Optimization of Process Parameters in Wire EDM of SS316, SS321, SS17-4 PH and H13 Hard Steels with Brass and Zinc Coated Brass Wire Electrodes

A Dissertation work

Submitted in Partial Fulfilment of the

Requirements for the Award of the Degree of

DOCTOR OF PHILOSOPHY

By

Lokeswara Rao Thatuku

(Roll No. 701006)

DEPARTMENT OF MECHANICAL ENGINEERING

NATIONAL INSTITUTE OF TECHNOLOGY

WARANGAL-506004 (T.S), INDIA

SEPTEMBER -2015

Optimization of Process Parameters in Wire EDM of SS316, SS321, SS17-4 PH and H13 Hard Steels with Brass and Zinc Coated Brass Wire Electrodes

A Dissertation work
Submitted in Partial Fulfilment of the
Requirements for the Award of the Degree of

DOCTOR OF PHILOSOPHY

By

Lokeswara Rao Thatuku
(Roll No. 701006)

Under the Guidance of

Prof. N. Selvaraj
Supervisor
Mechanical Engineering Department
National Institute of Technology
Warangal – 506004

DEPARTMENT OF MECHANICAL ENGINEERING
NATIONAL INSTITUTE OF TECHNOLOGY
WARANGAL-506004 (T.S), INDIA
SEPTEMBER -2015

To

My Parents

&

Family Members

DEPARTMENT OF MECHANICAL ENGINEERING
NATIONAL INSTITUTE OF TECHNOLOGY
WARANGAL-506004 (T.S), INDIA.

CERTIFICATE

This is to certify that the work presented in this thesis entitled "**Optimization of Process Parameters in Wire EDM of SS316, SS321, SS17-4 PH and H13 Hard Steels with Brass and Zinc Coated Brass Wire Electrodes"** submitted by Mr**. Lokeswara Rao Thatuku (Roll No.701006),** is an authentic work submitted to National Institute of Technology, Warangal in partial fulfillment of the requirements for the award of the degree of **Doctor of philosophy in Mechanical Engineering.**

To the best of our knowledge, the work embodied in the thesis has not been submitted to any other university or institute for the award of any other degree.

Prof. N. Selvaraj
Supervisor
Mechanical Engineering Department
National Institute of Technology
Warangal – 506004

Chapter 1

Introduction

1.1 INTRODUCTION

The development of manufacturing industry, the demands for alloy materials having high hardness, toughness and impact resistance are increasing. In the present advance manufacturing technology world requires unique and exact methodology for machining the high strength materials. There can be many solutions to this each having their own advantages and disadvantages.

The high strength materials are difficult to machine by traditional machining methods. Hence, unconventional machining method involves the use of modern and advanced technology for machine processing. There is no physical contact between the tool and the work piece in such process. Tools used for cutting in unconventional methods are laser beams, electric beam, electric arc, infrared beam, Plasma cutting and so on depending on the type of working material. For example, Abrasive Jet Machining (AJM), Ultrasonic Machining (USM), Water Jet and Abrasive Water Jet Machining (WJM and AWJM), Electro-discharge Machining (EDM), and Wire EDM are some of the Unconventional Machining Processes (UCMP) etc. are applied to machine such difficult to machine materials. Wire EDM process with a thin wire as an electrode transforms electrical energy to thermal energy for cutting materials. With this process, alloy steels, composite alloys, conductive ceramics and aerospace materials can be machined irrespective to their hardness and toughness. Wire EDM is capable of producing a fine, precise, corrosion and wear resistant surface.

1.2 TYPES OF EDM

1.2.1 RAM EDM

Ram EDM, also known as conventional EDM, sinker EDM, die sinker, vertical EDM and plunge EDM, is generally used to produce blind cavities as shown in Figure 1.1. In Ram EDM, sparks jump from the electrode to the work piece. This causes material to be removed from the work piece.

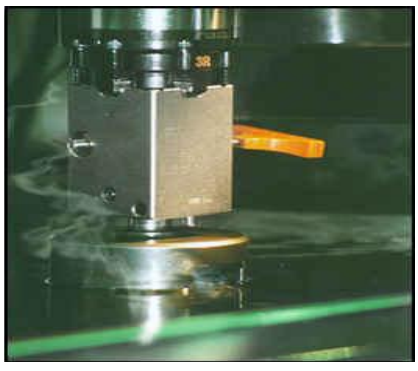

Figure 1.1: Sinker EDM used to produce blind cavities

In addition, EDM does not make direct contact between the electrode and the work piece eliminating mechanical stresses, chatter and vibration problems during machining. Today, an electrode as small as 0.1 mm can be used to drill holes into curved surfaces at steep angles without drill.

1.2.2 SMALL HOLE EDM DRILLING

Small Hole EDM Drilling, also known as fast hole EDM drilling, uses a hollow electrode to drill holes by means of electrical discharge machining by eroding material from the work piece as shown in the Figure 1.2.

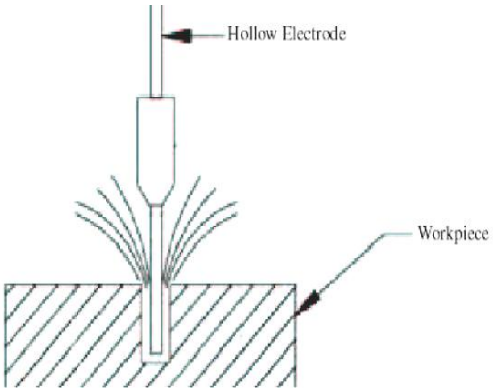

Figure 1.2: Working principle of micro-hole drilling EDM

1.2.3 WIRE EDM

Machining of high strength material is the most important issue in the manufacturing industry (Leunda et al, 2012). During the processing of such materials, the expectation is for high surface quality, reduced tool wear, as well as tool-based problems that cause increased machining cost and surface roughness (Ding et al, 2010). This problem can be tackle by non conventional machining process i.e. Wire EDM. Electrical discharge wire cutting, more commonly known as wire electrical discharge machining (Wire EDM).

Wire EDM machining (Electrical Discharge Machining) is an electro thermal production process in which a thin single-strand metal wire in conjunction with de-ionized water (used to conduct electricity) allows the wire to cut through metal by the use of heat from electrical sparks. Due to the inherent properties of the process, wire EDM can easily machine complex parts and precision components out of hard conductive materials. Wire EDM machining works by creating an electrical discharge between the wire or electrode and the workpiece. As the spark jumps across the gap, material is removed from both the workpiece and the electrode. To stop the sparking process from shorting out, a non conductive fluid or dielectric is also applied. The waste material is removed by the dielectric, and the

process continues. In wire EDM machining, a thin single-strand metal wire, usually brass, is fed through the work piece.

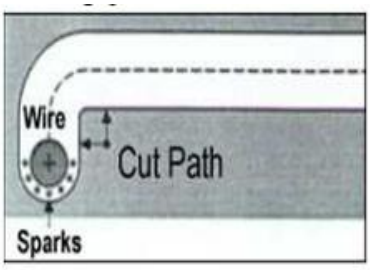

Figure 1.3: Wire travel showing sparks during cutting

Figure 1.4: Single strand wire in work piece

Figure 1.3 and Figure 1.4 shows the cutting process of a work piece by a single stranded thin wire. The wire, which is constantly fed from a spool, is held between upper and lower guides. The guides move in the X-Y plane, and sometimes the upper guide can also move independently giving rise to transitioning shapes (circle on the bottom square at the top). This gives the Wire EDM the ability to be programmed to cut very intricate and delicate shapes. The wire-cut uses water as its dielectric with the water's resistivity and other electrical properties carefully controlled by filters and de-ionizer units. Pure water is an insulator, but tap water usually contains minerals that cause the water to be too conductive for Wire EDM, The de-ionized water cools and flushes away the small particles from the gap (Goswami and Kumar Jatinder., 2013).

1.3 IMPORTANCE OF WIRE EDM IN PRESENT DAY MANUFACTURING

Wire electrical discharge machining (WireEDM) technology has grown tremendously since it was first applied more than 40 years ago. In 1974, D.H. Dulebohn applied the optical line follower system to automatically control the shape of the components to be machined by the Wire EDM process. By 1975, its popularity rapidly increased, as the process and its capabilities were better understood by the industry. It was only towards the end of the 1970s,

when computer numerical control (CNC) system was initiated into Wire EDM, which brought about a major evolution of the machining process (Ho et al., 2004).

The present application of Wire EDM process includes automotive, aerospace, mould, tool and die making industries. Wire EDM applications can also be found in the medical, optical, dental, jewellary industries. The machine's ability to operate unattended for hours or even days further increases the attractiveness of the process. Machining thick sections of material, as thick as 200 mm, in addition to using computer to accurately scale the size of the part, make this process especially valuable for the fabrication of dies of various types.

The machining of press stamping dies is simplified because the punch, die, punch plate and stripper, all can be machined from a common CNC program. Without Wire EDM, the fabrication process requires many hours of electrodes fabrication for the conventional EDM technique, as well as many hours of manual grinding and polishing. With Wire EDM the overall fabrication time is reduced by 37%, however, the processing time is reduced by 66%. Another popular application for Wire EDM is the machining of extrusion dies and dies for powder metal (PM) compaction.

As a highly-accurate tooling method that uses electrical energy to cut, drill, etch and machine metal parts, wire EDM has a long list of applications such as stripper plates, gears, punches, stamping die components, and producing plastic molds.

1.4 BASIC PRINCIPLE OF WIRE EDM PROCESS

In wire EDM, the conductive materials are machined with a series of electrical discharges (sparks) that are produced between an accurately positioned moving wire (the electrode) and the workpiece. High frequency pulses of alternating or direct current is discharged from the wire to the workpiece with a very small spark gap through an insulated dielectric fluid (water). Many sparks can be observed at one time. This is because actual discharges can occur more than one hundred thousand times per second, with discharge sparks lasting in the range of 1/1,000,000 of a second or less. The volume of metal removed during this short period of spark discharge depends on the desired cutting speed and the surface finish required. The heat of each electrical spark, estimated at around 15,000°to 21,000°Fahrenheit, erodes away a tiny bit of material that is vaporized and melted from the workpiece. (Some of the wire material is also eroded away) These particles (chips) are flushed away from the cut with a stream of de-ionized water through the top and bottom flushing nozzles. The water also prevents heat build-up in the workpiece. Without this cooling, thermal expansion of the part would affect size and positional accuracy. Keep in mind that it is the ON

and OFF time of the spark that is repeated over and over that removes material, not just the flow of electric current (Wil Gaffga, 2006). Figure 1.5 shows removal of material from workpiece as follows :(Donald B Moulton., 2010).

1. A charged wire approaches the workpiece in a dielectric fluid.
2. At a certain distance, the charge arc to the workpiece.
3. The wire and workpiece are heated and vacuum is formed.
4. Material is stripped off the wire and workpiece.
5. There is small implosion and more material is removed from the work piece and wire.

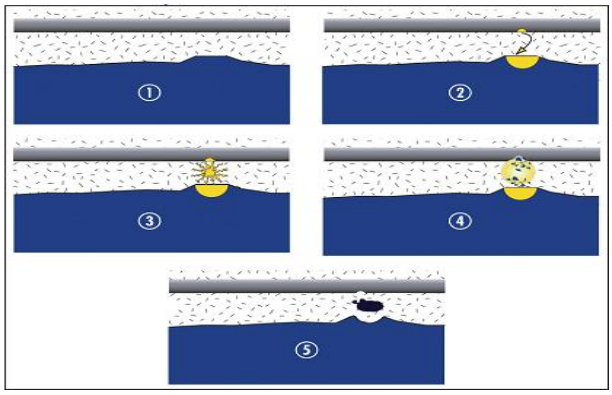

Figure 1.5: How the Wire EDM cuts through material

The degree of accuracy of workpiece dimensions obtainable and the fine surface finishes make Wire EDM particularly valuable for applications involving manufacture of stamping dies, extrusion dies and prototype parts. Without Wire EDM the fabrication of precision workpiece requires many hours of manual grinding and polishing.

The most important performance measures in Wire EDM are material removal rate (or cutting speed), workpiece surface finish and kerf (cutting width). Pulse on, pulse off, wire speed, wire tension and dielectric flushing conditions are the machining parameters which affect the performance measures (Tosun et al, 2004).

Among the other performance measures, the kerf (Figure 1.6), which determines the dimensional accuracy of the finished part, is of utmost importance. The internal corner radius to be produced in Wire EDM operations is also limited by the kerf. The wire–workpiece gap usually ranges from 0.025 to 0.075mm and is constantly maintained by a computer controlled positioning system. The kerf is calculated by summing up the wire diameter (ranges 0.05–0.4 mm) to 2 × "wire–workpiece gap distance".

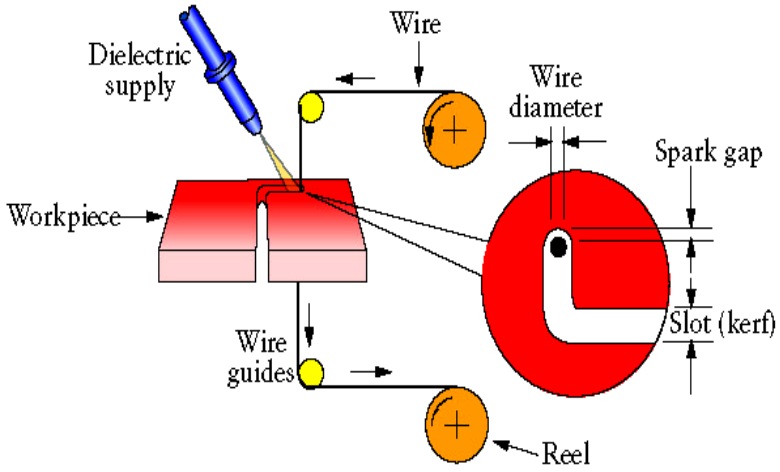

Figure 1.6: Schematic Diagram of the Wire EDM Process

In Wire EDM operations, material removal rate (MRR) determines the economics of machining and rate of production. In setting the machining parameters, the main goal is the maximum MRR with the minimum kerf. The setting of machining parameters relies strongly on the experience of operators and machining parameter tables provided by machine tool builders. It is difficult to utilize the optimal functions of a machine owing to there being too many adjustable machining parameters (Scott et al, 1991).

1.5 MECHANISM OF MATERIAL REMOVAL IN WIRE EDM PROCESS

The removal of material in electrical discharge machining is based upon the erosion effect of electric sparks occurring between two electrodes. Several theories have been forwarded in attempts to explain the complex phenomenon of "erosive spark".

The following are the theories:

a. Electro-Mechanical Theory
b. Thermo-Mechanical Theory
c. Thermo-Electric Theory

Electro-Mechanical Theory suggests that abrasion of material particles takes place as a result of the concentrated electric fluid. The theory proposes that the electric field separates the material particles of the work piece as it exceeds the forces of cohesion in the lattice of the material. This theory neglects any thermal effects. Experimental evidence lacks supports for this theory.

Whereby, Thermo-Mechanical Theory suggests that material removal in EDM operations is attributed to the melting of material caused by "Flame Jets". These so-called

flame jets are formed as a result of various electrical effects of the discharge. However, this theory does not agree with experimental data and fails to give a reasonable explanation of the effect of spark erosion.

Thermo-Electric Theory is best-supported by experimental evidence, suggests that metal removal in EDM operations takes place as a result of the generation of extremely high temperature generated by the high intensity of the discharge current. Although well supported, this theory cannot be considered as definite and complete because of difficulties in interpretation.

1.6 ADVANTAGES OF WIRE EDM PROCESS

1. Efficient Production Capabilities

Because of the precision and high-speed of wire EDM machines, manufacturers are increasingly discovering that many parts can be more economically produced with wire EDM, rather than with conventional machining.

2. Production Reliability

The constant reliability of wire EDM is one of the greater advantages of this process. Because the programs are computer generated and the electrode is constantly being fed from a spool (the wire electrode is used only once), the last part is identical to the first part. The cutter wear found in conventional machining does not exist. In addition, tighter machining tolerances can be maintained without additional cost.

3. Without Wire EDM Impossible to Machine

As more and more engineers, tool designers, and machinists understand the wire EDM process, many unique machining processes can be performed that can only be done with wire EDM. To understand the wire EDM process, visualize a super precision band saw with independent axis on top and bottom cutting any electrical conductive material, even tungsten carbide, with a thin (.010 inch and smaller) wire, cutting tapers up to 45 degrees.

4. Reduced Costs

To be competitive in today's market it is important to take advantage of every cost-saving procedure available. The high-speed cutting wire EDM machines of today have

dramatically reduced costs for many manufactured parts. Conventional machining leaves sharp edges and often burrs when machined, but a radius can be made with wire EDM without any additional cost. This eliminates a filling or sanding operation.

5. Stress-Free and Burr-Free Cutting

Wire EDM is a non-contact, force-free, metal-removing process which eliminates cutting stress and resultant mechanical distortion. Extremely thin sections can be machined because the wire electrode never contacts the material being cut. Materials cut with wire EDM are totally burr-free, and the edges are perfectly straight. Thin parts can be stacked and cut without leaving any burrs.

6. Tight Tolerances and Excellent Finishes

The wire path is controlled by a CNC computer-generated program, with part accuracies up to +/- .0001" (.0025 mm). Dowel holes can be produced with wire EDM to be either press or slip fit. The extremely fine finish from the standard wire EDM process often eliminates the need for grinding or other finishing procedures.

7. Program Files Downloadable

If the parts to be machined are programmed on a CAD system, many job shops can accept the files directly into their systems. Electronically transmitting these files eliminates the need for reprogramming the parts.

1.7 DISADVANTAGES OF WIRE EDM PROCESS

1. High capital cost is required for wire EDM process.
2. There is a problem regarding the formation of recast layer.
3. Wire EDM process exhibits very slow cutting rate.
4. It is not applicable to very large work piece.

1.8 APPLICATIONS OF WIRE EDM PROCESS

The present application of Wire EDM process includes automotive, aerospace, mould, tool and die making industries. Wire EDM applications can also be found in the medical, optical, dental, jewellary industries. The machine's ability to operate unattended for hours or even days further increases the attractiveness of the process. Machining thick sections of

material, as thick as 200 mm, in addition to using computer to accurately scale the size of the part, make this process especially valuable for the fabrication of dies of various types.

The machining of press stamping dies is simplified because the punch, die, punch plate and stripper, all can be machined from a common CNC program. Without Wire EDM, the fabrication process requires many hours of electrodes fabrication for the conventional EDM technique, as well as many hours of manual grinding and polishing. With Wire EDM the overall fabrication time is reduced by 37%, however, the processing time is reduced by 66%. Another popular application for Wire EDM is the machining of extrusion dies and dies for powder metal (PM) compaction.

As a highly-accurate tooling method that uses electrical energy to cut, drill, etch and machine metal parts, wire EDM has a long list of applications such as stripper plates, gears, punches, stamping die components, and producing plastic molds.

1.9 WORK PIECE MATERIALS

Wire EDM process is used to machine difficulty to cut materials such as hard steels tool steels, alloy steels, composites, and ceramic materials. The following materials have been widely used in automotive, aerospace, chemical, marine, mould; tool and die making industries are chosen for machining by Wire EDM process.

1. Stainless Steel 316 (Here after designated as SS316)
2. Stainless Steel 321(Here after designated as SS321)
3. Stainless Steel 17-4 PH (Here after designated as SS17-4 PH)
4. H13 Tool Steel (Here after designated as H13)

1.10 TOOL MATERIALS

In Wire EDM process electrode materials plays a major role and effect the process characteristics. By varying the electrodes while machining a hard material is a subject of researchers for long time [ ]. The following electrodes are used in Wire EDM process.

Plain Wires: While in the fashion world plain might be a derogatory term, in the EDM wire business "plain" merely refers that the wire consists of a single homogeneous component and does not have a coated or composite construction.

Coated Wires: Coated wires are produced by plating or hot-dipping re-draw wire (.9 mm) and subsequently drawing it to final size. This is a difficult process, since the plated surface

zinc has to "survive" the final drawing process and still present a uniform coating to the cut. Currently, no EDM wires are manufactured by a process in which the coating is deposited at finish wire size.

1. Brass Wire (Figure - 1.7): Brass was the first logical alternatives to copper when early EDM'ers were looking for better performance. Brass EDM wire is a combination of copper and zinc, typically alloyed in the range of 63-65% Cu and 35-37% Zn. In this work brass wire electrode is designated as $E_{B.}$

Figure 1.7: Brass wire (E_B)

1. Zinc Coated Brass Wire (Figure - 1.8): Zinc coated Brass wire was one of the first attempts to present more zinc to the wire's cutting surface. This wire consists of a thin (approximately 5 micron) zinc coating, a core which is one of the standard EDM brass alloys. This wire offers a significant increase in cutting speed over plain brass wires, without any sacrifice in any of the other critical properties. Zinc coated Brass wires produce exceptional surface finishes when cutting Tungsten carbide and are often utilized for cutting PCD and graphite. These wires are also utilized in those circumstances in which brass wires produce unacceptable Brass plating on the work piece. Zinc coated brass wire electrode is designated as $E_{C.}$

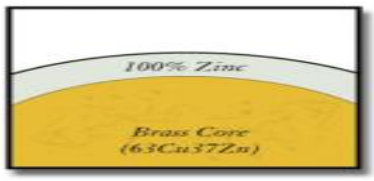

Figure 1.8: Zinc Coated Brass wire (E_C)

1.11 ORGANIZATON OF THE THESIS

1. Chapter – I presents introduction to Unconventional Machining process and salient features of Wire Electrical Discharge Machining process, work materials and electrode materials.
2. Chapter – II provide review of literature on the work done in the field of Wire EDM and Identified gaps from literature. The objectives of the present work and experimentation problem formulation were presented.

3. Chapter –III give the complete details of the experimental setup and the measurement of the output parameters for qualitative assessment of wire EDM study.
4. Chapter –IV provides the modeling methodology using Taguchi and Grey Relational Analysis methods for optimization of process parameters.
5. Chapter –V the results for wire EDM of Hard steels using Brass wire and Zinc Coated Brass wires. The experimental values and their analysis is done by taguchi method and presented.
6. Chapter – VI the results for wire EDM of Hard steels using brass and Zinc Coated Brass wires and discussions on the experimental values and their analysis are done by grey relational analysis and presented.
7. Chapter –VII Comparison of results for Hard Steels using Brass and Zinc Coated Brass wires. The regression equations and SEM studies are done for both the combinations.
8. Chapter –VIII present the conclusions drawn in this work and their industrial relevance.

1.12 SUMMARY

The present chapter gives the introduction about the conventional and unconventional machining process and the importance of the Wire EDM in the preset day manufacturing industry. The working principle of Wire EDM process and mechanism of material removal in Wire EDM process are discussed. The Wire EDM process advantages and disadvantages for present manufacturing industry. The present chapter provides the workpiece materials, mechanical properties of the materials and wire electrode materials chosen for the experimentation. It provides the organization of the thesis.

Chapter 2

Literature Review

2.1 INTRODUCTON

The technologies of wire electrical discharge machining (Wire EDM) have been emphasized significantly and have improved rapidly in recent years owing to the requirements in various manufacturing fields, especially in the precision industries. Good rigidity and the dynamic characteristic of the machine are pre-requisites to achieving optimal machining performance. In addition, proper machining parameters setting of Wire EDM also plays an important role. Several researchers have attempted to improve the performance characteristics namely the surface roughness, cutting speed, dimensional accuracy and material removal rate. But the full potential utilization of this process is not completely solved because of its complex and stochastic nature and more number of variables involved in this operation (Spedding and Wang, 1997; Scott et al., 1991).

2.2 BACKGROUND RESEARCH ON WIRE EDM

Rajurkar et al., (1991) used a factorial design method, to determine the optimal combination of control parameters in Wire EDM considering the measures of machining performance as metal removal rate and the surface finish. The study concluded control factors discharge current, the pulse duration and the pulse frequency. Scott et al. (1991) developed mathematical models to predict material removal rate and surface finish while machining D-2 tool steel at different machining conditions. It was found that there is no single combination of levels of the different factors that can be optimal under all circumstances.

K.H. Ho et al., (1995) in their paper have discussed about wire EDM research involving the optimization of the process parameters surveying the influence of the various factors affecting the machining performance and productivity. The paper also highlights the adaptive monitoring and control of the process investigating the feasibility of the different control strategies of obtaining the optimal machining conditions. The final part of the paper discusses these developments and outlines the possible trends for future Wire EDM research. Tarng et. al. (1995) formulated a neural network model and simulated annealing algorithm in order to predict and optimize the surface roughness and cutting velocity of the Wire EDM process in machining of SUS-304 stainless steel materials.

Nihat Tosun et al., (1997) have investigated the effect of cutting parameters on wire electrode wear in Wire EDM. The experiments were conducted under different settings of pulse duration, open circuit voltage, wire speed and dielectric fluid pressure. Brass wire of 0.25 mm diameter and AISI 4140 steel of 10 mm thickness were used as tool and workpiece material. It was found experimentally that the increasing pulse duration and open circuit

voltage increase the wire wear ratio (WWR) whereas the increasing wire speed and dielectric fluid pressure decreases WWR. The variation of workpiece material removal rate and average surface roughness were also investigated in relation to the WWR. The variation of the WWR with machining parameters was modeled statistically by using regression analysis technique. The level of the machining parameters on the WWR was determined by using analysis of variance (ANOVA) method.

Lee et al, (1997) have studied the effect of machining parameters in EDM of tungsten carbide on the machining characteristics. The characteristics of EDM refer essentially to the output machining parameters such as material removal rate (MRR), relative wear ratio (RWR) and surface roughness (Ra). The machining parameters are the input parameters of the EDM process namely electrode material, polarity, open ckt voltage, peak current, pulse duration, pulse interval & flushing pressure.

Spedding et al., (1997) attempted to model the cutting speed and surface roughness of EDM process through the response-surface methodology and artificial neural networks (ANNs). The authors attempted further to optimize the surface roughness, surface waviness and used the artificial neural networks to predict the process performance. Liao et. al. (1997) performed an experimental study using SKD11 alloy steel as the workpiece material and established mathematical models relating the machine performance like MRR, SR and gap width with various machining parameters and then determined the optimal parametric settings for Wire EDM process applying feasible-direction method of non-linear programming.

Spedding et. al. (1997) attempted to optimize the process parametric combinations by modeling the process using artificial neural networks (ANN) and characterizing the Wire EDM machined surface through time series techniques. A feed-forward back-propagation neural network based on a central composite rotatable experimental design is developed to model the machining process. Optimal parametric combinations are selected for the process. The periodic component of the surface texture is identified and an autoregressive AR (3) model is used to describe its stochastic component.

Huang et al., (1999) investigated experimentally the effect of various machining parameters on the gap width, SR and the depth of white layer on the machined workpiece (SKD11alloy steel) surface. They adopted the feasible-direction non-linear programming method for determination of the optimal process settings. Hsue et al. (1999) introduced a useful concept of discharge-angle C and presented a systematic analysis for metal removal rate (MRR) in corner cutting. Discharge-angle C_θ and MRR dropped drastically to a minimum and then recovered to the same level of straight-path cutting sluggishly. The amount of the

drop at the corner apex was dependent on the angle of the turning corner. The drastic variation of sparking frequency in corner cutting could be interpreted as the symptom of the abrupt change of MRR. The sudden increase of gap-voltage could also be interpreted as the result of abrupt MRR drop.

Murphy et al., (2000) developed a combined structural-thermal model using energy balance approach to describe the vibration and stability characteristics of an EDM wire. High-temperature effects were also included resulting from the energy discharges. The thermal field was used to determine the induced thermal stresses in the wire. An equilibrium and Eigen value analysis (for small vibrations about the computed equilibrium) showed that the transport speed influenced the stability of the straight equilibrium configuration. The wire had an extended residency time in the kerf and the wire thermally buckled.

Yan et al., (2001) presented a feed forward neural network using a back propagation learning algorithm for the estimation of the work piece height in Wire EDM. The average error of work piece height estimation was 1.6 mm, and the transient response to change in work piece height was found reasonably satisfactory. The developed hierarchical adaptive control system enabled the machining stability and the machining speed to be improved by 15% compared with a commonly used gap voltage control system.

Lin et al., (2001) proposed a control strategy based on fuzzy logic to improve the machining accuracy. Multi-variables fuzzy logic controller was designed to determine the reduced percentage of sparking force. The objective of the total control was to improve the machining accuracy at corner parts, but still keep the cutting feed rate at fair values. As a result of experiments, machining errors of corner parts, especially in rough-cutting, could be reduced to less than 50% of those in normal machining, while the machining process time increased not more than 10% of the normal value.

Lin et al., (2001) reported a new approach for the optimization of the electrical discharge machining (EDM) process with multiple performance characteristics based on the orthogonal array with the grey relational analysis. Optimal machining parameters were determined by the grey relational grade obtained from the grey relational analysis as the performance index. The machining parameters, namely work piece polarity, pulse on time, duty factor, open discharge voltage, discharge current and dielectric fluid were optimized with considerations of multiple performance characteristics including material removal rate, surface roughness, and electrode wear ratio.

Radzi et al., (2002) in their paper discussed that in the cutting of Tungsten Carbide ceramic using electro-discharge machining (EDM) with a graphite electrode by using Taguchi

methodology formulated the experimental layout, to analyze the effect of each parameter on the machining characteristics, and to predict the optimal choice for each EDM parameter such as peak current, voltage, pulse duration and interval time. It is found that these parameters have a significant influence on machining characteristic such as metal removal rate (MRR), electrode wear rate (EWR) and surface roughness (SR). The analysis of the Taguchi method reveals that, in general the peak current significantly affects the EWR and SR, while, the pulse duration mainly affects the MRR.

J. L. Lin et al., (2002) have studied the optimization of multiple performance characteristics of Wire EDM using orthogonal array. In their paper, a new approach for optimization of the EDM with multiple performance characteristics based on the orthogonal array with grey relational analysis has been studied. A grey relational grade obtained from the grey relational analysis has been used to solve the EDM process with multiple performance characteristics. Optimal machining parameters are then determined by the grey relational grade as the performance index. In this study, the machining parameters considered are work piece polarity, pulse-on time, and duty factor, and open discharge-voltage, discharge-current and dielectric fluid. The performance characteristics studied are MRR, surface roughness, and electrode wear ratio.

O. Blatnik et al., (2003) have described machining parameters of the EDM process are assembled in different rough and different fine machining regimes. The selection of the rough regime depends on the size of the eroding surface. The optimal regions of the eroding surfaces for different rough regimes are established according to the following criteria: material removal rate, relative electrode wear and surface integrity. The obtained regions are compared with the regions given by the machine manufacturer. The established optimal regions will be used by the system for automatic selection of the rough regime. The experiments have been done on an IT E 200M-E machine with iso-energetic generator. The work piece material was hardened steel 210CR12. The electrode material was electrolytic copper and the dielectric was Erozol 25, which is suitable for all machining regimes.

Miller et al., (2003) investigated the effect of spark on-time duration and spark on-time ratio on the material removal rate (MRR) and surface integrity of four types of advanced material; porous metal foams, metal bond diamond grinding wheels, sintered Nd-Fe-B magnets and carbon– carbon bipolar plates. Regression analysis was applied to model the wire EDM MRR. Scanning electron microscopy (SEM) analysis was used to investigate effect of important EDM process parameters on surface finish. Machining the metal foams without damaging the ligaments and the diamond grinding wheel to precise shape was very

difficult. Sintered NdFe-B magnet material was found very brittle and easily chipped by using traditional machining methods. Carbon–carbon bipolar plate was delicate but could be machined easily by the EDM.

Huang et al.,(2003) reported the microstructure analysis for martensitic stainless steel quenched and then tempered at 600°C. Specimens of the material were finished with either 4 or 5 cutting passes. Negatively polarized wire electrode (NPWE) was applied in the first four cutting passes, except the last cutting pass, in which the positively polarized wire electrode (PPWE) was used. From the results of scanning electron microscopy (SEM) examination, craters and martensitic grains were registered in the micrograph of the finished surface machined after the 4th cutting pass. From the results of transmission electron microscopes TEM-examination, a heat-affected zone (HAZ) of 1.5µm thick was detected in the surface layer finished with NPWE.

Klocke et al., (2003) tested different electrical parameters in a series of experiments. The measuring sensor was positioned at the place where the discharges occurred and was electrically isolated in order to prevent measuring interference. Cutting speed was found to be lower for material containing more number of electrically non-conductive particles. The idle voltage pulse on-time and the discharge current had little influence on the crater dimensions. At lower idle voltages the craters became more elliptical. The discharge forces depended strongly on the electrical parameters and the machined materials. The forces were linearly proportional to the discharge current and the idle voltage.

Liao et al., (2003) presented a new concept of specific discharge energy (SDE), a material property in Wire EDM. The relative relationship of SDE between different materials remained fixed as long as the materials were machined under the same machining conditions. Under steady machining process, the smaller discharge gap resulted in higher discharge efficiency. The shorter the normal discharge on time, the higher was the discharge efficiency. Using the characteristics of SDE, determination of parameter settings of different materials could be greatly simplified.

Puri et al., (2003) performed analysis of wire-tool vibration in order to achieve a high precision and accuracy in Wire EDM with the system equation based on the force acting on the wire in a multiple discharge process. It was clarified from the solution that the wire vibration during machining got mainly manipulated by the first order mode (n = 1). Also, a high tension without wire rupture proved always beneficial to reduce the amplitude of wire-tool vibration.

Ho et al., (2003) reviewed the research work carried out from the inception to the development of diesinking EDM within the past decade. It reported on the EDM research

relating to improving performance measures, optimizing the Process variables, monitoring and control the sparking process, simplifying the electrode design and manufacture. A range of EDM applications were highlighted together with the development of hybrid machining processes.

Ebeid et al., (2003) designed a knowledge-based system (KBS) to select an optimal setting of process parameters and diagnose the machining conditions for Wire EDM. The system allowed a fast retrieval for information and ease of modification or of appending data. The sample results for alloy steel 2417 and Al 6061 of the various twelve tested materials were presented in the form of charts to aid Wire EDM users for improving the performance of the process.

Altpeter et al., (2003) carried out a survey on wire modeling and control of Wire EDM. They found that the numerous solutions have been proposed in the past for mastering wire slackness but very little publications deal with issues like vibration damping and amplification of process randomness.

Puri et al., (2003) employed Taguchi methodology involving thirteen control factors with three levels for an orthogonal array L27 (3^{13}) to find out the main parameters that affect the different machining criteria, such as average cutting speed, surface roughness values and the geometrical inaccuracy caused due to wire lag.

Tosun et al., (2003) studied the effect of the cutting parameters on size of erosion craters (diameter and depth) on wire electrode in Wire EDM. Brass wire of 0.25 mm diameter and AISI 4140 steel of 0.28 mm thickness were used as tool and work piece materials in the experiments. It was found that increases in the pulse duration, open circuit voltage and wire speed increases the crater size, whereas increase in the dielectric flushing pressure decreases the crater size. The variation of wire crater size with machining parameters was modelled mathematically by using a power function. The level of importance of the machining parameters on the wire crater size was determined through analysis of variance (ANOVA).

Liao et al., (2003) used the modified traditional circuit using low power for ignition for Wire EDM. With the assistance of Taguchi quality design, ANOVA and *F*-test, machining voltage, current-limiting resistance, type of pulse-generating circuit and capacitance were identified as the significant parameters affecting the surface roughness in finishing process. It was found that a low conductivity of dielectric should be incorporated for the discharge spark to take place. After analyzing the effect of each relevant factor on surface roughness, appropriate values of all parameters were chosen and a fine surface of roughness *R*a = 0.22 µm was achieved.

Saha et al., (2003) developed a new approach using finite element modeling and optimization procedures for analyzing the process of wire electro-discharge machining. The results of the modeling and optimization showed that non uniform heating is the most important variable affecting the temperature and thermal strains.

Tzeng et al., (2003) conducted experiments on castek-03 for medium carbon steel material having excellent wear resistance. The most important factors affecting the EDM process robustness were pulse on time, applied electric current in low voltage and sparking current in high voltage. The most important factors affecting the machining speed were pulse on time and applied electric current in low voltage. The gain of 13.17 dB was able to decrease the variation range to 21.84%, which improved process robustness by 4.6 times. Huang et al., (2003) presented the use of grey relational and S/N ratio analysis, for determining the optimal parameters setting of Wire EDM process. The results showed that the MRR and surface roughness are easily influenced by the table feed rate and pulse on time. Kuriakose et al., (2003) carried out experiments with titanium alloy (Ti-6Al-4V) and used a data-mining technique to study the effect of various input parameters of Wire EDM process on the cutting speed and SR. They reformulated the Wire EDM domain as a classification problem to identify the important decision parameters.

Puri et al., (2003) investigated the wire lag phenomenon in wire-cut electrical discharge machining process and the trend of variation of the geometrical inaccuracy caused due to wire lag with various control parameters. They found that the optimal parametric settings with respect to productivity, SR and geometrical inaccuracy due to wire lag were different.

Lin et al., (2004) reported the use of an orthogonal array, grey relational generating, grey relational coefficient, grey-fuzzy reasoning grade and analysis of variance to study the performance characteristics of the Wire EDM machining process. The machining parameters (pulse on time, duty factor and discharge current) with considerations of multiple responses (electrode wear ratio, material removal rate and surface roughness) were effective. The grey-fuzzy logic approach helped to optimize the electrical discharge machining process with multiple process responses. The process responses such as the electrode wear ratio, material removal rate and surface roughness in the electrical discharge machining process could be greatly improved.

Sarkar et al., (2004) performed experimental investigation on single pass cutting of wire electrical discharge machining of γ-TiAl alloy. The process was successfully modelled using additive model. Both surface roughness as well as dimensional deviation was independent of the pulse off time. The process was optimized using constrained optimization

and Pareto optimization algorithm. Based on constrained optimization algorithm the Wire EDM process was optimized under single constraint as well as multi-constraint condition. By using Pareto optimization algorithm, the 20 Pareto optimal solutions were searched out from the set of all 243 outputs.

Ho et al., (2004) reviewed the vast array of research work carried out from the spin-off from the EDM process to the development of the Wire EDM. It reported on the Wire EDM research involving the optimization of the process parameters surveying the influence of the various factors affecting the machining performance and productivity. The paper also highlighted the adaptive monitoring and control of the process investigating the feasibility of the different control strategies of obtaining the optimal machining conditions.

Tosun et al., (2004) investigated the effect and optimization of machining parameters on the kerf (cutting width) and material removal rate (MRR) in wire electrical discharge machining (Wire EDM) operations. Based on ANOVA method, the highly effective parameters on both the kerf and the MRR were found as open circuit voltage and pulse duration, whereas wire speed and dielectric flushing pressure were less effective factors. The results showed that open circuit voltage was about three times more important than the pulse duration for controlling the kerf, whereas open circuit voltage for controlling the MRR was about six times more important than pulse duration.

Yan et al., (2004) performed experiments on a FANUC W1 CNC wire electrical discharge machine for cutting both the 10 and 20 vol. % Al_2O_3 particles reinforced 6061Al alloys-based composite and 6061Al matrix material itself. Results indicated that the cutting speed (material removal rate), the surface roughness and the width of the slit of cutting test material significantly depend on volume fraction of reinforcement (Al_2O_3 particles).

Liao et al., (2004) used specific discharge energy (SDE) concept in Wire EDM. Experimental results revealed that the relative relationship of SDE between different materials is invariant as long as all materials are machined under the same machining conditions. By means of dimensional analysis of SDE, a quantitative relationship between the machining parameters and gap width in Wire EDM was obtained. Under the same machining conditions, the surface finish improved when there was a greater SDE and vice versa.

Manna et al., (2004) performed experiments using a typical four-axes Electronica Supercut-734 CNC-wire cut EDM machine on aluminium-reinforced silicon carbide metal matrix composite Al/SiCMMC. Open gap voltage and pulse on period are the most significant machining parameters, for controlling the metal removal rate. The open gap voltage affected the cutting speed significantly. Wire tension and wire feed rate were the most significant

machining parameters, for the surface roughness. Wire tension and spark gap voltage setting were the most significant for controlling spark gap.

Tosun et al., (2004) modelled the variation of response variables with the machining parameters in Wire EDM using regression analysis method and then applied simulated annealing approach searching for determination of the machining parameters that can simultaneously optimize all the performance measures, e.g. kerf and MRR.

Y. S. Tarng, et al, (2004) used a neural network model to estimate to the effects of parameters on the surface roughness as the response variable and machining speed. The parameters considered for the study were pulse duration, pulse interval, peak current, open circuit voltage, servo reference voltage, electric capacitance and Table speed. In this study, the experiments have been performed on a Sodick A350-S CNC wire EDM machine. They have suggested the optimum parameters for thickness of 10 mm work piece. Tool material used was brass wire for the study.

Ozdemir et al., (2005) investigated the machinability of standard GGG40 nodular cast iron by A300 Fine Sodick Mark XI Wire EDM using different parameters. The increase in surface roughness and cutting rate clearly followed the trend indicated with increasing discharge energy as a result of an increase in current and pulse on time, because the increased discharge energy produced larger and deeper discharge craters. Three zones were identified in rough regimes of machining for all samples: decarburized layer, heat affected layer, and bulk metal. Miller et. al. (2005) investigated effects of spark cycle and pulse on-time on wire EDM micro features. Tests were conducted on various materials viz. Nd–Fe–B magnetic material, carbon bipolar plate, and titanium for wire EDM cutting of minimum cross section thickness. A hypothesis was proposed based on the combined thermal and electrostatic force to cause the fracture of thinsection during wire EDM. This was supported by findings from SEM micrographs of EDM surface, subsurface and debris.

Mustafa Ilhan et al., (2005) have presented in their paper to select the most suitable cutting and offset parameter combination for the electrical discharge machining process in order to get the desired surface roughness value for the machined surface. A series of experiments have been conducted on 1040 steel material of thickness 30, 60 and 80 mm, and on 2379 and 2738 steel materials of thicknesses 30 and 60mm. The specimen have been cut using different cutting and offset parameter combinations of the Sodick Mark X1 A500 EDW wire electrical discharge machine.

Kuriakose et al., (2005) used titanium alloy (Ti-6Al-4V) as the work material and conducted experiments based on Taguchi's L-18 orthogonal array. Then they employed the

nondominated sorting genetic algorithm to determine the optimal process parameters that would optimize the cutting velocity and SR of Wire EDM process.

Swarup S. Mahapatra and Amar patnaik et al, (2006) have described in their paper about Parametric Optimization of Wire Electrical Discharge Machining (Wire EDM) Process using Taguchi Method. They have used Robofil 100 Wire EDM to conduct the experiment. The control factors selected are Discharge current, Pulse duration, Pulse frequency, wire speed, Wire tension and dielectric flow rate. The fixed parameters are Zinc coated copper wire, rectangular shaped product, 10mm thickness work piece and 0.25mm diameter wire with number of passes three. The responses measured are Surface finish (Ra) and MRR. They have used Taguchi technique for the optimization of process parameters. Orthogonal array used is L27. They have proposed some optimized parameter values for machining the work piece.

Chiang et al., (2006) presented an approach for the optimization of the Wire EDM process of Al_2O_3 particle reinforced material with two performance characteristics, e.g. SR and MRR, based on the grey relational analysis. Ramakrishnan et al. (2006) considered three response characteristics, e.g. MRR, SR and wire wear ratio (WWR) for a Wire EDM process and determined the optimal process settings by optimization of multiple response signal-to-noise (MRSN) ratio, which is the logarithmic transformation of the sum of the weighted normalized quality loss of individual response variable.

Manna et al., (2006) established mathematical models relating to the machining performance criteria like MRR, SR, spark gap and gap current using the Gauss elimination method for effective machining of Al/SiC-MMC. Mahapatra et al. (2006) conducted experiments on ROBOFIL 100 high precision 5 axes CNC Wire EDM to find the relationship between control factors and responses like MRRSF and kerf by means of nonlinear regression analysis. Genetic algorithm was employed to optimize the wire electrical discharge machining process with multiple objectives. The error associated with MRR, SF, and kerf were 3.14%, 1.95%, and 3.72%, respectively. The optimum search of machining parameter values for maximizing MRR and SF and minimizing kerf was formulated as a multi-objective, multivariable, non-linear optimization problem.

Hargrove et al., (2006) applied finite element method (FEM) to determine work piece temperature for different cutting parameters. They investigated the effect of Wire EDM parameters such as discharge voltage and pulse on-time on the damaged layer thickness of a machined work piece using low carbon steel (AISI 4340) as the cutting material. The thickness of the temperature affected layers for different cutting parameters was computed

based on a critical temperature value. Through minimizing the thickness of the temperature affected layers and satisfying a certain cutting speed, a set of the cutting process parameters was determined for work piece manufacture. A set of optimum parameters for this machining process was selected such that the condition of machine cutting speed was 1.2 mm/min, on time pulse was 8 µs and no load voltage was 4 volt. The analyzed results had a good agreement with testing results.

J. Prohaszka et al, (2007) in their paper have discussed about effect of electrode material on machinability in wire electro-discharge machining that will lead to the improvement of Wire EDM performance. Experiments have been conducted regarding the choice of suitable wire electrode materials and the influence of the properties of these materials on the machinability in Wire EDM. The machinability during Wire EDM is improved significantly with the proper combination of the electrical, mechanical, physical and geometrical properties of the wire electrode. The materials used for the fabrication of wire electrodes must be characterized by a small work function and high melting and evaporation temperatures. The coating of the already-used copper, brass, steel and molybdenum wires by a layer of a material possessing a small work function such as magnesium, alkaline metals and alkaline earth metals, may increase considerably the cutting efficiency during Wire EDM.

Y.S Liao et al., (2008) devised an approach to determine machining parameter settings for Wire EDM process .Based on the taguchi quality design and the analysis of variance (ANOVA), the significant factors affecting the machining performance such as MRR, gap width ,surface roughness ,sparking frequency ,average gap voltage, normal ratio(ratio of normal sparks to total sparks) are determined. By means of regression analysis, mathematical models relating the machining performance and various machining parameters are established. Based on the mathematical models developed, an objective function under the multi-constraint conditions is formulated. The optimization problem is solved by the feasible direction method, and the optimal machining parameters are obtained. Experimental results demonstrate that the machining models are appropriate and the derived machining parameters satisfy the real requirements in practice.

N. Tosun et al., (2008) have investigated theoretically and experimentally about the effect of the cutting parameters on size on erosion craters of wire electrode in Wire EDM. The experiments have been conducted under the different cutting parameters of pulse duration, open circuit voltage, wire speed and dielectric flushing pressure. Brass wire of 0.25 mm diameter and AISI 4140 steel of 0.28 mm thickness are used as tool and work piece materials in the experiments. They have found that increasing the pulse duration, open circuit voltage,

and wire speed increases the crater size, whereas increasing the dielectric flushing pressure decreases the crater size. The variation of wire crater size with machining parameters has been modeled mathematically by using a power function. The level of importance of the machining parameters on the wire crater size has been determined by using analysis of variance (ANOVA).

Scott F. Miller et al., (2009) have discussed about wire electrical discharge machining (EDM) of cross-section with minimum thickness and compliant mechanisms is studied. Effects of EDM process parameters, particularly the spark cycle time and spark on-time on thin cross-section cutting of Nd–Fe–B magnetic material, carbon bipolar plate, and titanium are investigated. Effects of spark cycle and pulse on-time on wire EDM micro features were investigated. Tests were conducted on various materials for minimum thickness wire EDM cutting. Applications of low MRR EDM cutting for machining of thin-section and compliant mechanisms were studied. A hypothesis was proposed based on the combined thermal and electrostatic force to cause the fracture of thin-section during wire EDM. This was supported by findings from SEM micrographs of EDM surface, subsurface, and debris

Mu-Tian yan, et al, (2010) have made an attempt towards process monitoring and control of micro wire EDM process by developing a new pulse discrimination and control system. This system functions by identifying 4 major gap states classified as open cut, normal spark, arc discharge, and short cut by observing the characteristics of gap voltage waveforms. The influence of pulse interval, machining feed rate, and work piece thickness on the normal ratio, arc ratio and short ratio. It could be concluded from the experiment that a longer pulse interval would result in increase of short ratio at constant machining feed rate. A high machining federate as well as increase of work piece height results in increase of short ratio. To achieve stability in machining a control strategy is proposed by regulating the pulse interval of each spark in real time basis by analyzing the normal ratio, arc ratio & short ratio. Experimental results show that the developed pulse discrimination system and control strategy is very useful in reducing both arc discharge and short sparking frequency which are undesirable during the process. Also with this process monitoring a stable machining under the condition where the instability of machining operation is prone to occur can be achievable.

C. L. Lin et al., (2010) have described, the grey relational analysis based on an orthogonal array and fuzzy-based Taguchi method is applied for optimizing the multi-response process. They have used both the grey relational analysis method without using the S/N (Signal/Noise) ratio and fuzzy logic analysis in orthogonal array Table in carrying out experiments for solving the multiple responses in the electrical discharge machining process.

After observing the experimental results, both methods can be used to optimize the machining parameters (Pulse-ON, Pulse-OFF, voltage, feed, wire feed, offset) by considering the multiple responses (Electrode wear ratio, metal removal rate, accuracy, surface finish) effectively.

R. Ramakrishnan et al., (2011) in their paper have applied the Taguchi's method, which is one of the methods of robust design of experiments to optimize multi responses of the wire cut electric discharge machining operations. Experimentation is carried out using Taguchi's L16 orthogonal array method. They had conducted each experiment under different cutting conditions of pulse-on time, wire tension, delay time, wire feed, speed, and ignition current intensity. They had taken material removal rate, surface roughness, and wire wear ratio as the multi responses; they had applied the Taguchi's L16 orthogonal array method to measure the performance characteristics deviating from the actual value. They carried out the experiment to identify the effectiveness of the Taguchi's method on the level of importance of the machining parameters on the multiple characteristics. By applying the Taguchi's method, a good improvement was obtained.

C. Bhaskar Reddy et al., (2012) have investigated for best parameter selection to obtain maximum Material Removal Rate (MRR) and better surface roughness (Ra) by conducting the experimentation on CONCORD DK7720C four axes CNC Wire Electrical Discharge Machining of P20 die tool steel with molybdenum wire of 0.18mm diameter as electrode.

Ballal Yuvaraj P et al, (2012) described the use and steps of Taguchi design of experiments and orthogonal array to find a specific range and combinations of turning parameters like cutting speed ,feed rate and depth of cut to achieve optimal values of response variables like surface finish, tool wear, material removal rate.

S. R. Nithin Aravind et al., (2012) investigated effect of five optimal control parameters input voltage, current, speed, pulse on/off time to maximize metal removal rate (MRR) and minimize surface roughness (SR) on Wire EDM (electrical discharge machining).

L. Li et al, (2013) investigated the characteristics of surface integrity vs. discharge energy in Wire EDM of Inconel 718. The results show that the EDM surface topography shows dominant coral reef microstructures at high discharge energy, while random micro voids are dominant at low discharge energy. Surface roughness is equivalent for parallel and perpendicular wire directions, and average roughness can be significantly reduced for low

discharge energy. The thick white layers are predominantly discontinuous and non-uniform at relative high discharge energy. Micro voids are confined within the thick white layers and no micro cracks were found in the subsurface. The thin white layers by trim cut at low discharge energy become more continuous, uniform, and are free of micro voids. Compared to the bulk material, white layers have dramatic reduction in micro hardness due to significant thermal degradation. In addition, surface alloying from wire electrode and water dielectric are obvious in main cut at high discharge energy, but it can be minimized in trim cuts at very low discharge energy.

Sreenivasa Rao M et al., (2013) reviewed the effects of various Wire EDM process parameters such as pulse on time, pulse off time, servo voltage, peak current, dielectric flow rate, wire speed, wire tension on different process response parameters such as material removal rate (MRR), surface roughness (Ra), kerf (width of cut), wire wear ratio (WWR) and surface integrity factors. This paper also reviews various optimization methods applied by the researchers and finally outlines the recommendations and future trends in Wire EDM research.

Danial Ghodsiyeh et al, (2013) reviewed the research trends in Wire EDM on relation between different process parameters, include pulse on time, pulse off time, servo voltage, peak current, dielectric flow rate, wire speed, wire tension on different process responses include material removal rate (MRR), surface roughness (Ra), sparking gap (Kerf width), wire lag (LAG) and wire wear ration (WWR) and surface integrity factors.

2.3 GAP ANALYSIS/ MOTIVATION OF THE WORK

After comprehensive study of the existing literature, a number of gaps have been observed in machining and optimization of wire EDM.

- Wire EDM studies of SS316, SS321, SS17-4PH and H13 with Brass and Zinc Coated Brass wires are unexplored.
- In Wire EDM, less work was done on the optimization of process parameters for hard Steels.
- Earlier researchers, they have considered only single objective performance of wire EDM with copper or Brass as the wire materials. Very few have considered the multi objective performance measures.

Thus present work aims at "optimization of process parameters on wired electrical discharged machining of hard steel like SS316, SS321, SS17-4 (PH) and H13 with brass and zinc coated brass wire electrodes" has been under taken keeping into consideration of the following objectives.

2.4 OBJECTIVE/ SCOPE OF THE RESEARCH

- To investigate the effect of process parameters like pulse on time, pulse off time, wire tension, wire feed and dielectric fluid pressure in wire EDM of Hard Steels namely SS316, SS321, SS17-4PH and H13 Tool Steel on material removal rate, surface roughness, kerf and dimensional deviation.
- Optimization of process parameters using Taguchi method on Wire EDM of Hard steel work materials with Brass and Zinc Coated Brass as wire electrodes.
- Development of mathematical models for performance measures with Brass and Zinc coated Brass wire electrodes using Regression analysis.
- Multi- objective optimization of process parameters using Grey Relational Analysis in Wire EDM studies of Hard Steel work materials with Brass and Zinc Coated Brass wire electrodes.
- Comparison of results of wire EDM of SS316, SS321, SS17-4 PH and H13 tool steel wok materials with Brass and Zinc coated brass as wire electrode materials.
- To study the microstructure and perform micro structural analysis using SEM.

2.5 PROBLEM FORMULATION / STATEMENT

The present work "Optimization of Process Parameter on Wire EDM using Taguchi and Grey Relational Analysis" has been undertaken keeping into consideration of the following objectives:

- It has been long recognized that cutting conditions such as pulse on time, pulse off time, servo voltage, peak current and other machining parameters should be selected to optimize the economics of machining operations as assessed by productivity, total manufacturing cost per component or other suitable criterion.

- High cost of numerically controlled machine tools, compared to their conventional counterparts, has forced us to operate these machines as efficiently as possible in order to obtain the required payback.

- New materials of increasing strengths and capabilities are being developed continuously and response characteristics are not only dependent on the machining

parameters but also on materials of the work part. SS316, SS321, SS17-4 PH and H13 hard steels are the one of such materials. These can be used in applications such as aerospace, automotive, mould, tool making industries. Which are not considered in yet with brass and zinc coated brass as an electrode wire materials.

2.6 OVERALL RESEARCH PLAN

The flow chart gives the overall research work plan, which includes the work materials and wire electrode materials and optimization methods to investigate the optimum parameters in Wire EDM process.

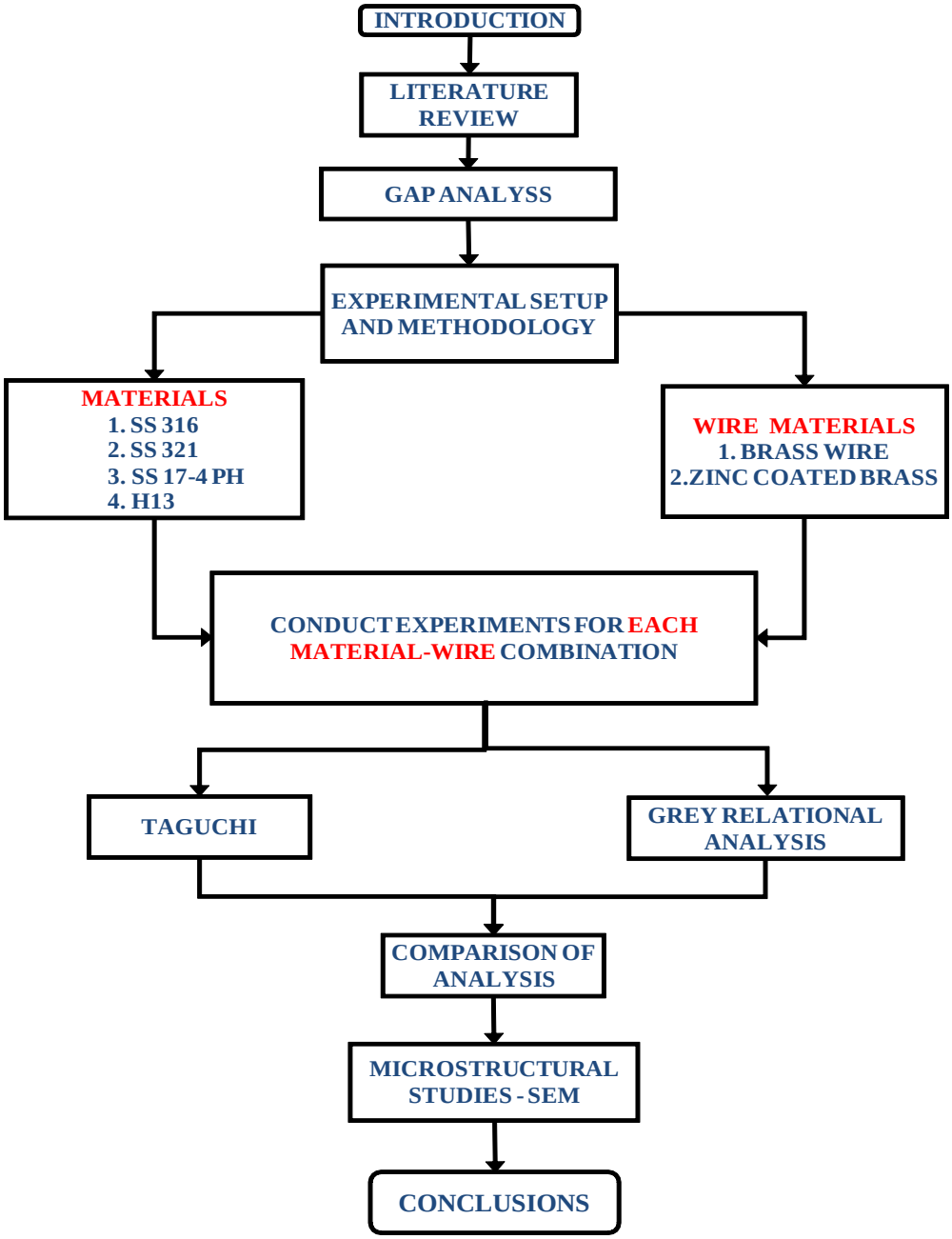

Figure 2.1 Scheme of the present work

2.7 SUMMARY

In this chapter, earlier works related to wire EDM machining process from available literature and the salient features of the works are briefly presented. In the present literature review, the researchers have been studied on different parameters of wire EDM process. From the literature most of the work was done on control process of Wire EDM process and very few of researchers has studied on optimization of Wire EDM process parameters. This chapter gives the information about gap analysis, objective of the research and problem formulation of the research. And also, the overall research work plan of the study.

Chapter 3

Experimental Set up and Process Parameters Selection

3.1 INTRODUCTION

The experiments are performed on JOEMARS WTT-655 five axes CNC Wire EDM machine. The basic parts of the Wire EDM machine consists of a wire electrode, a work table, a servo control system, a power supply and dielectric supply system. The JOEMERS WTT-655 allows the operator to choose input parameters according to the material and height of the work piece from a manual provided by the Wire EDM manufacturer. The input process parameters and machine specifications are given in the Table 3.1 and Table 3.2

Table 3.1: Terms used in Wire EDM and Parameters

S.No	Terms	Description	Unit	Fixed Parameters	
1	Servo voltage	It is the voltage which is responsible for setting the width of the spark gap	Volts	Wire used	Brass and Zinc coated wire of diameter 0.25 mm
2	Offset distance	It is the gap between the tool periphery and work piece surface	mm	Shape cut	5mm square
3	Feed	It is the advance of work piece over the tool for a given particular interval of time	Microns/s	Location of the work piece on work table	At the center of table
4	Pulse on	Sparking time	µsec	Angle of cut	Vertical
5	Pulse off	Spark pause time	µsec	Thickness/Height of the work piece	23mm
6	Wire feed	It is the movement of the tool through the work piece for a given particular interval of time	mm/min	Stability	Servo control
7	Flush rate	It is the amount of dielectric used to flush the molten metal at the interface of tool and work piece.	Ltr/min	Number of passes	One

Table 3.2: Specifications of the Wire EDM Machine

Machine Make and Model No.	JOEMERS WTT-655
Max table speed (L x W)	420x280 mm
Max. Work piece weight	5000 gm
Main table traverse (X,Y)	200x250 mm
Max. work piece thickness	250 mm
Dimensions (WxDxH)	1300x900 x1500 mm^3
Auxiliary table Traverse (u,v)	20x20 mm
Max. Wire spool capacity.	350 meters
Max. Taper angle	+/- 3^o Max./100 mm
Resolution	0.001 mm
Wire electrode diameter	0.18 mm (std), 0.25 mm (optional), 0.12 mm (optional)
Interpolation	Linear and circular
Programming	Incremental method
Least input increment	0.001 mm
Least command input	0.001 mm
Max. programmable dimensions	+/-999.999
Max. block display	999
Data input/output	1.44Mb floppy disc, regular key board, Mouse Can read Auto CAD DXF
Input power supply	3PH, 415V, 50Hz, with neutral and earth
Connected Load	1.5KVA
Die electric fluid	Soft water + coolant/ Soap cake
Die electric tank capacity	55litres
Paper filter	One in fluid tank
Air condition	Not required up to 40^oC

3.1.1 JOEMARS WT-655 Wire EDM MACHINE

The experiments were performed on JOEMARS WT-655 five axes CNC Wire EDM machine as shown in Figure 3. The basic parts of the WEDM machine consists of a wire electrode, a work table, a servo control system, a power supply and dielectric supply system. The JOEMARS WT-655 allows the operator to choose input parameters according to the material and height of the work piece from a manual provided by the Wire EDM manufacturer. The experiments are conducted on SS316, SS321, SS17-4 PH and H13 hard steel materials with E_B and E_C wire electrodes using the following wire EDM machine (Figure 3.1)

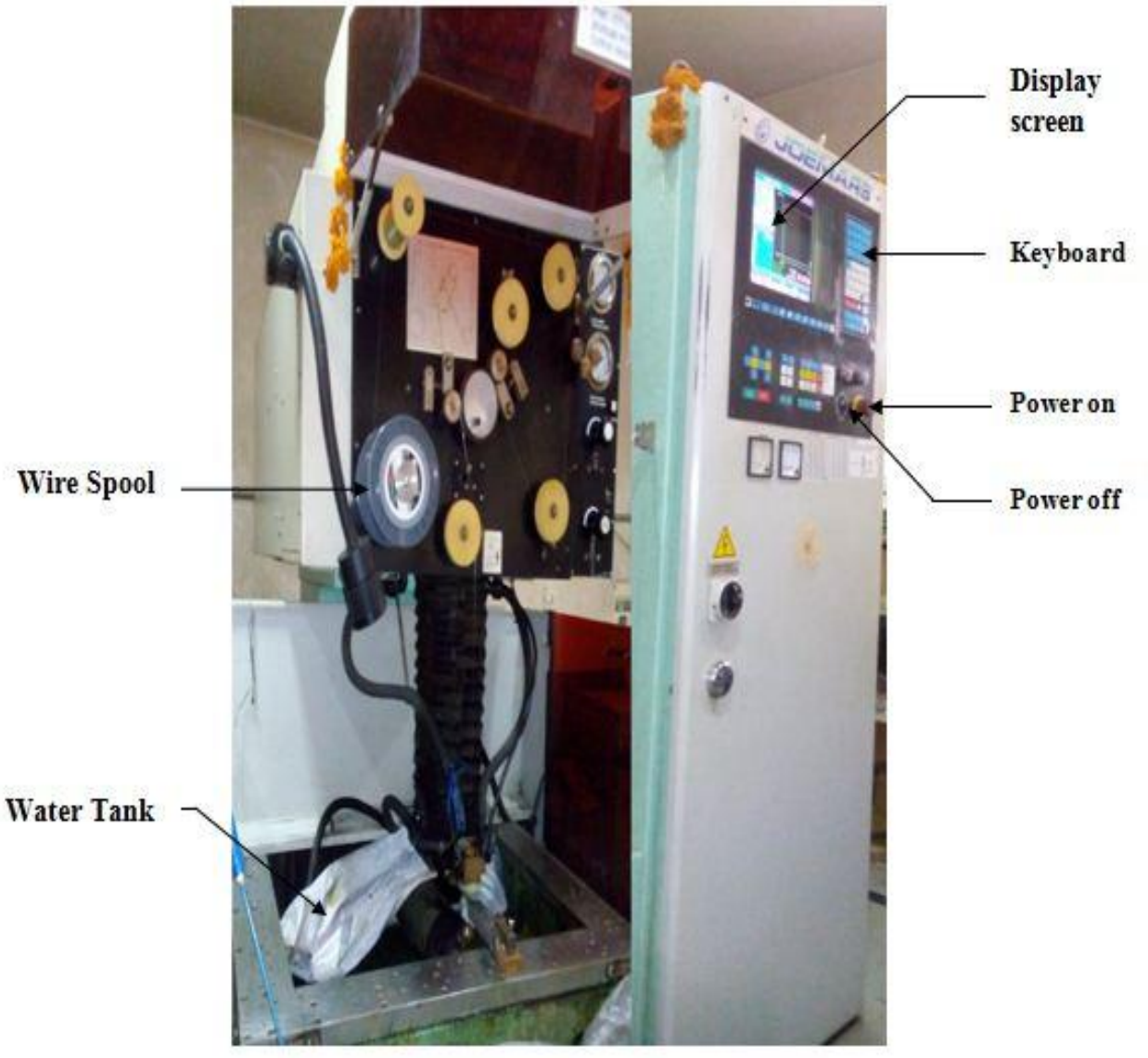

Figure 3.1: The Wire EDM Machine used in Experimentation

3.2 WORK MATERIALS USED IN WIRE EDM PROCESS

The following work materials are selected from the hard steels to machine on wire EDM process. The materials chemical composition tables, EDAX diagrams, mechanical prosperities (Table 3.7), and applications of each material are given in following subsections.

3.2.1 SS 316 Work piece Material

Grade 316 is the standard molybdenum-bearing grade, amongst the austenitic stainless steels. The molybdenum gives 316 better overall corrosion resistant properties than other Grades, particularly higher resistance to pitting and crevice corrosion in chloride environments. It has excellent forming and welding characteristics. It is readily brake or roll formed into a variety of parts for applications in the industrial, architectural, and transportation fields. Grade 316 also has outstanding welding characteristics. Post-weld annealing is not required when welding thin sections. The austenitic structure also gives these grades excellent toughness, even down to cryogenic temperatures. The chemical composition in Table 3.3 and Edax diagram Figure 3.2 are as shown below.

Table 3.3: Chemical composition of SS316 Material

SS316	C	Mn	P	S	Si	Cr	Ni	Mo	N
(%)	0.08	2.00	0.0045	0.030	0.75	16-18	10-14	2.00-3.00	0.10

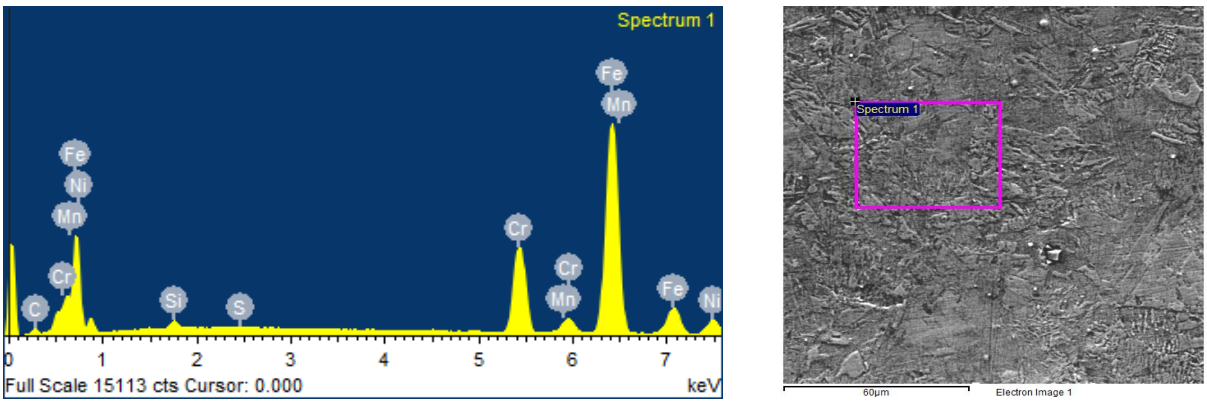

Figure 3.2: EDAX Diagram for Chemical composition of SS316 Material

3.2.2 SS321 Work piece Material

Type 321 is a stabilized stainless steel which offers as its main advantage an excellent resistance to inter-granular corrosion following exposure to temperatures in the chromium carbide precipitation range from 800 to 1500° F (427 to 816° C). Type 321 is stabilized against chromium carbide formation by the addition of titanium.

While Type 321 continues to be employed for prolonged service in the 800 to 1500° F (427 to 816° C) temperature range, Type 304L has supplanted this stabilized grade for applications involving only welding or short time heating.

Type 321 stainless steels also advantageous for high temperature service because of its good mechanical properties. Type 321 stainless steel offers higher creep and stress rupture properties.ype SS 321 resists scaling and vibration fatigue. The chemical composition in Table 3.4 and Edax diagram Figure 3.3 are as shown below.

Table 3.4: Chemical composition of SS321 Material

Material SS321 (%)	C	Mn	P	S	Si	Cr	Ni	Ti	N
	0.08	2.0	0.045	0.030	0.75	17-19	9-12	0.70	0.10

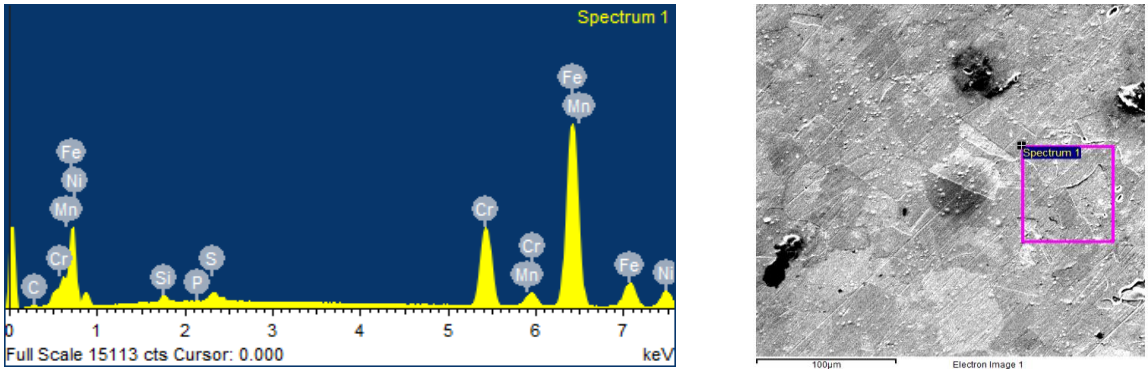

Figure 3.3: EDAX Diagram for Chemical composition of SS321 Material

3.2.3 SS17-4 PH Work piece Material

Precipitation hardening stainless steels are chromium and nickel containing steels that provide an optimum combination of the properties of martensitic and austenitic grades. The martensitic grades, they are known for their ability to gain strength through heat treatment and they are also having the corrosion resistance of austenitic stainless steels.

The high tensile strengths of precipitation hardening stainless steels come after a heat treatment process that leads to precipitation hardening of martensitic or austenitic matrix. Hardening is achieved through the addition of one or more of the elements copper, aluminium, titanium, niobium and molybdenum.

The most well known precipitation hardening steel is 17-4 PH. The name comes from the additions of 17% chromium and 4% nickel. 17-4 PH is also known as stainless steels grade 630. The chemical composition in Table 3.5 and Edax diagram Figure 3.4 are as shown below.

Table 3.5: Chemical composition of SS 17-4 PH Material

SS17-4 PH (%)	C	S	O	N	P	Si	Cr	Ni	Cu	Mn	Mo	Cb
	0.011	0.005	0.23	0.018	0.009	0.86	17.34	4.61	3.92	0.20	0.02	0.26

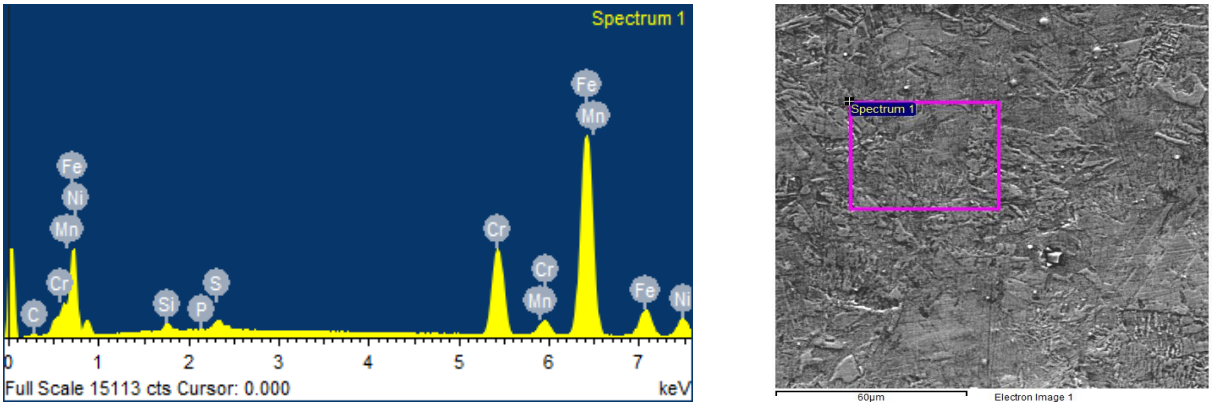

Figure 3.4: EDAX Diagram for Chemical composition of SS 17-4 PH Material

3.2.4 H13 Tool Steel Work piece Material

H13 hot tool steel is a chemical composton of chromium, molybdenum, and vanadium alloyed tool steel. This is used in die casting applications where a high level of heat resistance along with good toughness and ductility are required. H13 is also used in most other hot work applications such as forging dies and extrusion tooling components as well as plastic molds. The chemical composition in Table 3.6 and Edax diagram Figure 3.5 are as shown below.

Table 3.6: Chemical composition of H13 Material

Material H13 (%)	C	Mn	Si	Cr	Mo	V
	0.39	0.35	1.00	5.10	1.25	0.90

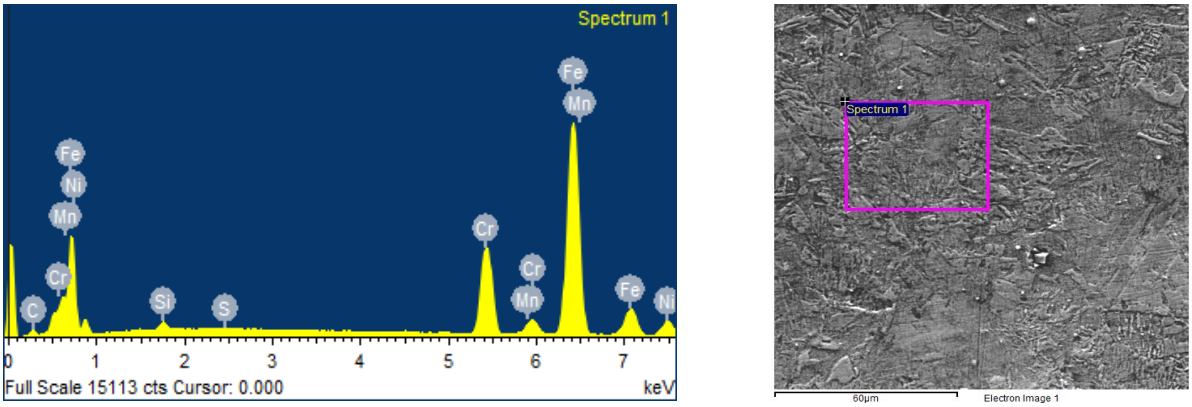

Figure 3.5: EDAX Diagram for Chemical composition of H13 Material

Table 3.7: Mechanical properties of the Work Materials

Materials					
Material Properties	Units	**SS316**	**SS321**	**SS 17-4PH**	**H13**
Density	g/cc	8	8	7.8	7.8
Hardness, Rockwell	C	79 B	80 B	45 C	52 C
Ultimate Tensile Strength	MPa	580	620	1448	1990
Tensile Strength, Yield	MPa	290	240	1379	1650
Modulus of Elasticity	GPa	193	200	200	210
Electrical Resistivity	ohm-cm	7.4e-005	7.2e-005	0.0000770	0.0000960
Thermal Conductivity	W/m-K	16.3	16.1	17.9	28.6
Melting Point	°C	1370 -1400	1400 -1425	1404-1440	1400-1427

3.3 TOOL ELECTRODE MATERIALS USED IN WIRE EDM PROCESS

Brass and zinc coated brass wires are selected for our experiments to compare its effect on performance measures such as Surface Roughness (Ra), Material Removal Rate (MRR), Kerf (cutting width) and Dimensional Deviation. Here after the brass and zinc coated brass wire electrodes are considered as E_B and E_C. The wire electrode material properties are given in Table 3.8.

Table 3.8: Wire Electrode Material Properties

Wire name	Brass	Zinc-Coated Brass
Material	Brass Special Composition	CuZnBrass,63/37Core Composition with Zinc Coating
Tensile Strength	900N/mm^2	1000N/mm^2
Wire Diameter	Ø 0.25mm	Ø 0.25mm
Symbol	E_B	E_C

3.4 THE SPECIMEN SAMPLES MACHINED IN WIRE EDM PROCESS

The experiments are carried out on all work material of SS316, SS321, SS17-4 and H13 hard steel plates of 100mm x100 x 24mm sizes. These work materials are mounted on JOEMARS WTT-655 five axes CNC Wire EDM machine and specimens of 5mm x 5mm x 24mm sizes are cut from the work piece materials. The machining of the specimen cutting operation is as shown in figure 3.6. The set of cut specimens along with work materials of SS316, SS321, SS17-4 and H13 hard steel are as shown in the following Figure 3.7(a, b, c, d, e, and f).

Figure 3.6: The Specimen Sample Machining Process of Wire EDM

(a) SS316 Material

(b) SS321 Material

(c) SS17-4 PH Material

(d) H13 Tool Steel Material

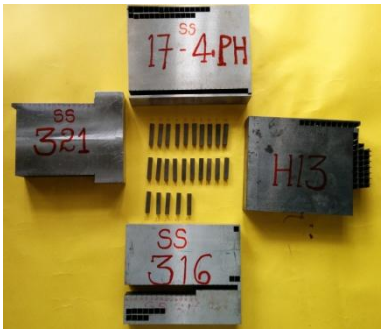

(e) All Work Materials

(f) specimens in vertical direction

Figure 3.7: The Work Material with Specimen Samples Machined in Wire EDM Process

3.5 MEASUREMENT OF EXPERIMENTAL PARAMETERS

The most important performance measures in Wire EDM are Material Removal Rate (MRR), Surface Roughness (SR), Kerf (Cutting Width) and Dimensional Deviation (DD). Cutting time and speed for each experiment are obtained from machine.

3.5.1 Cutting Speed (CS)

The Wire EDM cutting speed is a desirable characteristic and it should be as high as possible to give least machine cycle time leading to increased productivity. In the present study cutting speed is a measure of job cutting which is digitally displayed on the screen of

the machine and is given quantitatively in mm/min (Figure 3.8).

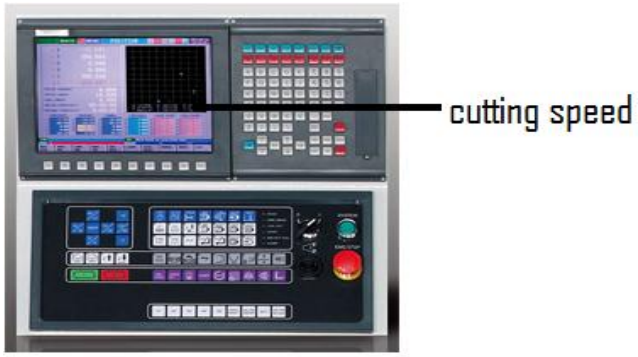

Figure 3.8: Cutting Speed Displayed on Screen in Wire EDM Process

3.5.2 Material Removal Rate (MRR)

The MRR for each Wire EDM operation was calculated manually by using following mathematical Equation.

Material removal rate (MRR) = Cs * L mm^2/min.

Where Cs = Cutting Speed in mm/min.

L = Thickness of the work piece in mm.

3.5.3 Surface Roughness (SR)

Roughness is often a good predictor of the performance of a mechanical component, since irregularities on the surface may form nucleation sites for cracks or corrosion. Roughness is a measure of the texture of a surface. It is quantified by the vertical deviations of a real surface from its ideal form. If the deviations are large the surface is rough; if small, the surface is smooth. Roughness is typically considered to be the high frequency, short wavelength component of a measured surface. The surface roughness value (µm) is obtained by the mean absolute deviation from the average surface level using the Handy surf surface measuring unit.

Figure 3.9 represents the setup used to calculate the Surface Roughness. Using the Handy Surf instrument surface roughness along the length and across the length was measured. In the present study, roughness was measured along parallel to the direction of the wire movement in machining. The total readings had taken for 50 specimens and tabulated (Ref. chapter 5 Table 5.9 and 5.10)

Figure 3.9: Setup to calculate Surface Roughness

3.5.4 Kerf (Cutting width)

Kerf (cutting width) is also an important process performance measure of the wire electro-discharge machining process. The kerf was measured using the Tool Makers Microscope (x100). The average of five measurements made from the work piece along cut length.

3.5.5 Dimensional Deviation (DD)

The specimen cross-section is measured with the help of a digital micrometer having the least count of 0.001 mm as shown in figure 3.10 and the deviation of the measured dimension is calculated in percentage using the following expression

$$\text{Dimensional Deviation} = \frac{(\text{Observed value} - \text{Actual value})}{\text{Actual value}} \times 100$$

Figure 3.10: Setup for measurement of Dimensional Deviation

3.6 EXPERIMENTATION

The experiments were accomplished on JOEMARS WT-655 five axes CNC Wire EDM machine. Following steps were followed in the cutting operation:

1. The wire was arranged vertically with the help of vertical block.
2. The work piece was located and clamped on the work table.
3. A reference point on the work piece was set for setting work co-ordinate system (WCS). The programming was done with the reference to the WCS. The reference point was defined by the bottom edges of the work piece.
4. A CNC program was written for cutting profile of 5mm x 5 mm square on work piece.

While performing various experiments, the following precautionary measures were taken:

1. Each experiment was repeated two times on trial conditions. Because in order to reduce experimental set up error.
2. The order and replication of experiment was randomized to avoid bias, if any, in the results.
3. Each set of experiments was performed at room temperature in a narrow temperature range (32 ± 2^{o} C).
4. Before taking measurements of surface roughness, the work piece was cleaned with acetone in order to get accurate values.

3.7 SELECTION OF PROCESS PARAMETERS

In order to identify the process parameters that may affect the machining characteristics of Wire EDM machined parts, the following factors are considered. This is as shown in the constructed Figure 3.11. The following electrode parameters, electrical parameters, no electrical parameters and work piece materials are considered for the Wire EDM experimentation.

Figure 3.11: Factors affecting the Wire EDM Process

3.8 SELECTION OF PROCESS PARAMETERS BASED ON PILOT EXERIMENTS

A number of pilot experiments were carried out by varying the process parameters like pulse on time, pulse off time, wire tension, wire feed, wire tension and dielectric pressure to study their effect on output parameters such as cutting seed, material removal rate, surface roughness, and dimensional deviation. The ranges of these process parameters are given in Table 3.7. From these ranges of the process parameters, different levels of process parameters would be selected by using Taguchi experimental design and experimental design methodology.

Table – 3.8: Levels of Various Process Parameters in Wire EDM

S.NO	Process Parameters	Units	Symbol	Range
1.	Pulse On	µs	A	8-16
2.	Pulse Off	µs	B	18-34
3.	Wire Tension	Kg-f	C	4-12
4.	Wire feed	mm/min	D	7-11
5.	Dielectric fluid pressure	Kg/cm^2	E	3-7

3.9 SUMMARY

This chapter gives the information about the JOEMARS WTT-655 five axes CNC Wire EDM machine specifications and the fixed parameters considered to conduct the experimentation. It provides the details about the work materials, applications and EDAX diagram for chemical composition using Scanning Electron Microscope. Further, the preparations of the specimen size and performance measures for the experimental parameters are also discussed. It gives the information about the selection of process parameters by conducting the pilot experiments. The tabular column gives the range of each parameter as an input, to the Wire EDM process.

Chapter 4

Experimental Design and Solution Methodology

4.1 INTRODUCTION

A scientific approach to plan the experiments is a necessity for efficient conduct of experiments. By the statistical design of experiments the process of planning the experiment is carried out, so that appropriate data will be collected and analyzed by statistical methods resulting in valid and objective conclusions. When the problem involves data that are subjected to experimental error, statistical methodology is the only objective approach to analysis. Thus, there are two aspects of an experimental problem: the design of the experiments and the statistical analysis of the data. These two points are closely related since the method of analysis depends directly on the design of experiments employed. The advantages of design of experiments are as follows:

- Numbers of trials is significantly reduced.
- Important decision variables which control and improve the performance of the product or the process can be identified.
- Optimal setting of the parameters can be found out.
- Qualitative estimation of parameters can be made.
- Experimental error can be estimated.
- Inference regarding the effect of parameters on the characteristics of the process can be made.

In present work, the Taguchi's method, and the grey relational analysis (GRA) have been used to plan the experiments and subsequent analysis of the data were collected.

4.2 TAGUCHI EXPERIMENTAL DESIGN AND ANALYSIS

4.2.1 Taguchi's Philosophy

Taguchi's comprehensive system of quality engineering is one of the greatest engineering achievements of the 20th century. His methods focus on the effective application of engineering strategies rather than advanced statistical techniques. It includes both upstream and shop-floor quality engineering. Upstream methods efficiently use small-scale experiments to reduce variability and remain cost-effective, and robust designs for large-scale production and market place. Shop-floor techniques provide cost-based, real time methods for monitoring and maintaining quality in production. The further upstream a quality method is applied, the greater leverages it produces on the improvement, and the more it reduces the cost and time. Taguchi's philosophy is founded on the following three very simple and fundamental concepts (Ross, 1988; Roy, 1990):

- Quality should be designed into the product and not inspected into it.
- Quality is best achieved by minimizing the deviations from the target. The product or process should be so designed that it is immune to uncontrollable environmental variables.
- The cost of quality should be measured as a function of deviation from the standard and the losses should be measured system-wide.

Taguchi proposes an "off-line" strategy for quality improvement as an alternative to an attempt to inspect quality into a product on the production line. He observes that poor quality cannot be improved by the process of inspection, screening and salvaging. No amount of inspection cannot put quality back the product. Taguchi recommends a three-stage process: system design, parameter design and tolerance design (Ross, 1988, Roy, 1990). In the present work Taguchi's parameter design approach is used to study the effect of process parameters on the various responses of the Wire EDM process.

4.2.2 Experimental Design Strategy

Taguchi recommends orthogonal array (OA) for layout of experiments. These OA's are generalized Graeco-Latin squares. To design an experiment is to select the most suitable OA and to assign the parameters and interactions of interest to the appropriate columns. The use of linear graphs and triangular tables suggested by Taguchi makes the assignment of parameters simple. The array forces all experimenters to design almost identical experiments (Roy, 1990).

In the Taguchi method the results of the experiments are analyzed to achieve one or more of the following objectives (Ross, 1988):

- To establish the best or the optimum condition for a product or process
- To estimate the contribution of individual parameters and interactions
- To estimate the response under the optimum condition

The optimum condition is identified by studying the main effects of each of the parameters. The main effects indicate the general trends of influence of each parameter. The knowledge of contribution of individual parameters is a key in deciding the nature of control to be established on a production process. The analysis of variance (ANOVA) is the statistical treatment most commonly applied to the results of the experiments in determining the

percentage contribution of each parameter against a stated level of confidence. Study of ANOVA table for a given analysis helps to determine which of the parameters need control (Ross, 1988).

Taguchi suggests (Roy, 1990) two different routes to carry out the complete analysis. First, the standard approach, where the results of a single run or the average of repetitive runs are processed through main effect and ANOVA analysis (Raw data analysis). The second approach which Taguchi strongly recommends for multiple runs is to use signal- to- noise ratio (S/N) for the same steps in the analysis. The S/N ratio is a concurrent quality metric linked to the loss function (Barker, 1990). By maximizing the S/N ratio, the loss associated can be minimized. The S/N ratio determines the most robust set of operating conditions from variation within the results. The S/N ratio is treated as a response (transform of raw data) of the experiment. Taguchi recommends (Ross, 1988) the use of outer OA to force the noise variation into the experiment i.e. the noise is intentionally introduced into experiment. However, processes are often times subject to many noise factors that in combination, strongly influence the variation of the response. For extremely "noisy" systems, it is not generally necessary to identify specific noise factors and to deliberately control them during experimentation. It is sufficient to generate repetitions at each experimental condition of the controllable parameters and analyze them using an appropriate S/N ratio (Byrne and Taguchi, 1987).

In the present investigation, the raw data analysis and S/N data analysis have been performed. The effects of the selected Wire EDM process parameters on the selected quality characteristics have been investigated through the plots of the main effects based on raw data. The optimum condition for each of the quality characteristics has been established through S/N data analysis aided by the raw data analysis. No outer array has been used and instead, experiments have been repeated three times at each experimental condition.

4.2.3 Loss Function

The heart of Taguchi method is his definition of the nebulous and elusive term 'quality' as the characteristic that avoids loss to the society from the time the product is shipped (Braker, 1986). Loss is measured in terms of monetary units and is related to quantifiable product characteristic.

Taguchi defines quality loss via his "loss function". He unites the financial loss with the functional specification through a quadratic relationship that comes from a Taylor series expansion. The quadratic function takes the form of a parabola. Taguchi defines the loss function as a quantity proportional to the deviation from the nominal quality characteristic

(Roy, 1990). He has found the following quadratic form to be a useful workable function (Roy, 1990):

$$L(y) = k (y-m)^2 \quad \ldots\ldots (4.1)$$

Where,

L = Loss in monetary units

m = value at which the characteristic should be set

y = actual value of the characteristic

k = constant depending on the magnitude of the characteristic and the monetary unit involved

The loss function represented in Eq. 4.1 is graphically shown in Figure 4.1(a). The characteristics of the loss function are (Roy, 1990):

- The further the product's characteristic varies from the target value, the greater is the loss. The loss must be zero when the quality characteristic of a product meets its target value.
- The loss is a continuous function and not a sudden step as in the case of traditional (goal post) approach (Figure 4.1b). This consequence of the continuous loss function illustrates the point that merely making a product within the specification limits does not necessarily mean that product is of good quality.

4.2.3.1 Average loss-function for product population

In a mass production process, the average loss per unit is expressed as (Roy 1990):

$$L(y) = \frac{1}{n}\{k (y_1 - m)^2 + k (y_2 - m)^2 + \ldots + k (y_n - m)^2\} \quad \ldots\ldots (4.2)$$

Where,

$y_1, y_2 \ldots y_n$ = Actual value of the characteristic for unit 1, 2 . . . n respectively

n = Number of units in a given sample

k = Constant depending on the magnitude of the characteristic and the monetary unit involved

m = Target value at which the characteristic should be set

The Eq. 4.2 can be simplified as:

$$L(y) = k (MSD_{NB}) \quad \ldots\ldots (4.3)$$

Where,

MSD_{NB} = Mean squared deviation or the average of squares of all deviations from the target or nominal value

NB = "Nominal is Best"

4.2.3.2 Other loss functions

The loss-function can also be applied to product characteristics other than the situation where the nominal value is the best value (m).

The loss-function for a "smaller is better" type of product characteristic lower the better (LB) is shown in Figure 4.2a. The loss function is identical to the "nominal-is-best" type of situation when m=0, which is the best value for "smaller is better" characteristic (no negative value). The loss function for a "larger-is-better" type of product characteristic higher the better (HB) is also shown in Figure 4.2b, where also m=0.

4.2.4 Signal to Noise Ratio

The loss-function discussed above is an effective figure of merit for making engineering design decisions. However, to establish an appropriate loss-function with its K value to use as a figure of merit is not always cost-effective and easy. Recognizing the dilemma, Taguchi created a transform function for the loss-function which is named as signal -to-noise (S/N) ratio (Barker, 1990).

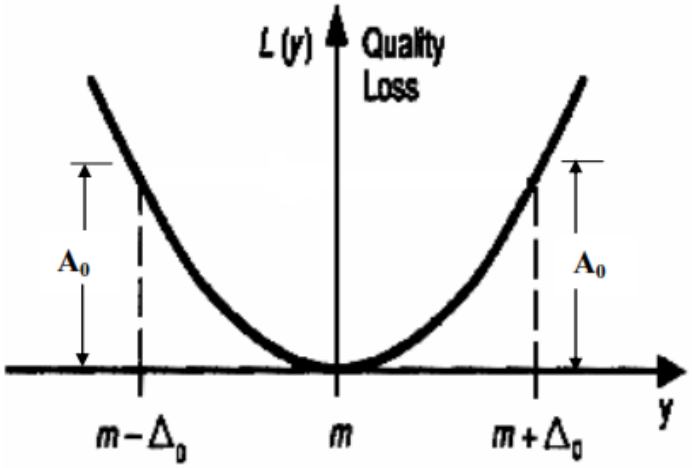

Figure 4.1(a): Taguchi Loss Function

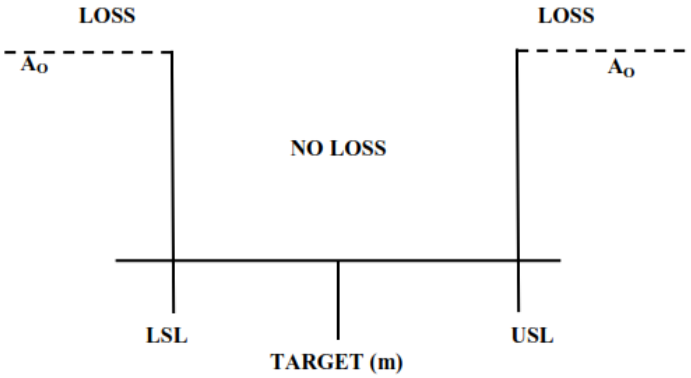

Figure 4.1(b): Traditional Approach

Figure 4.1: The Taguchi Loss-Function and the Traditional Approach (Ross, 1988)

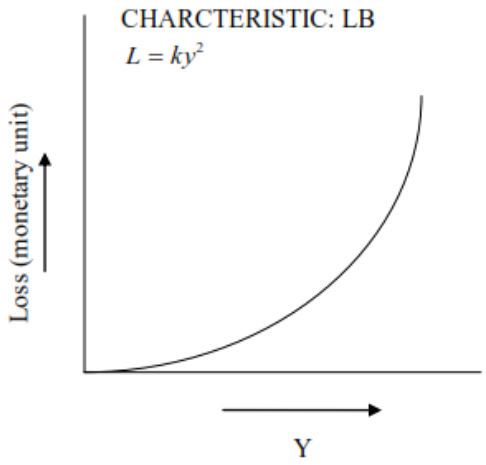

Figure 4.2(a): The Taguchi Loss-Function for Lower is Better (LB)

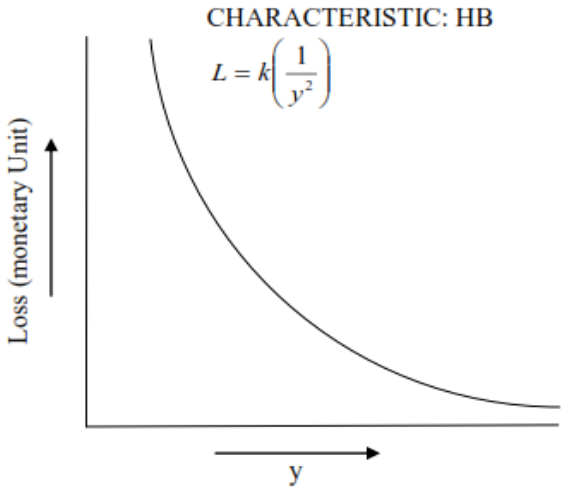

Figure 4.2(b): The Taguchi Loss-Function for Higher is Better (HB)

Figure 4.2: The Taguchi Loss-Function for LB and HB Characteristics (Barker, 1990)

The S/N ratio, as stated earlier, is a concurrent statistic. A concurrent statistic is able to look at two characteristics of a distribution and roll these characteristics into a single number or figure of merit. The S/N ratio combines both the parameters (the mean level of the quality characteristic and variance around this mean) into a single metric (Barker, 1990).

A high value of S/N implies that signal is much higher than the random effects of noise factors. Process operation consistent with highest S/N always yields optimum quality with minimum variation (Barker, 1990).

The S/N ratio consolidates several repetitions (at least two data points are required) into one value. The equation for calculating S/N ratios for "smaller is better"(LB), "larger is better" (HB) and "nominal is best" (NB) types of characteristics are as follows (Ross, 1988):

1. Larger the Better:

$(S/N)_{HB} = -10\log(MSD_{HB})$ ……..…….....(4.4)

Where,

$MSD_{HB} = \frac{1}{R}\sum_{j=1}^{R} (1/y_j^2)$

2. Smaller the Better:

$(S/N)_{LB} = -10\log(MSD_{LB})$ ……..……..…(4.5)

Where,

$MSD_{LB} = \frac{1}{R}\sum_{j=1}^{R} (y_j^2)$

3. Nominal the Best

$(S/N)_{NB} = -10\log(MSD_{NB})$ …….....…….....…(4.6)

Where,

$MSD_{LB} = \frac{1}{R}\sum_{j=1}^{R} (y_j - y_o)^2$

R = Number of repetitions

The mean squared deviation (MSD) is a statistical quantity that reflects the deviation from the target value. The expressions for MSD are different for different quality characteristics. For the "nominal is best" characteristic, the standard definition of MSD is used. For the other two characteristics the definition is slightly modified. For "smaller is better", the unstated target value is zero. For "larger is better", the inverse of each large value becomes a small value and again, the unstated target value is zero. Thus for all three expressions, the smallest magnitude of MSD is being sought.

4.2.5 Relation between S/N Ratio and Loss Function

Figure 4.2a shows a single sided quadratic loss function with minimum loss at the zero value of the desired characteristic. As the value of y increases, the loss grows. Since, loss is to be minimized the target in this situation for y is zero.

The basic loss function (Eq. 4.1) is:

$L(y) = k (y-m)^2$

If $m = 0$

$L(y) = k (y)^2$

The loss may be generalized by using k=1 and the expected value of loss may be found by summing all the losses for a population and dividing by the number of samples R taken from this population. This in turn gives the following expression (Barker, 1990).

EL = Expected loss = $(\sum y^2/R)$……...……(4.7)

The above expression is a figure of demerit. The negative of this demerit expression produces a positive quality function. This is the thought process that goes into the creation of S/N ratio from the basic quadratic loss function. Taguchi adds the final touch to this transformed loss-function by taking the log (base 10) of the negative expected loss and then he multiplies by 10 to put the metric into the decibel terminology (Barker, 1990). The final expression for "smaller-is-better" S/N ratio takes from the Equation 4.2. The same thought pattern follows in creation of other S/N ratios.

4.3 STEPS INVOLVED IN TAGUCHI EXPERIMENTAL DESIGN AND ANALYSIS

The Taguchi method involves reducing the variation in a process through robust design of experiments. The overall objective of the method is to produce high quality product at low cost to the manufacturer. The Taguchi method was developed by Dr. Genichi Taguchi of Japan who maintained that variation. The experimental design proposed by Taguchi involves using orthogonal arrays to organize the parameters affecting the process and the levels at which they should be varied; it allows for the collection of the necessary data to determine which factors most affect product quality with a minimum amount of experimentation, thus saving time and resources.

The general steps involved in the Taguchi Method are as follows;

1. Define the process objective, or more specifically, a target value for a performance measure of the process. This may be a flow rate, temperature etc. The target of a process may also be a minimum or maximum; for example, the goal may be to maximize the output flow rate. The deviation in the performance characteristic from the target value is used to define the loss function for the process.

2. Determine the design parameters affecting the process. Parameters are variables within the process that affect the performance measure such as temperatures, pressures, etc. that can be easily controlled. The number of levels that the parameters should be varied at must be specified. For example, a temperature might be varied to a low and high value of 40 C and 80 C. increasing the number of levels to vary a parameter at increases the number of experiments to be conducted.

3. Create orthogonal arrays for the parameter design indicating the number of and conditions for each experiment. The selection of orthogonal arrays is based on the number of parameters and the levels of variation for each parameter.

4. Conduct the experiments indicated in the completed array to collect data on the effect on the performance measure.

5. Complete data analysis to determine the effect of the different parameters on the performance measure.

Taguchi has tabulated 18 basic orthogonal arrays that are called standard orthogonal arrays. In many case studies, one of the arrays from Table 4.1 can be used directly to plan a matrix experiment. An arrays name indicates the number of rows and columns it has, and also the number of levels in each of the columns. The 18 standard orthogonal arrays along with the number of columns at different levels for these arrays are listed in Table 4.1.

Table 4.1: Standards Orthogonal Array [21]

Orthogonal array	Number rows	Maximum number of Factors	Maximum number of columns of these levels			
			2	3	4	5
L_4	4	3	3	-	-	-
L_8	8	7	7	-	-	-
L_9	9	4	-	4	-	-
L_{12}	12	11	11	-	-	-
L_{16}	16	15	15	-	-	-
L'_{16}	16	5	-	-	5	-
L_{18}	18	8	1	7	-	-
L_{25}	**25**	**6**	**-**	**-**	**-**	**6**
L_{27}	27	13	-	13	-	-
L_{32}	32	31	31	-	-	-
L'_{32}	32	10	1	-	9	-
L_{36}	36	23	11	12	-	-
L'_{36}	36	16	3	13	-	-
L_{50}	50	12	1	-	-	11
L_{54}	54	26	1	25	-	-
L_{64}	64	63	63	-	-	-
L_{64}	64	21	-	-	21	-
L_{81}	81	40	-	40	-	-

The number of rows of an orthogonal array represents the number of experiments. In order for an array to be a viable choice, the number of rows must be at least equal to the degrees of freedom required for the case study. The number of columns of an array represents the maximum number of factors that can be studied using that array. Further, in order to use a

standard orthogonal array directly, one must be able to match the number of levels of the factors with the number of levels of the columns in the array. Usually, it is expensive to conduct experiments. Therefore, the designer uses the smallest possible orthogonal array that meets the requirements of the case study.

4.4 EXPERIMENTATION AND DATA COLLECTION

The experiment is performed against each of the trial conditions of the inner array. Each experiment at a trial condition is repeated simply (if outer array is not used) or according to the outer array (if used). Randomization should be carried to reduce bias in the experiment. The data (raw data) are recorded against each trial condition and S/N ratios of the repeated data points are calculated and recorded against each trial condition.

4.4.1 Data analysis

A number of methods have been suggested by Taguchi for analyzing the data: observation method, ranking method, column effect method, ANOVA, S/N ANOVA, plot of average response curves etc. (Ross, 1988). However, in the present investigation the following methods have been used:

- Plot of average response curves
- ANOVA for raw data
- ANOVA for S/N data
- Residual graphs

The plot of average responses at each level of a parameter indicates the trend. It is a pictorial representation of the effect of parameter on the response. The change in the response characteristic with the change in levels of a parameter can easily be visualized from these curves. Typically, ANOVA for OA's are conducted in the same manner as other structured experiments (Ross, 1988). The S/N ratio is treated as a response of the experiment, which is a measure of the variation within a trial when noise factors are present. A standard ANOVA can be conducted on S/N ratio which will identify the significant parameters (mean and variation). Interaction graphs are used to select the best combination of interactive parameters (Peace, 1993). Residual graphs are used to check the accuracy.

4.5 PARAMETERS DESIGN STRATEGY

4.5.1 Parameter classification and selection of optimal levels

When the ANOVA on the raw data (identifies process parameters which affect average) and S/N data (identifies control parameters which affect variation) are completed, the control parameters may be put into four classes (Ross1988):

Class I : Parameters which affect both average and variation
(Significant in both i.e. raw data ANOVA and S/N ANOVA)

Class II : Parameters which affect variation only
(Significant in S/N ANOVA only)

The parameters design strategy is to select the proper levels of class I and class II parameters to reduce variation.

4.5.2 Prediction of the mean

After determination of the optimum condition, the mean of the response (η) at the optimum condition is predicted. The mean is estimated only from the significant parameters. The ANOVA identifies the significant parameters. Suppose, parameters A and B are significant and A_2B_2 (second level of A=A_2, second level of B=B_2) is the optimal treatment condition. Then, the mean at the optimal condition (optimal value of the response characteristic) is estimated as (Ross, 1988):

$$\eta = (T + (A_2\text{-}T) + (B_2 - T))$$

$$= A_2 + B_2\text{-}T$$

Where

T = Overall mean of the response

A_2, B_2 = Average values of response at the second levels of parameters A and B respectively

It may also so happen that the prescribed combination of parameter levels (optimal treatment condition) is identical to one of those in the experiment. If this situation exists, then the most direct way to estimate the mean for that treatment condition is to average out all the results for the trials which are set at those particular levels (Ross, 1988).

4.5.3 Determination of confidence interval

The estimate of the mean (η) is only a point estimate based on the average of results obtained from the experiment. Statistically this provides a 50% chance of the true average

being greater than η. It is therefore customary to represent the values of a statistical parameter as a range within which it is likely to fall, for a given level of confidence (Ross, 1988). This range is termed as the confidence interval (CI). In other words, the confidence interval is a maximum and minimum value between which the true average should fall at some stated percentage of confidence (Ross, 1988).

The following equation is used to find out the confidence interval is suggested by Taguchi in regards to the estimated mean of the optimal treatment condition (Ross, 1988).

1. Around the estimated average of a treatment condition predicted from the experiment. This type of confidence interval is designated as CI_{POP} (confidence interval for the population).

$$CI_{POP} = \sqrt{\frac{F\alpha\,(1,fe)\,Ve}{neff}} \quad \text{.....(4.8)}$$

Where,

$F_\alpha\,(1, f_e)$ = The F ratio at a confidence level of (1-a) against Degrees of Freedom (DOF) 1, and error degree of freedom f_e

$$n_{eff} = \frac{N}{1 + [\text{Total DOF associated in the estimate of the mean}]}$$

N = Total number of results

4.5.4 Confirmation Experiment

The confirmation experiment is a final step in verifying the conclusions from the previous round of experimentation. The optimum conditions are set for the significant parameters (the insignificant parameters are set at economic levels) and a selected number of tests are run under specified conditions. The average of the confirmation experiment results is compared with the anticipated average based on the parameters and levels tested. The confirmation experiment is a crucial step and is highly recommended to verify the experimental conclusion (Ross, 1988).

4.6 GREY RELATIONAL ANALYSIS

The Grey theory established by Dr. Deng (1982) includes Grey relational analysis (GRA), Grey modelling, prediction and decision making of a system in which the model is unsure or the information is incomplete.GRA is based on geometrical mathematics, which

compliance with the principles of normality, symmetry, entirety, and proximity. It provides an efficient solution to the uncertainty, multi-input and discrete data problem. The relation between machining parameters and machining performance can be found out using the Grey relational analysis. And this kind of interaction is mainly through the connection among parameters and some conditions that are already known. Also, it will indicate the relational degree between two sequences with the help of Grey relational analysis. Moreover, the Grey relational grade will utilize the discrete measurement method to measure the distance.

GRA is suitable for solving complicated interrelationships between multiple factors and variables and has been successfully applied on cluster analysis, robot path planning, project selection, prediction analysis, performance evaluation, and factor effect evaluation and multiple criteria decision.

Comparing to regression analysis and factor analysis in mathematic statistics, grey relational has some merits such as small sample, having no use for typical distribution, no requirement for independency and small amount of calculation. Additionally, GRA analysis is already proved to be simple and accurate method for selecting factors especially for those problems with unique characteristic..Grey Relational Analysis (GRA) a normalization evaluation technique is extended to solve the complicated multi-performance characteristics optimization effectively.

Single objective optimization is done by regression equation analysis but not possible for multiple objective optimization. multiple objectives as a performance parameter have been considered in this work. Hence Grey relational analysis method is used to get optimal solution for this work.

4.6.1 Optimization Steps in Grey Relational Analysis

Step I: In this step, the original response values are transformed into S/N ratio values. Further analysis is carried out based on these S/N ratio values. The material removal rate is a higher-the-better performance characteristic, since the maximization of the quality characteristic of interest is sought and can be expressed as (Muthu kumar et al, 2010)

$$\frac{S}{N} Ratio = -\log_{10}\left(\frac{1}{n}\sum_{i=1}^{n}\frac{1}{y_{ij}^2}\right) \quad \text{.....(4.9)}$$

Where n = number of replications and

y_{ij}= observed response value

Where i =1, 2.....n;

j = 1, 2…..k.

The surface roughness and kerf width are the lower-the-better performance characteristic and the loss function for the same can be expressed as

$$\frac{S}{N} Ratio = -\log_{10}\left(\frac{1}{n}\sum_{i=1}^{n} y_{ij}^{2}\right) \quad \text{.....(4.10)}$$

Step II: In the grey relational analysis, a data pre-processing is first performed in order to normalize the raw data for analysis. Normalization is a transformation performed on a single data input to distribute the data evenly and scale it into an acceptable range for further analysis. In this work, a linear normalization of the S/N ratio is performed in the range between zero and unity, which is also called the grey relational generating. y_{ij} is normalized as Z_{ij}($0 \leq Zij \leq 1$) by the following formula to avoid the effect of adopting different units and to reduce the variability. The normalized material removal rate corresponding to the larger-the-better criterion can be expressed as (Muthu kumar et al, 2010)

$$Z_{ij} = \frac{y_{ij} - \min\left(y_{ij,} i = 1,2,.....n\right)}{\max\left(y_{ij,} i = 1,2,.....n\right) - \min\left(y_{ij,} i = 1,2,.....n\right)} \quad \text{.....(4.11)}$$

The surface roughness and kerf width should follow the lower-the-better criterion and can be expressed as

$$Z_{ij} = \frac{\max\left(y_{ij,} i = 1,2,.....n\right) - y_{ij}}{\max\left(y_{ij,} i = 1,2,.....n\right) - \min\left(y_{ij,} i = 1,2,.....n\right)} \quad \text{...……..…(4.12)}$$

Step III: The grey relational coefficient is calculated to express the relationship between the ideal (best) and actual normalized actual results. The grey relational coefficient can be expressed as (Muthu kumar et al, 2010)

$$\gamma\left(y_{o}(k), y_{i}(k)\right) = \frac{\Delta\min + \xi\Delta\max}{\Delta_{oj}(k) + \xi\Delta\max} \quad \text{.....(4.13)}$$

Where

j = 1, 2...n;

k = 1, 2...m, n is the number of actual data items and m is the number of responses.

y_o(k) is the reference sequence (y_o(k) = 1, k = 1,2...m);

y_j(k) is the specific comparison sequence.

$\Delta_{oj} = \|y_o(k) - y_j(k)\|$ -The absolute value of the difference between y_0(k) and y_j(k).

$\Delta \min = \min_{\forall j \in i} \min_{\forall k} \|y_o(k) - y_j(k)\|$ is the smallest value of y_j(k)

$\Delta \max = \max_{\forall j \in i} \max_{\forall k} \|y_o(k) - y_j(k)\|$ is the largest value of y_j(k)

Where ξ is the distinguishing coefficients, which is defined in the range 0≤ ξ ≤1.The Wire EDM process parameters, are equally weighted in this study, and therefore ξ is 0.5.

***Step IV*:** The grey relational grade is determined by averaging the grey relational coefficient corresponding to each performance characteristic. The overall performance characteristic of the multiple response process depends on the calculated grey relational grade. The grey relational coefficient can be expressed as (Muthu kumar et al, 2010)

$$\overline{\gamma_j} = \frac{1}{k}\sum_{i=1}^{m} \gamma_{ij} \quad \text{.....(4.14)}$$

Where $\overline{\gamma_j}$ the grey relational grade for the jth experiment and k is the number of performance characteristics.

Step V: Determine the optimal factor and its level combination (Muthu kumar et al, 2010)

4.7 SUMMARY

In this chapter, the experimental design using Taguchi methodology is discussed and the experimental results solution methodology is also presented. Taguchi's design and analysis is used for single objective and Grey relational analysis is used for multi-objective analysis. This chapter provides the details about the steps involved in Taguchi's design methodology and grey relational analysis for multi objective analysis for Wire EDM experimental results.

Chapter 5

Results and Analysis by Taguchi Method

5.1 INTRODUCTION

The present chapter gives the application of the Taguchi experimental design method for single objective optimization. The scheme of carrying out experiments was selected and the experiments were conducted to investigate the effect of process parameters on the output responses e.g. cutting speed, material removal rate, surface roughness, kerf (cutting width) and dimensional deviation. The experimental results are discussed subsequently in the following sections.

5.2 SELECTION OF ORTHOGONAL ARRAY AND PROCESS PARAMETERS

For the present experimental work, five process parameters each at five levels have been decided. It is desirable to have five levels of process parameters to reflect the true behaviour of output parameters of study. The process parameters, their corresponding symbols and the levels of the individual process parameters are given in Table 5.1.

Table 5.1: Levels of Various Process Parameters in Wire EDM Process

S.NO	Process Parameters	Units	symbol	Levels				
				L1	L2	L3	L4	L5
1.	Pulse On time	µs	A	8	10	12	14	16
2.	Pulse Off time	µs	B	18	22	26	30	34
3.	Wire Tension	Kg-f	C	4	6	8	10	12
4.	Wire feed	m/min	D	7	8	9	10	11
5.	Dielectric fluid pressure	Kg/cm^2	E	3	4	5	6	7

5.3 RESULTS, ANALYSIS AND DISCUSSIONS ON EXPERIMENTS USING BRASS (E_B) AND ZINC COATED BRASS (E_C) WIRE ELECTRODES

The Wire EDM experiments were conducted to study the effect of process parameters over the output response characteristics with brass (E_B) and zinc coated brass(E_C) wires are as electrode materials for machining on hard steels like SS316, SS321, SS17-4 and H13; Cutting speed, material removal rate, surface roughness, kerf and dimensional deviation are the responses. The effect of process parameters on each response in terms of response plots, residual plots, analysis of variance (ANOVA) tables and response tables are presented in the following sections. Orthogonal Array (OA) L_{25} experiments were conducted using Taguchi experimental design methodology (Table 5.2) and each experiment was repeated two times for obtaining S/N values. Minitab statistical software is used for the above study.

Table 5.2: Taguchi's L_{25} Standard Orthogonal Array

S.No	A	B	C	D	E	Response (Raw data)		S/N Ratio
						R1	R2	
1	1	1	1	1	1			
2	1	2	2	2	2			
3	1	3	3	3	3			
4	1	4	4	4	4			
5	1	5	5	5	5			
6	2	1	2	3	4			
7	2	2	3	4	5			
8	2	3	4	5	1			
9	2	4	5	1	2			
10	2	5	1	2	3			
11	3	1	3	5	2			
12	3	2	4	1	3			
13	3	3	5	2	4			
14	3	4	1	3	5			
15	3	5	2	4	1			
16	4	1	4	2	5			
17	4	2	5	3	1			
18	4	3	1	4	2			
19	4	4	2	5	3			
20	4	5	3	1	4			
21	5	1	5	4	3			
22	5	2	1	5	4			
23	5	3	2	1	5			
24	5	4	3	2	1			
25	5	5	4	3	2			

R1 and R2 represent response values for two repetitions of each trial. The 1's, 2's, 3's, 4's and 5's represent levels 1, 2, 3, 4, and 5 of the variables, which appear at the top of the column.

5.4 RESULTS ANALYSIS AND DISCUSSION FOR SS316 USING E_B AND E_C

The Wire EDM experiments were conducted using the Taguchi's L_{25} orthogonal array (OA) with E_B and E_C electrodes and SS316 as work material. The experimental results are shown in Table 5.3 and Table 5.4 respectively. The effect of individual Wire EDM process parameters on the selected quality characteristics such as cutting speed (CS), material removal rate (MRR), surface roughness (SR), kerf (cutting width) and dimensional deviation (DD) are presented and analyzed. The average value and S/N ratio of the response characteristics for each variable at different levels were calculated from experimental data. The main effect of process variables both for experimental data and S/N data were plotted. The response curves

(main effects) are used for examining the parametric effects on the response characteristics. The analysis of variance (ANOVA) of experimental data and S/N data is carried out to identify the significant variables and to quantify their effects on the response characteristics. The most favourable values (optimal settings) of process parameters in terms of mean response characteristics are established by analyzing the response curves and the ANOVA tables.

5.4.1 Effect of Process Parameters on Cutting Speed (CS)

The average values of cutting speed (CS) for each of input (Pon, Poff, Wt, Wf and Wp) parameters at level 1 and 2 for experimental data and S/N data are plotted using E_B and E_C electrodes.

Table 5.3: Cutting Speed (CS) Results for SS316 using Electrode E_B

S.No	A	B	C	D	E	CS		S/N Ratio
						R1	R2	
1	1	1	1	1	1	0.534	0.542	-5.44917
2	1	2	2	2	2	0.425	0.418	-7.43222
3	1	3	3	3	3	0.330	0.326	-9.62972
4	1	4	4	4	4	0.697	0.712	-3.13534
5	1	5	5	5	5	0.754	0.762	-2.45257
6	2	1	2	3	4	0.805	0.811	-1.88408
7	2	2	3	4	5	0.945	0.942	-0.49136
8	2	3	4	5	1	0.833	0.828	-1.58710
9	2	4	5	1	2	0.470	0.465	-6.55804
10	2	5	1	2	3	0.405	0.413	-7.85090
11	3	1	3	5	2	1.832	1.835	5.25851
12	3	2	4	1	3	1.715	1.721	4.68528
13	3	3	5	2	4	1.064	1.071	0.53883
14	3	4	1	3	5	1.247	1.242	1.91733
15	3	5	2	4	1	0.892	0.886	-0.99270
16	4	1	4	2	5	1.925	1.932	5.68861
17	4	2	5	3	1	1.810	1.814	5.15357
18	4	3	1	4	2	1.105	1.113	0.86725
19	4	4	2	5	3	1.240	1.235	1.86843
20	4	5	3	1	4	0.912	0.918	-0.80010
21	5	1	5	4	3	2.186	2.184	6.79300
22	5	2	1	5	4	2.025	2.022	6.12850
23	5	3	2	1	5	1.916	1.916	5.64791
24	5	4	3	2	1	1.525	1.523	3.66540
25	5	5	4	3	2	1.289	1.286	2.20506

Table 5.4: Cutting Speed (CS) Results for SS316 using Electrode E_C

S.No	A	B	C	D	E	CS		S/N Ratio
						R1	R2	
1	1	1	1	1	1	0.635	0.646	-5.44917
2	1	2	2	2	2	0.540	0.551	-7.43222
3	1	3	3	3	3	0.478	0.489	-9.62972
4	1	4	4	4	4	0.387	0.398	-3.13534
5	1	5	5	5	5	0.335	0.346	-2.45257
6	2	1	2	3	4	1.011	1.023	-1.88408
7	2	2	3	4	5	0.835	0.847	-0.49136
8	2	3	4	5	1	0.675	0.687	-1.58710
9	2	4	5	1	2	0.587	0.599	-6.55804
10	2	5	1	2	3	0.552	0.564	-7.85090
11	3	1	3	5	2	1.876	1.888	5.25851
12	3	2	4	1	3	1.328	1.34	4.68528
13	3	3	5	2	4	0.934	0.945	0.53883
14	3	4	1	3	5	0.894	0.905	1.91733
15	3	5	2	4	1	0.735	0.746	-0.99270
16	4	1	4	2	5	2.205	2.216	5.68861
17	4	2	5	3	1	1.918	1.929	5.15357
18	4	3	1	4	2	1.315	1.326	0.86725
19	4	4	2	5	3	1.018	1.029	1.86843
20	4	5	3	1	4	0.870	0.881	-0.80010
21	5	1	5	4	3	2.625	2.637	6.79300
22	5	2	1	5	4	2.418	2.43	6.12850
23	5	3	2	1	5	1.924	1.936	5.64791
24	5	4	3	2	1	1.689	1.701	3.66540
25	5	5	4	3	2	1.315	1.327	2.20506

Figures 5.1(a, b) and 5.2(a, b) shows that the cutting speed increases with the increase of pulse on time, wire feed and water pressure, decreases with increase in pulse off time and wire tension. This is because the discharge energy increases with the pulse on time and wire feed leading to a faster cutting speed. As the pulse off time decreases, the number of discharges within a given period is more and thus lead to a higher cutting speed. The effects of wire feed and wire tension on cutting speed are very significant. It is also evident that cutting speed is minimum at first level of pulse on time and maximum at first level of pulse off time. It is seen from the Figures 5.1(a, b) and 5.2(a, b) that there is very weak interaction between the process parameters on the cutting speed.

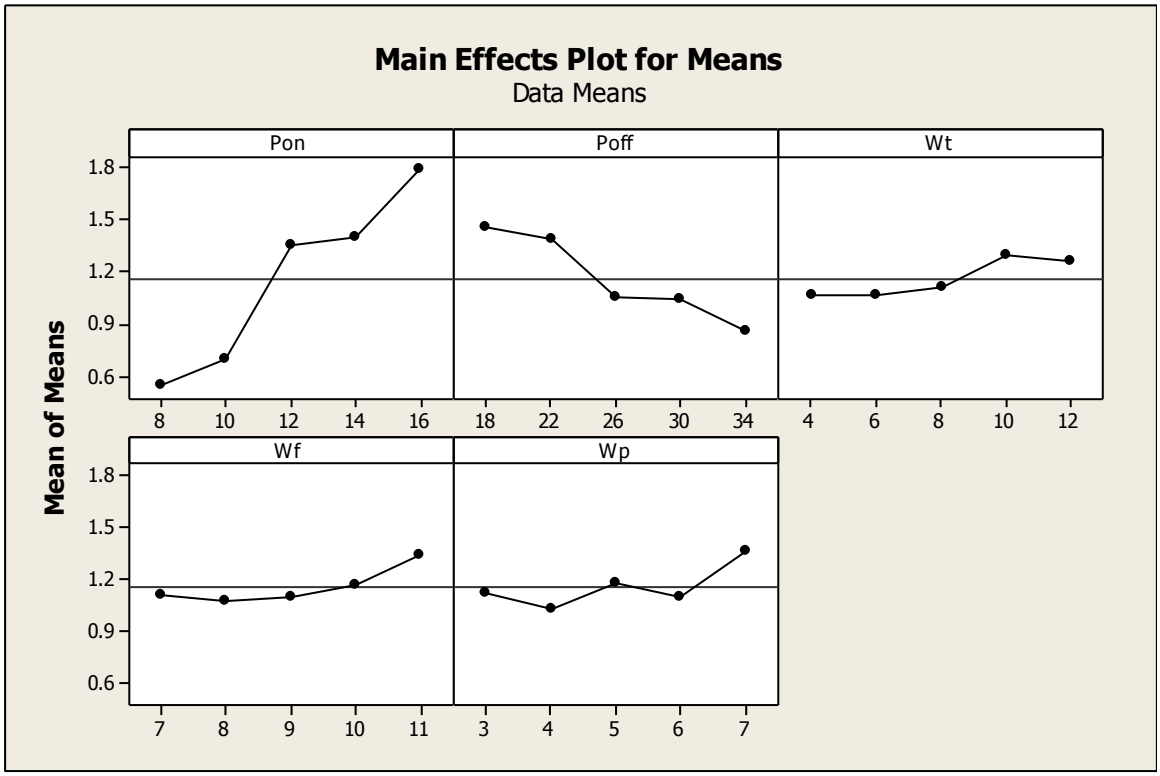

Figure 5.1(a): Effects of Process Parameters on Cutting Speed (Experimental Data)

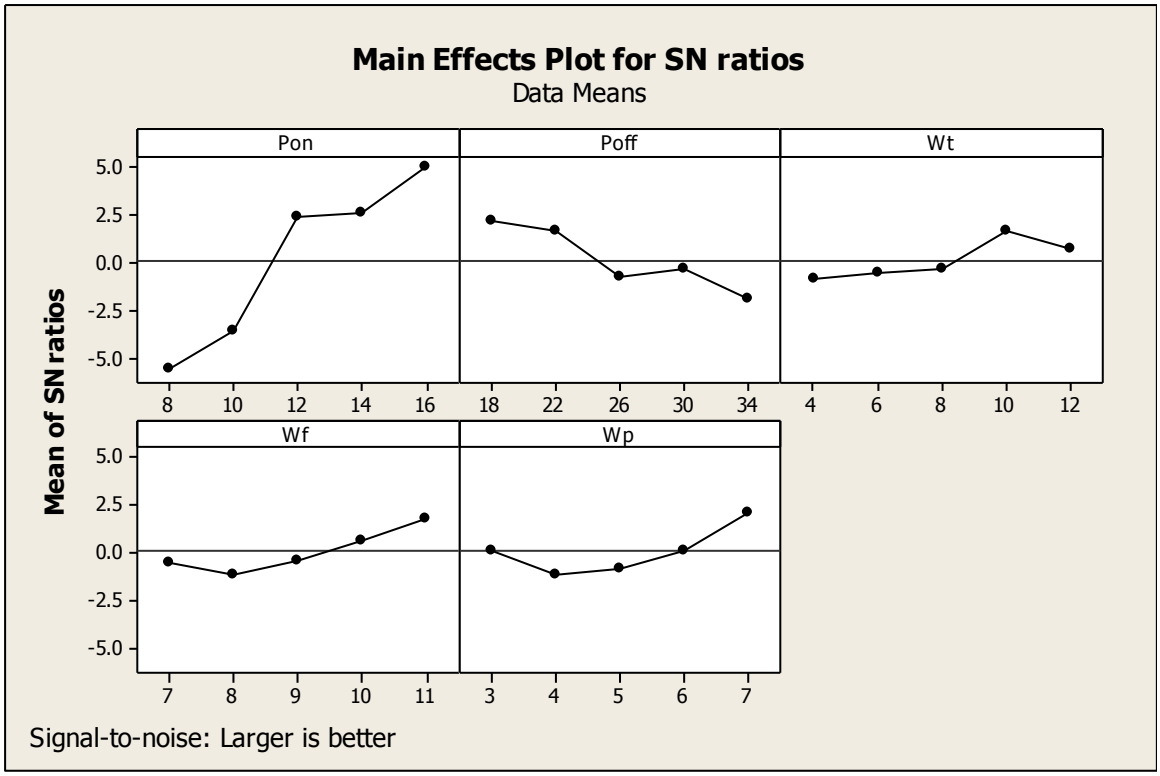

Figure 5.1(b): Effects of Process Parameters on Cutting Speed (S/N Data)

Figure 5.1(a, b): Effects of Process Parameters on Cutting Speed using Electrode E_B

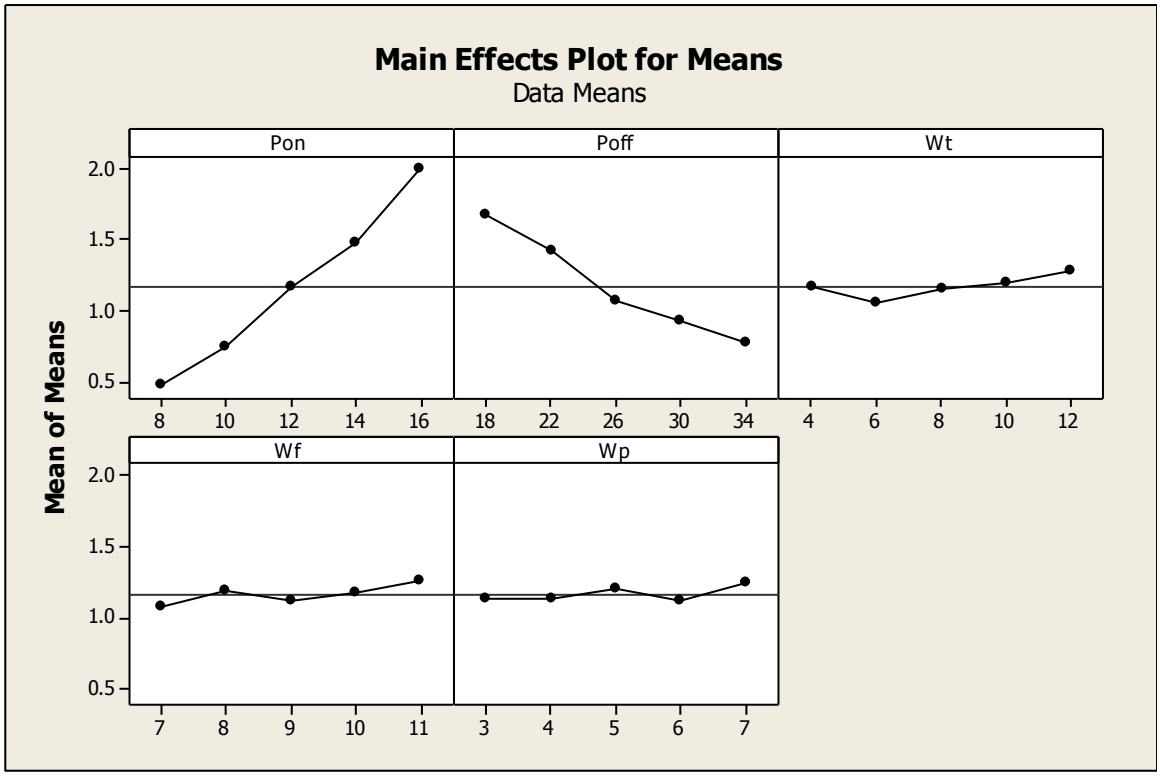

Figure 5.2(a): Effects of Process Parameters on Cutting Speed (Experimental Data)

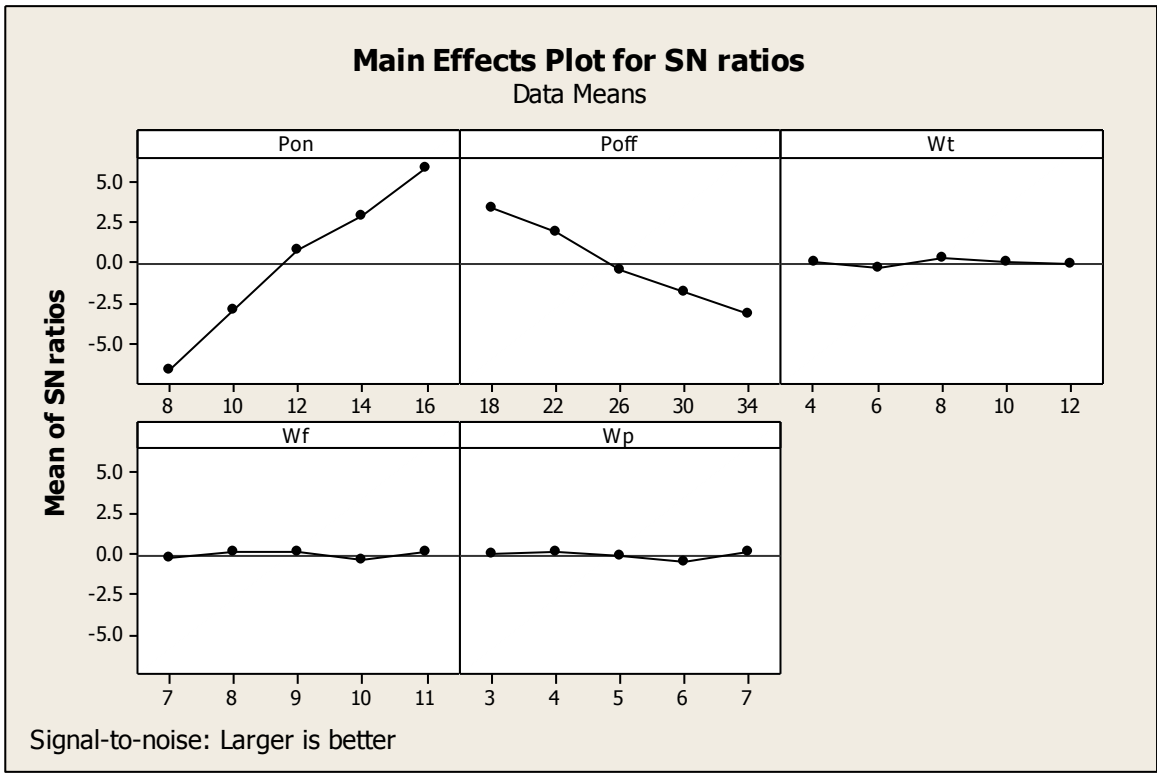

Figure 5.2(b): Effects of Process Parameters on Cutting Speed (S/N Data)

Figure 5.2(a, b): Effects of Process Parameters on Cutting Speed using Electrode E_C

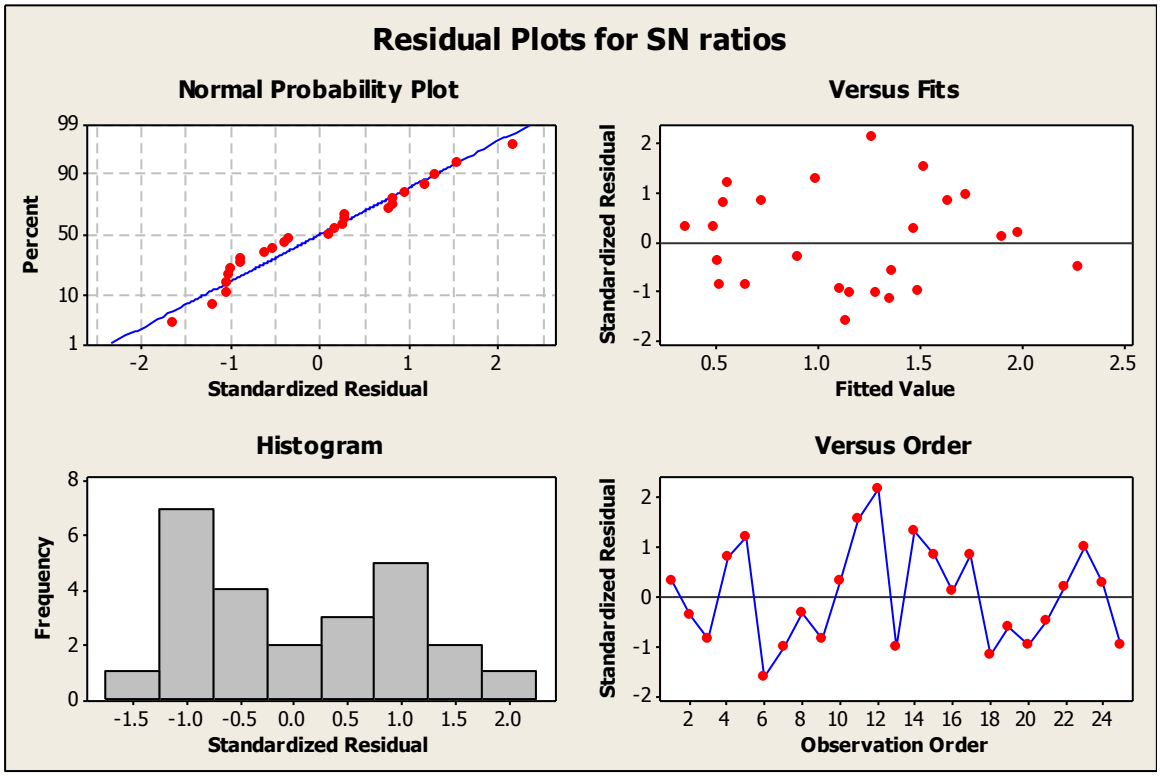

Figure 5.3: Residual Plots for Cutting Speed (S/N Data) using Electrode E_B

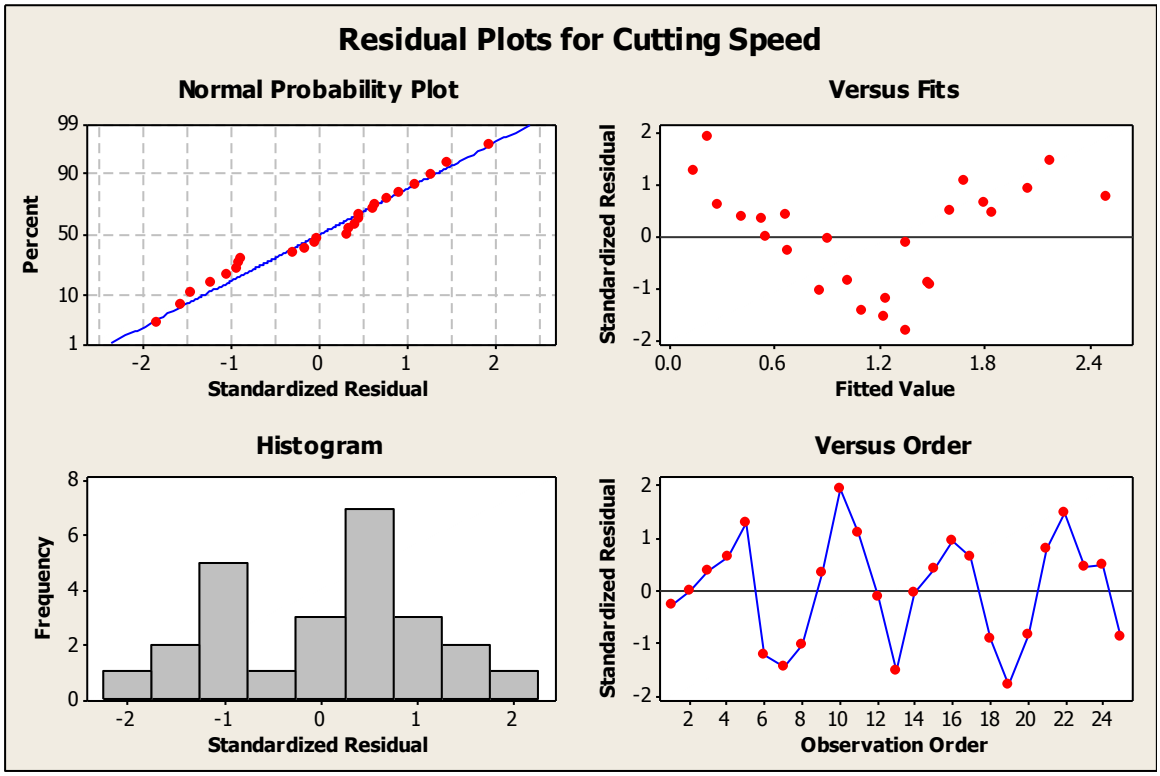

Figure 5.4: Residual Plots for Cutting Speed (S/N Data) using Electrode E_C

Residual plots are used to evaluate the data for the problems like non normality, non random variation, non constant variance, higher-order relationships, and outliers. It can be seen from Figures 5.3 and 5.4 that the residuals follow an approximately straight line in normal probability plot and approximate symmetric nature of histogram indicates that the

residuals are normally distributed. Residuals possess constant variance as they are scattered randomly around zero in residuals versus the fitted values. Since residuals exhibit no clear pattern, there is no error due to time or data collection order.

5.4.1.1 Selection of optimal levels for Cutting Speed using E_B and E_C Electrodes

In order to study the significance of the process parameters towards cutting speed, analysis of variance (ANOVA) was performed. It was found that wire tension and wire feed are least significant on process parameters for cutting speed. Non significant parameters are pooled and the pooled versions of ANOVA of the S/N data and the raw data for cutting speed are given in Tables 5.5(a, b) and 5.7(a, b) respectively. From these tables, it is clear that pulse on time, pulse off time, wire feed, water pressure significantly affect both the mean and the variation in the cutting speed (CS) values. The response tables (Table 5.6 and 5.8) shows the average of each response characteristic (means) for each level of each parameter. The tables include ranks based on delta statistics, which compare the relative magnitude of effects. The delta statistic is the highest minus the lowest average for each parameter. Minitab assigns ranks based on delta values; rank 1 to the highest delta value, rank 2 to the second highest, and so on. The ranks indicate the relative importance of each factor to the response. The ranks and the delta values show that pulse on time have the greatest effect on cutting speed and is followed by pulse off time , wire feed, water pressure in that order. The cutting speed is "higher the better" type quality characteristic, it can be seen from Figure 5.1 that the fifth level of pulse on time (A_5), first level of pulse off time (B_1), fourth level of wire tension (C_4), fifth level of wire feed (D_5) and fifth level of water pressure (E_5) provide maximum value of cutting speed using electrode E_B. Figure 5.2 shows that the fifth level of pulse on time(A_5), first level of pulse off time(B_1), fifth level of wire tension (C_5), fifth level of wire feed (D_5) and fifth level of water pressure (E_5) provide maximum value of cutting speed using electrode E_C .

Table 5.5(a): Analysis of Variance (ANOVA) for Cutting Speed (S/N Data) using E_B

Analysis of Variance for SN ratios						
Source	DF	Seq SS	Adj SS	Adj MS	F	P
Pon	4	403.37	403.37	100.842	25.08	0.004
Poff	4	58.45	58.45	14.613	7.64	0.020
Wt	4	20.78	20.78	5.195	7.29	0.025
Wf	4	26.69	26.69	6.672	7.66	0.018
Wp	4	31.17	31.17	7.791	7.94	0.016
Residual Error	4	16.08	16.08	4.020		
Total	24	556.54				

Table 5.5(b): Analysis of Variance for Cutting Speed (Experimental Data) using E_B

Analysis of Variance for Means					
Source	DF	Seq SS	Adj SS	Adj MS	F	P
Pon	4	5.4070	5.4070	1.35175	20.16	0.006
Poff	4	1.3069	1.3069	0.32673	7.87	0.037
Wt	4	0.2476	0.2476	0.06190	7.92	0.030
Wf	4	0.2306	0.2306	0.05765	7.86	0.039
Wp	4	0.3138	0.3138	0.07844	7.17	0.041
Residual Error	4	0.2683	0.2683	0.06707		
Total	24	7.7741				
DF - degrees of freedom, SS - sum of squares, MS - mean squares(Variance), F-ratio of variance of a source to variance of error, P < 0.05 - determines significance of a parameter at 95% confidence level						

Table 5.6: Response Table for Cutting Speed (Experimental Data) using E_B

Response Table for Means					
Level	Pon	Poff	Wt	Wf	Wp
1	0.5480	**1.4564**	1.0632	1.1094	1.1188
2	0.6916	1.3840	1.0556	1.0688	1.0242
3	1.3500	1.0496	1.1088	1.0962	1.1752
4	1.3984	1.0358	**1.2918**	1.1650	1.1006
5	**1.7882**	0.8504	1.2568	**1.3368**	**1.3574**
Delta	1.2402	0.6060	0.2362	0.2680	0.3332
Rank	1	2	5	4	3

Table 5.7(a): Analysis of Variance (ANOVA) for Cutting Speed (S/N Data) using E_C

Analysis of Variance for SN ratios						
Source	DF	Seq SS	Adj SS	Adj MS	F	P
Pon	4	472.173	472.173	118.043	76.59	0.000
Poff	4	142.564	142.564	35.641	23.12	0.005
Wt	4	0.959	0.959	0.240	13.16	0.008
Wf	4	1.140	1.140	0.285	15.18	0.005
Wp	4	1.032	1.032	0.258	16.17	0.004
Residual Error	4	6.165	6.165	1.541		
Total	24	624.033				
DF - degrees of freedom, SS - sum of squares, MS - mean squares(Variance), F-ratio of variance of a source to variance of error, P < 0.05 - determines significance of a parameter at 95% confidence level						

Table 5.7(b): Analysis of Variance for Cutting Speed (Experimental Data) using E_C

Analysis of Variance for Means					
Source	DF	Seq SS	Adj SS	Adj MS	F	P
Pon	4	7.2071	7.20705	1.80176	15.64	0.010
Poff	4	2.7486	2.74864	0.68716	8.97	0.026
Wt	4	0.1398	0.13980	0.03495	6.30	0.033
Wf	4	0.1072	0.10722	0.02681	7.23	0.027
Wp	4	0.0550	0.05502	0.01375	10.12	0.018
Residual Error	4	0.4608	0.46078	0.11519		
Total	24	10.7185				

DF - degrees of freedom, SS - sum of squares, MS - mean squares(Variance), F-ratio of variance of a source to variance of error, P < 0.05 - determines significance of a parameter at 95% confidence level

Table 5.8: Response Table for Cutting Speed (Experimental Data) using E_C

Response Table for Means					
Level	Pon	Poff	Wt	Wf	Wp
1	0.4750	**1.6704**	1.1628	1.0688	1.1304
2	0.7320	1.4078	1.0456	1.1840	1.1266
3	1.1534	1.0652	1.1496	1.1232	1.2002
4	1.4652	0.9150	1.1820	1.1794	1.1240
5	**1.9942**	0.7614	**1.2386**	**1.2644**	**1.2798**
Delta	1.5192	0.9090	0.2342	0.1956	0.1146
Rank	1	2	5	4	3

5.4.1.2 The Optimal and Predicted Values for SS316 using E_B and E_C Electrodes

In this section, the optimal values of the response characteristics (cutting speed, surface roughness, kerf, dimensional deviation) along with their respective confidence intervals have been predicted. The results of experiments are also presented to validate the optimal results. The optimal levels of the process parameters for the selected response characteristics have already been identified and are reported in the previous section.

The optimal value of each response characteristic is predicted considering the effect of the significant parameters only. However, the average values of quality characteristics obtained from the experiments may or may not lie within 95% confidence interval, CI (calculated for the mean of the population, equation 4.8). The Taguchi approach for predicting the mean of response characteristics and determination of confidence intervals for the predicted means has been presented.

5.4.1.3 Cutting Speed using Electrode E_B

The optimum value of Cutting Speed (CS) is predicted at the optimal levels of significant parameters which have already been selected as pulse on time (A_5), pulse off time (B_1), surface Roughness (C_4), kerf (D_5) and dimensional deviation (E_5). The estimated mean of the response characteristic (CS) can be determined (Kumar, 1993 and Roy, 1990) as

$\eta_{CS} = A_5+B_1+C_4+D_5+E_5 - 4T$

Where,

T = overall mean of cutting rate = $(\sum R_1+ \sum R_2)$ /50 = 1.1552 mm/min

Where, R_1, R_2 values are taken from the Table 5.3 and the values of A_5, B_1, C_4, D_5, and E_5, are taken from the Table 5.6

A_5 = Average value of cutting speed at the fifth level of pulse on time = 1.7882 mm/min

B_1 = Average value of cutting speed at the first level of pulse off time = 1.4564 mm/min

C_4 = Average value of cutting speed at the fourth level of wire tension = 1.2918 mm/min

D_5 = Average value of cutting speed at the fifth level of pulse wire feed = 1.3368 mm/min

E_5 = Average value of cutting speed at the fifth level of water pressure = 1.3574 mm/min

Substituting the values of various terms in the above equation,

$\eta_{CS} = A_5+B_1+C_4+D_5+E_5 - 4T$

$\eta_{CS} = 1.7882+ 1.4564 + 1.2918 + 1.3368 +1.3574 - 4 (1.1552) = 2.325$ mm/min

The 95 % confidence interval of the population (CI) is calculated by using the Equation 4.8 as rewritten below for ready reference:

$$CI_{POP} = \sqrt{\frac{F\alpha\ (1,fe\ )\ Ve}{neff}}$$

$$n_{eff} = \frac{N}{1+[\text{DOF associated in the estimate of mean response }]}$$

N = Total number of results = 25 x 2 = 50

Ve = Error variance = 0.06707 (Table 5.5b)

f_e = error DOF = 4 (Table 5.5b)

$F_{0.05}$ (1, 4) = 3.4115 (Tabulated F value; Roy, 1990)

So, CI_{POP} = ± 0.3100

Therefore, the predicted 95% confidence interval of the population is:

Mean η_{CS}- CI_{POP} < η_{CS} > Mean η_{CS} + CI_{POP}

2.015 < η_{CS} > 2.635

5.4.1.4 Cutting Speed using Electrode E_C

The optimum value of Cutting Speed (CS) is predicted at the optimal levels of significant variables which have already been selected as pulse on time (A_5), pulse off time (B_1), surface Roughness (C_5), kerf (D_5) and dimensional deviation (E_5). The estimated mean of the response characteristic (CS) can be determined (Kumar, 1993 and Roy, 1990) as

$\eta_{CS} = A_5+B_1+C_5+D_5+E_5 – 4T$

Where,

T = overall mean of cutting rate = 1.1834 mm/min

Where, R_1, R_2 values are taken from the Table 5.4 and the values of A_5, B_1, C_5, D_5, and E_5, are taken from the Table 5.8

A_5 = Average value of cutting speed at the fifth level of pulse on time = 1.9942 mm/min

B_1 = Average value of cutting speed at the first level of pulse off time = 1.6704 mm/min

C_5 = Average value of cutting speed at the fifth level of wire tension = 1.2386 mm/min

D_5 = Average value of cutting speed at the fifth level of wire feed = 1.2644 mm/min

E_5 = Average value of cutting speed at the fifth level of water pressure = 1.2798 mm/min

Substituting the values of various terms in the above equation,

$\eta_{CS} = A_5+B_1+C_5+D_5+E_5 – 4T$

$\eta_{CS} = 1.9942 + 1.6704 + 1.2386 + 1.2644 +1.2798 – 4\ (1.1834) = 2.786$ mm/min

The 95 % confidence interval of the population (CI) is calculated by using the Equations 4.8 as rewritten below for ready reference:

$$CI_{POP} = \sqrt{\frac{F\alpha\ (1,fe\ )\ Ve}{neff}}$$

$$n_{eff} = \frac{N}{1+[\text{DOF associated in the estimate of mean response }]}$$

N = Total number of results = 25 x 2 = 50

Ve = Error variance = 0.11519 (Table 5.7b)

f_e = error DOF = 4 (Table 5.7b)

$F_{0.05}$ (1, 4) = 5.5675 (Tabulated F value; Roy, 1990)

So, $CI_{POP} = \pm 0.5190$

Therefore, the predicted 95% confidence interval of the population is:

Mean η_{CS}- $CI_{POP} < \eta_{CS} >$ Mean $\eta_{CS} + CI_{POP}$

$2.267 < \eta_{CS} > 3.305$

5.4.2 Effect of Process Parameters on Surface Roughness (SR)

The variation of average surface roughness is plotted for all the input parameters such as Pon, Poff, Wt, Wf and Wp for both experimental data and S/N data using E_B and E_C electrodes respectively.

Table 5.9: Surface Roughness Results for SS316 using Electrode (E_B)

S.No	A	B	C	D	E	SR		S/N Ratio
						R1	R2	
1	1	1	1	1	1	2.60	2.61	-8.2995
2	1	2	2	2	2	2.54	2.66	-8.0967
3	1	3	3	3	3	2.40	2.51	-7.6042
4	1	4	4	4	4	2.28	2.29	-7.1587
5	1	5	5	5	5	2.24	2.36	-7.0050
6	2	1	2	3	4	2.65	2.66	-8.4649
7	2	2	3	4	5	2.54	2.55	-8.0967
8	2	3	4	5	1	2.35	2.47	-7.4214
9	2	4	5	1	2	2.32	2.43	-7.3098
10	2	5	1	2	3	2.69	2.72	-8.5950
11	3	1	3	5	2	2.60	2.72	-8.2995
12	3	2	4	1	3	2.52	2.53	-8.0280
13	3	3	5	2	4	2.35	2.36	-7.4214
14	3	4	1	3	5	2.32	2.44	-7.3098
15	3	5	2	4	1	2.30	2.41	-7.2346
16	4	1	4	2	5	2.76	2.77	-8.8182
17	4	2	5	3	1	2.75	2.87	-8.7867
18	4	3	1	4	2	2.48	2.49	-7.8890
19	4	4	2	5	3	2.43	2.44	-7.7121
20	4	5	3	1	4	2.33	2.45	-7.3471
21	5	1	5	4	3	2.89	2.86	-9.2180
22	5	2	1	5	4	2.76	2.77	-8.8182
23	5	3	2	1	5	2.65	2.77	-8.4649
24	5	4	3	2	1	2.40	2.41	-7.6042
25	5	5	4	3	2	2.35	2.36	-7.4214

Table 5.10: Surface Roughness Results for SS316 using Electrode (E_C)

S.No	A	B	C	D	E	SR		S/N Ratio
						R1	R2	
1	1	1	1	1	1	2.92	2.93	-9.3077
2	1	2	2	2	2	2.72	2.84	-8.6914
3	1	3	3	3	3	2.64	2.75	-8.4321
4	1	4	4	4	4	2.65	2.66	-8.4649
5	1	5	5	5	5	2.28	2.32	-7.1587
6	2	1	2	3	4	2.16	2.17	-6.6891
7	2	2	3	4	5	2.95	2.96	-9.3964
8	2	3	4	5	1	2.86	2.98	-9.1273
9	2	4	5	1	2	2.82	2.93	-9.0050
10	2	5	1	2	3	2.85	2.86	-9.0969
11	3	1	3	5	2	2.84	2.96	-9.0664
12	3	2	4	1	3	2.72	2.73	-8.6914
13	3	3	5	2	4	2.66	2.67	-8.4976
14	3	4	1	3	5	2.28	2.36	-7.1587
15	3	5	2	4	1	2.17	2.28	-6.7292
16	4	1	4	2	5	3.06	3.07	-9.7144
17	4	2	5	3	1	2.97	3.09	-9.4551
18	4	3	1	4	2	2.84	2.85	-9.0664
19	4	4	2	5	3	2.74	2.75	-8.7550
20	4	5	3	1	4	2.45	2.57	-7.7833
21	5	1	5	4	3	3.22	3.33	-10.1571
22	5	2	1	5	4	2.94	2.95	-9.3669
23	5	3	2	1	5	2.85	2.97	-9.0969
24	5	4	3	2	1	2.72	2.73	-8.6914
25	5	5	4	3	2	2.06	2.07	-6.2773

It is seen from the Figures 5.5(a, b) and 5.6(a, b) that the Surface Roughness (SR) increases with the increase of pulse on time, wire feed and water pressure, decreases with increase in pulse off time. The discharge energy increases with the pulse on time and wire feed and larger discharge energy produces a larger crater, causing a larger surface roughness value on the work piece. As the pulse off time decreases, the number of discharges increases which causes poor surface roughness. With decrease in wire feed the average discharge gap gets widened resulting into better surface accuracy due to stable machining .The effects of wire tension are not very significant. It is noticed from Figures 5.5 and 5.6 that there is a least interaction between pulse off time and wire tension while there is very weak interaction

between all the other process parameters in affecting the surface roughness since the responses at different levels of process parameters for a given level of parameter value are almost parallel. Residual plots do not show any problem in the distribution of the data and model assumptions (Figure 5.7 and 5.8).

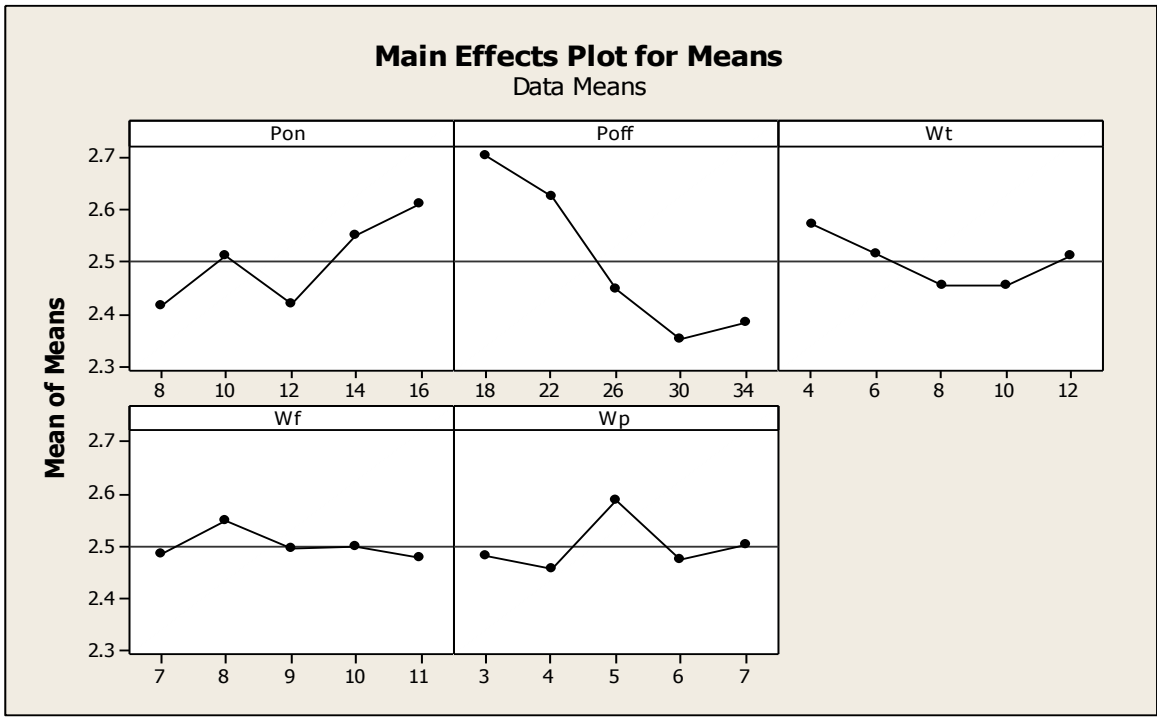

Figure 5.5(a): Effects of Process Parameters on Surface Roughness (Experimental Data)

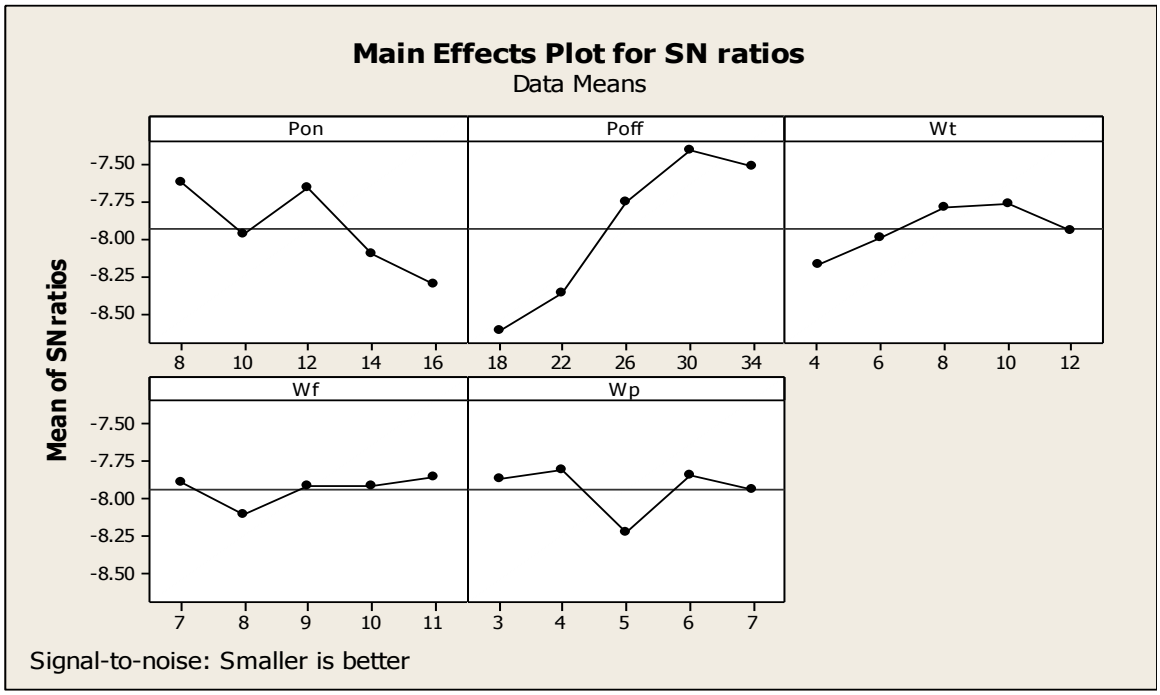

Figure 5.5(b): Effects of Process Parameters on Surface Roughness (S/N Data)

Figure 5.5(a, b): Effects of Process Parameters on Surface Roughness using Electrode E_B

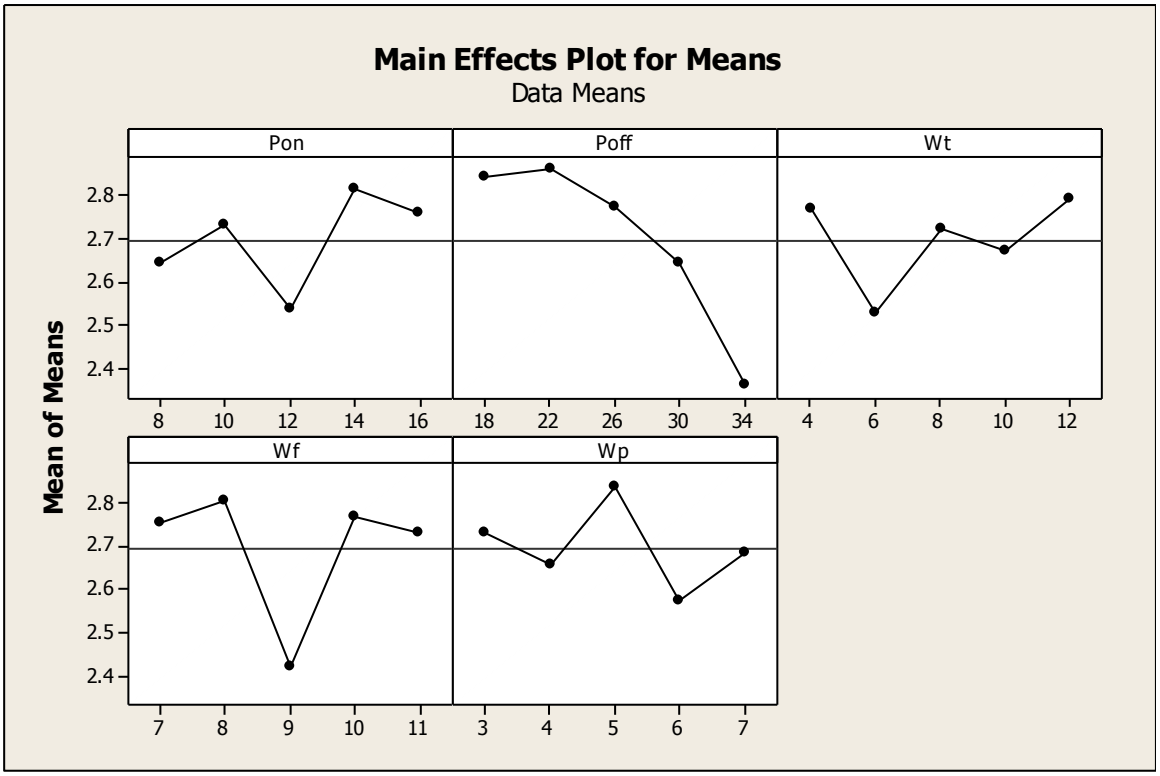

Figure 5.6(a): Effects of Process Parameters on Surface Roughness (Experimental Data)

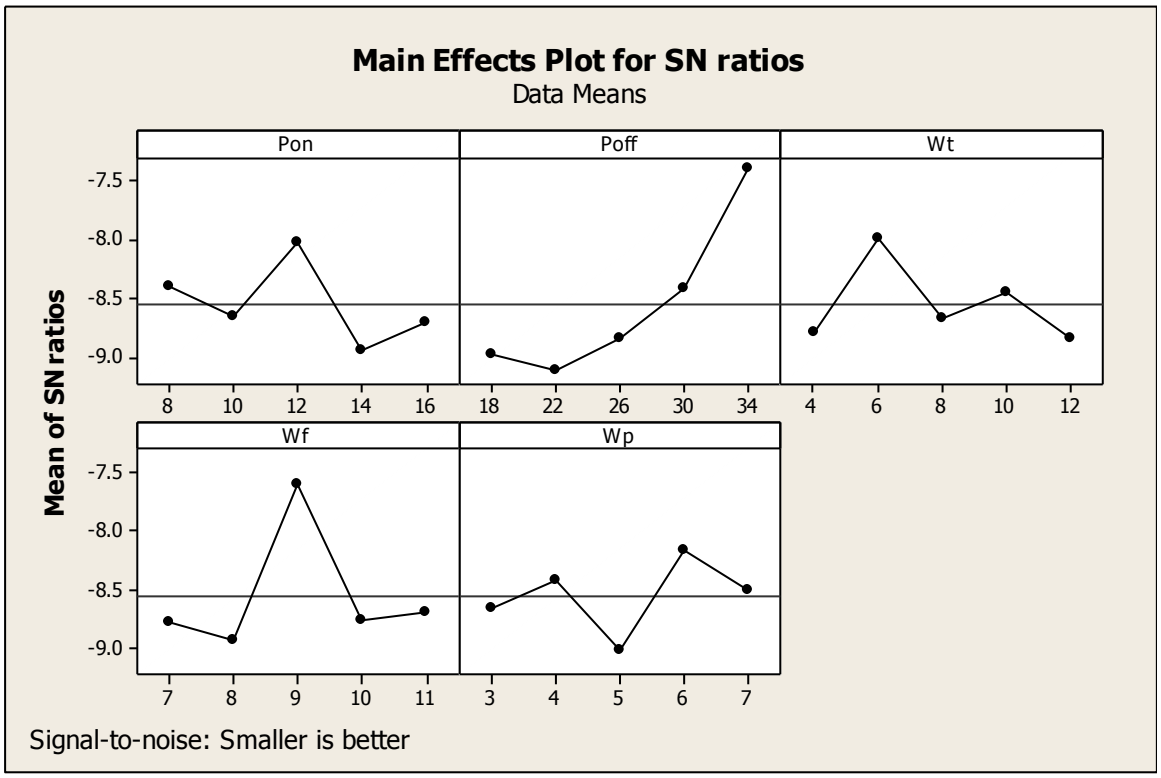

Figure 5.6(b): Effects of Process Parameters on Surface Roughness (S/N Data)

Figure 5.6(a,b): Effects of Process Parameters on Surface Roughness using Electrode E_C

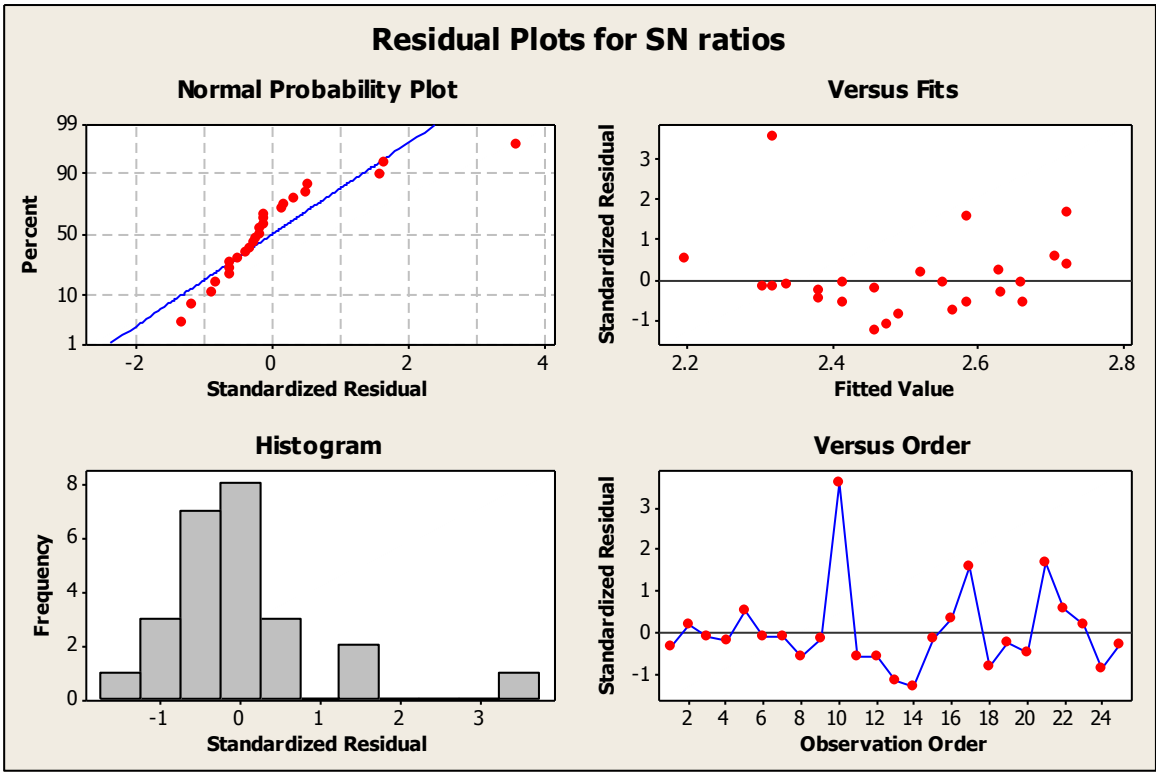

Figure 5.7: Residual Plots for Surface Roughness (S/N Data) using Electrode E_B

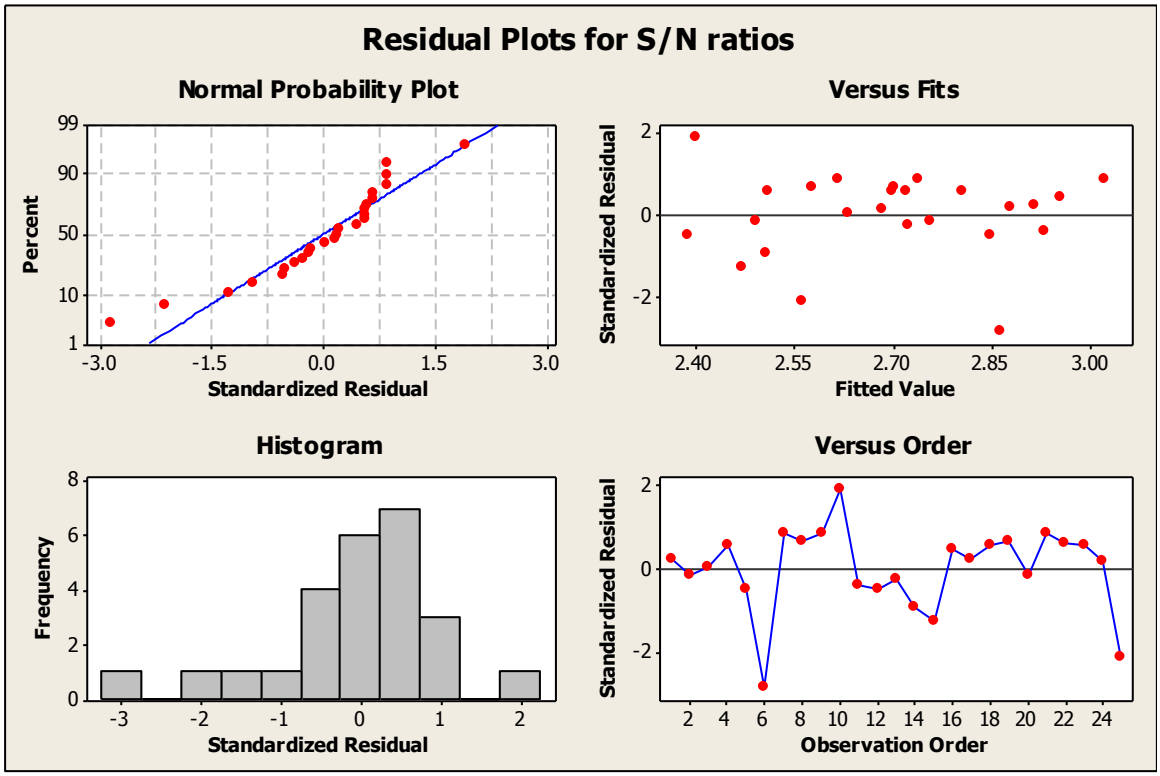

Figure 5.8: Residual Plots for Surface Roughness (S/N Data) using Electrode E_C

Residual plots are used to evaluate the data for the problems like non normality, non random variation, non constant variance, higher-order relationships, and outliers. It can be seen from Figure 5.7 and 5.8 that the residuals follow an approximately straight line in normal

probability plot and approximate symmetric nature of histogram indicates that the residuals are normally distributed.

5. 4.2.1 Selection of optimal levels for Surface Roughness using E_B and E_C Electrodes

In order to study the significance of the process variables towards surface roughness, analysis of variance (ANOVA) was performed. It was found that wire tension is significant process parameter for Surface Roughness. From these tables, it is clear that pulse on time, pulse off time, wire feed, water pressure significantly affect both the mean and the variation in the surface roughness values. The response tables (Tables 5.12 and 14) shows the average of each response characteristic (means) for each level of each parameter. The tables include ranks based on delta statistics, which compare the relative magnitude of effects. The delta statistic is the highest minus the lowest average for each factor. Minitab assigns ranks based on delta values; rank 1 to the highest delta value, rank 2 to the second highest, and so on. The ranks indicate the relative importance of each factor to the response. The ranks and the delta values show that pulse on time have the greatest effect on surface roughness and is followed by pulse off time , wire feed, water pressure in that order. As surface roughness is the "lower the better" type quality characteristic, Figure 5.5 shows that the second level of pulse on time(A_2), first level of pulse off time(B_1), fourth level of wire tension (C_4), fifth level of wire feed (D_5) and third level of water pressure (E_3) provide minimum value of surface roughness using electrode E_B. The S/N data analysis also suggests the same levels of the variables as the best levels for minimum surface roughness in Wire EDM process. Figure 5.6 shows that the second level of pulse on time(A_2), first level of pulse off time(B_1), fourth level of wire tension (C_4), fifth level of wire feed (D_5) and fifth level of water pressure (E_5) provide minimum value of surface roughness using electrode E_C.

Table 5.11(a): Analysis of Variance for Surface Roughness (S/N Data) using E_B

Analysis of Variance for SN ratios						
Source	DF	Seq SS	Adj SS	Adj MS	F	P
Pon	4	1.6874	1.6874	0.42185	8.26	0.025
Poff	4	5.6147	5.6147	1.40367	7.51	0.038
Wt	4	0.5659	0.5659	0.14147	8.76	0.013
Wf	4	0.1960	0.1960	0.04901	8.26	0.049
Wp	4	0.5910	0.5910	0.14776	8.79	0.047
Residual Error	4	0.7478	0.7478	0.18696		
Total	24	9.4029				

DF - degrees of freedom, SS - sum of squares, MS - mean squares(Variance), F-ratio of variance of a source to variance of error, P < 0.05 - determines significance of a parameter at 95% confidence level

Table 5.11(b): Analysis of Variance for Surface Roughness (Exp. Data) using E_B

Analysis of Variance for Means					
Source	DF	Seq SS	Adj SS	Adj MS	F	P
Pon	4	0.14584	0.14584	0.036460	8.25	0.026
Poff	4	0.47112	0.47112	0.117780	7.26	0.040
Wt	4	0.04808	0.04808	0.012020	8.74	0.011
Wf	4	0.01588	0.01588	0.003970	8.24	0.049
Wp	4	0.05120	0.05120	0.012800	8.79	0.048
Residual Error	4	0.06488	0.06488	0.016220		
Total	24	0.79700				
DF - degrees of freedom, SS - sum of squares, MS - mean squares(Variance), F-ratio of variance of a source to variance of error, P < 0.05 - determines significance of a parameter at 95% confidence level						

Table 5.12: Response Table for Surface Roughness (Exp. Data) using Electrode E_B

Response Table for Means					
Level	Pon	Poff	Wt	Wf	Wp
1	2.412	**2.700**	2.452	2.454	2.480
2	**2.510**	2.622	2.514	2.376	2.458
3	2.418	2.446	2.454	2.464	**2.586**
4	2.520	2.350	**2.510**	2.498	2.474
5	2.510	2.382	2.410	**2.476**	2.502
Delta	0.198	0.350	0.118	0.072	0.128
Rank	2	1	4	5	3

Table 5.13(a): Analysis of Variance for Surface Roughness (S/N Data) using E_C

Analysis of Variance for SN ratios						
Source	DF	Seq SS	Adj SS	Adj MS	F	P
Pon	4	2.479	2.479	0.6198	0.99	0.502
Poff	4	9.612	9.612	2.4029	3.86	0.110
Wt	4	2.451	2.451	0.6128	0.98	0.506
Wf	4	5.831	5.831	1.4578	2.34	0.215
Wp	4	2.049	2.049	0.5124	0.82	0.573
Residual Error	4	2.492	2.492	0.6231		
Total	24	24.915				
DF - degrees of freedom, SS - sum of squares, MS - mean squares(Variance), F-ratio of variance of a source to variance of error, P < 0.05 - determines significance of a parameter at 95% confidence level						

Table 5.13(b): Analysis of Variance for Surface Roughness (Exp. Data) using E_C

Analysis of Variance for Means					
Source	DF	Seq SS	Adj SS	Adj MS	F	P
Pon	4	0.2374	0.2374	0.05935	1.09	0.000
Poff	4	0.8379	0.8379	0.20947	3.85	0.000
Wt	4	0.2160	0.2160	0.05401	0.99	0.001
Wf	4	0.4782	0.4782	0.11955	2.20	0.000
Wp	4	0.1859	0.1859	0.04648	0.85	0.002
Residual Error	4	0.2175	0.2175	0.05437		
Total	24	2.1728				

DF - degrees of freedom, SS - sum of squares, MS - mean squares(Variance), F-ratio of variance of a source to variance of error, P < 0.05 - determines significance of a parameter at 95% confidence level

Table 5.14: Response Table for Surface Roughness (Exp. Data) using Electrode E_C

Response Table for Means					
Level	Pon	Poff	Wt	Wf	Wp
1	2.642	**2.840**	2.766	2.752	2.528
2	**2.812**	2.820	2.528	2.732	2.656
3	2.534	2.770	2.720	2.422	2.634
4	2.728	2.642	**2.790**	2.702	2.572
5	2.758	2.362	2.670	**2.802**	**2.834**
Delta	0.278	0.498	0.262	0.380	0.262
Rank	2	1	5	4	3

5.4.2.2 Surface Roughness (SR) using Electrode E_B

The optimum value of Surface Roughness (SR) is predicted at the optimal levels of significant variables which have already been selected as pulse on time (A_2), pulse off time (B_1), surface Roughness (C_4), kerf (D_5) and dimensional deviation (E_3). The estimated mean of the response characteristic (SR) can be determined (Kumar, 1993 and Roy, 1990) as

$\eta_{SR} = A_2+B_1+C_4+D_5+E_3 - 4T$

Where,

T = overall mean of cutting rate = $(\sum R_1+ \sum R_2)/50$ = 2.0642 μm

Where, R_1, R_2 values are taken from the Table 5.9 and the values of A_2, B_1, C_4, D_5, and E_3, are taken from the Table 5.12

A_2 = Average value of cutting speed at the second level of pulse on time = 2.510 μm

B_1 = Average value of cutting speed at the first level of pulse off time = 2.700 μm

C_4 = Average value of cutting speed at the fourth level of wire tension = 2.510 μm

D_5 = Average value of cutting speed at the fifth level of wire feed = 2.476 μm

E_3 = Average value of cutting speed at the third level of water pressure = 2.586 μm

Substituting the values of various terms in the above equation,

$\eta_{SR} = A_2+B_1+C_4+D_5+E_3 - 4T$

$\eta_{SR} = 2.32$ μm

The 95 % confidence interval of the population (CI) is calculated by using the Equation 4.8 as rewritten below for ready reference:

$$CI_{POP} = \sqrt{\frac{F\alpha\,(1,fe)\,Ve}{neff}}$$

$$n_{eff} = \frac{N}{1+[\text{DOF associated in the estimate of mean response}]}$$

N = Total number of results = 25 x 2 = 50

Ve = Error variance = 0.01622 (Table 5.11b)

f_e = error DOF = 4 (Table 5.11b)

$F_{0.05}$ (1, 4) = 3.1060 (Tabulated F value; Roy, 1990)

So, $CI_{POP} = \pm 0.460$

Therefore, the predicted 95% confidence interval of the population is:

Mean η_{SR}- CI_{POP} < η_{SR} >Mean η_{SR} + CI_{POP}

1.86< η_{SR} >2.78

5.4.2.3 Surface Roughness (SR) using Electrode E_C

The optimum value of Surface Roughness (SR) is predicted at the optimal levels of significant variables which have already been selected as pulse on time (A_2), pulse off time (B_1), surface Roughness (C_4), kerf (D_5) and dimensional deviation (E_5). The estimated mean of the response characteristic (SR) can be determined (Kumar, 1993 and Roy, 1990) as

$\eta_{SR} = A_2+B_1+C_4+D_5+E_5 - 4T$

Where,

T = overall mean of cutting rate = $(\sum R_1+ \sum R_2)/50$ = 2.0126 μm

Where, R_1, R_2 values are taken from the Table 5.10 and the values of A_2, B_1, C_4, D_5, and E_5, are taken from the Table 5.14

A_2 = Average value of cutting speed at the second level of pulse on time = 2.812 μm

B_1 = Average value of cutting speed at the first level of pulse off time = 2.840 μm

C_4 = Average value of cutting speed at the fourth level of wire tension = 2.790 μm

D_5 = Average value of cutting speed at the fifth level of wire feed = 2.802 μm

E_5 = Average value of cutting speed at the fifth level of water pressure = 2.834 μm

Substituting the values of various terms in the above equation,

$\eta_{SR} = A_2+B_1+C_4+D_5+E_5 - 4T$

$\eta_{SR} = 2.540$ μm

The 95 % confidence interval of the population (CI) is calculated by using the Equation 4.8 as rewritten below for ready reference:

$$CI_{POP} = \sqrt{\frac{F\alpha\,(1,fe)\,Ve}{neff}}$$

$$n_{eff} = \frac{N}{1+[\text{DOF associated in the estimate of mean response}]}$$

N = Total number of results = 25 x 2 = 50

Ve = Error variance = 0.05437 (Table 5.13b)

f_e = error DOF = 4 (Table 5.13b)

$F_{0.05}$ (1, 4) = 3.5720 (Tabulated F value; Roy, 1990)

So, $CI_{POP} = \pm 0.680$

Therefore, the predicted 95% confidence interval of the population is:

Mean η_{SR}- CI_{POP} < η_{SR} >Mean η_{SR} + CI_{POP}

1.86< η_{SR} >3.22

5.4.3 Effect of Process Parameters on KERF (cutting width)

The average values of KERF (cutting width) for each of input (Pon, Poff, Wt, Wf and Wp) parameters at level 1 and 2 for experimental data and S/N data are plotted using E_B and E_C electrodes.

Figures 5.9(a, b) and 5.10(a, b) shows that the KERF (cutting width) increases with the increase of pulse on time, wire feed and water pressure, decreases with increase in pulse

off time and wire tension. The discharge energy increases with the pulse on time and wire feed and larger discharge energy produces a larger crater, causing a larger cutting width value on the work piece. As the pulse off time decreases, the number of discharges increases which causes poor surface accuracy. With increase in wire feed the average discharge gap gets widened resulting into more Cutting width. The effects of wire tension are also very significant.

Table 5.15: KERF Results for SS316 using Electrode E_B

S.No	A	B	C	D	E	KERF		S/N Ratio
						R1	R2	
1	1	1	1	1	1	0.465	0.476	6.65094
2	1	2	2	2	2	0.456	0.467	6.82070
3	1	3	3	3	3	0.442	0.453	7.09155
4	1	4	4	4	4	0.426	0.437	7.41181
5	1	5	5	5	5	0.354	0.365	9.01993
6	2	1	2	3	4	0.438	0.450	7.17052
7	2	2	3	4	5	0.418	0.430	7.57647
8	2	3	4	5	1	0.393	0.405	8.11215
9	2	4	5	1	2	0.432	0.444	7.29033
10	2	5	1	2	3	0.426	0.438	7.41181
11	3	1	3	5	2	0.515	0.527	5.76386
12	3	2	4	1	3	0.532	0.544	5.48177
13	3	3	5	2	4	0.505	0.516	5.93417
14	3	4	1	3	5	0.479	0.490	6.39329
15	3	5	2	4	1	0.499	0.510	6.03799
16	4	1	4	2	5	0.465	0.476	6.65094
17	4	2	5	3	1	0.467	0.478	6.61366
18	4	3	1	4	2	0.489	0.512	6.21382
19	4	4	2	5	3	0.481	0.492	6.35710
20	4	5	3	1	4	0.538	0.549	5.38435
21	5	1	5	4	3	0.570	0.582	4.88250
22	5	2	1	5	4	0.484	0.496	6.30309
23	5	3	2	1	5	0.468	0.484	6.59508
24	5	4	3	2	1	0.480	0.492	6.37518
25	5	5	4	3	2	0.378	0.390	8.45016

Table 5.16: KERF Results for SS316 using Electrode E_C

S.No	A	B	C	D	E	KERF		S/N Ratio
						R1	R2	
1	1	1	1	1	1	0.438	0.449	7.17052
2	1	2	2	2	2	0.446	0.457	7.01330
3	1	3	3	3	3	0.412	0.423	7.70206
4	1	4	4	4	4	0.396	0.407	8.04610
5	1	5	5	5	5	0.362	0.373	8.82583
6	2	1	2	3	4	0.438	0.423	7.17052
7	2	2	3	4	5	0.458	0.472	6.78269
8	2	3	4	5	1	0.433	0.445	7.27024
9	2	4	5	1	2	0.432	0.444	7.29033
10	2	5	1	2	3	0.426	0.438	7.41181
11	3	1	3	5	2	0.485	0.497	6.28517
12	3	2	4	1	3	0.462	0.474	6.70716
13	3	3	5	2	4	0.465	0.476	6.65094
14	3	4	1	3	5	0.452	0.463	6.89723
15	3	5	2	4	1	0.434	0.445	7.25021
16	4	1	4	2	5	0.485	0.496	6.28517
17	4	2	5	3	1	0.452	0.463	6.89723
18	4	3	1	4	2	0.436	0.447	7.21027
19	4	4	2	5	3	0.434	0.445	7.25021
20	4	5	3	1	4	0.428	0.439	7.37112
21	5	1	5	4	3	0.530	0.542	5.51448
22	5	2	1	5	4	0.484	0.496	6.30309
23	5	3	2	1	5	0.458	0.475	6.78269
24	5	4	3	2	1	0.420	0.432	7.53501
25	5	5	4	3	2	0.358	0.372	8.92234

The residual plots (Figures 5.11 and 5.12) are drawn for estimating the accuracy of the model. The histogram plot indicates a mild tendency for the non normality; however the normal probability plots of these residuals do not reveal any abnormality. Residual versus fitted value and residual versus observation order plot do not indicate any undesirable effect.

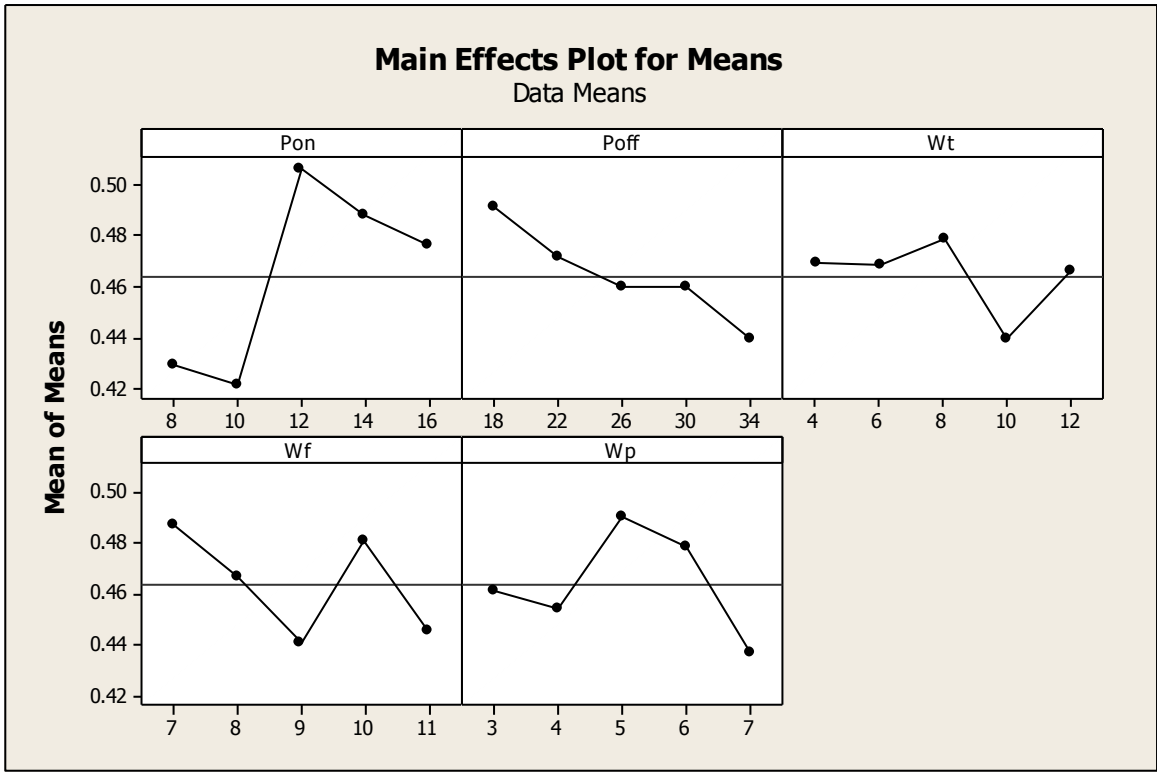

Figure 5.9(a): Effects of Process Parameters on KERF (Experimental Data)

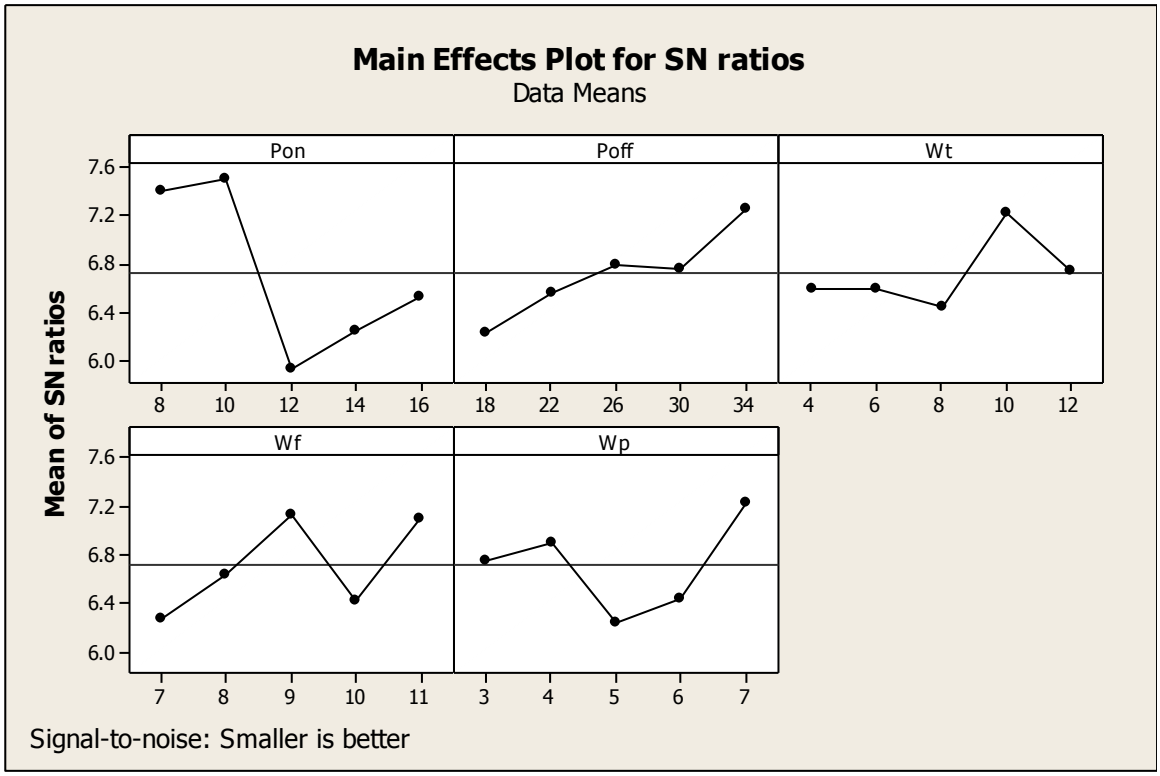

Figure 5.9(b): Effects of Process Parameters on KERF (S/N Data)

Figure 5.9(a,b): Effects of Process Parameters on KERF using Electrode E_B

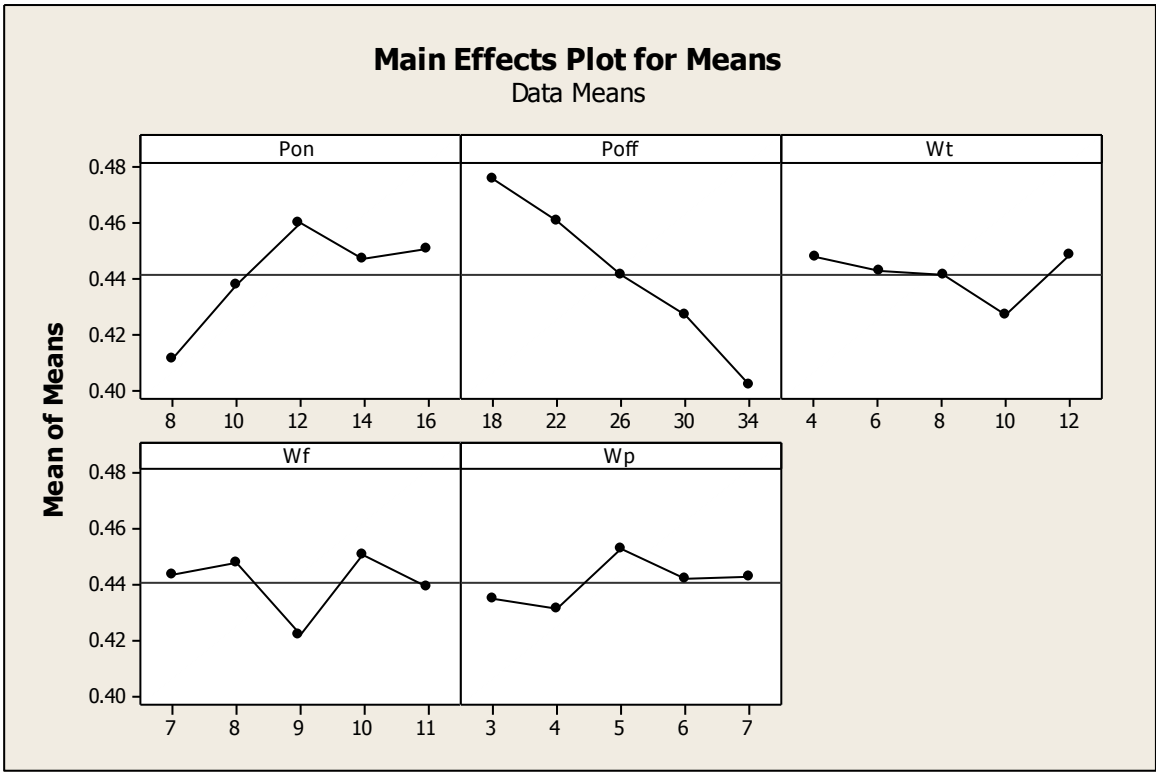

Figure 5.10(a): Effects of Process Parameters on KERF (Experimental Data)

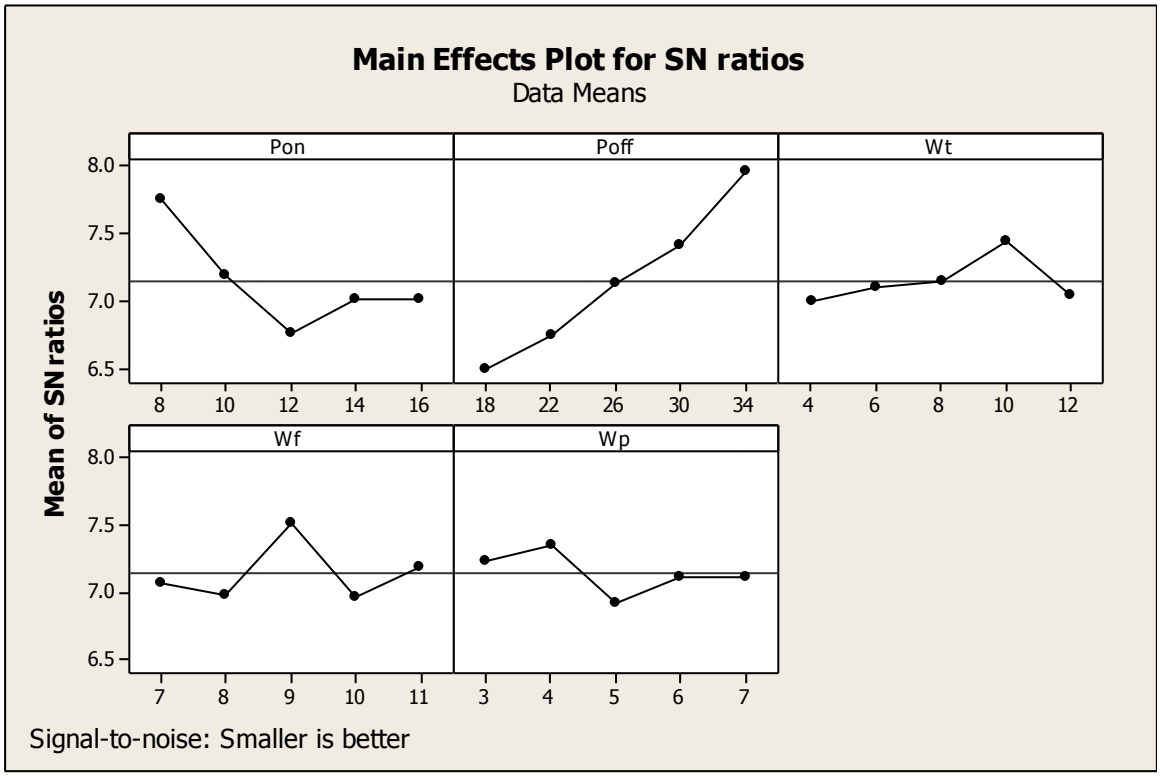

Figure 5.10(b): Effects of Process Parameters on KERF (S/N Data)

Figure 5.10(a, b): Effects of Process Parameters on KERF using Electrode E_C

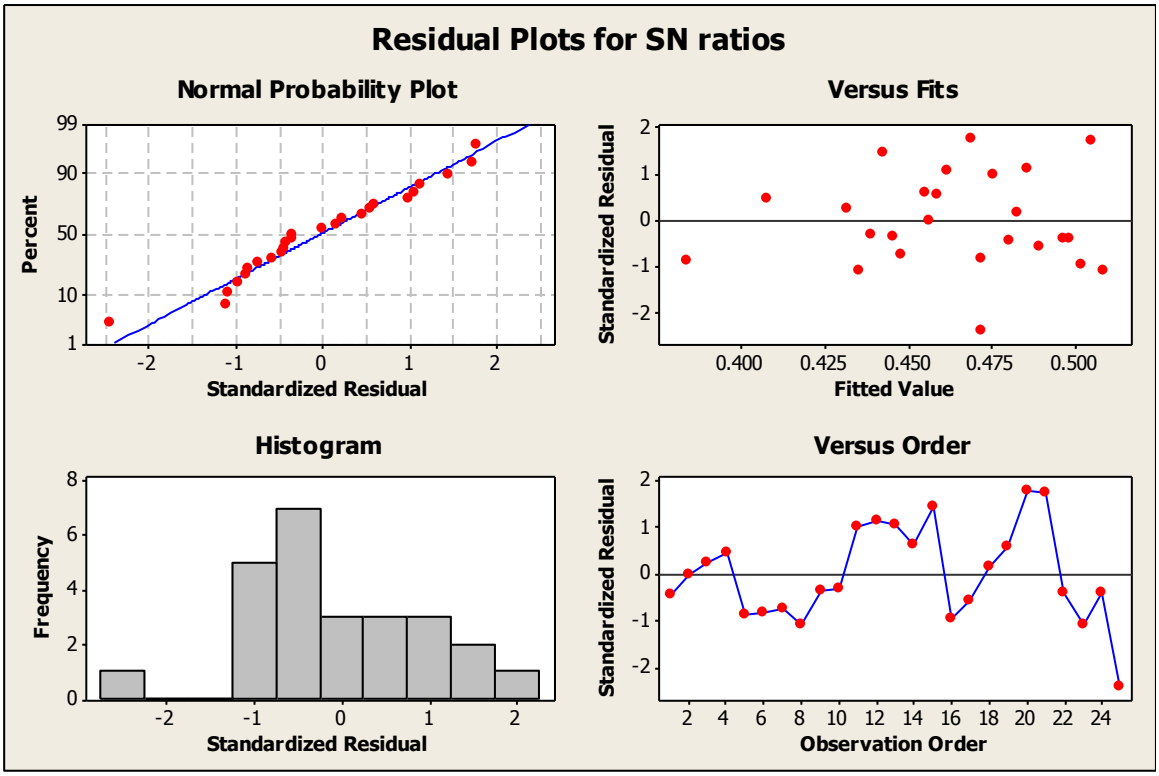

Figure 5.11: Residual Plots for KERF (S/N Data) using Electrode E_B

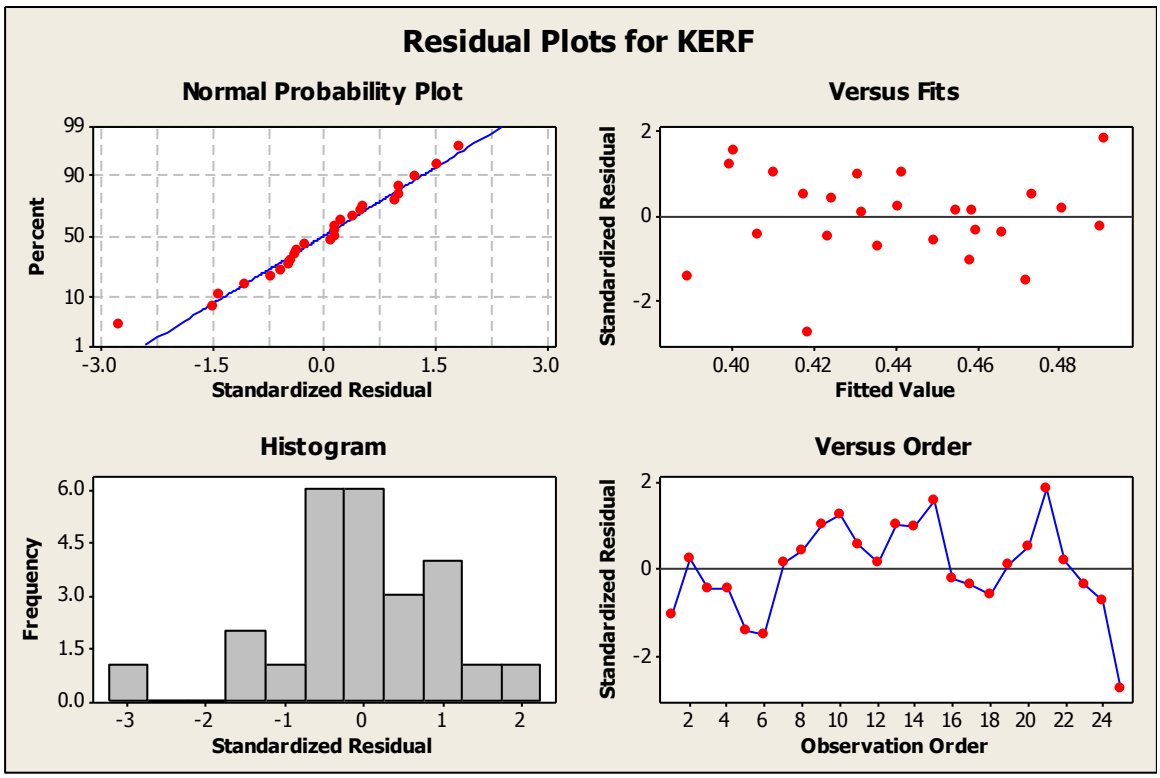

Figure 5.12: Residual Plots for KERF (S/N Data) using Electrode E_C

5.4.3.1 Selection of optimal levels for KERF

In order to study the significance of the process variables towards KERF (cutting width), analysis of variance (ANOVA) was performed. It was found that wire tension is a significant process parameter for KERF (cutting width). From these tables, it is clear that pulse on time, pulse off time, wire feed, water pressure significantly affect both the mean and the variation in the KERF (cutting width) values. The response table (Table 5.18 and 5.20) shows the average of each response characteristic (means) for each level of each parameter. The tables include ranks based on delta statistics, which compare the relative magnitude of effects. The delta statistic is the highest minus the lowest average for each factor. Minitab assigns ranks based on delta values; rank 1 to the highest delta value, rank 2 to the second highest, and so on. The ranks indicate the relative importance of each parameter to the response. The ranks and the delta values show that pulse on time have the greatest effect on KERF (cutting width)and is followed by pulse off time , wire feed, water pressure in that order. As KERF (cutting width) is the "lower the better" type quality characteristic, it can be seen from Figure 5.9(a, b) that the third level of pulse on time (A_3), first level of pulse off time (B_1), third level of wire tension (C_3), first level of wire feed (D_1) and third level of water pressure (E_3) provide minimum value of KERF (cutting width) using electrode E_B. Figure 5.10(a, b) shows that the third level of pulse on time(A_3), first level of pulse off time(B_1), fifth level of wire tension (C_5), fourth level of wire feed (D_4) and third level of water pressure (E_3) provide minimum value of KERF (cutting width) using electrode E_C.

Table 5.17(a): Analysis of Variance (ANOVA) for KERF (S/N Data) using Electrode E_B

Analysis of Variance for SN ratios						
Source	DF	Seq SS	Adj SS	Adj MS	F	P
Pon	4	9.956	9.956	2.4891	12.74	0.000
Poff	4	2.858	2.858	0.7144	7.22	0.029
Wt	4	1.813	1.813	0.4532	5.41	0.044
Wf	4	3.099	3.099	0.7748	8.41	0.008
Wp	4	3.091	3.091	0.7728	9.40	0.008
Residual Error	4	1.286	1.286	0.3214		
Total	24	22.103				

DF - degrees of freedom, SS - sum of squares, MS - mean squares(Variance), F-ratio of variance of a source to variance of error, $P < 0.05$ - determines significance of a parameter at 95% confidence level

Table 5.17(b): Analysis of Variance for KERF (Experimental Data) using Electrode E_B

Analysis of Variance for Means						
Source	DF	Seq SS	Adj SS	Adj MS	F	P
Pon	4	0.027760	0.027760	0.006940	15.00	0.003
Poff	4	0.007139	0.007139	0.001785	12.80	0.019
Wt	4	0.004456	0.004456	0.001114	7.12	0.047
Wf	4	0.008440	0.008440	0.002110	8.13	0.021
Wp	4	0.008691	0.008691	0.002173	9.19	0.013
Residual Error	4	0.003968	0.003968	0.000992		
Total	24	0.060454				

Table 5.18: Response Table for KERF (Experimental Data) using Electrode E_B

Response Table for Means					
Level	Pon	Poff	Wt	Wf	Wp
1	0.4286	**0.4906**	0.4686	**0.4870**	0.4608
2	0.4214	0.4714	0.4684	0.4664	0.4540
3	**0.5060**	0.4594	**0.4786**	0.4408	**0.4902**
4	0.4880	0.4596	0.4388	0.4804	0.4782
5	0.4760	0.4390	0.4656	0.4454	0.4368
Delta	0.0846	0.0516	0.0398	0.0462	0.0534
Rank	2	1	4	3	5

Table 5.19(a): Analysis of Variance (ANOVA) for KERF (S/N Data) using Electrode E_C

Analysis of Variance for SN ratios						
Source	DF	Seq SS	Adj SS	Adj MS	F	P
Pon	4	2.7859	2.7859	0.6965	1.80	0.000
Poff	4	6.6219	6.6219	1.6555	4.29	0.000
Wt	4	0.6340	0.6340	0.1585	0.41	0.000
Wf	4	1.0433	1.0433	0.2608	0.68	0.000
Wp	4	0.5009	0.5009	0.1252	0.32	0.000
Residual Error	4	1.5436	1.5436	0.3859		
Total	24	13.1296				

DF - degrees of freedom, SS - sum of squares, MS - mean squares(Variance), F-ratio of variance of a source to variance of error, $P < 0.05$ - determines significance of a parameter at 95% confidence level

Table 5.19(b): Analysis of Variance for KERF (Experimental Data) using Electrode E_C

Analysis of Variance for Means						
Source	DF	Seq SS	Adj SS	Adj MS	F	P
Pon	4	0.006940	0.006940	0.001735	1.80	0.000
Poff	4	0.016500	0.016500	0.004125	4.29	0.000
Wt	4	0.001465	0.001465	0.000366	0.38	0.000
Wf	4	0.002527	0.002527	0.000632	0.66	0.003
Wp	4	0.001341	0.001341	0.000335	0.35	0.004
Residual Error	4	0.003847	0.003847	0.000962		
Total	24	0.032621				
DF - degrees of freedom, SS - sum of squares, MS - mean squares(Variance), F-ratio of variance of a source to variance of error, P < 0.05 - determines significance of a parameter at 95% confidence level						

Table 5.20: Response Table for KERF (Experimental Data) using Electrode E_C

Response Table for Means					
Level	Pon	Poff	Wt	Wf	Wp
1	0.4108	**0.4752**	0.4472	0.4436	0.4354
2	0.4374	0.4604	0.4420	0.4484	0.4314
3	**0.4596**	0.4408	0.4406	0.4224	**0.4528**
4	0.4470	0.4268	0.4268	**0.4508**	0.4422
5	0.4500	0.4016	**0.4482**	0.4396	0.4430
Delta	0.0488	0.0736	0.0214	0.0284	0.0214
Rank	2	1	4	3	5

5.4.3.2 KERF (Cutting Width) using Electrode E_B

The optimum value of KERF (Cutting Width) is predicted at the optimal levels of significant variables which have already been selected as pulse on time (A_3), pulse off time (B_1), surface Roughness (C_3), kerf (D_1) and dimensional deviation (E_3). The estimated mean of the response characteristic (KERF) can be determined (Kumar, 1993 and Roy, 1990) as

$\eta_{KERF} = A_3+B_1+C_3+D_1+E_3 - 4T$

Where,

T = overall mean of cutting rate = $(\sum R_1 + \sum R_2)/50 = 0.464$ μm

Where, R_1, R_2 values are taken from the Table 5.15 and the values of A_3, B_1, C_3, D_1, and E_3, are taken from the Table 5.18

A_3 = Average value of cutting speed at the third level of pulse on time = 0.5060 μm

B_1= Average value of cutting speed at the first level of pulse off time = 0.4906 μm

C_3 = Average value of cutting speed at the third level of wire tension = 0.4786 μm

D_1 = Average value of cutting speed at the first level of wire feed = 0.4870 μm

E_3 = Average value of cutting speed at the third level of water pressure = 0.4902 μm

Substituting the values of various terms in the above equation,

$\eta_{KERF} = A_3+B_1+C_3+D_1+E_3 - 4T$

$\eta_{KERF} = 0.395$ μm

The 95 % confidence interval of the population (CI) is calculated by using the Equation 4.8 as rewritten below for ready reference:

$$CI_{POP} = \sqrt{\frac{F\alpha\,(1,fe)\,Ve}{neff}}$$

$$n_{eff} = \frac{N}{1+[\text{DOF associated in the estimate of mean response}]}$$

N = Total number of results = 25 x 2 = 50

Ve = Error variance = 0.000992 (Table 5.17b)

f_e = error DOF = 4 (Table 5.17b)

$F_{0.05}$ (1, 4) = 6.2136 (Tabulated F value; Roy, 1990)

So, $CI_{POP} = \pm 0.0490$

Therefore, the predicted 95% confidence interval of the population is:

Mean η_{KERF}- CI_{POP} < η_{KERF} > Mean η_{KERF} + CI_{POP}

0.346 < η_{KERF} > 0.444

5.4.3.3 KERF (Cutting Width) using Electrode E_C

The optimum value of KERF (Cutting Width) is predicted at the optimal levels of significant variables which have already been selected as pulse on time (A_3), pulse off time (B_1), surface Roughness (C_5), kerf (D_4) and dimensional deviation (E_3). The estimated mean of the response characteristic (KERF) can be determined (Kumar, 1993 and Roy, 1990) as

$\eta_{KERF} = A_3+B_1+C_5+D_4+E_3 - 4T$

Where,

T = overall mean of cutting rate = $(\sum R_1 + \sum R_2)/50$ = 0.44096 μm

Where, R_1, R_2 values are taken from the Table 5.16 and the values of A_3, B_1, C_5, D_4, and E_3, are taken from the Table 5.20

A_3 = Average value of cutting speed at the third level of pulse on time = 0.4596 μm

B_1 = Average value of cutting speed at the first level of pulse off time = 0.4752 μm

C_5 = Average value of cutting speed at the fifth level of wire tension = 0.4482 μm

D_4 = Average value of cutting speed at the fourth level of wire feed = 0.4508 μm

E_3 = Average value of cutting speed at the third level of water pressure = 0.4528 μm

Substituting the values of various terms in the above equation,

$\eta_{KERF} = A_3+B_1+C_5+D_4+E_3 - 4T$

$\eta_{KERF} = 0.364$ μm

The 95 % confidence interval of the population (CI) is calculated by using the Equation 4.8 as rewritten below for ready reference:

$$CI_{POP} = \sqrt{\frac{F\alpha\,(1,fe)\,Ve}{neff}}$$

$$n_{eff} = \frac{N}{1+[\text{DOF associated in the estimate of mean response}]}$$

N = Total number of results = 25 x 2 = 50

Ve = Error variance = 0.000962 (Table 5.19b)

f_e = error DOF = 4 (Table 5.19b)

$F_{0.05}$ (1, 4) = 0.5568 (Tabulated F value; Roy, 1990)

So, $CI_{POP} = \pm 0.0150$

Therefore, the predicted 95% confidence interval of the population is:

Mean η_{KERF} - CI_{POP} < η_{KERF} > Mean η_{KERF} + CI_{POP}

$0.346 < \eta_{KERF} > 0.379$

5.4.4 Effect of Process Parameters on Dimensional Deviation (DD)

The average values of Dimensional Deviation (DD) for each of input (Pon, Poff, Wt, Wf and Wp) parameters at level 1 and 2 for experimental data and S/N data are plotted using E_B and E_C electrodes.

Table 5.21: Dimensional Deviation (DD) Results for SS316 using Electrode E_B

S.No	A	B	C	D	E	DD		S/N Ratio
						R1	R2	
1	1	1	1	1	1	0.453	0.464	6.8780
2	1	2	2	2	2	0.346	0.357	9.2185
3	1	3	3	3	3	0.264	0.275	11.5679
4	1	4	4	4	4	0.244	0.255	12.2522
5	1	5	5	5	5	0.128	0.139	17.8558
6	2	1	2	3	4	0.247	0.259	12.1461
7	2	2	3	4	5	0.465	0.477	6.6509
8	2	3	4	5	1	0.368	0.382	8.6830
9	2	4	5	1	2	0.643	0.655	3.8358
10	2	5	1	2	3	0.468	0.480	6.5951
11	3	1	3	5	2	0.489	0.501	6.2138
12	3	2	4	1	3	0.346	0.358	9.2185
13	3	3	5	2	4	0.328	0.339	9.6825
14	3	4	1	3	5	0.287	0.298	10.8424
15	3	5	2	4	1	0.244	0.255	12.2522
16	4	1	4	2	5	0.466	0.477	6.6323
17	4	2	5	3	1	0.126	0.137	17.9926
18	4	3	1	4	2	0.136	0.147	17.3292
19	4	4	2	5	3	0.265	0.276	11.5351
20	4	5	3	1	4	0.356	0.367	8.9710
21	5	1	5	4	3	0.534	0.546	5.4492
22	5	2	1	5	4	0.428	0.442	7.3711
23	5	3	2	1	5	0.436	0.448	7.2103
24	5	4	3	2	1	0.324	0.336	9.7891
25	5	5	4	3	2	0.485	0.497	6.2852

Figures 5.13(a, b) and 5.14(a, b) shows that the dimensional deviation decreases with the increase of pulse on time and increases with increase in pulse off time. Increasing wire tension and wire feed values leads to higher dimensional deviation. The forces acting on wire electrode are the main causes of geometrical inaccuracy of the machined parts. The efficiency

and accuracy of the process are limited by the process parameters as well. Dimensional deviation value increases if the energy contained in a pulse increases to a large value. That's why when pulse on time is very high the dimensional deviation increases. With increase in wire tension the vibration and deflection of the wire change resulting into increase of dimensional deviation.

Table 5.22: Dimensional Deviation (DD) Results for SS316 using Electrode E_C

S.No	A	B	C	D	E	DD		S/N Ratio
						R1	R2	
1	1	1	1	1	1	0.564	0.575	4.9744
2	1	2	2	2	2	0.492	0.503	6.1607
3	1	3	3	3	3	0.324	0.335	9.7891
4	1	4	4	4	4	0.372	0.383	8.5891
5	1	5	5	5	5	0.134	0.145	17.4579
6	2	1	2	3	4	0.456	0.468	6.8207
7	2	2	3	4	5	0.436	0.448	7.2103
8	2	3	4	5	1	0.468	0.472	6.5951
9	2	4	5	1	2	0.444	0.456	7.0523
10	2	5	1	2	3	0.372	0.384	8.5891
11	3	1	3	5	2	0.556	0.568	5.0985
12	3	2	4	1	3	0.384	0.396	8.3134
13	3	3	5	2	4	0.318	0.329	9.9515
14	3	4	1	3	5	0.224	0.235	12.9950
15	3	5	2	4	1	0.248	0.259	12.1110
16	4	1	4	2	5	0.516	0.527	5.7470
17	4	2	5	3	1	0.484	0.495	6.3031
18	4	3	1	4	2	0.232	0.243	12.6902
19	4	4	2	5	3	0.185	0.196	14.6566
20	4	5	3	1	4	0.196	0.207	14.1549
21	5	1	5	4	3	0.634	0.646	3.9582
22	5	2	1	5	4	0.428	0.436	7.3711
23	5	3	2	1	5	0.316	0.328	10.0063
24	5	4	3	2	1	0.322	0.334	9.8429
25	5	5	4	3	2	0.296	0.308	10.5742

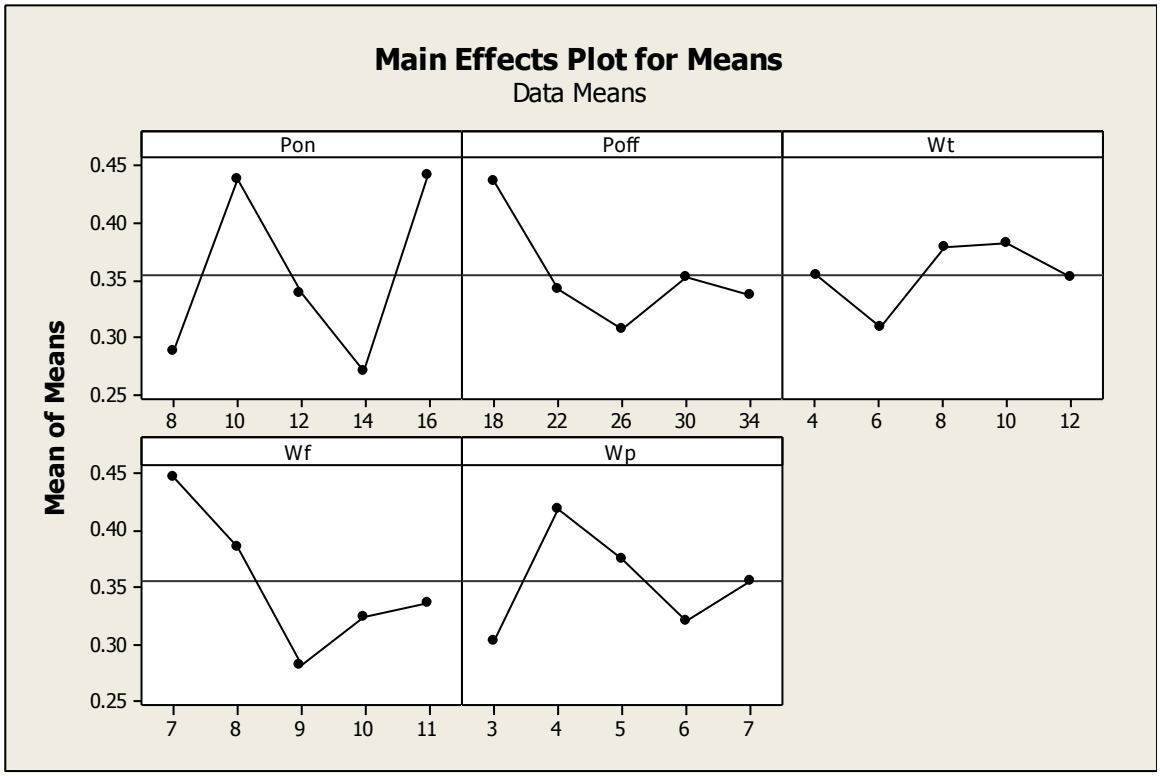

Figure 5.13(a): Effects of Process Parameters on Dimensional Deviation (Exp. Data)

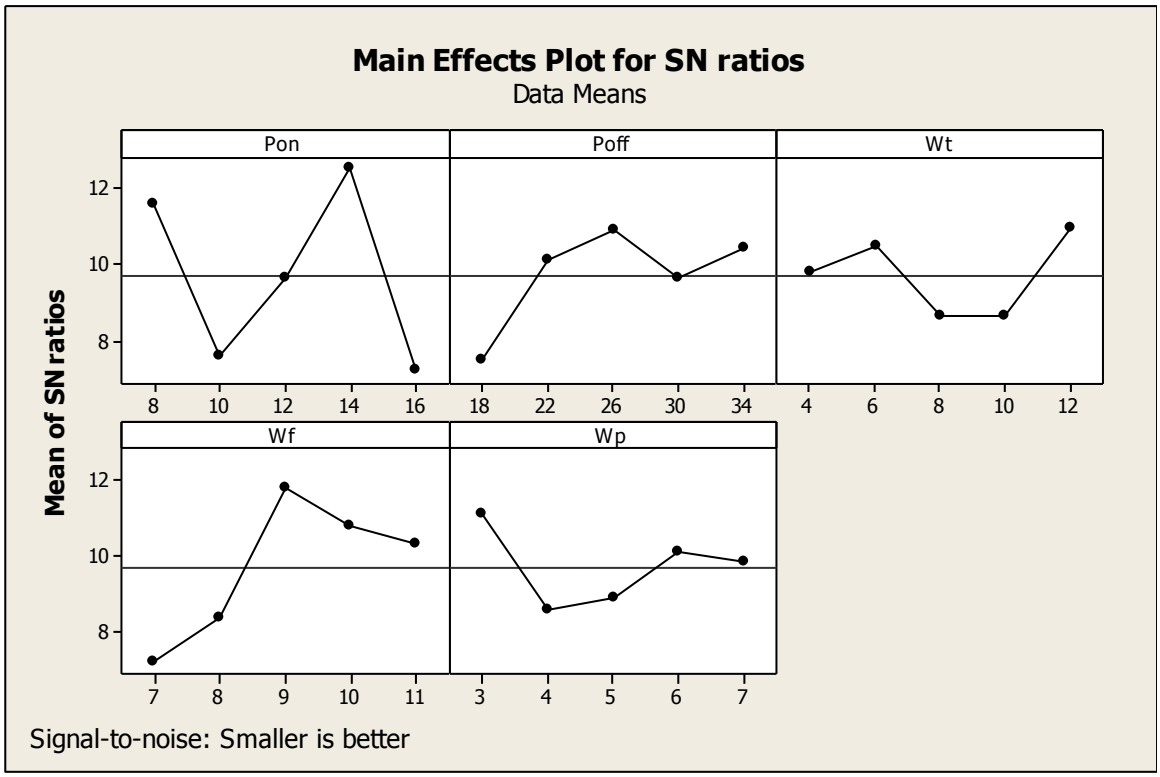

Figure 5.13(b): Effects of Process Parameters on Dimensional Deviation (S/N Data)

Figure 5.13(a, b): Effects of Process Parameters on Dimensional Deviation using E_B

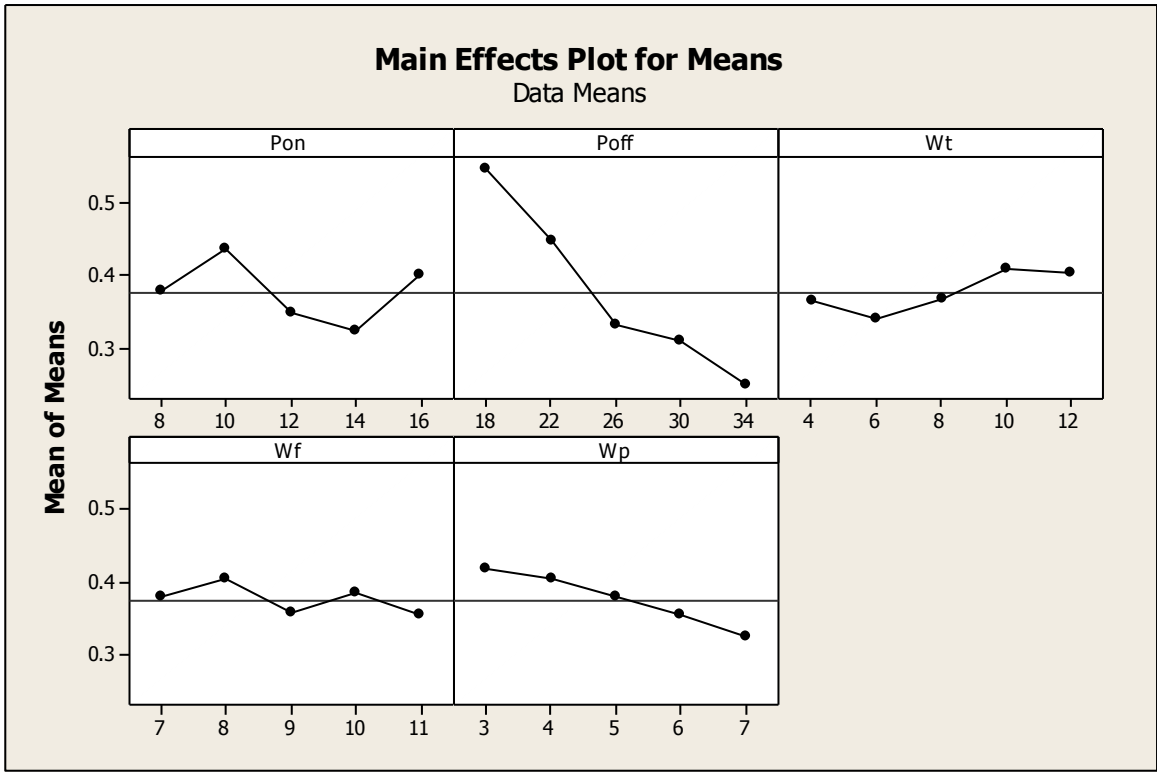

Figure 5.14(a): Effects of Process Parameters on Dimensional Deviation (Exp. Data)

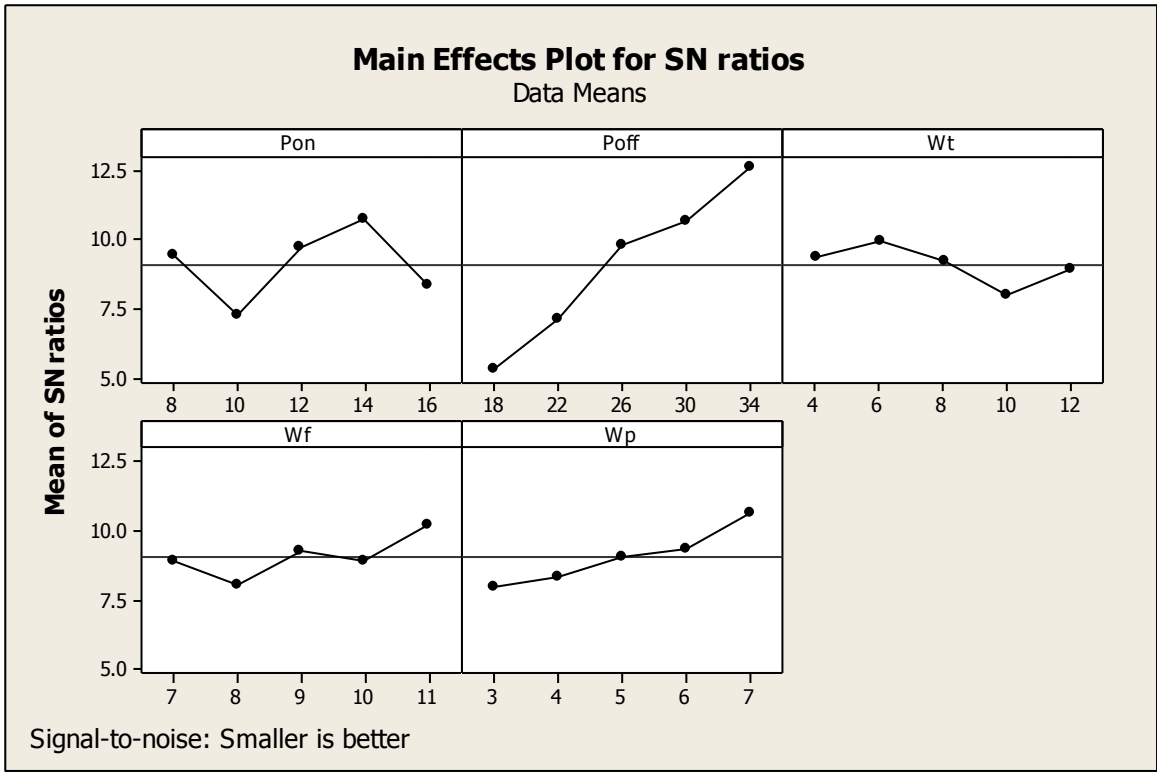

Figure 5.14(b): Effects of Process Parameters on Dimensional Deviation (S/N Data)

Figure 5.14(a, b): Effects of Process Parameters on Dimensional Deviation using E_C

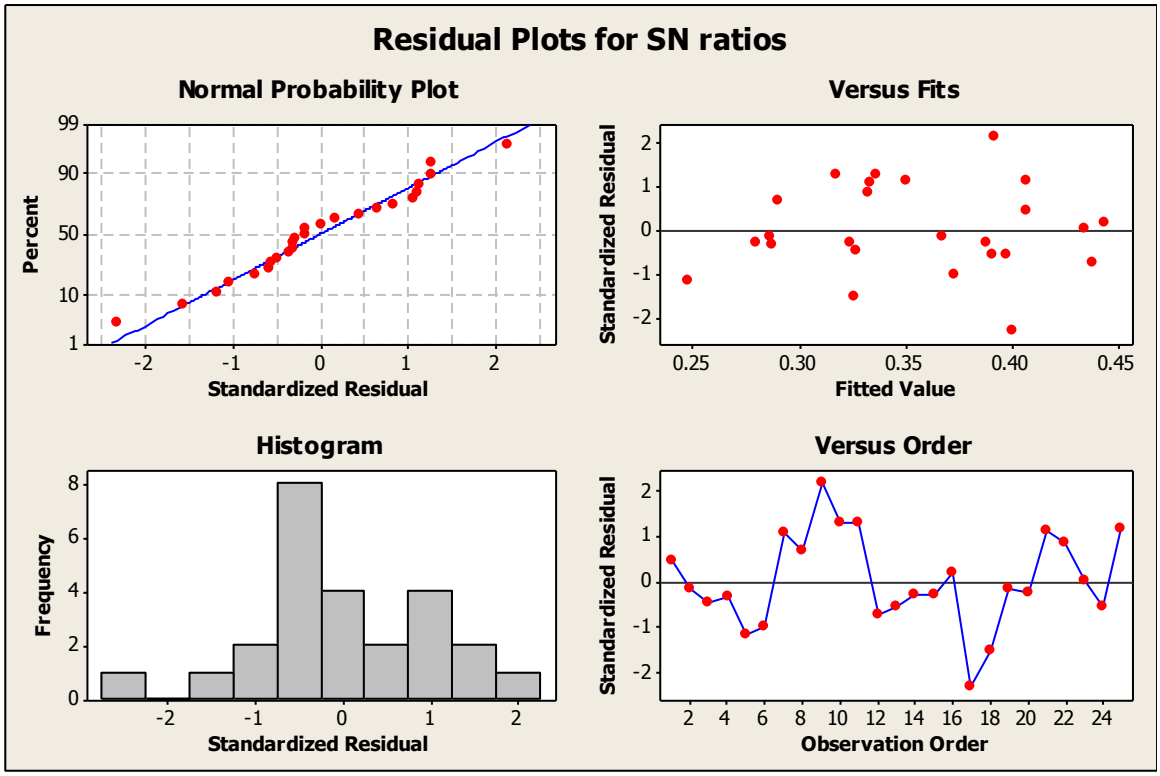

Figure 5.15: Residual Plots for Dimensional Deviation (S/N Data) using Electrode E_B

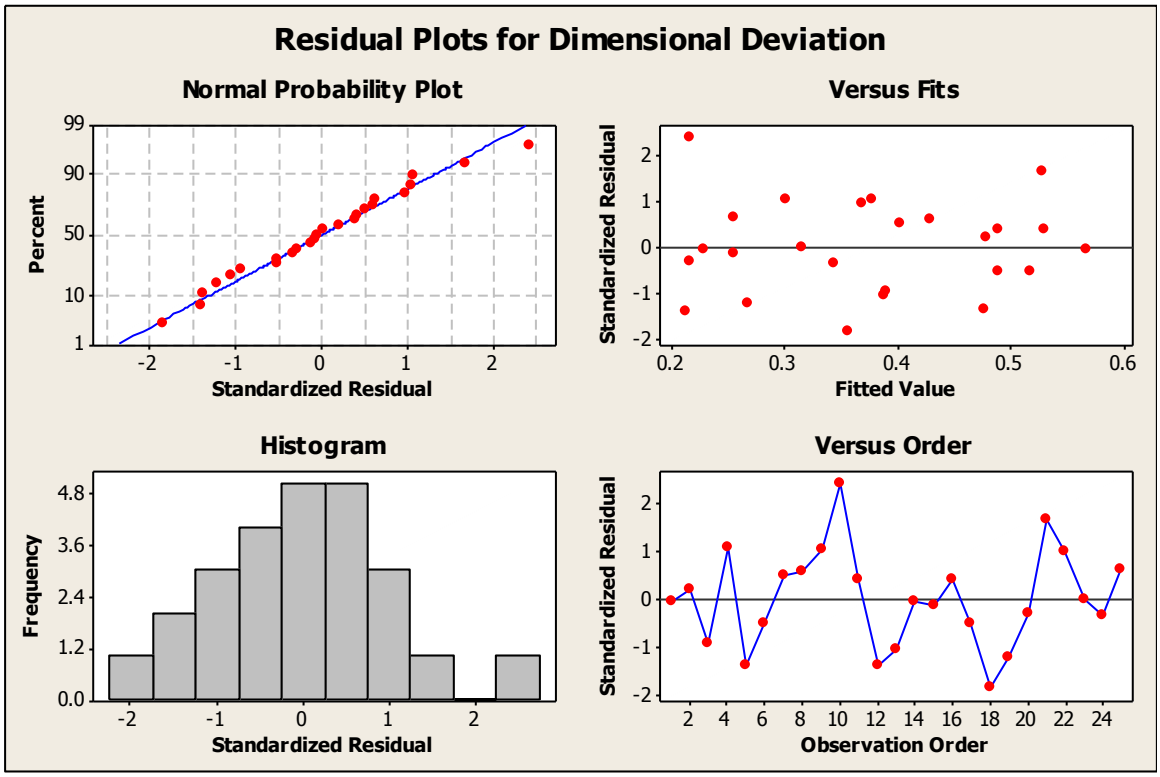

Figure 5.16: Residual Plots for Dimensional Deviation (S/N Data) using Electrode E_C

Residual plots are drawn to check for data for the non normality, non random variation, non constant variance, higher-order relationships, and outliers (Figures 5.15 and 5.16). The residual versus fitted value indicates a little tendency for variance of the residuals to increase as the dimensional deviation value increases. The problem, however, is not severe

enough to have any dramatic impact on the analysis and conclusions. The normal probability plot, histogram plot, and residual versus observation order plot of these residuals do not reveal any problem.

5.4.4.1 Selection of optimal levels for Dimensional Deviation (DD)

In order to study the significance of the process variables towards Dimensional Deviation (DD), analysis of variance (ANOVA) was performed. It was found that wire tension is significant process parameter for Dimensional Deviation (DD). From these tables, it is clear that pulse on time, pulse off time, wire tension, wire feed and water pressure significantly affect both the mean and the variation in the Dimensional Deviation (DD) values. The response table (Table 5.24 and 5.26) shows the average of each response characteristic (means) for each level of each factor. The tables include ranks based on delta statistics, which compare the relative magnitude of effects. The delta statistic is the highest minus the lowest average for each factor. Minitab assigns ranks based on delta values; rank 1 to the highest delta value, rank 2 to the second highest, and so on. The ranks indicate the relative importance of each factor to the response. The ranks and the delta values show that pulse on time, wire tension have the greatest effect on Dimensional Deviation (DD) and is followed by pulse off time , wire feed, water pressure in that order. As Dimensional Deviation (DD) is the "lower the better" type quality characteristic, it can be seen from Figure 5.13(a, b) shows that the fifth level of pulse on time (A_5), first level of pulse off time (B_1), fourth level of wire tension (C_4), first level of wire feed (D_1) and second level of water pressure (E_2) provide minimum value of Dimensional Deviation (DD) using electrode E_B. Figure 5.14(a, b) shows that the second level of pulse on time (A_2), first level of pulse off time (B_1), fourth level of wire tension (C_4), second level of wire feed (D_2) and first level of water pressure (E_1) provide minimum value of Dimensional Deviation (DD) using electrode E_C.

Table 5.23(a): Analysis of Variance for Dimensional Deviation (S/N Data) using E_B

Analysis of Variance for SN ratios						
Source	DF	Seq SS	Adj SS	Adj MS	F	P
Pon	4	109.34	109.34	27.336	15.21	0.000
Poff	4	35.30	35.30	8.826	10.39	0.000
Wt	4	22.54	22.54	5.636	7.25	0.002
Wf	4	68.61	68.61	17.153	9.76	0.001
Wp	4	20.63	20.63	5.158	11.23	0.000
Residual Error	4	90.47	90.47	22.619		
Total	24	346.91				

Table 5.23(b): Analysis of Variance for Dimensional Deviation (Exp. Data) using E_B

Analysis of Variance for Means					
Source	DF	Seq SS	Adj SS	Adj MS	F	P
Pon	4	0.13266	0.13266	0.033166	9.36	0.000
Poff	4	0.04870	0.04870	0.012176	6.50	0.002
Wt	4	0.01790	0.01790	0.004476	4.18	0.009
Wf	4	0.08036	0.08036	0.020090	7.82	0.000
Wp	4	0.04252	0.04252	0.010631	6.44	0.000
Residual Error	4	0.09764	0.09764	0.024409		
Total	24	0.41979				

DF - degrees of freedom, SS - sum of squares, MS - mean squares(Variance), F-ratio of variance of a source to variance of error, P < 0.05 - determines significance of a parameter at 95% confidence level

Table 5.24: Response Table for Dimensional Deviation (Exp. Data) using Electrode E_B

Response Table for Means					
Level	Pon	Poff	Wt	Wf	Wp
1	0.2870	**0.4378**	0.3544	**0.4468**	0.3030
2	0.4382	0.3422	0.3076	0.3864	0.4198
3	0.3388	0.3064	0.3796	0.2818	0.3754
4	0.2698	0.3526	**0.3818**	0.3246	0.3206
5	**0.4414**	0.3362	0.3518	0.3356	**0.3564**
Delta	0.1716	0.1314	0.0742	0.1650	0.1168
Rank	1	3	2	5	4

Table 5.25(a): Analysis of Variance for Dimensional Deviation (S/N Data) using E_C

Analysis of Variance for SN ratios						
Source	DF	Seq SS	Adj SS	Adj MS	F	P
Pon	4	35.01	35.01	8.752	1.11	0.002
Poff	4	166.63	166.63	41.657	5.26	0.068
Wt	4	10.51	10.51	2.627	0.33	0.005
Wf	4	12.44	12.44	3.109	0.39	0.006
Wp	4	22.43	22.43	5.609	0.71	0.004
Residual Error	4	31.66	31.66	7.916		
Total	24	278.68				

DF - degrees of freedom, SS - sum of squares, MS - mean squares(Variance), F-ratio of variance of a source to variance of error, P < 0.05 - determines significance of a parameter at 95% confidence level

Table 5.25(b): Analysis of Variance for Dimensional Deviation (Exp. Data) using E_C

Analysis of Variance for Means						
Source	DF	Seq SS	Adj SS	Adj MS	F	P
Pon	4	0.038979	0.038979	0.009745	0.96	0.000
Poff	4	0.279236	0.279236	0.069809	6.87	0.000
Wt	4	0.016299	0.016299	0.004075	0.40	0.005
Wf	4	0.008607	0.008607	0.002152	0.21	0.001
Wp	4	0.027803	0.027803	0.006951	0.68	0.002
Residual Error	4	0.040644	0.040644	0.010161		
Total	24	0.411569				

DF - degrees of freedom, SS - sum of squares, MS - mean squares(Variance), F-ratio of variance of a source to variance of error, P < 0.05 - determines significance of a parameter at 95% confidence level

Table 5.26: Response Table for Dimensional Deviation (Exp. Data) using Electrode E_C

Response Table for Means					
Level	Pon	Poff	Wt	Wf	Wp
1	0.3772	**0.5452**	0.3640	0.3808	**0.4172**
2	**0.4352**	0.4448	0.3394	**0.4040**	0.4040
3	0.3460	0.3316	0.3668	0.3568	0.3798
4	0.3226	0.3094	**0.4072**	0.3844	0.3540
5	0.3992	0.2492	0.4028	0.3542	0.3252
Delta	0.1126	0.2960	0.0678	0.0498	0.0920
Rank	2	1	4	5	3

5.4.4.2 Dimensional Deviation (DD) using Electrode E_B

The optimum value of Dimensional Deviation (DD) is predicted at the optimal levels of significant variables which have already been selected as pulse on time (A_5), pulse off time (B_1), surface Roughness (C_4), kerf (D_1) and dimensional deviation (E_2). The estimated mean of the response characteristic (DD) can be determined (Kumar, 1993 and Roy, 1990) as

$\eta_{DD} = A_5+B_1+C_4+D_1+E_2 - 4T$

Where,

T = overall mean of cutting rate = $(\sum R_1+ \sum R_2)/50 = 0.35504$

Where, R_1, R_2 values are taken from the Table 5.21 and the values of A_5, B_1, C_4, D_1, and E_2, are taken from the Table 5.24

A_5 = Average value of cutting speed at the fifth level of pulse on time = 0.4414

B_1 = Average value of cutting speed at the first level of pulse off time = 0.4378

C_4 = Average value of cutting speed at the fourth level of wire tension = 0.3818

D_1 = Average value of cutting speed at the first level of wire feed = 0.4468

E_2 = Average value of cutting speed at the second level of water pressure = 0.4198

Substituting the values of various terms in the above equation,

$$\eta_{DD} = A_5+B_1+C_4+D_1+E_2 - 4T$$

$$\eta_{DD} = 0.126$$

The 95 % confidence interval of the population (CI) is calculated by using the Equation 4.8 as rewritten below for ready reference:

$$CI_{POP} = \sqrt{\frac{F\alpha\,(1,fe)\,Ve}{neff}}$$

$$n_{eff} = \frac{N}{1+[\text{DOF associated in the estimate of mean response}]}$$

N = Total number of results = 25 x 2 = 50

Ve = Error variance = 0.024409 (Table 5.23b)

f_e = error DOF = 4 (Table 5.23b)

$F_{0.05}$ (1, 4) = 0.2731 (Tabulated F value; Roy, 1990)

So, $CI_{POP} = \pm 0.022$

Therefore, the predicted 95% confidence interval of the population is:

Mean η_{DD}- CI_{POP} < η_{DD} >Mean η_{DD} + CI_{POP}

0.104 < η_{DD} >0.148

5.4.4.3 Dimensional Deviation (DD) using Electrode E_C

The optimum value of Dimensional Deviation (DD) is predicted at the optimal levels of significant variables which have already been selected as pulse on time (A_2), pulse off time (B_1), surface Roughness (C_4), kerf (D_2) and dimensional deviation (E_1). The estimated mean of the response characteristic (DD) can be determined (Kumar, 1993 and Roy, 1990) as

$$\eta_{DD} = A_2+B_1+C_4+D_2+E_1 - 4T$$

Where,

T = overall mean of cutting rate = $(\sum R_1 + \sum R_2)/50 = 0.37604$

Where, R_1, R_2 values are taken from the Table 5.22 and the values of A_2, B_1, C_4, D_2, and E_1, are taken from the Table 5.26

A_2 = Average value of cutting speed at the second level of pulse on time = 0.4352

B_1 = Average value of cutting speed at the first level of pulse off time = 0.5452

C_4 = Average value of cutting speed at the fourth level of wire tension = 0.4072

D_2 = Average value of cutting speed at the second level of wire feed = 0.4040

E_1 = Average value of cutting speed at the first level of water pressure = 0.4172

Substituting the values of various terms in the above equation,

$\eta_{DD} = A_2+B_1+C_4+D_2+E_1 - 4T$

$\eta_{DD} = 0.132$

The 95 % confidence interval of the population (CI) is calculated by using the Equation 4.8 as rewritten below for ready reference:

$$CI_{POP} = \sqrt{\frac{F\alpha\,(1,fe)\,Ve}{neff}}$$

$$n_{eff} = \frac{N}{1+[\text{DOF associated in the estimate of mean response}]}$$

N = Total number of results = 25 x 2 = 50

Ve = Error variance = 0010161 (Table 5.25b)

f_e = error DOF = 4 (Table 5.25b)

$F_{0.05}$ (1, 4) = 0.1536 (Tabulated F value; Roy, 1990)

So, $CI_{POP} = \pm 0.0260$

Therefore, the predicted 95% confidence interval of the population is:

Mean η_{DD}- CI_{POP} < η_{DD} >Mean η_{DD} + CI_{POP}

0.106 < η_{DD} >0.158

Experiments were conducted using Taguchi orthogonal array in order to find out the optimal set of process parameters for obtaining the quality output and percentage contribution of each parameter on the performance measures of the Wire EDM. The optimum process parameters for wire EDM of SS316 with E_B and E_C as wire electrode materials and the influence of five process parameters namely pulse on time, pulse off time, wire tension, wire feed and dielectric flow rate have been investigated on four machining characteristics namely CS, SR, Kerf, and DD. The similar Taguchi analysis is done for the remaining materials of SS321, SS17-4 PH and H13 tool steels. The experimental results for work piece materials are shown in Appendix I. Optimal setting of process parameters have been predicted and verified experimentally for all work materials using E_B and E_C electrodes with each machining characteristic. The results are shown in the following Tables (Table 27 to 34).

Table 27: The Optimal and Predicted values for SS316 using Electrode E_B

Performance Measures	Optimal set of parameters	Predicted Optimal Value	Predicted Confidence Interval at 95% confidence Level.	Experimental Value (average of two confirmation experiments)
CS	A_5 B_1 C_4 D_5 E_5	2.635mm/min.	$2.015 < \eta_{CS} > 2.635$	2.786 mm/min.
SR	A_1 B_4 C_3 D_5 E_2	2.24 μm	$1.86 < \eta_{SR} > 2.78$	2.26 μm
KERF	A_2 B_5 C_4 D_3 E_5	0.348mm	$0.336 < \eta_{KERF} > 0.444$	0.354mm
DD	A_4 B_2 C_2 D_3 E_1	0.114%	$0.106 < \eta_{DD} > 0.158$	0.126%

Table 28: The Optimal and Predicted values for SS321 using Electrode E_B

Performance Measures	Optimal set of parameters	Predicted Optimal Value	Predicted Confidence Interval at 95% confidence Level.	Experimental Value (average of two confirmation experiments)
CS	A_5 B_1 C_3 D_2 E_5	2.480 mm/min	$2.367 < \eta_{CS} > 2.783$	2.625 mm/min.
SR	A_1 B_2 C_1 D_3 E_2	2.38 μm	$2.35 < \eta_{SR} > 2.74$	2.65 μm
KERF	A_4 B_2 C_3 D_3 E_2	0.358mm	$0.372 < \eta_{KERF} > 0.435$	0.412mm
DD	A_2 B_1 C_1 D_1 E_3	0.125%	$0.126 < \eta_{DD} > 0.172$	0.154%

Table 29: The Optimal and Predicted values for SS17-4 PH using Electrode E_B

Performance Measures	Optimal set of parameters	Predicted Optimal Value	Predicted Confidence Interval at 95% confidence Level.	Experimental Value (average of two confirmation experiments)
CS	A_5 B_1 C_3 D_2 E_4	2.552mm/min	2.467 < η_{CS} > 2.957	2.964mm/min.
SR	A_1 B_3 C_2 D_3 E_2	2.35 μm	2.42 < η_{SR} > 2.95	2.82 μm
KERF	A_3 B_2 C_3 D_3 E_4	0.365mm	0.382 < η_{KERF} >0.453	0.418mm
DD	A_2 B_1 C_1 D_1 E_4	0.136%	0.125 < η_{DD} > 0.164	0.158%

Table 30: The Optimal and Predicted values for H13 using Electrode E_B

Performance Measures	Optimal set of parameters	Predicted Optimal Value	Predicted Confidence Interval at 95% confidence Level	Experimental Value (average of two confirmation experiments)
CS	A_5 B_2 C_3 D_2 E_5	1.96mm/min.	1.85 < η_{CS} > 2.536	2.315 mm/min.
SR	A_1 B_3 C_1 D_3 E_3	2. 28μm	2.35 < η_{SR} > 2.78	2.65 μm
KERF	A_3 B_2 C_4 D_3 E_2	0.386mm	0.395 < η_{KERF} >0.483	0.432mm
DD	A_2 B_1 C_1 D_2 E_3	0.106%	0.124 < η_{DD} > 0.195	0.138%

Table 31: The Optimal and Predicted values for SS316 using Electrode E_C

Performance Measures	Optimal set of parameters	Predicted Optimal Value	Predicted Confidence Interval at 95% confidence	Experimental Value (average of two confirmation
CS	A_5 B_1 C_3 D_2 E_5	2.865mm/min.	2.267 < η_{CS} > 3.305	2.925 mm/min.
SR	A_1 B_3 C_1 D_3 E_2	1.95 μm	1.86 < η_{SR} > 3.22	2.18 μm
KERF	A_3 B_2 C_3 D_3 E_3	0.349mm	0.346 < η_{KERF} >0.379	0.364mm
DD	A_2 B_1 C_1 D_1 E_2	0.112 %	0.147 < η_{DD} > 0.148	0.118%

Table 32: The Optimal and Predicted values for SS321 using Electrode E_C

Performance Measures	Optimal set of parameters	Predicted Optimal Value	Predicted Confidence Interval at 95% confidence level.	Experimental Value (average of two confirmation experiments)
CS	A_5 B_1 C_3 D_2 E_4	2.715mm/min.	2.627 < η_{CS} > 2.968	2.931mm/min.
SR	A_1 B_3 C_2 D_3 E_2	1.85μm	1.92 < η_{SR} > 2.15	1.98 μm
KERF	A_3 B_2 C_2 D_3 E_2	0.375mm	0.382 < η_{KERF} >0.425	0.382mm
DD	A_2 B_1 C_1 D_1 E_3	0.145%	0.136 < η_{DD} > 0.198	0.164 %

Table 33: The Optimal and Predicted values for SS17-4 PH using Electrode E_C

Performance Measures	Optimal set of parameters	Predicted Optimal Value	Predicted Confidence Interval at 95% confidence level.	Experimental Value (average of two confirmation experiments)
CS	A_5 B_1 C_4 D_3 E_5	2.827mm/min.	$2.658 < \eta_{CS} > 2.985$	2.953 mm/min.
SR	A_1 B_3 C_2 D_3 E_3	1.73 μm	$1.84 < \eta_{SR} > 2.15$	1.96 μm
KERF	A_4 B_2 C_3 D_3 E_2	0.379mm	$0.384 < \eta_{KERF} > 0.426$	0.413mm
DD	A_2 B_1 C_2 D_1 E_3	0.162%	$0.174 < \eta_{DD} > 0.198$	0.185%

Table 34: The Optimal and Predicted values for H13 using Electrode E_C

Performance Measures	Optimal set of parameters	Predicted Optimal Value	Predicted Confidence Interval at 95% confidence level.	Experimental Value (average of two confirmation experiments)
CS	A_5 B_1 C_3 D_2 E_5	2.419mm/min.	$2.425 < \eta_{CS} > 2.785$	2.638mm/min.
SR	A_1 B_3 C_2 D_3 E_2	1.86 μm	$1.95 < \eta_{SR} > 2.28$	2.15 μm
KERF	A_3 B_2 C_3 D_3 E_3	0.389mm	$0.394 < \eta_{KERF} > 0.436$	0.423mm
DD	A_2 B_1 C_1 D_1 E_3	0.174%	$0.172 < \eta_{DD} > 0.198$	0.195%

SUMMARY

The present chapter give the results analysis and discussions for SS316 work material using E_B and E_C electrodes. The results analysis is done for single objective optimization by Taguchi design method. The experiments were conducted for four work materials to investigate the effect of process parameters on the output responses such as cutting speed, material removal rate, surface roughness, kerf (cutting width) and dimensional deviation using E_B and E_C electrodes. The predicted and experimental results are presented for all work materials with the combinations of E_B and E_C electrodes.

Chapter 6

Results and Analysis by Grey Relational Analysis

6.1 INTRODUCTION

The Grey theory established by Dr. Deng (1982) which includes Grey relational analysis, Grey modelling, prediction and decision making of a system in which the model is unsure or the information is incomplete. Grey Relational Analysis (GRA) is based on geometrical mathematics, which compliance with the principles of normality, symmetry, entirety, and proximity. It provides an efficient solution to the uncertainty, multi-input and discrete data problem. The relation between machining parameters and machining performance can be found out using the Grey relational analysis. And this kind of interaction is mainly through the connection among parameters and some conditions that are already known. Also, it will indicate the relational degree between two sequences with the help of Grey relational analysis. Moreover, the Grey relational grade will utilize the discrete measurement method to measure the distance.

Grey Relational Analysis (GRA) is suitable for solving complicated interrelationships between multiple factors and variables and has been successfully applied on cluster analysis, robot path planning, project selection, prediction analysis, performance evaluation, factor effect evaluation and multiple criteria decision.

Comparing to regression analysis and factor analysis in mathematic statistics, grey relational has some merits such as small sample, having no use for typical distribution, no requirement for independency and small amount of calculation. Additionally, GRA analysis is already proved to be simple and accurate method for selecting factors especially for those problems with unique characteristic. Grey Relational Analysis (GRA) a normalization evaluation technique is extended to solve the complicated multi-performance characteristics optimization effectively.

Single objective optimization is done by regression equation analysis but not possible for multiple objective optimization. The multi-objective optimization is done by grey relational analysis. Hence Grey relational analysis method is used to get optimal solution for the experimental results.

6.2 RESULTS ANALYSIS FOR SS316 USING E_B AND E_C ELECTRODES

Table 6.1 and 6.2 shows the twenty five experimental results of SS316 with the assigned levels of the process parameters according to the selected L_{25} orthogonal layout (Ref. Table 4.1 in Chapter 4).

Table 6.1: Orthogonal Array and Experimental Results Using Electrode E_B

Exp No.	Process Parameters					Responses				
	P on	P off	Wt	Wf	Wp	CS	MRR	SR	KERF	DD
1	1	1	1	1	1	0.534	12.81	2.60	0.465	0.453
2	1	2	2	2	2	0.425	10.20	2.54	0.456	0.346
3	1	3	3	3	3	0.330	7.92	2.40	0.442	0.264
4	1	4	4	4	4	0.697	7.12	2.28	0.426	0.244
5	1	5	5	5	5	0.754	6.09	2.24	0.354	0.128
6	2	1	2	3	4	0.805	19.32	2.65	0.438	0.247
7	2	2	3	4	5	0.945	15.48	2.54	0.418	0.465
8	2	3	4	5	1	0.833	12.79	2.35	0.393	0.368
9	2	4	5	1	2	0.470	11.28	2.32	0.432	0.643
10	2	5	1	2	3	0.405	9.72	2.69	0.426	0.468
11	3	1	3	5	2	1.832	43.96	2.60	0.515	0.489
12	3	2	4	1	3	1.715	41.16	2.52	0.532	0.346
13	3	3	5	2	4	1.064	20.73	2.35	0.505	0.328
14	3	4	1	3	5	1.247	15.52	2.32	0.479	0.287
15	3	5	2	4	1	0.892	11.80	2.30	0.499	0.244
16	4	1	4	2	5	1.925	46.20	2.76	0.465	0.466
17	4	2	5	3	1	1.810	43.44	2.75	0.467	0.126
18	4	3	1	4	2	1.105	21.72	2.48	0.489	0.136
19	4	4	2	5	3	1.240	17.76	2.43	0.481	0.265
20	4	5	3	1	4	0.912	17.08	2.33	0.538	0.356
21	5	1	5	4	3	2.186	52.46	2.89	0.570	0.534
22	5	2	1	5	4	2.025	48.60	2.76	0.484	0.428
23	5	3	2	1	5	1.916	45.98	2.65	0.468	0.436
24	5	4	3	2	1	1.525	36.60	2.40	0.480	0.324
25	5	5	4	3	2	1.289	30.93	2.35	0.378	0.485

Table 6.2: Orthogonal Array and Experimental Results Using Electrode E_C

Exp No.	Process Parameters					Responses				
	P on	P off	Wt	Wf	Wp	CS	MRR	SR	KERF	DD
1	1	1	1	1	1	0.635	15.24	2.92	0.438	0.564
2	1	2	2	2	2	0.540	12.96	2.72	0.446	0.492
3	1	3	3	3	3	0.478	11.47	2.64	0.412	0.324
4	1	4	4	4	4	0.387	9.28	2.65	0.396	0.372
5	1	5	5	5	5	0.335	8.04	2.28	0.362	0.134
6	2	1	2	3	4	1.011	24.26	2.16	0.438	0.456
7	2	2	3	4	5	0.835	20.04	2.95	0.458	0.436
8	2	3	4	5	1	0.675	16.20	2.86	0.433	0.468
9	2	4	5	1	2	0.587	14.08	2.82	0.432	0.444
10	2	5	1	2	3	0.552	13.24	2.85	0.426	0.372
11	3	1	3	5	2	1.876	45.02	2.84	0.485	0.556
12	3	2	4	1	3	1.328	31.87	2.72	0.462	0.384
13	3	3	5	2	4	0.934	22.41	2.66	0.465	0.318
14	3	4	1	3	5	0.894	21.45	2.28	0.452	0.224
15	3	5	2	4	1	0.735	17.64	2.17	0.434	0.248
16	4	1	4	2	5	2.205	52.92	3.06	0.485	0.516
17	4	2	5	3	1	1.918	46.03	2.97	0.452	0.484
18	4	3	1	4	2	1.315	31.56	2.84	0.436	0.232
19	4	4	2	5	3	1.018	24.43	2.74	0.434	0.185
20	4	5	3	1	4	0.870	20.88	2.45	0.428	0.196
21	5	1	5	4	3	2.625	63.00	3.22	0.530	0.634
22	5	2	1	5	4	2.418	58.03	2.94	0.484	0.428
23	5	3	2	1	5	1.924	46.17	2.85	0.458	0.316
24	5	4	3	2	1	1.689	40.53	2.72	0.420	0.322
25	5	5	4	3	2	1.315	31.56	2.06	0.358	0.296

6.2.1 OPTIMIZATION STEPS USING GREY RELATIONAL ANALYSIS FOR SS316

***Step I*:** In this step, the experimental response values are transformed into S/N ratio values. Further analysis is carried out based on these S/N ratio values. The material removal rate is a higher-the-better performance characteristic, since the maximization of the quality characteristic of interest is sought and can be expressed as (Muthu kumar et al, 2010).

$$\frac{S}{N} Ratio = -\log_{10}\left(\frac{1}{n}\sum_{i=1}^{n}\frac{1}{y_{ij}^2}\right) \quad \text{.....(6.1)}$$

Where n= number of replications and

y_{ij} = observed response value y_{ij}

Where i=1, 2... ....n;

j = 1, 2...k.

The S/N ratio values for the Experimental results for Electrode E_B were calculated and presented in Table 6.3.

Table 6.3: S/N Ratio values for Electrode E_B

Exp No	Process Parameters					S/N ratio		
	P on	P off	Wt	Wf	Wp	MRR	SR	KERF
1	1	1	1	1	1	21.10145	-8.94316	9.2
2	1	2	2	2	2	19.756	-8.66417	11.9
3	1	3	3	3	3	18.71623	-8.44154	12.2
4	1	4	4	4	4	17.7175	-8.40645	12.3
5	1	5	5	5	5	16.7398	-8.25743	13.2
6	2	1	2	3	4	17.39031	-8.47532	17.3
7	2	2	3	4	5	17.82462	-8.29337	16.4
8	2	3	4	5	1	18.06816	-8.12238	16.7
9	2	4	5	1	2	18.20882	-7.92392	17.1
10	2	5	1	2	3	18.22376	-7.72759	17.4
11	3	1	3	5	2	18.55876	-8.03411	19.1
12	3	2	4	1	3	18.85552	-8.24261	18.3
13	3	3	5	2	4	19.08613	-8.32309	18.0
14	3	4	1	3	5	19.25031	-8.34065	18.1
15	3	5	2	4	1	19.32296	-8.29526	18.2
16	4	1	4	2	5	19.58079	-8.51074	20.3
17	4	2	5	3	1	19.80424	-8.65211	19.5
18	4	3	1	4	2	19.98191	-8.75506	19.0
19	4	4	2	5	3	20.12086	-8.82796	18.8
20	4	5	3	1	4	20.23025	-8.87343	18.7
21	5	1	5	4	3	20.42501	-9.04615	20.9
22	5	2	1	5	4	20.59752	-9.1538	20.7
23	5	3	2	1	5	20.74998	-9.17696	20.0
24	5	4	3	2	1	20.87626	-9.19021	20.0
25	5	5	4	3	2	20.97476	-9.15787	20.1

The surface roughness and kerf are the lower-the-better performance characteristic and the loss function for the same can be expressed as

$$\frac{S}{N} Ratio = -\log_{10}\left(\frac{1}{n}\sum_{i=1}^{n} y_{ij}^2\right) \quad \text{.....(6.2)}$$

The S/N ratio values for the Experimental results for Electrode E_C were calculated and presented in Table 6.4

Table 6.4: S/N Ratio values for Electrode E_C

Exp No	Process Parameters					S/N ratio		
	P on	P off	Wt	Wf	Wp	MRR	SR	KERF
1	1	1	1	1	1	24.65382	-5.39026	9.978815
2	1	2	2	2	2	22.77049	-5.25019	12.12894
3	1	3	3	3	3	21.59151	-4.68898	11.59192
4	1	4	4	4	4	20.77312	-4.20005	12.45023
5	1	5	5	5	5	19.73394	-3.81444	13.27487
6	2	1	2	3	4	20.36911	-4.73297	17.6244
7	2	2	3	4	5	20.79693	-5.07235	17.42198
8	2	3	4	5	1	21.05956	-5.2094	17.88076
9	2	4	5	1	2	21.12499	-5.23527	17.92393
10	2	5	1	2	3	21.14572	-5.09133	18.26825
11	3	1	3	5	2	21.5007	-5.44573	19.40936
12	3	2	4	1	3	21.77433	-5.58156	19.28806
13	3	3	5	2	4	21.97525	-5.66204	19.07655
14	3	4	1	3	5	22.13068	-5.70216	19.10032
15	3	5	2	4	1	22.21213	-5.6938	18.17235
16	4	1	4	2	5	22.45598	-5.9223	20.93931
17	4	2	5	3	1	22.66443	-5.97415	20.04881
18	4	3	1	4	2	22.84439	-6.05464	19.90358
19	4	4	2	5	3	22.98656	-6.08802	20.05778
20	4	5	3	1	4	23.1034	-6.0955	19.04829
21	5	1	5	4	3	23.29385	-6.25614	20.59332
22	5	2	1	5	4	23.46819	-6.35678	20.97995
23	5	3	2	1	5	23.61478	-6.40689	21.21456
24	5	4	3	2	1	23.7318	-6.46987	21.42025
25	5	5	4	3	2	23.82505	-6.49259	20.61168

Step II: In the grey relational analysis, a data pre-processing is first performed in order to normalize the raw data for analysis. Normalization is a transformation performed on a single data input to distribute the data evenly and scale it into an acceptable range for further analysis. In this study, a linear normalization of the S/N ratio is performed in the range between zero and unity, which is also called the grey relational generating. $y_{ij}$is normalized as Z_{ij}($0 \leq Zij \leq 1$) by the following formula to avoid the effect of adopting different units and to reduce the variability. The normalized material removal rate corresponding to the larger-the-

better criterion can be expressed (Muthu kumar et al, 2010) and as shown in Table 6.5 and Table 6.6 respectively.

$$Z_{ij} = \frac{y_{ij} - \min\left(y_{ij,} i = 1,2,.....n\right)}{\max\left(y_{ij,} i = 1,2,.....n\right) - \min\left(y_{ij,} i = 1,2,.....n\right)} \quad \text{.....(6.3)}$$

Table 6.5: Normalized S/N ratio values for Electrode E_B

Exp No.	Process Parameters					Normalized S/N ratio		
	P on	P off	Wt	Wf	Wp	MRR	SR	KERF
1	1	1	1	1	1	0.1986	0.5104	0.93582888
2	1	2	2	2	2	0.1123	0.6042	0.86631016
3	1	3	3	3	3	0.0672	0.6667	0.52406417
4	1	4	4	4	4	0.0298	0.6146	0.18181818
5	1	5	5	5	5	0.0000	0.7188	0.1657754
6	2	1	2	3	4	0.3751	0.4271	1.0000000
7	2	2	3	4	5	0.2452	0.8021	0.63636364
8	2	3	4	5	1	0.1673	0.8438	0.5828877
9	2	4	5	1	2	0.1390	0.9427	0.55614973
10	2	5	1	2	3	0.1008	1.0000	0.51336898
11	3	1	3	5	2	0.4431	0.2656	0.81818182
12	3	2	4	1	3	0.4293	0.3125	0.52941176
13	3	3	5	2	4	0.3247	0.4688	0.36363636
14	3	4	1	3	5	0.2506	0.5729	0.29411765
15	3	5	2	4	1	0.1742	0.7188	0.22459893
16	4	1	4	2	5	0.8930	0.1458	0.71122995
17	4	2	5	3	1	0.6272	0.2344	0.45454545
18	4	3	1	4	2	0.427	0.2813	0.22994652
19	4	4	2	5	3	0.3384	0.3281	0.10160428
20	4	5	3	1	4	0.2926	0.3854	0.0000000
21	5	1	5	4	3	1.0000	0.00000	0.57754011
22	5	2	1	5	4	0.7204	0.1302	0.47058824
23	5	3	2	1	5	0.5875	0.3854	0.22459893
24	5	4	3	2	1	0.4584	0.4167	0.17112299
25	5	5	4	3	2	0.3685	0.6146	0.13368984

The surface roughness and kerf width should follow the lower-the-better criterion and can be expressed as

$$Z_{ij} = \frac{\max\left(y_{ij,} i = 1,2,.....n\right) - y_{ij}}{\max\left(y_{ij,} i = 1,2,.....n\right) - \min\left(y_{ij,} i = 1,2,.....n\right)} \quad \text{.....(6.4)}$$

Table 6.6: Normalized S/N ratio values for Electrode E_C

Exp No.	Process Parameters					Normalized S/N ratio		
	P on	P off	Wt	Wf	Wp	MRR	SR	KERF
1	1	1	1	1	1	0.260025	0.571429	1.000000
2	1	2	2	2	2	0.122807	0.612245	0.818681
3	1	3	3	3	3	0.072055	0.843537	0.236264
4	1	4	4	4	4	0.045739	0.952381	0.120879
5	1	5	5	5	5	0.000000	1.000000	0.076923
6	2	1	2	3	4	0.404762	0.197279	0.972527
7	2	2	3	4	5	0.278822	0.367347	0.785714
8	2	3	4	5	1	0.206767	0.469388	0.758242
9	2	4	5	1	2	0.130952	0.564626	0.648352
10	2	5	1	2	3	0.118421	0.816327	0.620879
11	3	1	3	5	2	0.619674	0.136054	0.791209
12	3	2	4	1	3	0.414160	0.340136	0.675824
13	3	3	5	2	4	0.312657	0.394558	0.538462
14	3	4	1	3	5	0.273810	0.448980	0.461538
15	3	5	2	4	1	0.206767	0.544218	0.115385
16	4	1	4	2	5	0.761278	0.047619	0.769231
17	4	2	5	3	1	0.582080	0.360544	0.489011
18	4	3	1	4	2	0.497494	0.272109	0.384615
19	4	4	2	5	3	0.395363	0.374150	0.362637
20	4	5	3	1	4	0.351504	0.442177	0.000000
21	5	1	5	4	3	1.000000	0.000000	0.390110
22	5	2	1	5	4	0.854637	0.115646	0.439560
23	5	3	2	1	5	0.614035	0.244898	0.450549
24	5	4	3	2	1	0.471805	0.183673	0.456044
25	5	5	4	3	2	0.399749	0.312925	0.181319

Step III: The grey relational coefficient is calculated to express the relationship between the ideal (best) and normalized experimental results. The grey relational coefficient can be expressed as (Muthu kumar et al, 2010)

$$\gamma\left(y_o(k), y_i(k)\right) = \frac{\Delta\min + \xi\Delta\max}{\Delta_{oj}(k) + \xi\Delta\max} \qquad \text{.....(6.5)}$$

Where; j = 1, 2...n;

k = 1, 2...m, n is the number of experimental data items and

m is the number of responses.

y_o(k) is the reference sequence (y_o(k) = 1, k = 1,2...m);

y_j(k) is the specific comparison sequence.

$\Delta_{oj} = \|y_o(k) - y_j(k)\|$ -The absolute value of the difference between y_0(k) and y_j(k).

$\Delta \min = \min_{\forall j \in i} \min_{\forall k} \|y_o(k) - y_j(k)\|$ is the smallest value of y_j(k)

$\Delta \max = \max_{\forall j \in i} \max_{\forall k} \|y_o(k) - y_j(k)\|$ is the largest value of y_j(k)

Where ξ is the distinguishing coefficient, which is defined in the range 0≤ ξ ≤1.The Wire EDM process parameters, is equally weighted in this study, and therefore ξ is 0.5.

Step IV: The grey relational grade is determined by averaging the grey relational coefficient corresponding to each performance characteristic. The overall performance characteristic of the multiple response process depends on the calculated grey relational grade. The grey relational coefficient can be expressed as (Muthu kumar et al, 2010)

$$\overline{\gamma_j} = \frac{1}{k}\sum_{i=1}^{m} \gamma_{ij} \quad \text{.....(6.6)}$$

Where $\overline{\gamma_j}$ the grey relational grade for the jth experiment and k is the number of performance characteristics.

This approach converts a multiple response process optimization problem into a single response optimization situation with the objective function of an overall grey relational grade. Table 6.7 shows the grey relation coefficient and grey relational grade for each experiment using the L_{25} orthogonal array. The higher grey relational grade reveals that the corresponding actual result is closer to the ideally normalized value. Experiment no 6 for electrode E_B wire similarly experiment no 1 for electrode E_C wire has the best multiple performance characteristic shown among 25 experiments, because it has the highest grey relational grade shown in Table, comparatively in Figure 6.1 and 6.2. The higher the value of the grey relational grade, the closer the corresponding factor combination is, to the optimal. A higher

grey relational grade implies better product quality; therefore, on the basis of the grey relational grade, the factor effect can be estimated and the optimal level for each controllable factor can also be determined.

Table 6.7: Grey Relational Co-efficient and Grey Relational Grade Using Electrode E_B

Exp No.	Process Parameters					Grey Relational Co-efficient			Grey grade
	P on	P off	Wt	Wf	Wp	MRR	SR	KERF	
1	1	1	1	1	1	0.067010	0.845304	0.86875	0.5919093
2	1	2	2	2	2	0.042096	0.955801	1.072595	0.5691591
3	1	3	3	3	3	0.024914	1.000000	0.4125	0.4871007
4	1	4	4	4	4	0.008591	0.878453	0.0750	0.4280348
5	1	5	5	5	5	0.000000	0.900552	0.1625	0.4493609
6	2	1	2	3	4	0.682131	0.712707	0.6250	**0.6452338**
7	2	2	3	4	5	0.573024	0.828729	0.7500	0.5646140
8	2	3	4	5	1	0.438144	0.878453	0.90625	0.5607570
9	2	4	5	1	2	0.359107	0.900552	0.6625	0.5981094
10	2	5	1	2	3	0.327320	0.883978	0.7000	0.6213774
11	3	1	3	5	2	0.719931	0.558011	0.14375	0.5371573
12	3	2	4	1	3	0.706186	0.403315	0.0375	0.4677346
13	3	3	5	2	4	0.604811	0.436464	0.20625	0.4500876
14	3	4	1	3	5	0.524313	0.646409	0.36875	0.4513811
15	3	5	2	4	1	0.448454	0.707182	0.24375	0.4697194
16	4	1	4	2	5	1.000000	0.215470	0.45625	0.6089725
17	4	2	5	3	1	0.621993	0.265193	0.44375	0.4820630
18	4	3	1	4	2	0.615979	0.337017	0.30625	0.4233142
19	4	4	2	5	3	0.596220	0.392265	0.35625	0.4048899
20	4	5	3	1	4	0.537801	0.000000	0.00000	0.3986803
21	5	1	5	4	3	0.365979	0.127072	0.4250	0.6251207
22	5	2	1	5	4	0.326460	0.281768	0.3375	0.4973618
23	5	3	2	1	5	0.310137	0.331492	0.4375	0.4628532
24	5	4	3	2	1	0.325601	0.403315	0.3625	0.4392702
25	5	5	4	3	2	0.352234	0.767956	1.0000	0.4575121

Table 6.8: Grey Relational Co-efficient and Grey Relational Grade Using Electrode E_C

Exp No.	Process Parameters					Grey Relational Co-efficient			Grey grade
	P on	P off	Wt	Wf	Wp	MRR	SR	KERF	
1	1	1	1	1	1	0.348921	0.763713	1.169851	**0.656128**
2	1	2	2	2	2	0.342958	0.918782	0.459770	0.573837
3	1	3	3	3	3	0.338963	1.000000	0.350877	0.563280
4	1	4	4	4	4	0.335253	0.804444	0.373832	0.504510
5	1	5	5	5	5	0.333333	0.834101	0.571429	0.579621
6	2	1	2	3	4	0.611345	0.635088	0.666667	0.637700
7	2	2	3	4	5	0.539388	0.744856	0.842105	0.708783
8	2	3	4	5	1	0.470874	0.804444	0.597015	0.624111
9	2	4	5	1	2	0.438253	0.834101	0.625000	0.632451
10	2	5	1	2	3	0.426374	0.811659	0.368664	0.535565
11	3	1	3	5	2	0.640969	0.530792	0.341880	0.504547
12	3	2	4	1	3	0.629870	0.455919	0.386473	0.490754
13	3	3	5	2	4	0.558541	0.470130	0.441989	0.490220
14	3	4	1	3	5	0.512459	0.585761	0.398010	0.498743
15	3	5	2	4	1	0.475490	0.630662	0.479042	0.528398
16	4	1	4	2	5	1.000000	0.389247	0.473373	0.620873
17	4	2	5	3	1	0.569472	0.404922	0.418848	0.464414
18	4	3	1	4	2	0.565598	0.429929	0.437158	0.477562
19	4	4	2	5	3	0.553232	0.451372	0.333333	0.445979
20	4	5	3	1	4	0.519643	0.333333	0.465116	0.439364
21	5	1	5	4	3	0.440909	0.364185	0.430108	0.411734
22	5	2	1	5	4	0.426061	0.410431	0.470588	0.435694
23	5	3	2	1	5	0.420217	0.427896	0.439560	0.429224
24	5	4	3	2	1	0.425750	0.455919	1.000000	0.627223
25	5	5	4	3	2	0.435629	0.683019	1.000000	0.606216

Since the actual design is orthogonal, it is possible to separate out the effect of each machining parameter on the grey relational grade at different levels.

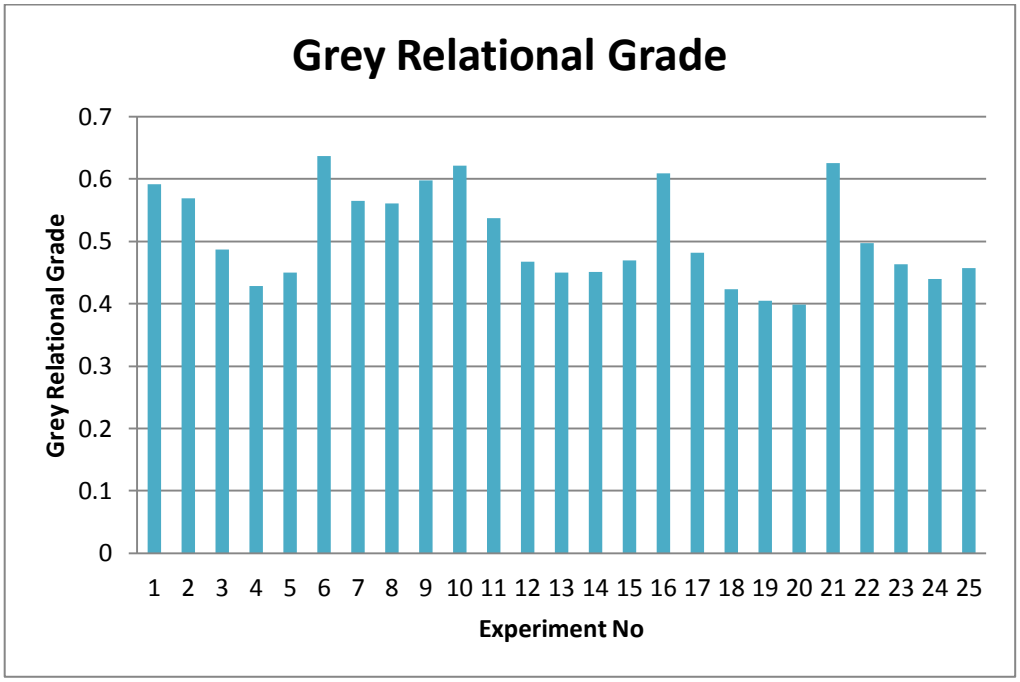

Figure 6.1: Grey Relational Grades for max MRR, min SR and min kerf Using Electrode E_B

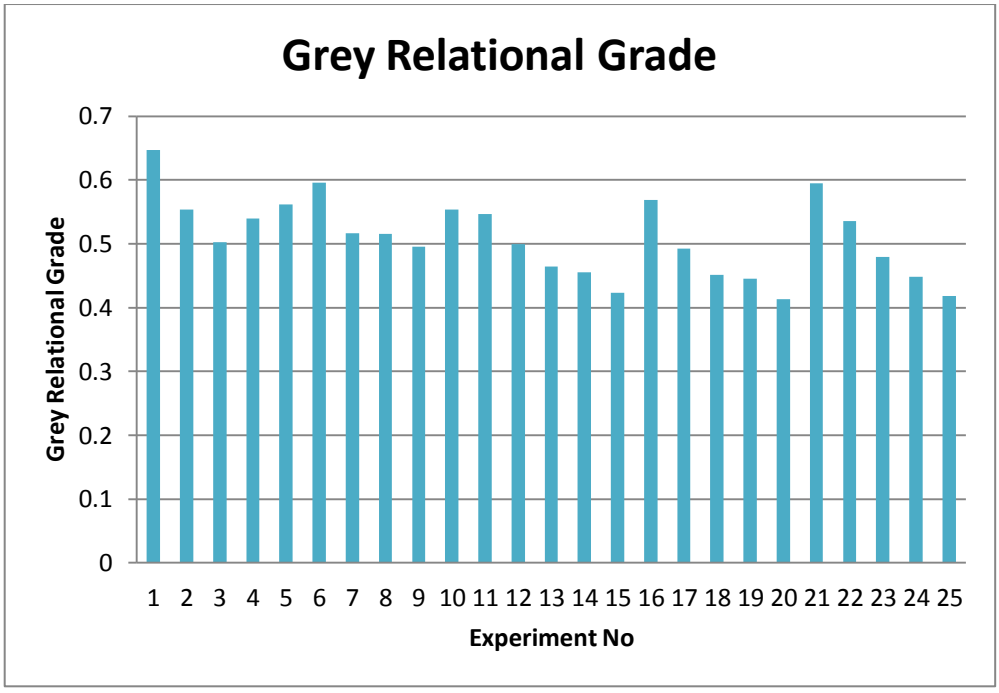

Figure 6.2: Grey Relational Grades for max MRR, min SR and min kerf Using Electrode E_C

The mean of the grey relational grade for each level of the other machining parameters can be computed in a similar manner. The mean of the grey relational grade for each level of the machining parameters is summarized and as shown in Table 6.9 and 6.10.

Table 6.9: Main effects of the Parameters on the Grey Relational Grade Using Electrode E_B

Symbol	Process Parameters	Level 1	Level 2	Level 3	Level4	Level5	Max-min
A	Pon	0.505113	0.596339	0.475216	0.463584	0.496424	0.13275
B	Poff	**2.999994**	2.580933	2.384114	2.321686	2.39665	0.67830
C	Wt	2.585344	2.543456	2.426823	**2.523012**	**2.60474**	0.17791
D	Wf	2.519287	**2.688867**	2.514891	2.510804	2.449528	0.23933
E	Wp	2.54372	2.585252	**2.606224**	2.410999	2.537182	0.19522

Table 6.10: Main effects of the Parameters on the Grey Relational Grade Using E_C

Symbol	Process Parameters	Level 1	Level 2	Level 3	Level4	Level5	Max-min
A	Pon	**0.560893**	0.535589	0.477831	0.474356	0.49535	0.061233
B	Poff	**2.953024**	2.598258	2.413376	2.384229	2.37124	0.581785
C	Wt	**2.643446**	2.498266	2.428254	**2.541205**	2.60895	0.180702
D	Wf	2.535768	2.588653	2.464528	2.526407	**2.60477**	0.01612
E	Wp	2.527193	2.465343	**2.595958**	2.549957	2.58167	0.046002

Step V: Determine the optimal process parameters and its level combination (Muthu kumar et al, 2010)

Figure 6.3 shows the grey relational grade Bar chart. Generally, the larger grey relational grade, the better is the multiple performance characteristic. However, the relative importance among the machining parameters for the multiple performance characteristics still needs to be known, so that the optimal combinations of the machining parameter levels can be determined more accurately. The optimal parametric combinations are shown in Table 6.9 and 6.10. Comparatively shown in Figure 6.3 further it is also bolded in the tables. The optimal process parameter setting becomes A_5 (pulse on time, 16 µs), B_1 (pulse off time, 18 µs), C_2 (Wire tension, 6 Kg-f), D_3 (wire feed rate, 9 mm/min) and E_4 (water flushing pressure, 6 Kg/cm2) for electrode E_B wire and A_5 (pulse on time, 8 µs), B_1(pulse off time, 18 µs), C_4(Wire tension, 10 Kg-f), D_2(wire feed rate, 8 mm/min), E_5(water flushing pressure 5 Kg/cm2) for electrode E_C wire respectively.

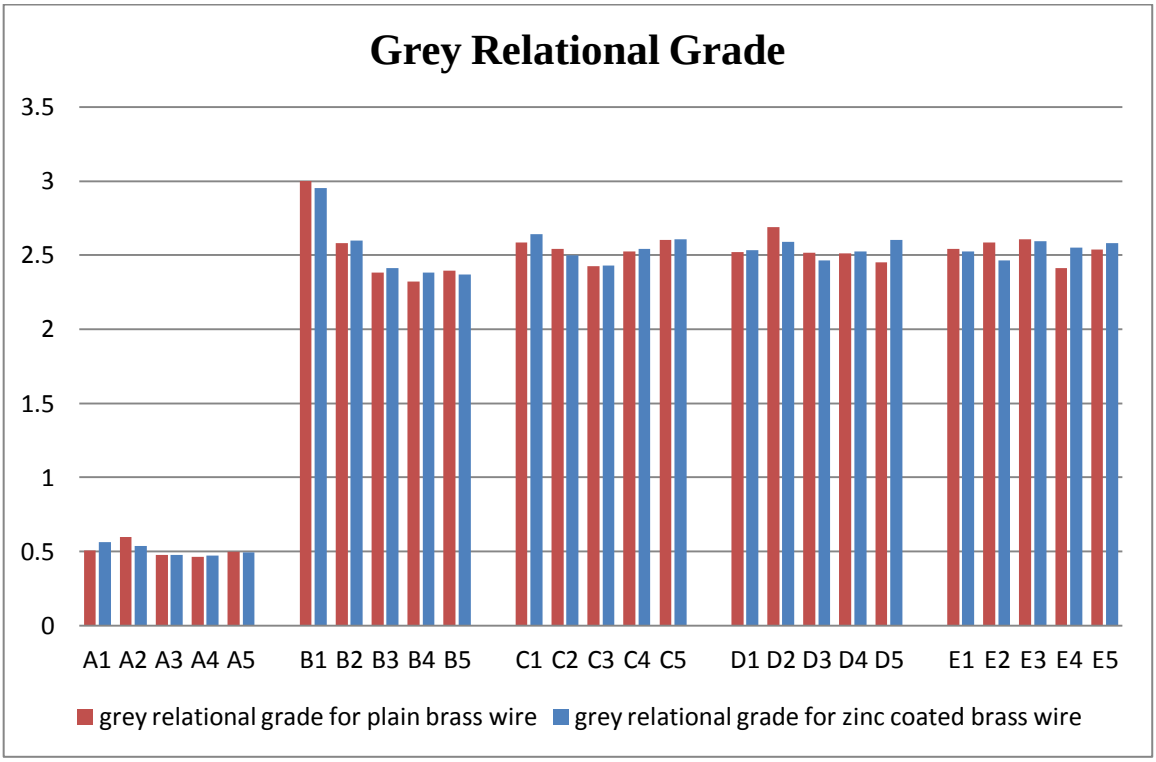

Figure 6.3: Response graph of average Grey Relational Grade Using Electrodes E_B and E_C

6.2.2 VALIDATION OF THE EXPERIMENTAL RESULTS

The confirmation test for the optimal parameter setting with its selected levels was conducted to evaluate the quality characteristics for Wire EDM machining on SS316 work material using brass and zinc coated brass wire electrode materials. (Muthu kumar et al, 2010)

Experiment 6 (Table 6.7) and experiment 1 (Table 6.8) shows the highest grey relational grade for brass wire and zinc coated brass wire respectively, indicating the optimal process parameter set of $A_5B_1C_2D_3E_4$ (electrode E_B) and $A_5B_1C_4D_2E_5$ (electrode E_C) has the best multiple performance characteristics among the twenty five experiments, which can be compared with results of confirmation experiment for validation of results. Table 6.11 shows the comparison of the actual results of machining on Wire EDM process parameters on SS316 work material using brass wire and zinc coated brass wire. The response values obtained from the confirmation experiment are MRR = 53.232mm^2/min, SR = 2.28 µm and kerf = 0.398 mm for brass wire and MRR= 63.696mm^2/min, SR = 2.34µm, Kerf = 0.386mm for zinc coated brass wire. The Material Removal Rate shows an increased from 53.232mm^2/min to 63.696mm^2/min, the Surface Roughness shows value of 2.28µm to 2.34µm and the kerf width shows a reduced value of 0.398 to 0.386 mm for brass wire and zinc coated brass wire.

Table – 6.11: Experimental results for SS316 using Electrodes E_B and E_C

S.No.	Machining Characteristics	Experimental Value for brass	Experimental Value for zinc coated brass
1.	Optimal parameters	$A_5B_1C_2D_3E_4$	$A_5B_1C_4D_2E_5$
2.	Cutting Speed (CS)	2.218 mm/min	2.654mm/min
3.	Material Removal Rate (MRR)	53.232mm^2/min	63.696mm^2/min
4.	Surface Roughness (SR)	2.28 μm	2.34μm
5.	Cutting Width (KERF)	0.398 mm	0.386mm
6.	Dimensional Deviation (DD)	0.136%	0.124%
7.	Grey Relation Grade	0.6452	0.6561

6.3 RESULTS ANALYSIS FOR SS321 USING E_B AND E_C ELECTRODES

Table 6.12: Orthogonal Array and Experimental Results using Electrode E_B

Exp No.	Process Parameters					Responses				
	P on	P off	Wt	Wf	Wp	CS	MRR	SR	KERF	DD
1	1	1	1	1	1	0.473	11.35	2.80	0.464	0.485
2	1	2	2	2	2	0.360	8.64	2.72	0.459	0.348
3	1	3	3	3	3	0.301	7.22	2.81	0.423	0.486
4	1	4	4	4	4	0.252	6.04	2.70	0.447	0.452
5	1	5	5	5	5	0.213	5.11	2.63	0.412	0.154
6	2	1	2	3	4	0.904	21.69	2.96	0.434	0.456
7	2	2	3	4	5	0.836	20.06	2.82	0.402	0.463
8	2	3	4	5	1	0.615	14.76	2.96	0.412	0.442
9	2	4	5	1	2	0.495	11.88	2.97	0.417	0.168
10	2	5	1	2	3	0.345	8.28	2.86	0.425	0.248
11	3	1	3	5	2	1.538	36.91	3.27	0.468	0.492
12	3	2	4	1	3	1.214	29.13	3.18	0.422	0.465
13	3	3	5	2	4	0.918	22.03	2.88	0.453	0.422
14	3	4	1	3	5	0.641	15.38	2.86	0.466	0.414
15	3	5	2	4	1	0.441	10.58	2.75	0.479	0.348
16	4	1	4	2	5	1.986	47.66	3.50	0.488	0.524
17	4	2	5	3	1	1.405	33.72	3.33	0.436	0.461
18	4	3	1	4	2	0.928	22.27	3.24	0.478	0.366
19	4	4	2	5	3	0.756	18.14	3.15	0.432	0.214
20	4	5	3	1	4	0.596	14.30	3.04	0.421	0.244
21	5	1	5	4	3	2.625	63.00	3.78	0.543	0.514
22	5	2	1	5	4	2.318	55.63	3.53	0.493	0.418
23	5	3	2	1	5	1.932	46.36	3.04	0.479	0.432
24	5	4	3	2	1	1.798	43.15	2.98	0.489	0.424
25	5	5	4	3	2	1.285	30.84	2.72	0.456	0.484

Table 6.12 and 6.13 shows the twenty five experimental results of SS321 with the assigned levels of the process parameters according to the selected L_{25} orthogonal layout (Ref. Table 4.1 in Chapter 4).

Table 6.13: Orthogonal Array and Experimental Results using Electrode E_C

Exp No.	Process Parameters					Responses				
	P on	P off	Wt	Wf	Wp	CS	MRR	SR	KERF	DD
1	1	1	1	1	1	0.712	17.08	2.26	0.457	0.422
2	1	2	2	2	2	0.493	11.83	2.28	0.435	0.352
3	1	3	3	3	3	0.412	9.88	2.24	0.436	0.336
4	1	4	4	4	4	0.370	8.88	2.12	0.395	0.189
5	1	5	5	5	5	0.297	7.12	1.98	0.382	0.164
6	2	1	2	3	4	0.943	22.63	2.41	0.422	0.484
7	2	2	3	4	5	0.742	17.80	2.16	0.456	0.433
8	2	3	4	5	1	0.627	15.04	2.05	0.441	0.336
9	2	4	5	1	2	0.506	12.14	2.08	0.446	0.228
10	2	5	1	2	3	0.486	11.66	1.95	0.436	0.168
11	3	1	3	5	2	1.826	43.82	2.15	0.445	0.542
12	3	2	4	1	3	1.358	32.59	2.24	0.446	0.428
13	3	3	5	2	4	0.976	23.42	2.12	0.472	0.435
14	3	4	1	3	5	0.734	17.61	2.04	0.422	0.328
15	3	5	2	4	1	0.627	15.04	2.20	0.436	0.232
16	4	1	4	2	5	2.125	51.00	2.63	0.459	0.516
17	4	2	5	3	1	1.926	46.22	2.17	0.451	0.468
18	4	3	1	4	2	1.391	33.38	2.30	0.429	0.324
19	4	4	2	5	3	0.928	22.27	2.15	0.433	0.352
20	4	5	3	1	4	0.858	20.59	2.05	0.429	0.268
21	5	1	5	4	3	2.931	70.34	2.70	0.528	0.636
22	5	2	1	5	4	2.661	63.86	2.53	0.519	0.484
23	5	3	2	1	5	2.017	48.40	2.34	0.487	0.365
24	5	4	3	2	1	1.864	44.73	2.43	0.456	0.228
25	5	5	4	3	2	0.935	22.44	2.24	0.436	0.234

6.3.1 OPTIMIZATION STEPS USING GREY RELATIONAL ANALYSIS FOR SS321

Step I: In this step, the Experimental response values are transformed into S/N ratio values. Further analysis is carried out based on these S/N ratio values. The material removal rate is a higher-the-better performance characteristic, since the maximization of the quality characteristic of interest is sought and can be expressed as (Muthu kumar et al, 2010)

$$\frac{S}{N}Ratio = -\log_{10}(\frac{1}{n}\sum_{i=1}^{n}\frac{1}{y_{ij}^2})$$

Where n= number of replications and

y_{ij} = observed response value y_{ij}

Where i=1, 2... ....n; j = 1, 2...k.

Table 6.14: S/N Ratio values for Electrode E_B

Exp No.	Process Parameters					S/N ratio		
	P on	P off	Wt	Wf	Wp	MRR	SR	KERF
1	1	1	1	1	1	21.10145	-8.94316	9.22
2	1	2	2	2	2	19.756	-8.66417	11.9
3	1	3	3	3	3	18.71623	-8.44154	12.2
4	1	4	4	4	4	17.7175	-8.40645	12.3
5	1	5	5	5	5	16.7398	-8.25743	13.2
6	2	1	2	3	4	17.39031	-8.47532	17.3
7	2	2	3	4	5	17.82462	-8.29337	16.4
8	2	3	4	5	1	18.06816	-8.12238	16.7
9	2	4	5	1	2	18.20882	-7.92392	17.1
10	2	5	1	2	3	18.22376	-7.72759	17.4
11	3	1	3	5	2	18.55876	-8.03411	19.1
12	3	2	4	1	3	18.85552	-8.24261	18.3
13	3	3	5	2	4	19.08613	-8.32309	18
14	3	4	1	3	5	19.25031	-8.34065	18.1
15	3	5	2	4	1	19.32296	-8.29526	18.2
16	4	1	4	2	5	19.58079	-8.51074	20.3
17	4	2	5	3	1	19.80424	-8.65211	19.5
18	4	3	1	4	2	19.98191	-8.75506	19
19	4	4	2	5	3	20.12086	-8.82796	18.8
20	4	5	3	1	4	20.23025	-8.87343	18.7
21	5	1	5	4	3	20.42501	-9.04615	20.9
22	5	2	1	5	4	20.59752	-9.1538	20.7
23	5	3	2	1	5	20.74998	-9.17696	20
24	5	4	3	2	1	20.87626	-9.19021	20
25	5	5	4	3	2	20.97476	-9.15787	20.1

The surface roughness and kerf width are the lower-the-better performance characteristic and the loss function for the same can be expressed as

$$\frac{S}{N}Ratio = -\log_{10}(\frac{1}{n}\sum_{i=1}^{n}y_{ij}^2)$$

The S/N ratio values for the Experimental results for brass wire (E_B) were calculated and presented in Table 6.14. The S/N ratio values for the Experimental results for zinc coated brass wire (E_C) were calculated and presented in Table 6.15

Table 6.15: S/N Ratio values for Electrode E_C

Exp No.	Process Parameters					S/N ratio		
	P on	P off	Wt	Wf	Wp	MRR	SR	KERF
1	1	1	1	1	1	24.65382	-5.39026	9.978815
2	1	2	2	2	2	22.77049	-5.25019	12.12894
3	1	3	3	3	3	21.59151	-4.68898	11.59192
4	1	4	4	4	4	20.77312	-4.20005	12.45023
5	1	5	5	5	5	19.73394	-3.81444	13.27487
6	2	1	2	3	4	20.36911	-4.73297	17.6244
7	2	2	3	4	5	20.79693	-5.07235	17.42198
8	2	3	4	5	1	21.05956	-5.2094	17.88076
9	2	4	5	1	2	21.12499	-5.23527	17.92393
10	2	5	1	2	3	21.14572	-5.09133	18.26825
11	3	1	3	5	2	21.5007	-5.44573	19.40936
12	3	2	4	1	3	21.77433	-5.58156	19.28806
13	3	3	5	2	4	21.97525	-5.66204	19.07655
14	3	4	1	3	5	22.13068	-5.70216	19.10032
15	3	5	2	4	1	22.21213	-5.6938	18.17235
16	4	1	4	2	5	22.45598	-5.9223	20.93931
17	4	2	5	3	1	22.66443	-5.97415	20.04881
18	4	3	1	4	2	22.84439	-6.05464	19.90358
19	4	4	2	5	3	22.98656	-6.08802	20.05778
20	4	5	3	1	4	23.1034	-6.0955	19.04829
21	5	1	5	4	3	23.29385	-6.25614	20.59332
22	5	2	1	5	4	23.46819	-6.35678	20.97995
23	5	3	2	1	5	23.61478	-6.40689	21.21456
24	5	4	3	2	1	23.7318	-6.46987	21.42025
25	5	5	4	3	2	23.82505	-6.49259	20.61168

Step II: In the grey relational analysis, a data pre-processing is first performed in order to normalize the raw data for analysis. Normalization is a transformation performed on a single

data input to distribute the data evenly and scale it into an acceptable range for further analysis. In this study, a linear normalization of the S/N ratio is performed in the range between zero and unity, which is also called the grey relational generating. $y_{ij}$is normalized as Z_{ij}($0 \leq Zij \leq 1$) by the following formula to avoid the effect of adopting different units and to

reduce the variability. The normalized material removal rate corresponding to the larger-the-better criterion can be expressed as (Muthu kumar et al, 2010) shown in Tables 6.16 and 6.17.

$$Z_{ij} = \frac{y_{ij} - \min\left(y_{ij}, i = 1,2,.....n\right)}{\max\left(y_{ij}, i = 1,2,.....n\right) - \min\left(y_{ij}, i = 1,2,.....n\right)}$$

Table 6.16: Normalized S/N ratio values for Electrode E_B

Exp No.	Process Parameters					Normalized S/N ratio		
	P on	P off	Wt	Wf	Wp	MRR	SR	KERF
1	1	1	1	1	1	0.1986	0.5104	0.93582888
2	1	2	2	2	2	0.1123	0.6042	0.86631016
3	1	3	3	3	3	0.0672	0.6667	0.52406417
4	1	4	4	4	4	0.0298	0.6146	0.18181818
5	1	5	5	5	5	0	0.7188	0.1657754
6	2	1	2	3	4	0.3751	0.4271	1
7	2	2	3	4	5	0.2452	0.8021	0.63636364
8	2	3	4	5	1	0.1673	0.8438	0.5828877
9	2	4	5	1	2	0.139	0.9427	0.55614973
10	2	5	1	2	3	0.1008	1	0.51336898
11	3	1	3	5	2	0.4431	0.2656	0.81818182
12	3	2	4	1	3	0.4293	0.3125	0.52941176
13	3	3	5	2	4	0.3247	0.4688	0.36363636
14	3	4	1	3	5	0.2506	0.5729	0.29411765
15	3	5	2	4	1	0.1742	0.7188	0.22459893
16	4	1	4	2	5	0.893	0.1458	0.71122995
17	4	2	5	3	1	0.6272	0.2344	0.45454545
18	4	3	1	4	2	0.427	0.2813	0.22994652
19	4	4	2	5	3	0.3384	0.3281	0.10160428
20	4	5	3	1	4	0.2926	0.3854	0
21	5	1	5	4	3	1	0	0.57754011
22	5	2	1	5	4	0.7204	0.1302	0.47058824
23	5	3	2	1	5	0.5875	0.3854	0.22459893
24	5	4	3	2	1	0.4584	0.4167	0.17112299
25	5	5	4	3	2	0.3685	0.6146	0.13368984

The surface roughness and kerf width should follow the lower-the-better criterion and can be expressed as

$$Z_{ij} = \frac{\max\left(y_{ij,} i = 1,2,.....n\right) - y_{ij}}{\max\left(y_{ij,} i = 1,2,.....n\right) - \min\left(y_{ij,} i = 1,2,.....n\right)}$$

Table 6.17: Normalized S/N ratio values for Electrode E_C

Exp No.	Process Parameters					Normalized S/N ratio		
	P on	P off	Wt	Wf	Wp	MRR	SR	KERF
1	1	1	1	1	1	0.260025	0.571429	1
2	1	2	2	2	2	0.122807	0.612245	0.818681
3	1	3	3	3	3	0.072055	0.843537	0.236264
4	1	4	4	4	4	0.045739	0.952381	0.120879
5	1	5	5	5	5	0	1	0.076923
6	2	1	2	3	4	0.404762	0.197279	0.972527
7	2	2	3	4	5	0.278822	0.367347	0.785714
8	2	3	4	5	1	0.206767	0.469388	0.758242
9	2	4	5	1	2	0.130952	0.564626	0.648352
10	2	5	1	2	3	0.118421	0.816327	0.620879
11	3	1	3	5	2	0.619674	0.136054	0.791209
12	3	2	4	1	3	0.41416	0.340136	0.675824
13	3	3	5	2	4	0.312657	0.394558	0.538462
14	3	4	1	3	5	0.27381	0.44898	0.461538
15	3	5	2	4	1	0.206767	0.544218	0.115385
16	4	1	4	2	5	0.761278	0.047619	0.769231
17	4	2	5	3	1	0.58208	0.360544	0.489011
18	4	3	1	4	2	0.497494	0.272109	0.384615
19	4	4	2	5	3	0.395363	0.37415	0.362637
20	4	5	3	1	4	0.351504	0.442177	0
21	5	1	5	4	3	1	0	0.39011
22	5	2	1	5	4	0.854637	0.115646	0.43956
23	5	3	2	1	5	0.614035	0.244898	0.450549
24	5	4	3	2	1	0.471805	0.183673	0.456044
25	5	5	4	3	2	0.399749	0.312925	0.181319

Step III: The grey relational coefficient is calculated to express the relationship between the ideal (best) and normalized results. The grey relational coefficient can be expressed as (Muthu kumar et al, 2010)

$$\gamma\left(y_o(k), y_i(k)\right) = \frac{\Delta\min + \xi\Delta\max}{\Delta_{oj}(k) + \xi\Delta\max}$$

Where; j = 1, 2...n;

k = 1, 2...m, n is the number of actual data items and m is the number of responses.

$y_o(k)$ is the reference sequence

($y_o(k) = 1$, k = 1,2...m); $y_j(k)$ is the specific comparison sequence.

$\Delta_{oj} = \|y_o(k) - y_j(k)\|$ -The absolute value of the difference between $y_0(k)$ and $y_j(k)$.

$\Delta \min = \min_{\forall j \in i} \min_{\forall k} \|y_o(k) - y_j(k)\|$ is the smallest value of $y_j(k)$

$\Delta \max = \max_{\forall j \in i} \max_{\forall k} \|y_o(k) - y_j(k)\|$ is the largest value of $y_j(k)$

Where ξ is the distinguishing coefficient, which is defined in the range $0 \leq \xi \leq 1$.The Wire EDM process parameters, is equally weighted in this study, and therefore ξ is 0.5.

Step IV: The grey relational grade is determined by averaging the grey relational coefficient corresponding to each performance characteristic. The overall performance characteristic of the multiple response process depends on the calculated grey relational grade. The grey relational coefficient can be expressed as (Muthu kumar et al, 2010)

$$\overline{\gamma_j} = \frac{1}{k} \sum_{i=1}^{m} \gamma_{ij}$$

Where $\overline{\gamma_j}$ the grey relational grade for the jth experiment and k is the number of performance characteristics.

This approach converts a multiple response process optimization problem into a single response optimization situation with the objective function of an overall grey relational grade. Table 6.7 shows the grey relation coefficient and grey relational grade for each experiment using the L_{25} orthogonal array. The higher grey relational grade reveals that the corresponding actual result is closer to the ideally normalized value. Experiment no 21 for electrode E_B similarly experiment no 1for electrode E_C has the best multiple performance characteristic shown among 25 experiments, because it has the highest grey relational grade shown in Table 6.18 and 6.19 corresponding Figures shown in 6.4 and 6.5. The higher the value of the grey

relational grade, the closer the corresponding factor combination is, to the optimal. A higher grey relational grade implies better product quality; therefore, on the basis of the grey relational grade, the factor effect can be estimated and the optimal level for each controllable factor can also be determined.

Table 6.18: Grey Relational Co-efficient and Grey Relational Grade of Electrode E_B

Exp No.	Process Parameters					Grey Relational Co-efficient			Grey grade
	P on	P off	Wt	Wf	Wp	MRR	SR	KERF	
1	1	1	1	1	1	0.38420898	0.505263	0.8863	0.5919093
2	1	2	2	2	2	0.36030829	0.55814	0.789	0.5691591
3	1	3	3	3	3	0.34897361	0.6	0.5123	0.4871007
4	1	4	4	4	4	0.34008833	0.564706	0.3793	0.4280348
5	1	5	5	5	5	0.33333333	0.64	0.3747	0.4493609
6	2	1	2	3	4	0.44448217	0.466019	1	0.6368338
7	2	2	3	4	5	0.39847793	0.716418	0.5789	0.564614
8	2	3	4	5	1	0.37517913	0.761905	0.5452	0.560757
9	2	4	5	1	2	0.36738703	0.897196	0.5297	0.5981094
10	2	5	1	2	3	0.35735736	1	0.5068	0.6213774
11	3	1	3	5	2	0.47307553	0.405063	0.7333	0.5371573
12	3	2	4	1	3	0.46699964	0.421053	0.5152	0.4677346
13	3	3	5	2	4	0.42541436	0.484848	0.44	0.4500876
14	3	4	1	3	5	0.40018343	0.539326	0.4146	0.4513811
15	3	5	2	4	1	0.37712475	0.64	0.392	0.4697194
16	4	1	4	2	5	0.82378855	0.369231	0.6339	0.6089725
17	4	2	5	3	1	0.57286652	0.395062	0.4783	0.4820630
18	4	3	1	4	2	0.46600214	0.410256	0.3937	0.4233142
19	4	4	2	5	3	0.43045051	0.426667	0.3576	0.4048899
20	4	5	3	1	4	0.41410946	0.448598	0.3333	0.3986803
21	5	1	5	4	3	1	0.333333	0.542	**0.6475207**
22	5	2	1	5	4	0.64135228	0.365019	0.4857	0.4973618
23	5	3	2	1	5	0.547928	0.448598	0.392	0.4628532
24	5	4	3	2	1	0.48001467	0.461538	0.3763	0.4392702
25	5	5	4	3	2	0.4418814	0.564706	0.3659	0.4575121

Table 6.19: Grey Relational Co-efficient and Grey Relational Grade of Electrode E_C

Exp No.	Process Parameters					Grey Relational Co-efficient			Grey grade
	P on	P off	Wt	Wf	Wp	MRR	SR	KERF	
1	1	1	1	1	1	0.403234	0.538462	1	**0.646832**
2	1	2	2	2	2	0.363057	0.563218	0.733871	0.553382
3	1	3	3	3	3	0.350154	0.761658	0.395652	0.502488
4	1	4	4	4	4	0.343817	0.913043	0.36255	0.539804
5	1	5	5	5	5	0.333333	1	0.351351	0.561562
6	2	1	2	3	4	0.456522	0.383812	0.947917	0.596083
7	2	2	3	4	5	0.409441	0.441441	0.7	0.516961
8	2	3	4	5	1	0.386628	0.485149	0.674074	0.515283
9	2	4	5	1	2	0.365217	0.534545	0.587097	0.49562
10	2	5	1	2	3	0.361905	0.731343	0.56875	0.553999
11	3	1	3	5	2	0.567972	0.366584	0.705426	0.54666
12	3	2	4	1	3	0.460473	0.431085	0.606667	0.499408
13	3	3	5	2	4	0.421108	0.452308	0.52	0.464472
14	3	4	1	3	5	0.407767	0.475728	0.481481	0.454992
15	3	5	2	4	1	0.386628	0.523132	0.361111	0.423624
16	4	1	4	2	5	0.676845	0.344262	0.684211	0.568439
17	4	2	5	3	1	0.54471	0.438806	0.494565	0.492694
18	4	3	1	4	2	0.49875	0.407202	0.448276	0.451409
19	4	4	2	5	3	0.452638	0.444109	0.439614	0.445453
20	4	5	3	1	4	0.435352	0.472669	0.333333	0.413785
21	5	1	5	4	3	1	0.333333	0.450495	0.594609
22	5	2	1	5	4	0.774757	0.361179	0.471503	0.535813
23	5	3	2	1	5	0.564356	0.398374	0.47644	0.479723
24	5	4	3	2	1	0.486289	0.379845	0.478947	0.44836
25	5	5	4	3	2	0.454442	0.421203	0.379167	0.418271

Since the actual design is orthogonal, it is possible to separate out the effect of each machining parameter on the grey relational grade at different levels.

The mean of the grey relational grade for each level of the other machining parameters can be computed in a similar manner. The mean of the grey relational grade for each level of the machining parameters is summarized and as shown in Table 6.18 and 6.19.

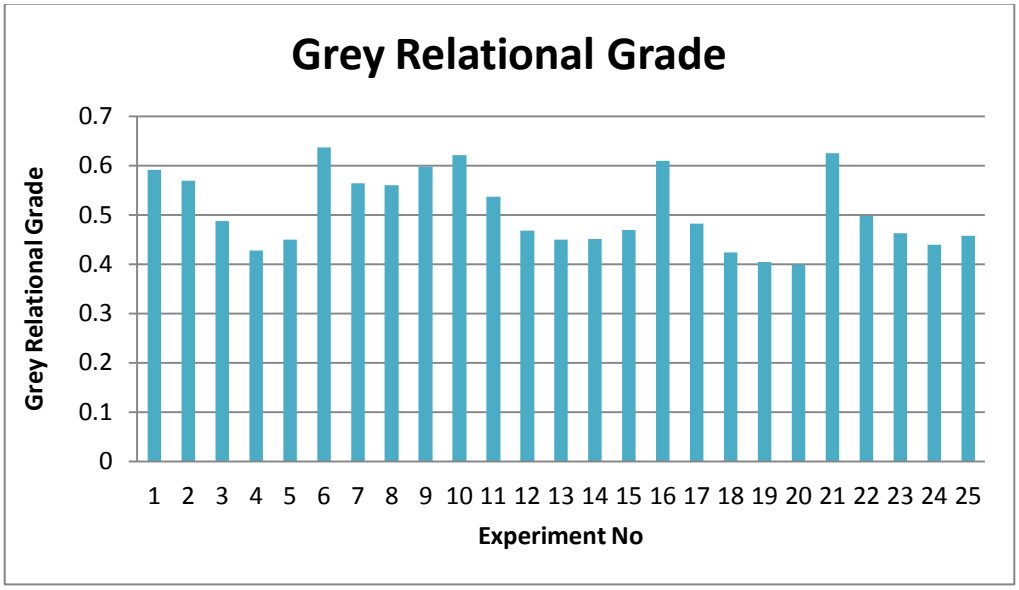

Figure 6.4 Grey Relational Grades for max MRR, min SR and min KERF for Electrode E_B

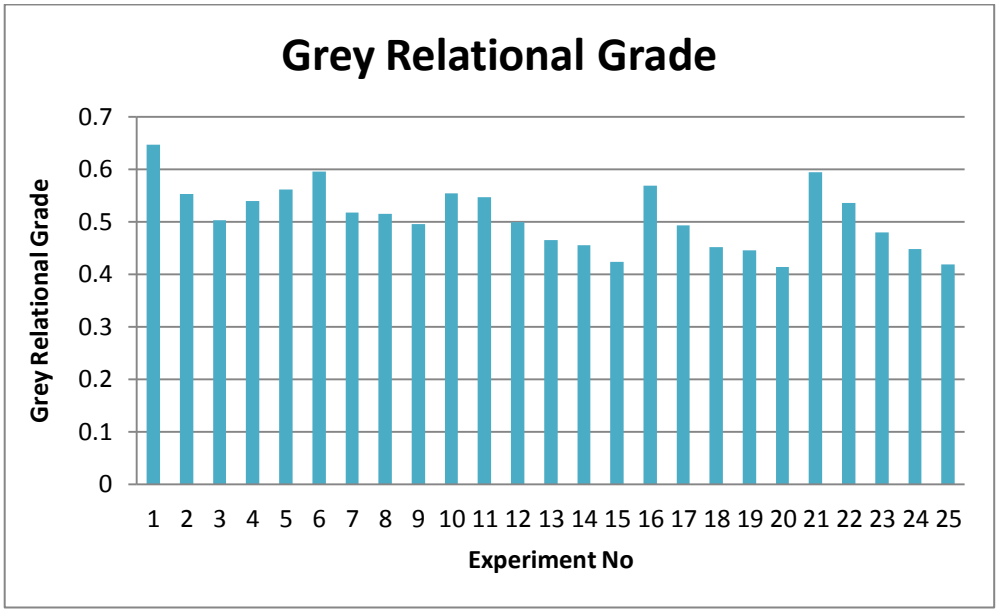

Figure 6.5 Grey Relational Grades for max MRR, min SR and min KERF for Electrode E_C

Table 6.20: Main effects of the Factors on the Grey Relational Grade for Electrode E_B

Symbol	Process Parameters	Level 1	Level 2	Level 3	Level4	Level5	Max-min
A	Pon	0.505113	0.596329	0.472211	0.431235	0.69642	0.134755
B	Poff	**2.876994**	2.521933	2.383214	2.322186	2.39665	0.678708
C	Wt	2.562134	2.643456	2.432823	2.528812	**2.50237**	0.177976
D	Wf	2.512878	**2.583739**	2.524891	2.516660	2.46395	0.239377
E	Wp	2.543721	2.585252	**2.623224**	2.410999	2.53221	0.195224

Table 6.21: Main effects of the Factors on the Grey Relational Grade for Electrode E_C

Symbol	Process Parameters	Level 1	Level 2	Level 3	Level4	Level5	Max-min
A	Pon	**0.570893**	0.634589	0.567831	0.584356	0.55355	0.061333
B	Poff	**2.963024**	2.698258	2.513376	2.484229	2.47124	0.581585
C	Wt	2.543446	2.598266	2.528254	**2.641205**	2.638957	0.181402
D	Wf	2.435768	2.488653	2.564528	2.676407	**2.612272**	0.011212
E	Wp	2.627193	2.665343	**2.695958**	2.582957	2.581277	0.056002

Step V: Determine the optimal factor and its level combination (Muthu kumar et al, 2010)

Figure 6.6 shows the grey relational grade bar chart. Generally, the larger the grey relational grade, is better in the multiple performance characteristic. However, the relative importance among the machining parameters for the multiple performance characteristics still needs to be known, so that the optimal combinations of the machining parameter levels can be determined more accurately. The optimal parametric combinations are shown in Table 6.20 and 6.21. Comparatively shown in Figure 6.6 further it is also bolded in the tables. The optimal process parameter setting becomes A_5 (pulse on time, 16 µs), B_1 (pulse off time, 18 µs), C_3 (Wire tension, 6 Kg-f), D_3 (wire feed rate, 9 mm/min) and E_5 (water flushing pressure, 6 Kg/cm2) for brass wire and A_5 (pulse on time, 8 µs), B_1(pulse off time, 18 µs), C_3 (Wire tension, 10 Kg-f), D_3 (wire feed rate, 8 mm/min), E_5 (water flushing pressure 5 Kg/cm2) for zinc coated brass wire.

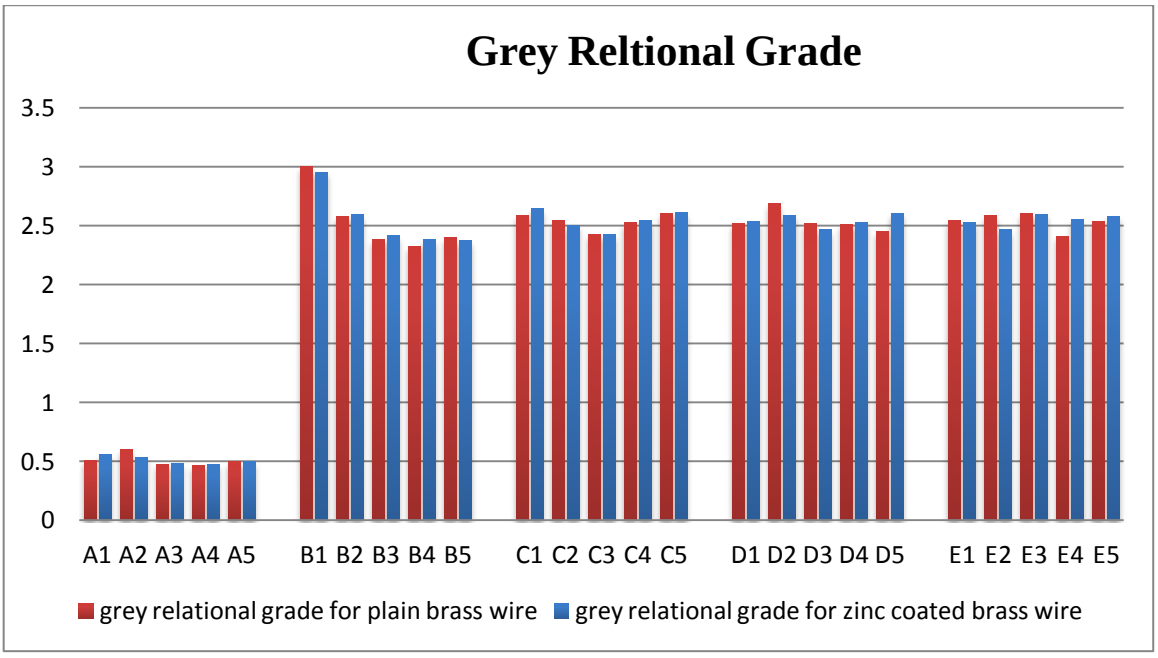

Figure 6.6 Response graphs of average Grey Relational Grade for electrodes E_B and E_C

6.3.2 VALIDATION OF THE EXPERIMENTAL RESULTS

The confirmation test for the optimal parameter setting with its selected levels was conducted to evaluate the quality characteristics for Wire EDM machining on SS321 work material using brass and zinc coated brass wire electrode materials. (Muthu kumar et al, 2010)

Experiment 21 (Table 6.18) and experiment 1 (Table 6.19) shows the highest grey relational grade for brass wire and zinc coated brass wire respectively, indicating the optimal process parameter set of $A_5B_1C_3D_3E_5$ (Brass wire) and $A_5B_1C_3D_3E_5$ (zinc coated brass wire) has the best multiple performance characteristics among the twenty five experiments, which can be compared with results of confirmation experiment for validation of results. Table 6.22 shows the comparison of the actual results of machining on Wire EDM process parameters on SS321 work material using brass wire and zinc coated brass wire. The response values obtained from the confirmation experiment are MRR = 55.472mm^2/min, SR = 2.82 μm and kerf = 0.421 mm for brass wire and MRR= 68.304mm^2/min, SR = 1.95μm, Kerf = 0.395mm for zinc coated brass wire. The Material Removal Rate shows an increased from 55.472mm^2/min to 68.304mm^2/min, the Surface Roughness shows value of 2.82μm to 1.95μm and the kerf width shows a reduced value of 0.421 to 0.395 mm for Electrodes E_B and E_C.

Table – 6.22: Experimental results for SS321 using Electrodes E_B and E_C

S.No.	Machining Characteristics	Experimental Value for Electrode E_B	Experimental Value for Electrode E_C
1.	Optimal parameters	$A_5B_1C_3D_3E_5$	$A_5B_1C_3D_3E_5$
2.	Cutting Speed (CS)	2.528 mm/min	2.846 mm/min
3.	Material Removal Rate (MRR)	55.472mm^2/min	68.304 mm^2/min
4.	Surface Roughness (SR)	2.82 μm	1.95 μm
5.	Cutting Width (KERF)	0.421mm	0.395mm
6.	Dimensional Deviation (DD)	0.186%	0.182%
7.	Grey Relation Grade	0.6475	0.6468

Similar calculation is done for SS17-4 PH and H13 tool steel materials using Grey relational Analysis (GRA). The Normalized S/N ratios for SS17-4 PH and H13 tool steel materials are shown in Appendix II. The Optimum Results SS17-4 PH and H13 tool steel materials using Electrodes E_B and E_C are shown in the following Tables 6.23 and 6.24.

Table 6.23: Experimental results for SS17-4 PH using Electrodes E_B and E_C

S.No.	Machining Characteristics	Experimental Value for Electrode E_B	Experimental Value for Electrode E_C
1.	Optimal parameters	$A_5B_1C_3D_3E_5$	$A_5B_1C_4D_3E_4$
2.	Cutting Speed (CS)	2.552 mm/min	2.869mm/min
3.	Material Removal Rate (MRR)	61.248mm^2/min	68.856mm^2/min
4.	Surface Roughness (SR)	2.75μm	1.75 μm
5.	Cutting Width (KERF)	0.386mm	0.426mm
6.	Dimensional Deviation (DD)	0.153 %	0.156%
7.	Grey Relation Grade	0.6578	0.6352

Table 6.24: Experimental results for H13 using Electrodes E_B and E_C

S.No.	Machining Characteristics	Experimental Value for Electrode E_B	Experimental Value for Electrode E_C
1.	Optimal parameters	$A_5B_1C_4D_3E_5$	$A_5B_1C_3D_3E_5$
2.	Cutting Speed (CS)	2.258 mm/min	2.527 mm/min
3.	Material Removal Rate (MRR)	54.192mm^2/min	60.648mm^2/min
4.	Surface Roughness (SR)	2.56 μm	2.04 μm
5.	Cutting Width (KERF)	0.415mm	0.396mm
6.	Dimensional Deviation (DD)	0.175 %	0.172 %
7.	Grey Relation Grade	0.6586	0.6826

6.4 SUMMARY

The present chapter gives the results analysis and discussions for SS316 and SS321 work material using E_B and E_C electrodes. The results analysis is done for multi-objective optimization by Grey Relational Analysis. The experiments were conducted for all the work materials to investigate the effect of process parameters on the output responses such as cutting speed, material removal rate, surface roughness, kerf (cutting width) and dimensional deviation using E_B and E_C electrodes. The experimental results are presented for all work materials with the combinations of E_B and E_C electrodes.

Chapter 7

Comparison of Results for Brass and Zinc Coated Brass Wires

7.1 INTRODUCTION

The present chapter gives the performance results of E_B and E_C electrode materials on SS316, SS321, SS17-4 PH and H13 tool steels. The comparison results of responses as cutting speed (CS), material removal rate (MRR), surface roughness (SR), cutting width (KERF) and dimensional deviation (DD) are presented and analyzed. Such as Pon, Poff, Wt, Wf, and Wp. The Wire EDM process parameters pulse on, pulse off, wire tension, wire feed and water pressure are considered as input parameters for the experimentation using taguchi design method. In this chapter the results were compared between for each wire and each work material combinations. The performance is depicted in terms of plots and tables for all possible combinations of work materials. The tabular columns and graphs are plotted for each work and electrode material combinations. The combinations of experimental results are presented in the following sections.

7.2 COMPARISON OF RESULTS FOR SS316 USING E_B AND E_C ELECTRODES

The Wire EDM machining performance of E_B and E_C electrodes while machining SS316 is shown in Figures 7.1 and 7.2 respectively. The performance characteristics Cutting Speed, Material Removal Rate, Surface Roughness, Cutting Width and Dimensional Deviation in Wire EDM of SS316 are experimentally measured and theoretically predicted (Ref: In chapter 5 Table 27 and 31). These results are also presented in Table 7.1.

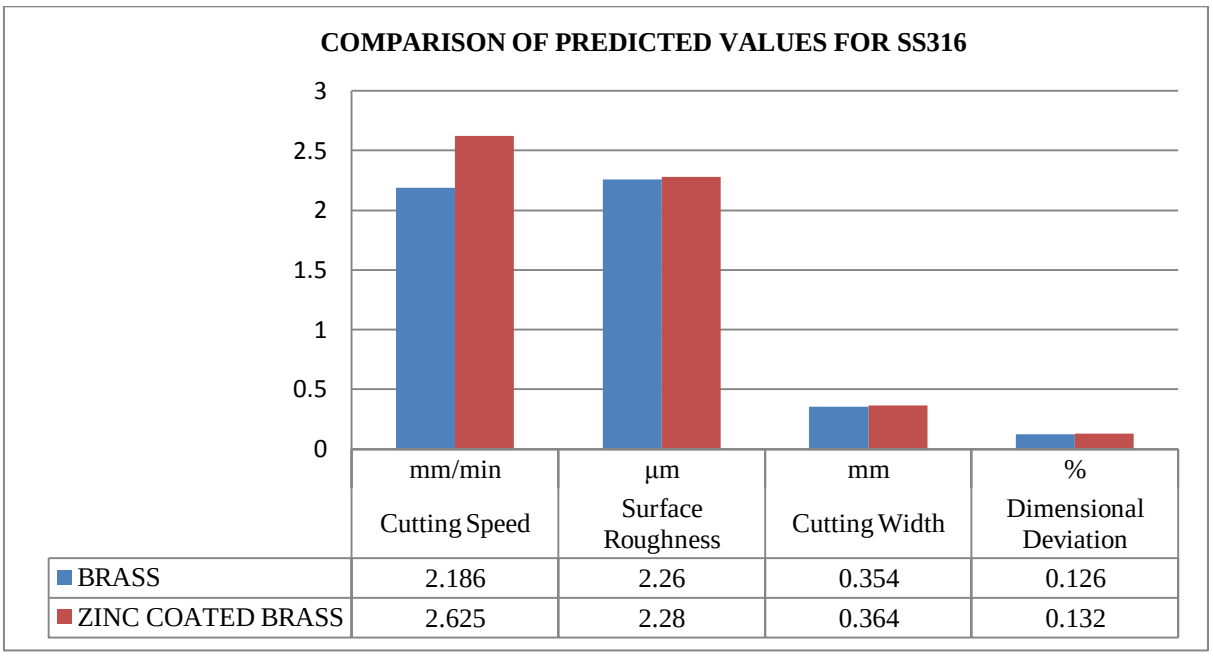

Figure 7.1: Comparison of Predicted Values for SS316

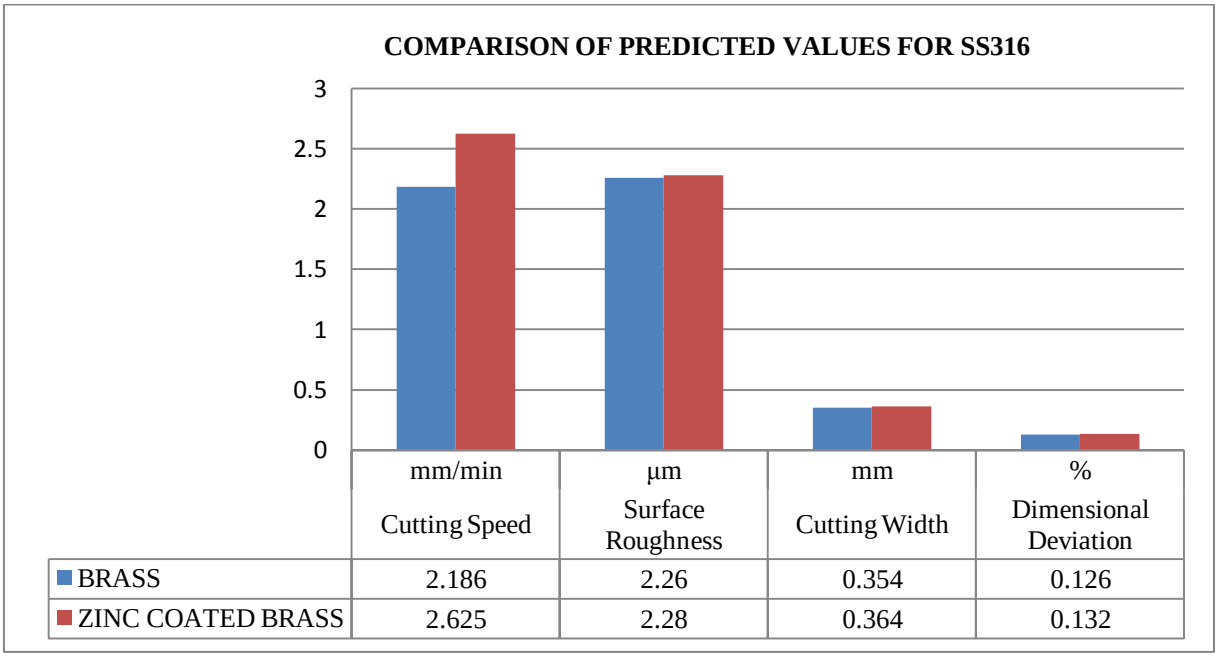

Figure 7.2: Comparison of Experimental Values for SS316

Table 7.1: Predicted and Experimental values comparison for SS316

S.No.	Machining Characteristics	units	Predicted Values		Experimental Values	
			Brass	Zinc Coated Brass	Brass	Zinc Coated Brass
1.	Cutting Speed	mm/min	2.064	2.359	2.186	2.625
2.	Material Removal Rate	mm^2/min	49.53	56.61	52.46	63.01
3.	Surface Roughness	µm	1.84	1.95	2.26	2.28
4.	Cutting Width (Kerf)	mm	0.338	0.349	0.354	0.364
5.	Dimensional Deviation	%	0.104	0.106	0.126	0.132

7.3 COMPARISON OF RESULTS FOR SS321 E_B AND E_C ELECTRODES

The results are compared for SS321 using Brass and Zinc Coated Brass wires as electrodes. The following Table 7.2 shows the comparison of predicted and experimental values for SS321 work material using brass and zinc coated brass as electrode materials. Figure 7.3 and 7.4 shows the comparison graphs for machining characteristics of Cutting Speed, Material Removal Rate, Surface Roughness, Cutting Width and Dimensional Deviation for SS316 using brass and zinc coated brass wires.

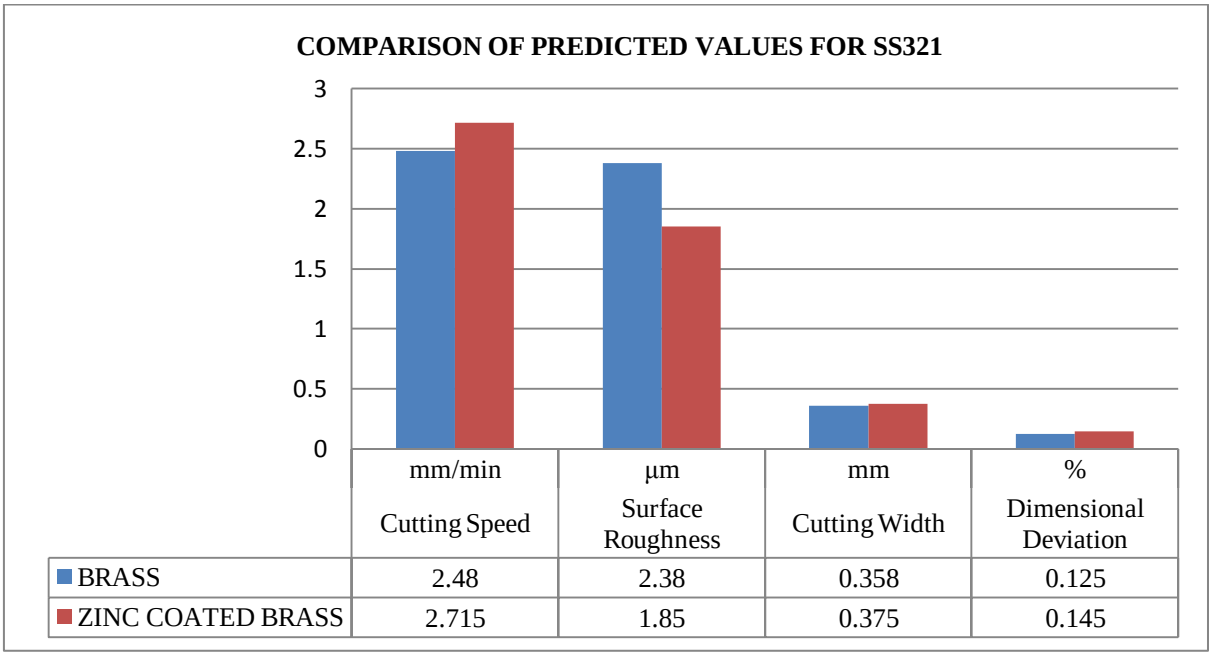

Figure 7.3: Comparison of Predicted Values for SS321

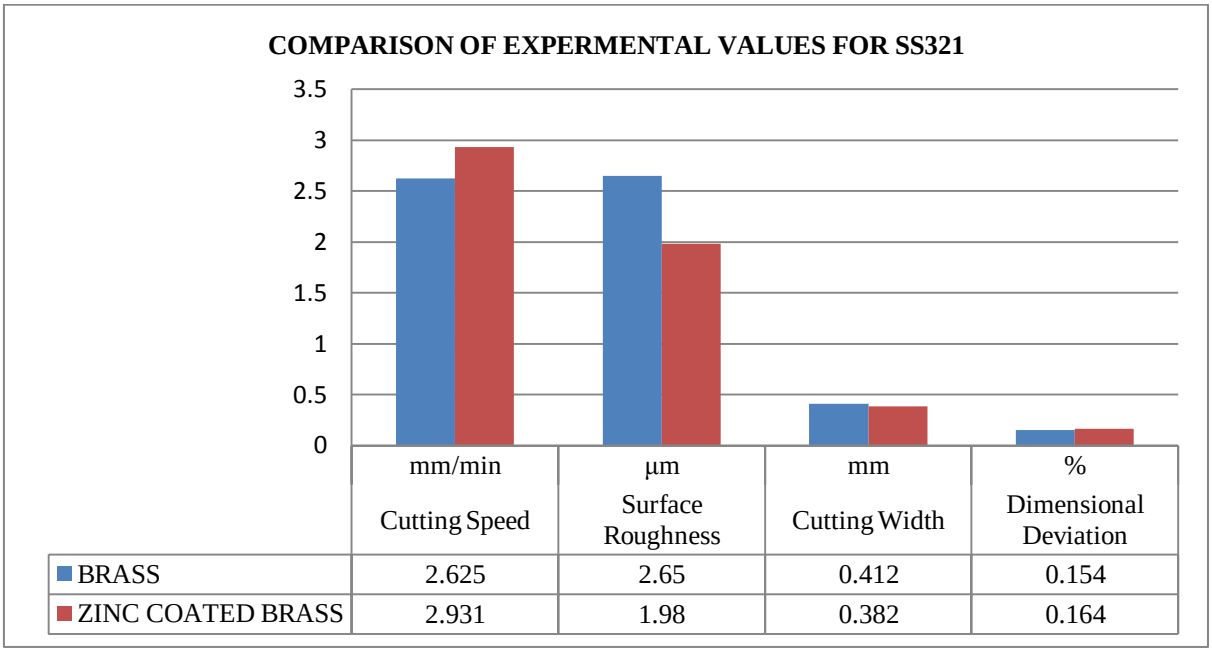

Figure 7.4: Comparison of Experimental Values for SS321

Table 7.2: Predicted and Experimental values comparison for SS321

S.No.	Machining Characteristics	units	Predicted Value		Experimental Value	
			Brass	Zinc Coated Brass	Brass	Zinc Coated Brass
1.	Cutting Speed	mm/min	2.480	2.715	2.625	2.931
2.	Material Removal Rate	mm^2/min	59.52	65.16	63.00	70.34
3.	Surface Roughness	µm	2.38	1.85	2.65	1.98
4.	Cutting Width (Kerf)	mm	0.358	0.375	0.412	0.382
5.	Dimensional Deviation	%	0.125	0.145	0.154	0.164

7.4 COMPARISON OF RESULTS FOR SS17- 4PH USING E_B AND E_C ELECTRODES

The Wire EDM machining performance of E_B and E_C electrodes while machining SS17-4 PH is shown in Figures 7.5 and 7.6 respectively. The performance characteristics Cutting Speed, Material Removal Rate, Surface Roughness, Cutting Width and Dimensional Deviation in Wire EDM of SS17-4 PH are experimentally measured and theoretically predicted (Ref: In chapter 5 Table 29 and 33). These results are also presented in Table 7.3.

Table 7.3: Predicted and Experimental values comparison for SS17-4 PH

S.No.	Machining Characteristics	units	Predicted Value		Experimental Value	
			Brass	Zinc Coated Brass	Brass	Zinc Coated Brass
1.	Cutting Speed	mm/min	2.552	2.827	2.964	2.953
2.	Material Removal Rate	mm^2/min	61.24	67.84	71.13	70.87
3.	Surface Roughness	µm	2.35	1.73	2.82	1.96
4.	Cutting Width (Kerf)	mm	0.365	0.379	0.418	0.413
5.	Dimensional Deviation	%	0.136	0.162	0.158	0.185

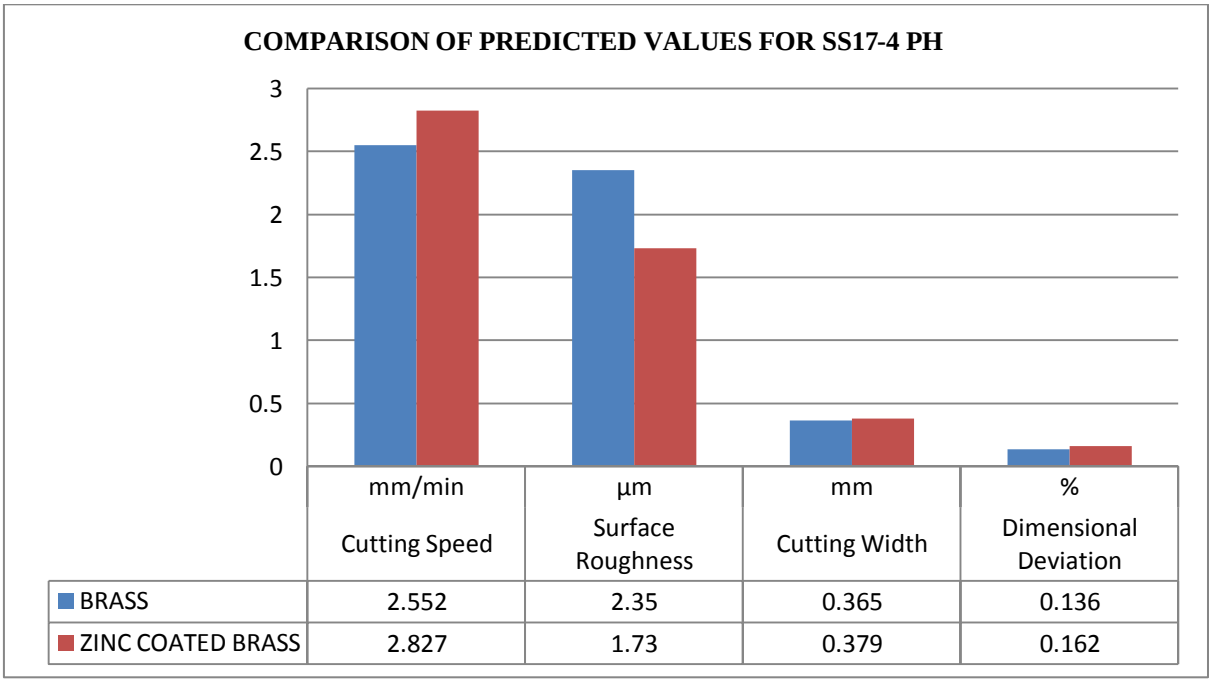

Figure 7.5: Comparison of Predicted Values for SS17-4 PH

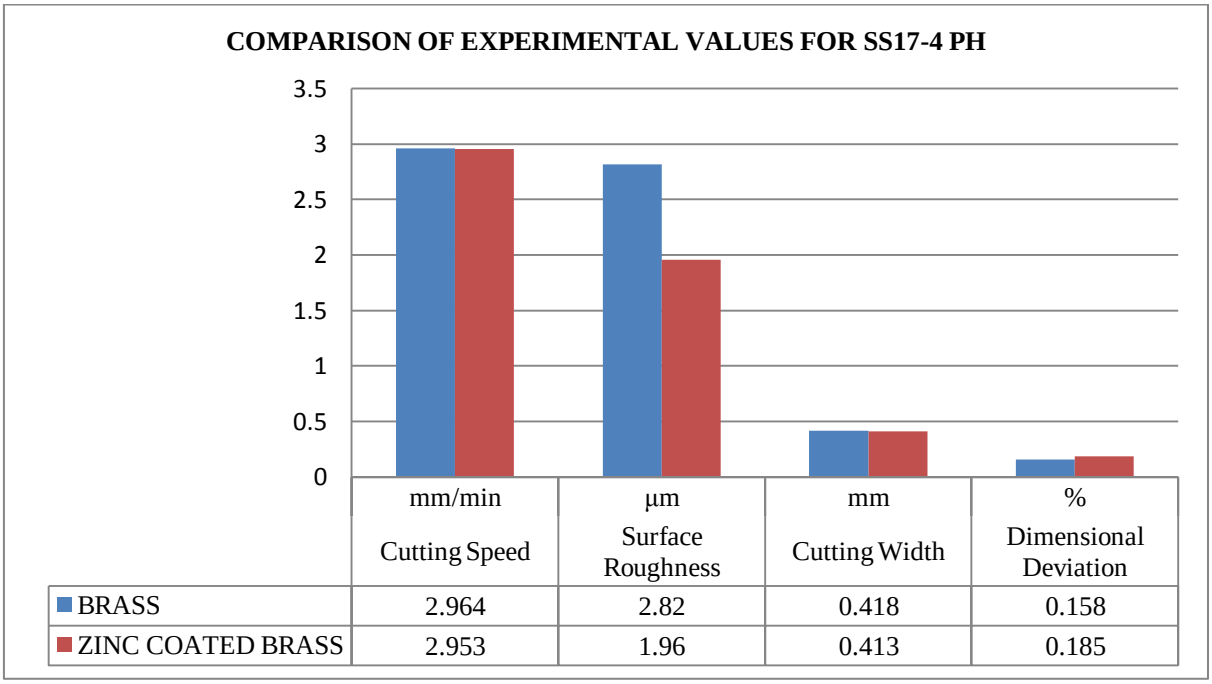

	mm/min Cutting Speed	µm Surface Roughness	mm Cutting Width	% Dimensional Deviation
BRASS	2.964	2.82	0.418	0.158
ZINC COATED BRASS	2.953	1.96	0.413	0.185

Figure 7.6: Comparison of Experimental Values for SS17-4 PH

7.5 COMPARISON OF RESULTS FOR H13 USING E_B AND E_C ELECTRODES

The Wire EDM machining performance of E_B and E_C electrodes while machining H13 is shown in Figures 7.7 and 7.8 respectively. The performance characteristics Cutting Speed, Material Removal Rate, Surface Roughness, Cutting Width and Dimensional Deviation in Wire EDM of H13 are experimentally measured and theoretically predicted (Ref: In chapter 5 Table 30 and 34). These results are also presented in Table 7.4.

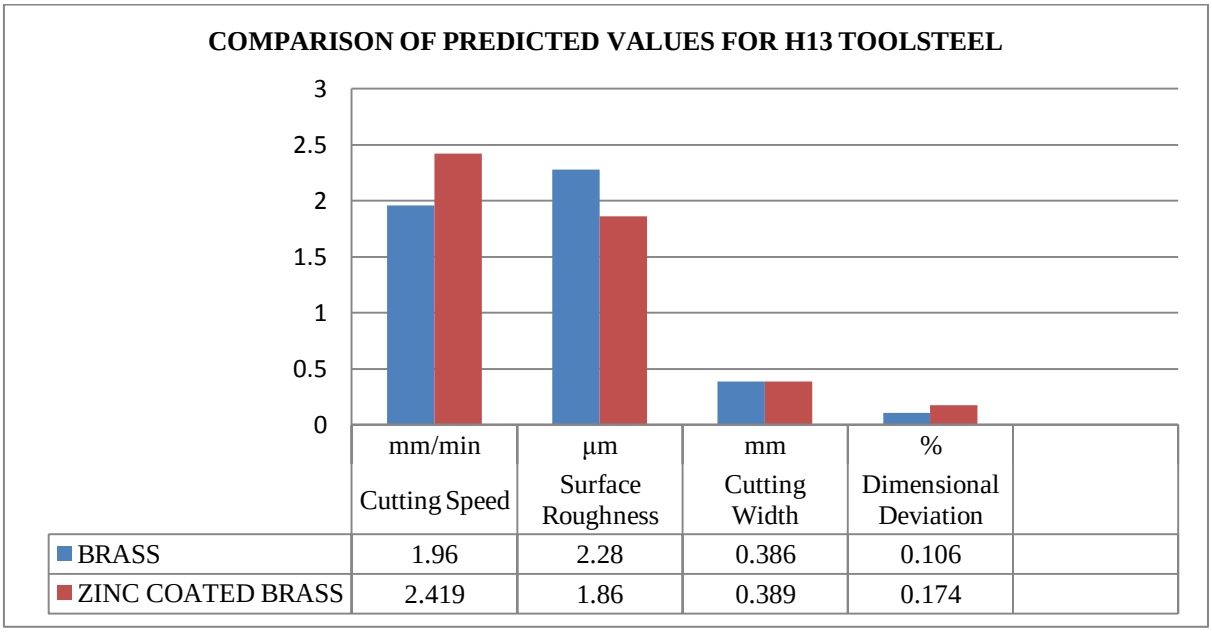

	mm/min Cutting Speed	µm Surface Roughness	mm Cutting Width	% Dimensional Deviation	
BRASS	1.96	2.28	0.386	0.106	
ZINC COATED BRASS	2.419	1.86	0.389	0.174	

Figure 7.7: Comparison of Predicted Values for H13 tool steel

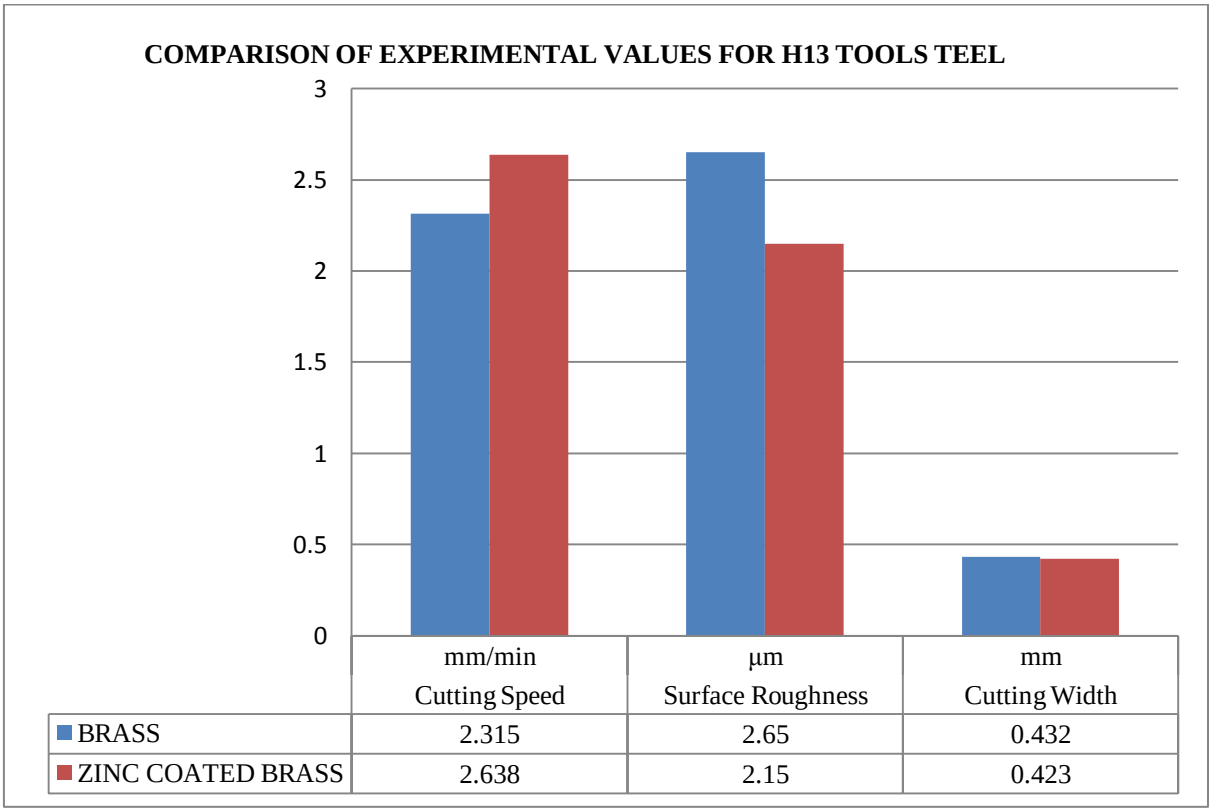

Figure 7.8: Comparison of Experimental Values for H13 tool steel

Table 7.4: Predicted and Experimental values comparison for H13 tool steel

S.No.	Machining Characteristics	units	Predicted Value		Experimental Value	
			Brass	Zinc Coated Brass	Brass	Zinc Coated Brass
1.	Cutting Speed	mm/min	1.960	2.419	2.315	2.638
2.	Material Removal Rate	mm^2/min	47.04	58.05	55.56	63.31
3.	Surface Roughness	µm	2.28	1.86	2.65	2.15
4.	Cutting Width (Kerf)	mm	0.386	0.389	0.432	0.423
5.	Dimensional Deviation	%	0.106	0.174	0.138	0.195

7.6 COMPARISON OF RESULTS BY GREY RELATIONAL ANALYSIS

The results are compared for the materials of SS316, SS321, SS17-4 PH and H13 tool steel with Brass and Zinc coated brass wire using the Taguchi's single objective optimization method and the comparison tables and graphs are drawn. Also the results were compared for the Multi-objective optimization using grey relational analysis for SS316, SS321, SS17-4 PH and H13 tool steel materials with Brass and Zinc coated brass wires. The SEM images are also compared for the materials of SS321, SS17-4 PH and H13 tool steel with Brass and Zinc coated brass wire as electrode materials.

7.6.1 COMPARISON OF RESULTS FOR SS316 USING E_B AND E_C ELECTRODES

The results are compared for SS316 using Brass and Zinc Coated Brass wires as electrodes. The following Table 7.5 shows the comparison of predicted and experimental values for SS316 work material using brass and zinc coated brass as electrode materials. Figure 7.9 shows the comparison graphs for machining characteristics of Cutting Speed, Material Removal Rate, Surface Roughness, Cutting Width and Dimensional Deviation for SS316 using brass and zinc coated brass wires.

Table 7.5: Experimental values comparison for SS316

S.No.	Machining Characteristics	units	Experimental Value	
			Brass	Zinc Coated Brass
1.	Optimal parameters		$A_5B_1C_2D_3E_4$	$A_5B_1C_3D_3E_5$
2.	Cutting Speed (CS)	mm/min	2.218	2.654
3.	Material Removal Rate (MRR)	mm^2/min	53.232	63.69
4.	Surface Roughness (SR)	µm	2.28	2.34
5.	Cutting Width (KERF)	mm	0.398	0.386
6.	Dimensional Deviation (DD)	%	0.136	0.124

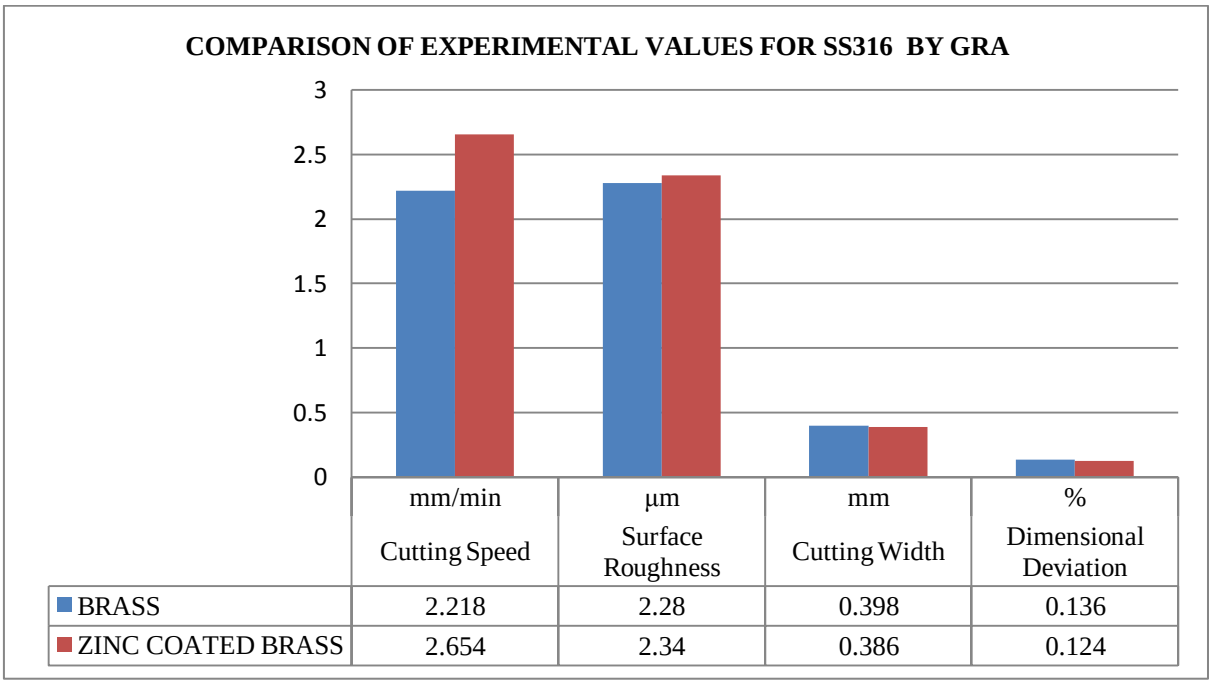

Figure 7.9: Comparison of Experimental Values for SS316

7.6.2 COMPARISON OF RESULTS FOR SS321 USING E_B AND E_C ELECTRODES

The results are compared for SS321 using Brass and Zinc Coated Brass wires as electrodes. The following Table 7.6 shows the comparison of predicted and experimental values for SS321 work material using brass and zinc coated brass as electrode materials. Figure 7.10 shows the comparison graphs for machining characteristics of Cutting Speed,

Material Removal Rate, Surface Roughness, Cutting Width and Dimensional Deviation for SS316 using brass and zinc coated brass wires.

Table 7.6: Experimental values comparison for SS321

S.No.	Machining Characteristics	units	Experimental Value	
			Brass	Zinc Coated Brass
1.	Optimal parameters		$A_5B_1C_3D_3E_5$	$A_5B_1C_3D_3E_5$
2.	Cutting Speed (CS)	mm/min	2.728	2.846
3.	Material Removal Rate (MRR)	mm^2/min	65.47	68.30
4.	Surface Roughness (SR)	µm	2.82	1.95
5.	Cutting Width (KERF)	mm	0.421	0.390
6.	Dimensional Deviation (DD)	%	0.186	0.182

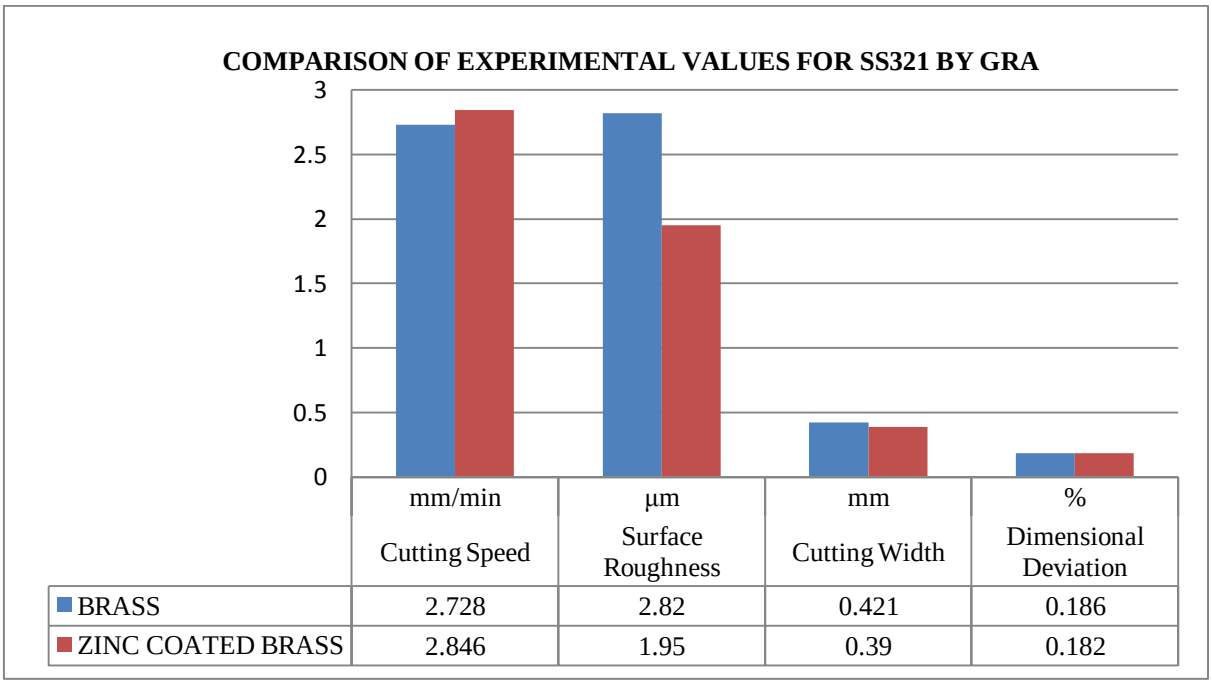

Figure 7.10: Comparison of Experimental Values for SS321

7.6.3 COMPARISON OF RESULTS FOR SS17-4 PH USING E_B AND E_C

The results are compared for SS17-4 using Brass and Zinc Coated Brass wires as electrodes. The following Table 7.7 shows the comparison of predicted and experimental values for SS17-4 work material using brass and zinc coated brass as electrode materials. Figure 7.11 shows the comparison graphs for machining characteristics of Cutting Speed, Material Removal Rate, Surface Roughness, Cutting Width and Dimensional Deviation for SS316 using brass and zinc coated brass wires.

Table 7.7: Experimental values comparison for SS17-4 PH

S.No.	Machining Characteristics	units	Experimental Value	
			Brass	Zinc Coated Brass
1.	Optimal parameters		$A_5B_1C_3D_3E_5$	$A_5B_1C_4D_3E_4$
2.	Cutting Speed (CS)	mm/min	2.852	2.869
3.	Material Removal Rate (MRR)	mm^2/min	68.44	68.86
4.	Surface Roughness (SR)	µm	2.75	1.75
5.	Cutting Width (KERF)	mm	0.386	0.426
6.	Dimensional Deviation (DD)	%	0.153	0.156

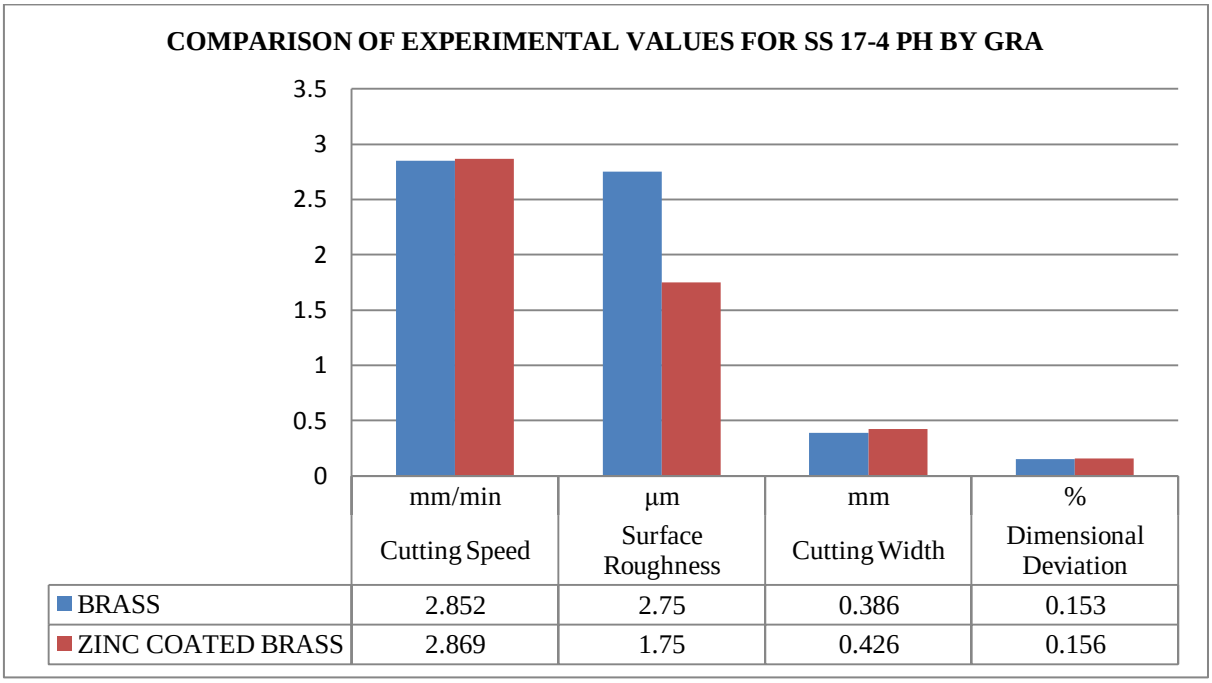

Figure 7.11: Comparison of Experimental Values for SS17-4 PH

7.6.4 COMPARISON OF RESULTS FOR H13 USING E_B AND E_C ELECTRODES

Table 7.8: Experimental values comparison for H13 Tool Steel

S.No.	Machining Characteristics	units	Experimental Value	
			Brass	Zinc Coated Brass
1.	Optimal parameters		$A_5B_1C_4D_3E_5$	$A_5B_1C_3D_3E_5$
2.	Cutting Speed (CS)	mm/min	2.258	2.527
3.	Material Removal Rate (MRR)	mm^2/min	54.19	60.64
4.	Surface Roughness (SR)	µm	2.56	2.04
5.	Cutting Width (KERF)	mm	0.415	0.396
6.	Dimensional Deviation (DD)	%	0.175	0.172

The results are compared for H13 tool steel using Brass and Zinc Coated Brass wires as electrodes. The following Table 7.8 shows the comparison of predicted and experimental values for H13 tool steel work material using brass and zinc coated brass as electrode materials. Figure 7.12 shows the comparison graphs for machining characteristics of

Cutting Speed, Material Removal Rate, Surface Roughness, Cutting Width and Dimensional Deviation for SS316 using brass and zinc coated brass wires. Figure 7.13 shows the comparison graph for brass and zinc coated brass wires as electrode materials on Wire EDM of hard steels like SS316, SS321, SS17-4 PH and H13 tool steel.

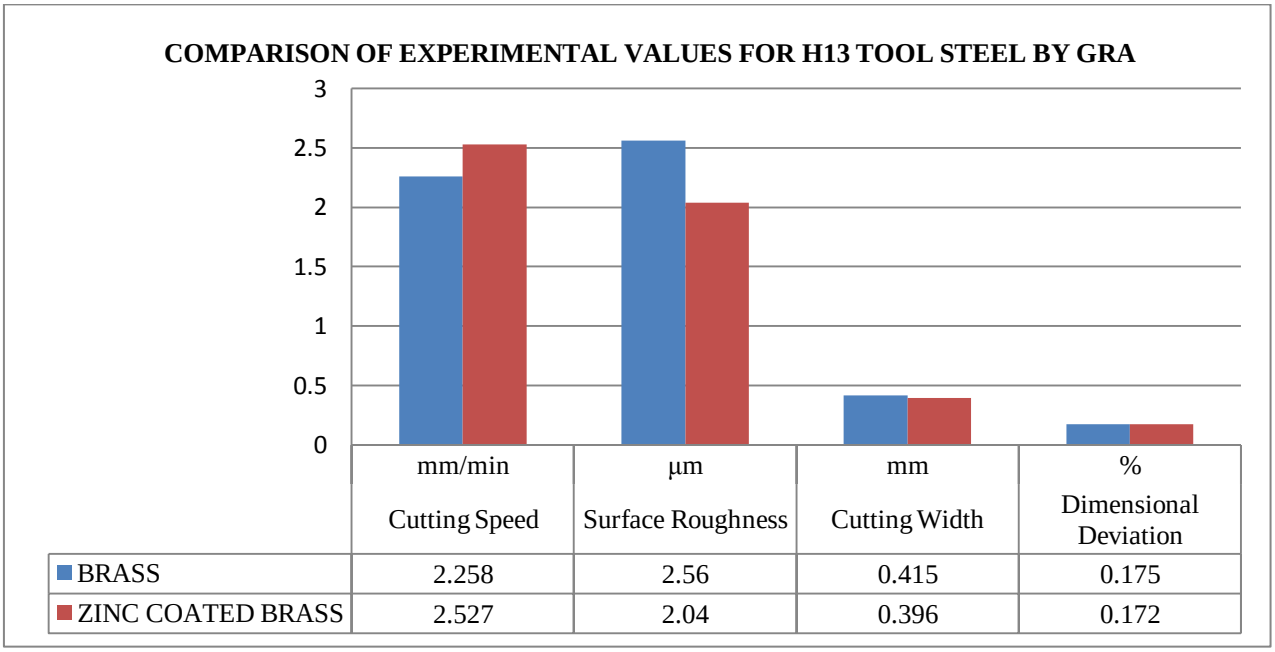

Figure 7.12: Comparison of Experimental Values for H13 Tool Steel

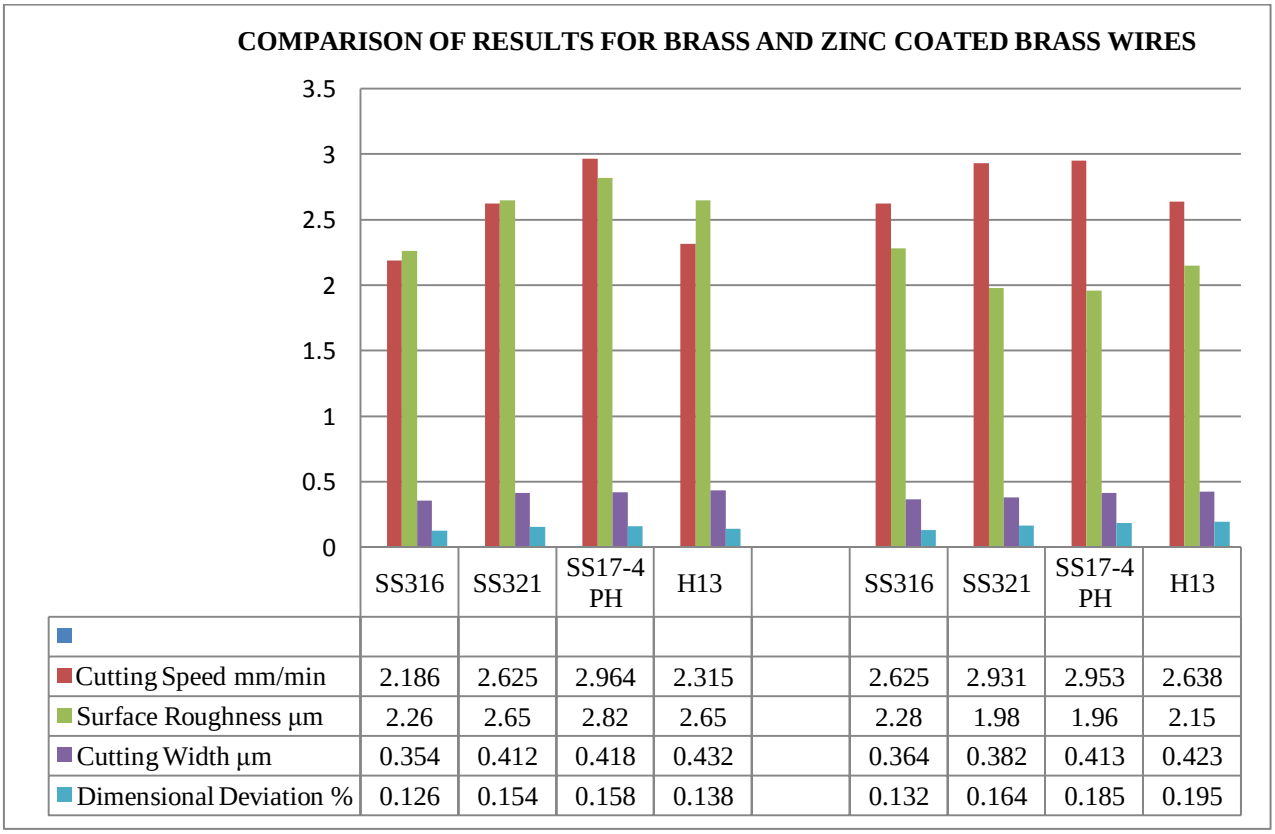

Figure 7.13: Comparison of Experimental Values for Brass and Zinc Coated Brass Wires

7.7 REGRESSION EQUATIONS

The regression equations are developed for the response machining characteristics in terms of process parameters of the Wire EDM. The five important process parameters namely pulse on, pulse off, wire tension, wire feed and water pressure has been investigated on machining of SS316, SS321, SS17-4 Ph and H13 work materials. The four machining characteristics namely cutting speed (CS), surface roughness (SR), kerf (cutting width) and dimensional deviation (DD) were observed on Wire EDM. The empirical models have been developed for all the hard steel materials and each machining characteristic as given below:

7.7.1 REGRESSION EQUATIONS FOR SS316 USING E_B ELECTRODE

The regression equation in terms of process parameters

Cutting Speed = - 0.765 + 0.159 * Pulse on - 0.0390 * Pulse off + 0.0312 * Wire Tension + 0.0551 * Wire Feed + 0.0554 * Water Pressure

The regression equation in terms of process parameters

Surface Roughness = 2.93 + 0.0218 * Pulse on - 0.0227 * Pulse off- 0.00910 * Wire Tension - 0.0066 * Wire Feed+ 0.0060 * Water Pressure

The regression equation in terms of process parameters

Kerf = 0.530 + 0.00807 * Pulse on - 0.00288 * Pulse off - 0.00178 * Wire Tension- 0.00692 * Wire Feed - 0.00238 * Water Pressure

The regression equation in terms of process parameters

Dimensional Deviation = 0.621 + 0.00702 * Pulse on - 0.00482 * Pulse off + 0.00345 * Wire Tension - 0.0284 * Wire Feed+ 0.0008 * Water Pressure

7.7.2 REGRESSION EQUATIONS FOR SS316 USING E_C ELECTRODE

The regression equation in terms of process parameters

Cutting Speed = - 0.200 + 0.189 * Pulse on - 0.0578 * Pulse off + 0.0185 * Wire Tension + 0.0387 * Wire Feed + 0.0214 * Water Pressure

The regression equation in terms of process parameters

Surface Roughness = 3.35 + 0.0158 * Pulse on - 0.0294 * Pulse off + 0.0095 * Wire Tension - 0.0076 * Wire Feed - 0.0172 * Water Pressure

The regression equation in terms of process parameters

Kerf = 0.503 + 0.00440 * Pulse on - 0.00452 * Pulse off - 0.00066 * Wire Tension - 0.00056 * Wire Feed + 0.00260 * Water Pressure

The regression equation in terms of process parameters

Dimensional Deviation = 1.01 - 0.00343 * Pulse on - 0.0182 * Pulse off + 0.00727 * Wire Tension - 0.0073 * Wire Feed- 0.0234 * Water Pressure

7.8 SEM STUDY AFTER WIRE EDM OPERATION

Two major surface flaws namely morphology (machined area) and surface projection (unmachined area) has been done on wire EDM machined samples using scanning electron microscope (SEM). Scanning Electron Microscopy (SEM) images of the Wire EDMed surfaces were taken in order to compare the effect of brass and zinc coated brass wire types on machining of SS316, SS321, SS17-4 PH and H13 work piece materials by analyzing surface integrity and characteristics. The SEM study is done for the specimens of the maximum metal removal rate, maximum surface roughness and minimum material removal rate, minimum surface roughness values of the experimental results for the brass and zinc coated brass wires. The SEM micrographs of Wire EDMed surfaces are taken at different magnifications of 100x, 200x, 500x, 1000x, 1500x, and 2000x. The SEM images are shown in the Figures below.

7.8.1 SEM IMAGES FOR SS316 USING E_B AND E_C ELECTRODES

In the present study, the SEM micrograph images are taken for SS316 work material at maximum and minimum material removal rate (MRR), maximum and minimum surface roughness (SR) of Wire EDM machined specimens with wire electrodes of brass and zinc coated brass.

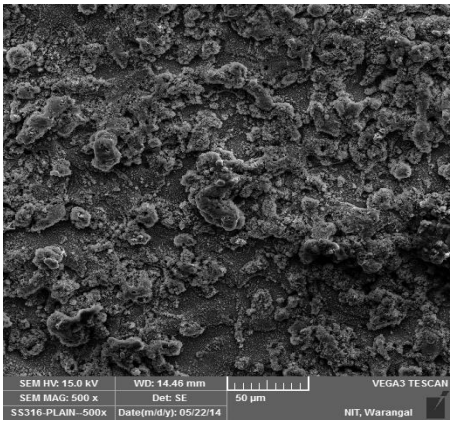

(a) Max MRR for brass

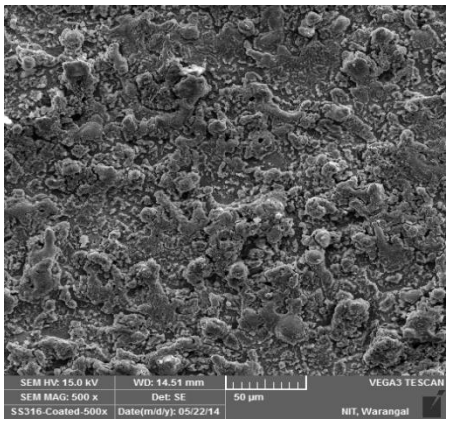

(b) Max MRR for zinc coated brass

Figure 7.14(a, b): The maximum MRR for SS316 with brass and zinc coated brass wires

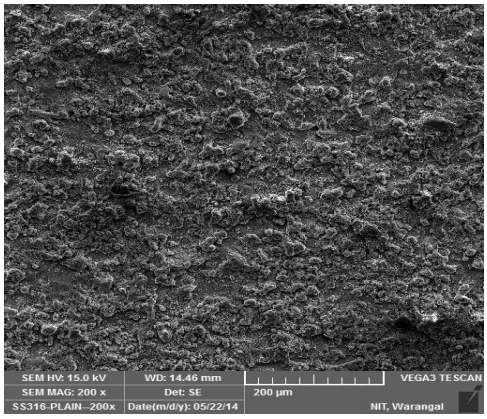

(a) Min MRR for brass

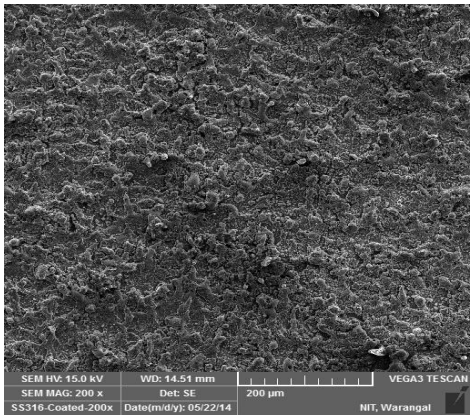

(b) Min MRR for zinc coated brass

Figure 7.15(a, b): The minimum MRR for SS316 with brass and zinc coated brass wires

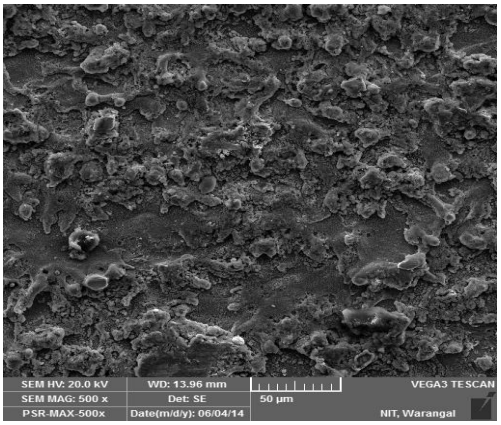

(a) Max SR for brass

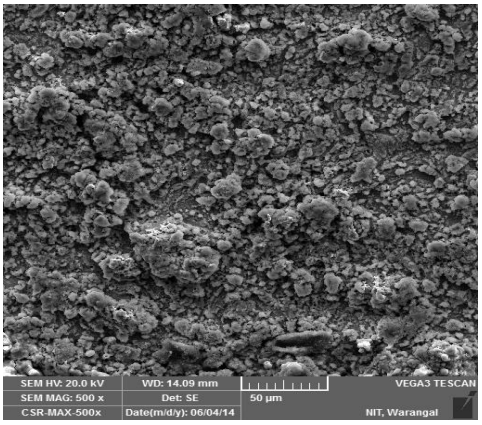

(b) Max SR for zinc coated brass

Figure 7.16(a, b): The maximum SR for SS316 with brass and zinc coated brass wires

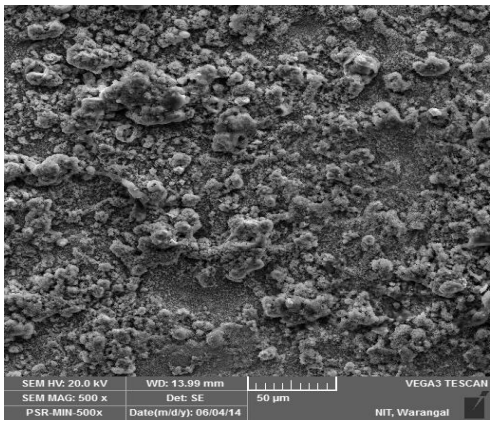

(a) Min SR for brass

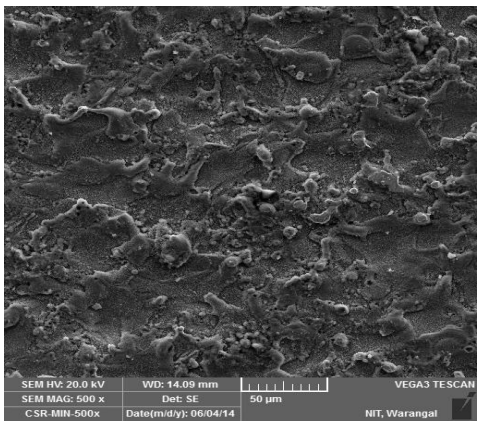

(b) Min SR for zinc coated brass

Figure 7.17(a, b): The minimum SR for SS316 with brass and zinc coated brass wires

Figures 7.14(a, b) and 7.15(a, b) shows the SEM images for maximum and minimum material removal rate of Wire EDM machined specimens with brass and zinc coated brass wire electrodes. Figures 7.16(a, b) and 7.17(a, b) shows the SEM micrographs for maximum and minimum surface roughness of Wire EDM machined specimens with both electrode

combinations. From the above images it is clear that the maximum material removal rate and minimum surface roughness images of zinc coated brass electrode wire has smooth surface, the least craters formation than the micrograph images of brass wire electrode.

7.8.2 SEM IMAGES FOR SS321 USING E_B AND E_C ELECTRODES

In the present study, the SEM micrograph images are taken for SS321 work material at maximum and minimum material removal rate (MRR), maximum and minimum surface roughness (SR) of Wire EDM machined specimens with wire electrodes of brass and zinc coated brass.

Figures 7.18(a, b) and 7.19(a, b) shows the SEM images for maximum and minimum material removal rate of Wire EDM machined specimens with brass and zinc coated brass wire electrodes. Figures 7.20(a, b) and 7.21(a, b) shows the SEM micrographs for maximum and minimum surface roughness of Wire EDM machined specimens with both electrode combinations. From the above images it is clear that the maximum material removal rate and minimum surface roughness images of zinc coated brass electrode wire has smooth surface, the least craters formation than the micrograph images of brass wire electrode. Zinc coated Brass wires was one of the first attempts to present more zinc to the wire's cutting surface. This wire consists of a thin coating of zinc (approximately 5 micron). Because of the zinc coating on the brass core material, the cutting speed is higher and produce exceptional surface finishes. These wires are particularly utilized for better surface accuracy than the brass wires. The brass wire electrodes are produce unacceptable Brass plating on the work piece.

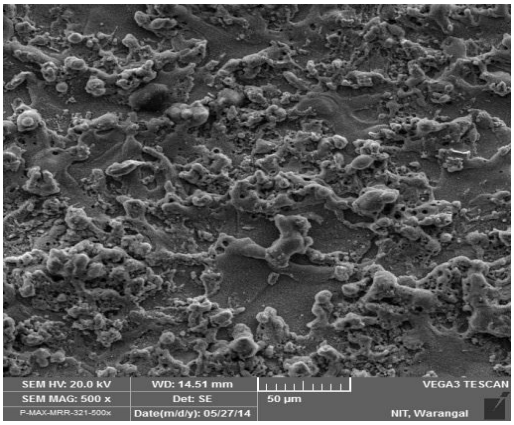

(a) Max MRR for brass

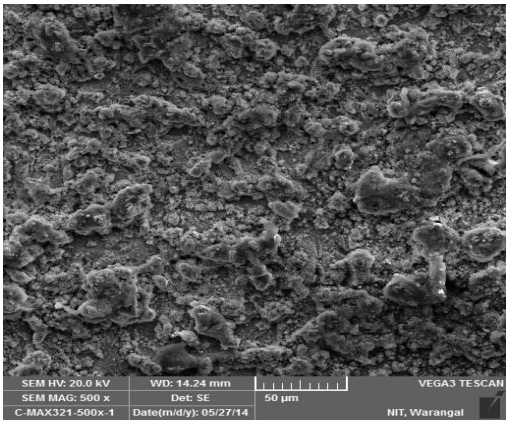

(b) Max MRR for zinc coated brass

Figure 7.18(a, b): The maximum MRR for SS321with brass and zinc coated brass wires

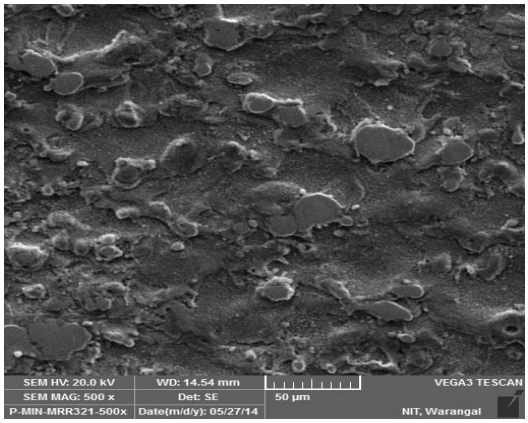

(a) Min MRR for brass

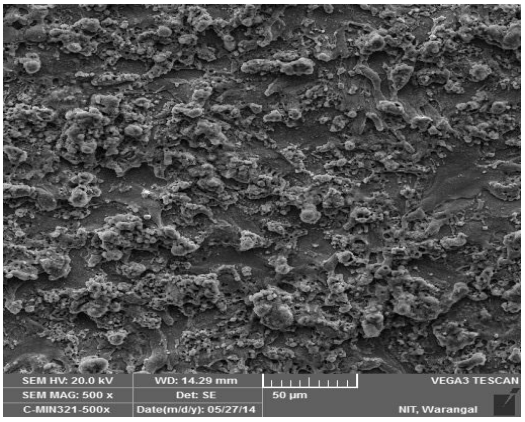

(b) Min MRR for zinc coated brass

Figure 7.19(a, b): The minimum MRR SS321 with for brass and zinc coated brass wires

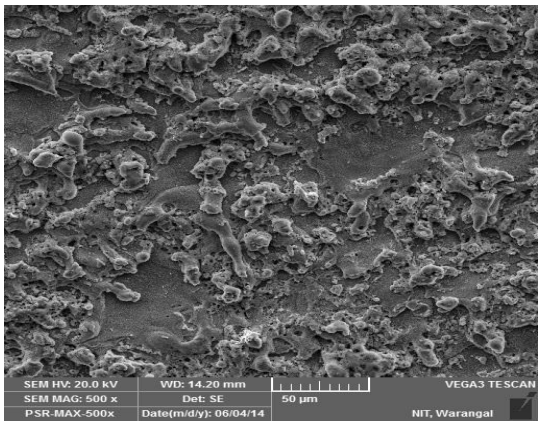

(a) Max SR for brass

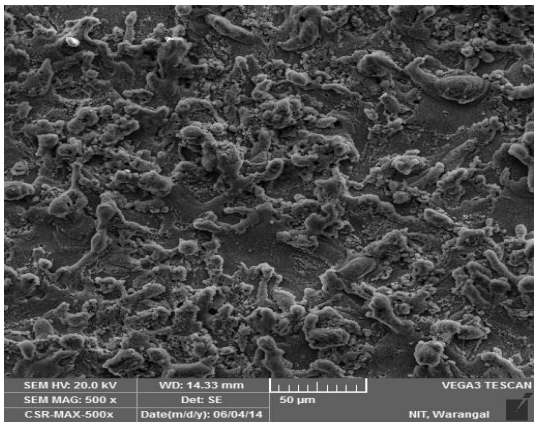

(b) Max SR for zinc coated brass

Figure 7.20(a, b): The maximum SR for SS321with brass and zinc coated brass wires

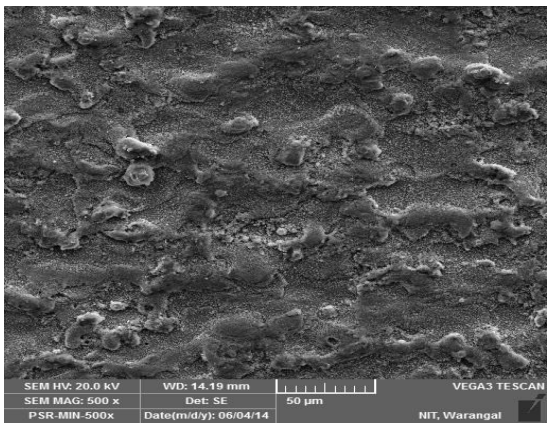

(a) Min SR for brass

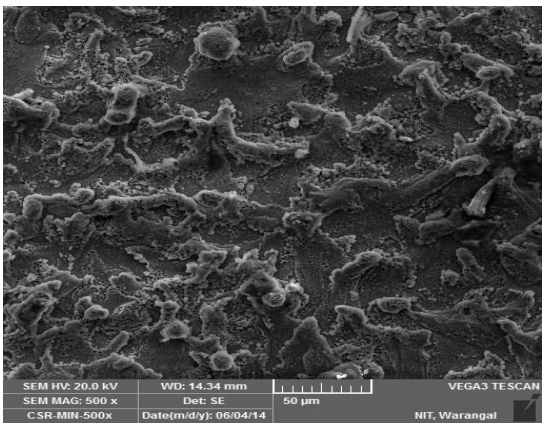

(b) Min SR for zinc coated brass

Figure 7.21(a, b): The minimum SR for SS321with brass and zinc coated brass wires

7.8.3 SEM IMAGES FOR SS17-4 USING E_B AND E_C ELECTRODES

In the present study, the SEM micrograph images are taken for SS17-4 PH work material at maximum and minimum material removal rate (MRR), maximum and minimum surface roughness (SR) of Wire EDM machined specimens with wire electrodes of brass and zinc coated brass.

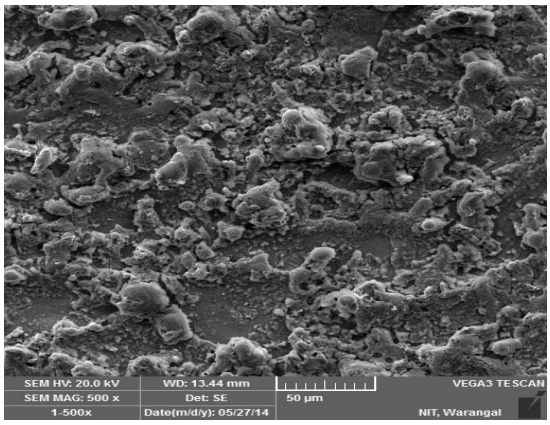

(a) Max MRR for brass

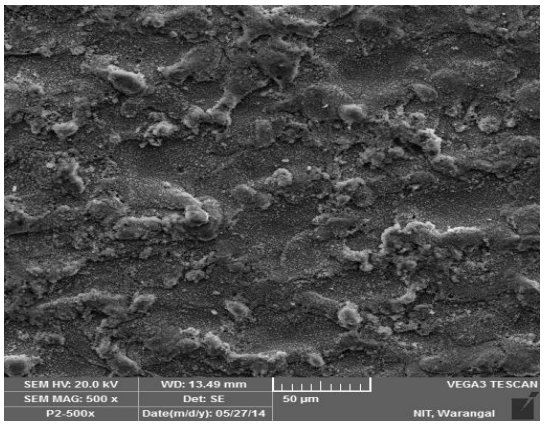

(b) Max MRR for zinc coated brass

Figure 7.22(a, b): The maximum MRR for SS17-4 with brass and zinc coated brass wires

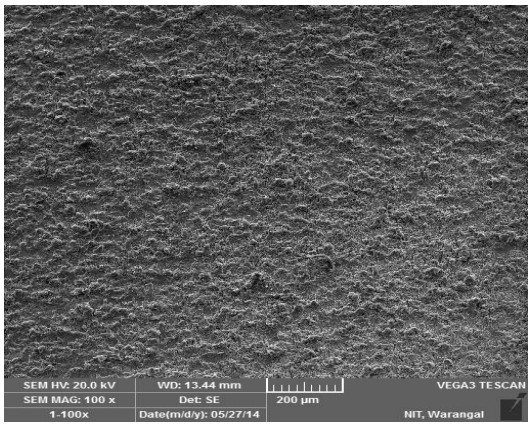

(a) Min MRR for brass

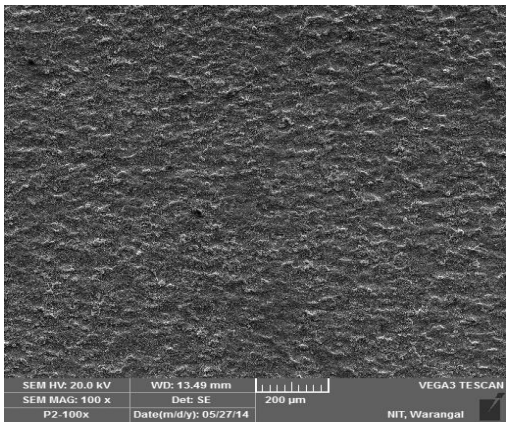

(b) Min MRR for zinc coated brass

Figure 7.23(a, b): The minimum MRR for SS17-4 with brass and zinc coated brass wires

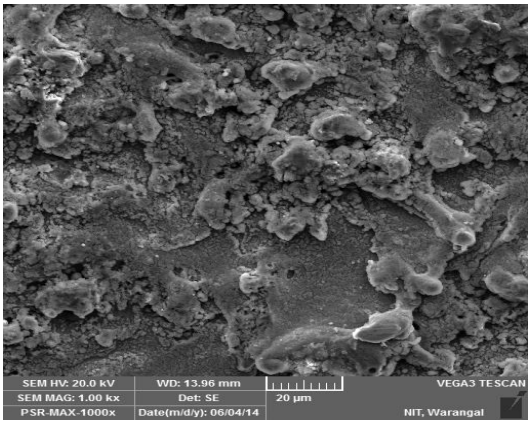

(a) Max SR for brass

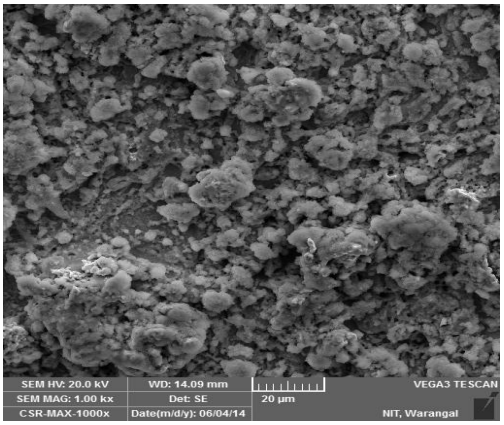

(b) Max SR for zinc coated brass

Figure 7.24(a, b): The maximum SR for SS17-4 with brass and zinc coated brass wires

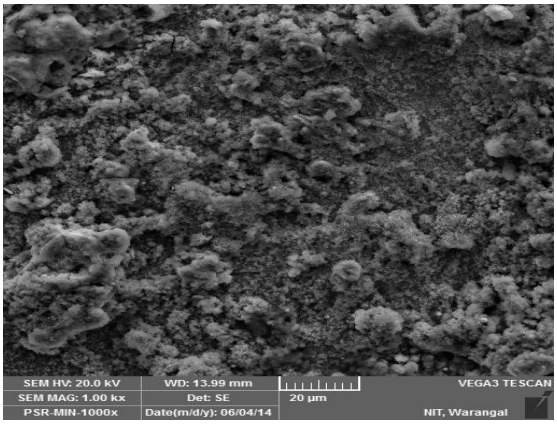

(a) Min SR for brass

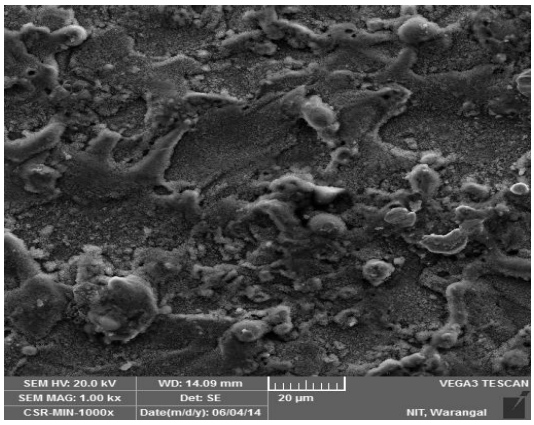

(b) Min SR for zinc coated brass

Figure 7.25(a, b): The minimum SR for SS17-4 with brass and zinc coated brass wires

Figures 7.22(a, b) and 7.23(a, b) shows the SEM images for maximum and minimum material removal rate of Wire EDM machined specimens with brass and zinc coated brass wire electrodes. Figures 7.24(a, b) and 7.25(a, b) shows the SEM micrographs for maximum and minimum surface roughness of Wire EDM machined specimens with both electrode combinations. It is clear from the SEM images, that the surface roughness is much better for the work pieces were cut by zinc coated brass wire **.**The craters formation is least in samples cutting by zinc coated brass wire. Using brass wire electrode cutting, the molten material has come out in chunks which gets stuck to the surface**.** In brass wire cutting, big size of droplets sticking to the surface, which indicates that the proper metal removal may lead to smooth surface finish has not taken place.

7.8.4 SEM IMAGES FOR H13 USING E_B AND E_C ELECTRODES

In the present study, the SEM micrograph images are taken for H13 work material at maximum and minimum material removal rate (MRR), maximum and minimum surface roughness (SR) of Wire EDM machined specimens with wire electrodes of brass and zinc coated brass.

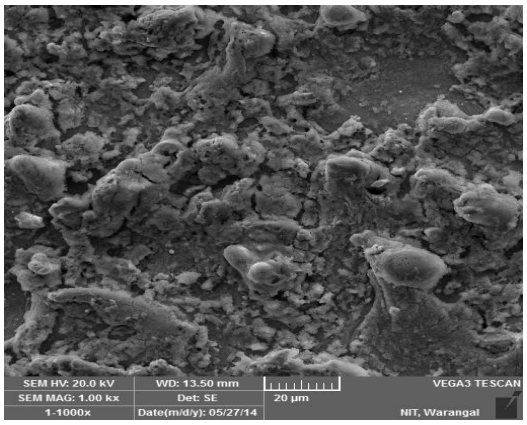

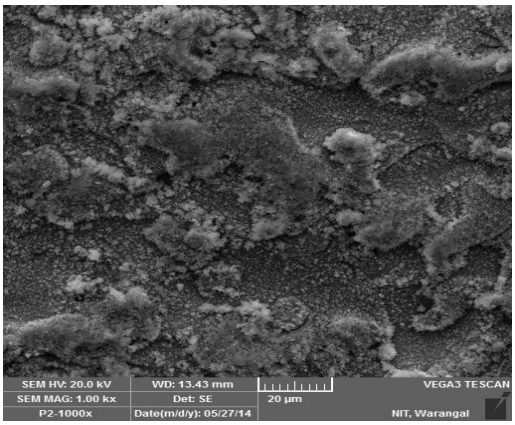

(a) Max MRR for brass (b) Max MRR for zinc coated brass

Figure 7.26(a, b): The maximum MRR for H13 with brass and zinc coated brass wires

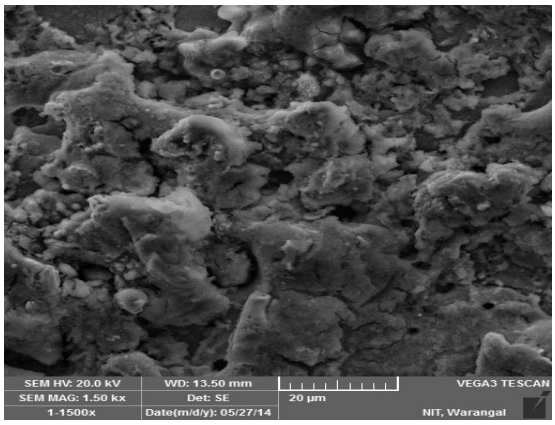

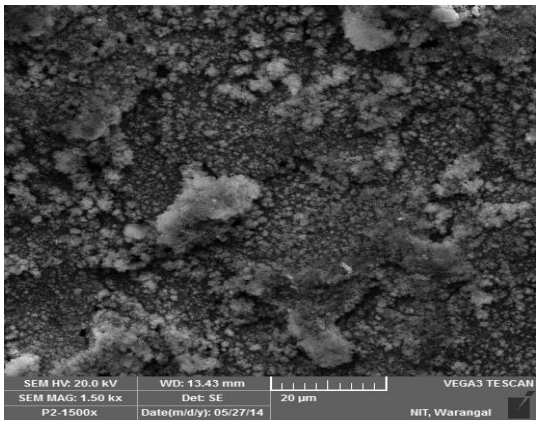

(a) Min MRR for brass (b) Min MRR for zinc coated brass

Figure 7.27(a, b): The minimum MRR for H13 with brass and zinc coated brass wires

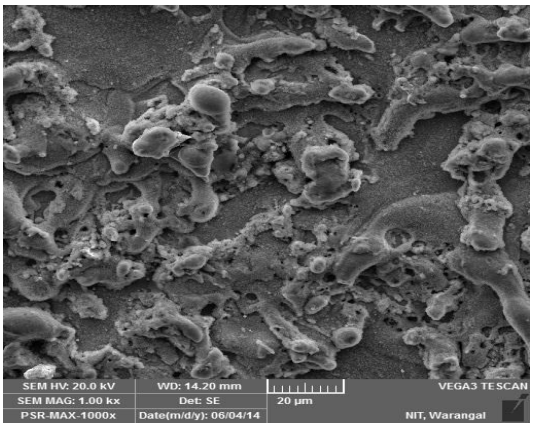

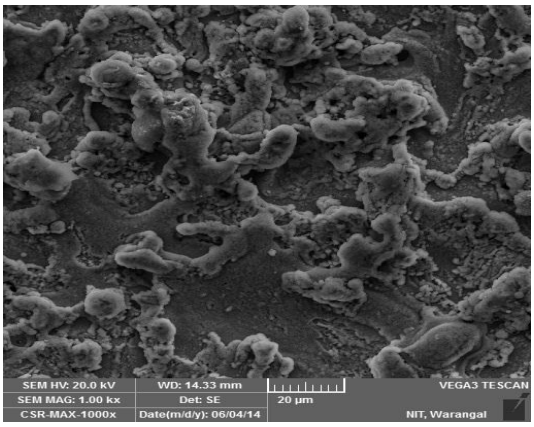

(a) Max SR for brass (b) Max SR for zinc coated brass

Figure 7.28(a, b): The maximum SR for H13 with brass and zinc coated brass wires

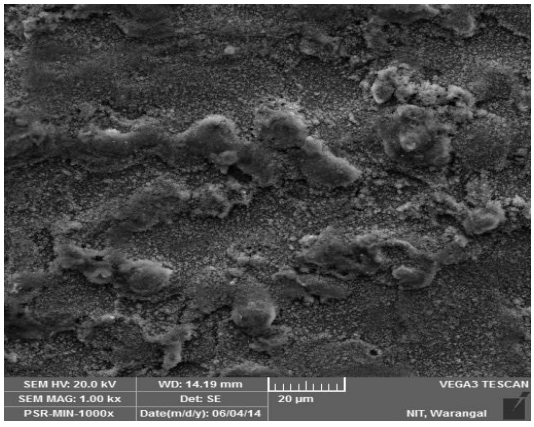

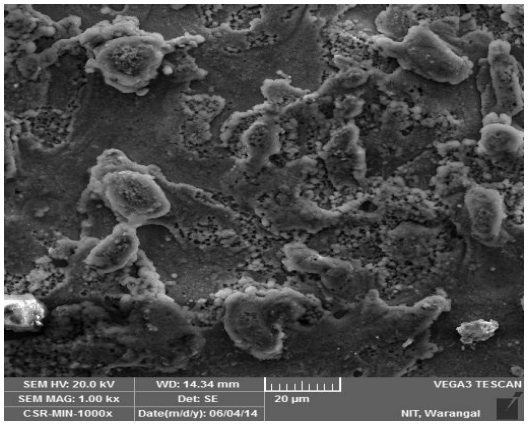

(a) Min SR for brass (b) Min SR for zinc coated brass

Figure 7.29(a, b): The minimum SR for H13 with brass and zinc coated brass wires

Figures 7.26(a, b) and 7.27(a, b) shows the SEM images for maximum and minimum material removal rate of Wire EDM machined specimens with brass and zinc coated brass wire electrodes. Figures 7.28(a, b) and 7.29(a, b) shows the SEM micrographs for maximum and minimum surface roughness of Wire EDM machined specimens with both electrode combinations. From the above images it is clear that the maximum material removal rate and minimum surface roughness images of zinc coated brass electrode wire has smooth surface, the least craters formation than the micrograph images of brass wire electrode.

The above figures shows the comparison between the SEM micrograph images for SS316, SS321, SS17-4 PH and H13 tool steel with Brass and Zinc coated brass wire electrodes on Wire EDM machined samples at maximum metal removal rate, surface roughness and minimum metal removal rate, surface roughness. All the work piece materials are machined in same conditions with brass wire and zinc coated brass wire electrodes. It is evident that the specimens are produced with brass wire in left side images have more melted drops, globules of debris, craters and cracks. As it can be seen in right side images have low melting temperature and high conductivity for the zinc coated wire produces better surface quality for all the work piece materials.

7.9 SUMMARY

In this chapter, the predicted results and experimental results with brass and zinc coated brass wire electrodes are compared for all the material combinations. The tabular columns and graphs are plotted for all the combinations. And also regression equations are developed for the SS316 material with electrodes of brass and zinc coated wires. The present chapter gives the information about SEM macrographs for maximum and minimum material removal rate, surface roughness of Wire EDM machined specimens.

Chapter 8

Conclusions

8.1 CONCLUSIONS

Wire EDM has been chosen as an alternative machining process to machine, difficulty to machine materials. Establishment of optimum process parameters is highly useful to the industry. In this study influence of brass wire (E_B) and zinc coated brass wire (Ec) while Wire EDM of SS316, SS321, and SS17-4PH and H13 materials,

Taguchi L25 orthogonal array is used to conduct experiments for varying Input parameters namely pulse on time (Pon), pulse off time (Poff), wire tension (Wt), wire feed (Wf) and dielectric flow rate (Wp). The output parameters of the study are cutting speed, Surface roughness, Kerf and dimensional deviation. The results of the experimentation were analyzed using Taguchi and Grey Relation Analysis techniques and the following conclusions are derived.

1. The range of Wire EDM input parameters have been established for conduct of complete L_{25} array of experimentation based on literature review and by performing one factor pilot experimentation. This cases correct fixation of levels for experimentation and enhance scope for reliable results. Further mathematical models were formulated for each output parameters and optimum output parameter value is obtained (predicted performance measures) by substitution of optimum set of input parameters.
2. The optimum Wire EDM input parameters for maximum metal removal rate have been observed to be as follows for two electrode and four work material combinations as shown in Table 8.1.

Table 8.1: Optimum Cutting Speed for All Work Materials Using E_B and E_C

S.No	Electrode-work material combination	Optimum set of parameters					Experimental value	Predicted value	%error
		Pon	Poff	Wt	Wf	Wp			
1	E_B -SS316	A_5	B_1	C_4	D_5	E_5	2.786	2.634	5.41
2	E_B -SS321	A_5	B_1	C_3	D_2	E_2	2.625	2.480	5.12
3	E_B -SS17-4PH	A_5	B_1	C_3	D_2	E_4	2.964	2.752	7.15
4	E_B -H13	A_5	B_2	C_3	D_2	E_5	2.315	2.245	3.02
5	E_C -SS316	A_5	B_1	C_3	D_2	E_5	2.625	2.359	7.13
6	E_C -SS321	A_5	B_1	C_3	D_2	E_4	2.931	2.715	6.67
7	E_C -17-4 PH	A_5	B_1	C_4	D_3	E_5	2.953	2.827	5.12
8	E_C -H13	A_5	B_1	C_3	D_2	E_5	2.638	2.419	7.84

It has been observed that Wire EDM of all the materials with Zinc coated brass electrode gives maximum material removal rate thus more productivity compared to that of brass electrode. The maximum deviation between experimental and predicted value is about 6% and hence the predicted values are Intune with experimental values and thus these mathematical models can be used for further studies as well

3. The optimum Wire EDM input parameters for minimum surface roughness have been observed to be as follows for two electrode and four work material combinations as shown in Table 8.2.

Table 8.2: Optimum Surface Roughness for All Work Materials Using E_B and E_C

S.No	Electrode-work material combination	Optimum set of parameters					Experimental value	Predicted value	%error
		Pon	Poff	Wt	Wf	Wp			
1	E_B -SS316	A_1	B_4	C_3	D_5	E_2	2.02	1.84	8.94
2	E_B -SS321	A_1	B_2	C_1	D_3	E_2	2.65	2.38	10.14
3	E_B -SS17-4PH	A_1	B_3	C_2	D_2	E_2	2.82	2.65	9.56
4	E_B -H13	A_1	B_2	C_3	D_2	E_3	2.28	2.25	1.13
5	E_C -SS316	A_1	B_3	C_1	D_3	E_2	2.28	2.15	4.48
6	E_C -SS321	A_1	B_3	C_2	D_3	E_2	1.98	1.85	6.66
7	E_C -17-4 PH	A_1	B_3	C_2	D_3	E_3	1.96	1.93	1.53
8	E_C -H13	A_1	B_3	C_2	D_3	E_2	2.05	1.96	4.39

It has been observed that Wire EDM of all the materials with Zinc coated brass electrode gives minimum surface roughness thus more quality compared to that of brass electrode. The maximum deviation between experimental and predicted value (>95% confidence level) are Intune with experimental values and these mathematical models can be used for further studies as well

4. The optimum Wire EDM input parameters for minimum cutting width have been observed to be as follows for two electrode and four work material combinations as shown in Table 8.3.

Table 8.3: Optimum Kerf (cutting width) for All Work Materials Using E_B and E_C

S.No	Electrode-work material combination	Optimum set of parameters					Experimental value	Predicted value	%error
		Pon	Poff	Wt	Wf	Wp			
1	E_B -SS316	A_2	B_5	C_4	D_3	E_5	0.354	0.338	4.51
2	E_B -SS321	A_4	B_2	C_1	D_3	E_2	0.412	0.398	3.39
3	E_B -SS17-4PH	A_3	B_2	C_3	D_3	E_4	0.418	0.395	4.26
4	E_B -H13	A_3	B_2	C_4	D_3	E_2	0.432	0.426	3.14
5	E_C -SS316	A_3	B_2	C_3	D_3	E_3	0.423	0.412	2.16
6	E_C -SS321	A_3	B_2	C_2	D_3	E_2	0.413	0.405	1.93
7	E_C -17-4 PH	A_4	B_2	C_3	D_1	E_2	0.382	0.375	1.83
8	E_C -H13	A_3	B_2	C_3	D_3	E_3	0.364	0.349	1.93

It has been observed that Wire EDM of all the materials with Zinc coated brass electrode gives minimum Kef (cutting width) thus more productivity compared to that of brass electrode. The maximum deviation between experimental and predicted value is about 6% and hence the predicted values are Intune with experimental values and these mathematical models can be used for further studies as well

5. The optimum Wire EDM input parameters for minimum dimensional deviation have been observed to be as follows for two electrode and four work material combinations as shown in Table 8.4.

Table 8.4: Optimum Dimensional Deviation for All Work Materials Using E_B and E_C

S.No	Electrode-work material combination	Optimum set of parameters					Experimental value	Predicted value	%error
		Pon	Poff	Wt	Wf	Wp			
1	E_B -SS316	A_4	B_2	C_2	D_3	E_1	0.126	0.114	9.52
2	E_B -SS321	A_2	B_1	C_1	D_1	E_3	0.154	0.145	5.84
3	E_B -SS17-4PH	A_2	B_1	C_1	D_1	E_4	0.158	0.146	7.59
4	E_B -H13	A_2	B_1	C_1	D_2	E_3	0.138	0.126	8.69
5	E_C -SS316	A_2	B_1	C_1	D_1	E_2	0.132	0.128	3.03
6	E_C -SS321	A_2	B_1	C_1	D_1	E_3	0.164	0.155	5.48
7	E_C -17-4 PH	A_2	B_1	C_2	D_1	E_3	0.185	0.172	7.02
8	E_C -H13	A_2	B_1	C_1	D_1	E_3	0.195	0.184	5.64

It has been observed that Wire EDM of all the materials with Zinc coated brass electrode gives minimum dimensional deviation thus more productivity compared to the brass electrode. The maximum deviation between experimental and predicted value (>95% confidence level) are

Intune with experimental values and these mathematical models can be used for further studies as well

6. Grey relational analysis (GRA) was performed for multi-level optimization i.e. maximization of MRR, Minimization of SR and KERF on all SS316, SS321, SS17-4 PH and H13 tool steel work materials and two electrode materials (E_B and E_C) combinations. The following optimization results were obtained.

Table 8.5: Optimum Results by Using GRA

S.No	Work material	Optimum parameters	Multilevel optimization values		% of Improvement
			Electrode E_B	Electrode E_C	
1	SS316	E_B - $A_5B_1C_2D_3E_4$ E_C - $A_5B_1C_4D_2E_5$	MRR =53.232 SR =2.28 KERF=0.398	MRR =63.696 SR =2.14 KERF=0.386	16.42 -6.54 -3.86
2	SS321	E_B - $A_5B_1C_3D_3E_5$ E_C - $A_5B_1C_3D_3E_5$	MRR =55.472 SR =2.6 KERF=0.421	MRR =68.304 SR =2.15 KERF=0.395	18.78 -16.15 -6.17
3	SS17-4 PH	E_B - $A_5B_1C_3D_3E_5$ E_C - $A_5B_1C_4D_3E_4$	MRR =61.248 SR =2.58 KERF=0.426	MRR =68.856 SR=2.2 KERF=0.386	11.06 -14.7 -9.38
4	H13	E_B - $A_5B_1C_4D_3E_5$ E_C - $A_5B_1C_3D_3E_5$	MRR= 54.192 SR =2.56 KERF=0.415	MRR=60.648 SR=2.04 KERF=0.396	10.64 -18.75 -4.57

In all the above cases performance of zinc coated were shows the better results on all the work materials considered. The corresponding optimum input parameters are listed in column-3 in the above table.

7. Wire EDM studies on SS316, SS321, SS17-4 PH and H13 tool steel work materials with Brass and Zinc coated Brass wire electrode is not available for industrial uses in the literature published so far. Hence these studies establish optimum machining parameters for individual responses of MRR, SR and KERF. Thus also establish optimum parameter for maximization or minimization of output responses combinedly. Grey Relational

Analysis (GRA) provides one best solution however other sets of non-dominated solution can be obtained as well.

8. The SEM micrograph images for SS316, SS321, SS17-4 PH and H13 tool steel with Brass and Zinc coated brass wire electrodes on Wire EDM machined samples at maximum metal removal rate, surface roughness and minimum metal removal rate, surface roughness. All the work piece materials are machined in same conditions with brass wire and zinc coated brass wire electrodes. It is evident that the specimens are produced with brass wire images have more melted drops, globules of debris, craters and cracks. It is observed that the images have low melting temperature and high conductivity for the zinc coated wire produces better surface quality for all the work piece materials.

8.2 SCOPE FOR FUTURE WORK

Although the Wire EDM machining has been thoroughly investigated for SS316, SS321, SS17-4 PH and H13 tool steel work materials, still there is a scope for further investigation. The following suggestions may prove useful for future work:

1. The optimization process parameters can be done Wire EDM for novel composite materials.

2. The effects of machining parameters on recast layer thickness and overcut should be investigated.

3. Efforts should be made to investigate the effects of Wire EDM process parameters on performance measures in a cryogenic cutting environment.

4. The weightages to be assigned to various characteristics in multi response optimization models should be based upon requirements of industries.

5. The effect of process parameters such as conductivity of dielectric, wire diameter, workpiece height etc. may also be investigated.

APPENDIX I

The Experimental results for SS321, SS17-4 PH, and H13 Tool Steel materials Using Electrodes E_B and E_C are given in the following Tables.

Table 1: Experimental results for SS321Using Electrode E_B

S.No	A	B	C	D	E	CS	SR	KERF	DD
1	1	1	1	1	1	0.473	2.80	0.464	0.485
2	1	2	2	2	2	0.360	2.72	0.459	0.348
3	1	3	3	3	3	0.301	2.81	0.423	0.486
4	1	4	4	4	4	0.252	2.70	0.447	0.452
5	1	5	5	5	5	0.213	2.63	0.412	0.154
6	2	1	2	3	4	0.904	2.96	0.434	0.456
7	2	2	3	4	5	0.836	2.82	0.402	0.463
8	2	3	4	5	1	0.615	2.96	0.412	0.442
9	2	4	5	1	2	0.495	2.97	0.417	0.168
10	2	5	1	2	3	0.345	2.86	0.425	0.248
11	3	1	3	5	2	1.538	3.27	0.468	0.492
12	3	2	4	1	3	1.214	3.18	0.422	0.465
13	3	3	5	2	4	0.918	2.88	0.453	0.422
14	3	4	1	3	5	0.641	2.86	0.466	0.414
15	3	5	2	4	1	0.441	2.75	0.479	0.348
16	4	1	4	2	5	1.986	3.50	0.488	0.524
17	4	2	5	3	1	1.405	3.33	0.436	0.461
18	4	3	1	4	2	0.928	3.24	0.478	0.366
19	4	4	2	5	3	0.756	3.15	0.432	0.214
20	4	5	3	1	4	0.596	3.04	0.421	0.244
21	5	1	5	4	3	2.625	3.78	0.543	0.514
22	5	2	1	5	4	2.318	3.53	0.493	0.418
23	5	3	2	1	5	1.932	3.04	0.479	0.432
24	5	4	3	2	1	1.798	2.98	0.489	0.424
25	5	5	4	3	2	1.285	2.72	0.456	0.484

Table 2: Experimental results for SS321Using Electrode E_C

S.No	A	B	C	D	E	CS	SR	KERF	DD
1	1	1	1	1	1	0.712	2.26	0.457	0.422
2	1	2	2	2	2	0.493	2.28	0.435	0.352
3	1	3	3	3	3	0.412	2.24	0.436	0.336
4	1	4	4	4	4	0.370	2.12	0.395	0.189
5	1	5	5	5	5	0.297	1.98	0.382	0.164
6	2	1	2	3	4	0.943	2.41	0.422	0.484
7	2	2	3	4	5	0.742	2.16	0.456	0.433
8	2	3	4	5	1	0.627	2.05	0.441	0.336
9	2	4	5	1	2	0.506	2.08	0.446	0.228
10	2	5	1	2	3	0.486	1.95	0.436	0.168
11	3	1	3	5	2	1.826	2.15	0.445	0.542
12	3	2	4	1	3	1.358	2.24	0.446	0.428
13	3	3	5	2	4	0.976	2.12	0.472	0.435
14	3	4	1	3	5	0.734	2.04	0.422	0.328
15	3	5	2	4	1	0.627	2.20	0.436	0.232
16	4	1	4	2	5	2.125	2.63	0.459	0.516
17	4	2	5	3	1	1.926	2.17	0.451	0.468
18	4	3	1	4	2	1.391	2.30	0.429	0.324
19	4	4	2	5	3	0.928	2.15	0.433	0.352
20	4	5	3	1	4	0.858	2.05	0.429	0.268
21	5	1	5	4	3	2.931	2.70	0.528	0.636
22	5	2	1	5	4	2.661	2.53	0.519	0.484
23	5	3	2	1	5	2.017	2.34	0.487	0.365
24	5	4	3	2	1	1.864	2.43	0.456	0.228
25	5	5	4	3	2	0.935	2.24	0.436	0.234

Table 3: Experimental results for SS17-4PH Using Electrode E_B

S.No	A	B	C	D	E	CS	SR	KERF	DD
1	1	1	1	1	1	0.872	2.96	0.437	0.458
2	1	2	2	2	2	0.604	2.96	0.424	0.345
3	1	3	3	3	3	0.484	2.88	0.435	0.284
4	1	4	4	4	4	0.382	2.85	0.421	0.164
5	1	5	5	5	5	0.326	2.82	0.418	0.158
6	2	1	2	3	4	1.324	3.14	0.440	0.447
7	2	2	3	4	5	1.042	3.15	0.433	0.465
8	2	3	4	5	1	0.712	2.95	0.434	0.363
9	2	4	5	1	2	0.562	2.92	0.456	0.243
10	2	5	1	2	3	0.504	2.96	0.467	0.268
11	3	1	3	5	2	1.362	2.90	0.493	0.589
12	3	2	4	1	3	1.302	2.98	0.454	0.446
13	3	3	5	2	4	1.004	2.85	0.442	0.428
14	3	4	1	3	5	0.832	2.86	0.427	0.387
15	3	5	2	4	1	0.662	2.88	0.433	0.234
16	4	1	4	2	5	2.274	3.14	0.428	0.466
17	4	2	5	3	1	1.624	3.05	0.445	0.326
18	4	3	1	4	2	1.232	3.12	0.432	0.246
19	4	4	2	5	3	1.046	3.05	0.437	0.165
20	4	5	3	1	4	0.862	3.18	0.432	0.186
21	5	1	5	4	3	2.964	3.15	0.513	0.538
22	5	2	1	5	4	2.352	3.6	0.453	0.458
23	5	3	2	1	5	2.146	3.11	0.431	0.446
24	5	4	3	2	1	1.662	2.96	0.427	0.334
25	5	5	4	3	2	1.206	2.92	0.446	0.465

Table 4: Experimental results for SS17-4 PH Using Electrode E_C

S.No	A	B	C	D	E	CS	SR	KERF	DD
1	1	1	1	1	1	0.876	2.36	0.437	0.422
2	1	2	2	2	2	0.636	2.28	0.424	0.352
3	1	3	3	3	3	0.547	2.25	0.435	0.336
4	1	4	4	4	4	0.458	2.12	0.421	0.196
5	1	5	5	5	5	0.379	1.96	0.413	0.185
6	2	1	2	3	4	1.402	2.38	0.420	0.584
7	2	2	3	4	5	1.006	2.16	0.433	0.463
8	2	3	4	5	1	0.834	2.25	0.434	0.346
9	2	4	5	1	2	0.683	2.18	0.446	0.268
10	2	5	1	2	3	0.569	1.98	0.437	0.198
11	3	1	3	5	2	1.387	2.15	0.479	0.562
12	3	2	4	1	3	1.030	2.24	0.454	0.458
13	3	3	5	2	4	0.884	2.22	0.442	0.435
14	3	4	1	3	5	0.826	2.14	0.427	0.358
15	3	5	2	4	1	0.719	2.25	0.433	0.212
16	4	1	4	2	5	2.357	2.68	0.488	0.546
17	4	2	5	3	1	1.983	2.37	0.445	0.478
18	4	3	1	4	2	1.741	2.34	0.432	0.344
19	4	4	2	5	3	1.354	2.25	0.437	0.262
20	4	5	3	1	4	1.116	2.15	0.432	0.189
21	5	1	5	4	3	2.953	2.70	0.493	0.566
22	5	2	1	5	4	2.330	2.53	0.463	0.494
23	5	3	2	1	5	2.157	2.34	0.431	0.375
24	5	4	3	2	1	1.527	2.25	0.427	0.268
25	5	5	4	3	2	1.381	2.28	0.426	0.294

Table 5: Experimental results for H13 Tool Steel Using Electrode E_B

S.No	A	B	C	D	E	CS	SR	KERF	DD
1	1	1	1	1	1	0.476	2.82	0.447	0.468
2	1	2	2	2	2	0.428	2.72	0.440	0.375
3	1	3	3	3	3	0.467	2.81	0.435	0.264
4	1	4	4	4	4	0.319	2.72	0.434	0.164
5	1	5	5	5	5	0.206	2.65	0.432	0.138
6	2	1	2	3	4	0.956	2.98	0.460	0.487
7	2	2	3	4	5	0.742	2.84	0.453	0.468
8	2	3	4	5	1	0.432	2.96	0.434	0.365
9	2	4	5	1	2	0.394	2.98	0.436	0.244
10	2	5	1	2	3	0.345	2.86	0.467	0.269
11	3	1	3	5	2	0.916	3.27	0.529	0.589
12	3	2	4	1	3	0.632	3.18	0.514	0.456
13	3	3	5	2	4	0.412	2.89	0.442	0.438
14	3	4	1	3	5	0.403	2.86	0.447	0.367
15	3	5	2	4	1	0.394	2.74	0.435	0.254
16	4	1	4	2	5	1.308	3.55	0.518	0.496
17	4	2	5	3	1	0.932	3.33	0.485	0.426
18	4	3	1	4	2	0.732	3.24	0.462	0.146
19	4	4	2	5	3	0.712	3.25	0.453	0.155
20	4	5	3	1	4	0.635	3.04	0.532	0.142
21	5	1	5	4	3	2.315	3.48	0.513	0.578
22	5	2	1	5	4	1.908	3.33	0.483	0.468
23	5	3	2	1	5	1.314	3.24	0.463	0.496
24	5	4	3	2	1	0.988	2.98	0.447	0.344
25	5	5	4	3	2	0.753	2.76	0.436	0.435

Table 6: Experimental results for H13 Tool Steel Using Electrode E_C

S.No	A	B	C	D	E	CS	SR	KERF	DD
1	1	1	1	1	1	0.597	2.68	0.477	0.416
2	1	2	2	2	2	0.549	2.54	0.454	0.352
3	1	3	3	3	3	0.588	2.35	0.435	0.336
4	1	4	4	4	4	0.44	2.22	0.431	0.198
5	1	5	5	5	5	0.327	2.15	0.423	0.195
6	2	1	2	3	4	1.007	2.78	0.480	0.586
7	2	2	3	4	5	0.663	2.56	0.463	0.465
8	2	3	4	5	1	0.553	2.35	0.454	0.343
9	2	4	5	1	2	0.515	2.28	0.456	0.266
10	2	5	1	2	3	0.466	2.48	0.447	0.198
11	3	1	3	5	2	1.336	2.95	0.479	0.569
12	3	2	4	1	3	0.953	2.74	0.454	0.448
13	3	3	5	2	4	0.756	2.62	0.442	0.345
14	3	4	1	3	5	0.633	2.44	0.427	0.258
15	3	5	2	4	1	0.551	2.25	0.433	0.198
16	4	1	4	2	5	1.429	2.98	0.498	0.548
17	4	2	5	3	1	1.053	2.77	0.445	0.476
18	4	3	1	4	2	0.853	2.54	0.442	0.354
19	4	4	2	5	3	0.833	2.35	0.437	0.272
20	4	5	3	1	4	0.756	2.15	0.432	0.219
21	5	1	5	4	3	2.638	3.28	0.513	0.566
22	5	2	1	5	4	2.219	2.83	0.502	0.485
23	5	3	2	1	5	1.602	2.54	0.461	0.345
24	5	4	3	2	1	1.219	2.45	0.437	0.258
25	5	5	4	3	2	0.984	2.38	0.432	0.354

APPENDIX II

Table 1: Normalized S/N Ratios for SS17-4 PH Using Electrode E_B

Exp No.	Process Parameters					Normalized S/N ratio		
	P on	P off	Wt	Wf	Wp	MRR	SR	KERF
1	1	1	1	1	1	0.1986	0.5104	0.93582888
2	1	2	2	2	2	0.1123	0.6042	0.86631016
3	1	3	3	3	3	0.0672	0.6667	0.52406417
4	1	4	4	4	4	0.0298	0.6146	0.18181818
5	1	5	5	5	5	0.0000	0.7188	0.1657754
6	2	1	2	3	4	0.3751	0.4271	1.0000000
7	2	2	3	4	5	0.2452	0.8021	0.63636364
8	2	3	4	5	1	0.1673	0.8438	0.5828877
9	2	4	5	1	2	0.1390	0.9427	0.55614973
10	2	5	1	2	3	0.1008	1.0000	0.51336898
11	3	1	3	5	2	0.4431	0.2656	0.81818182
12	3	2	4	1	3	0.4293	0.3125	0.52941176
13	3	3	5	2	4	0.3247	0.4688	0.36363636
14	3	4	1	3	5	0.2506	0.5729	0.29411765
15	3	5	2	4	1	0.1742	0.7188	0.22459893
16	4	1	4	2	5	0.8930	0.1458	0.71122995
17	4	2	5	3	1	0.6272	0.2344	0.45454545
18	4	3	1	4	2	0.427	0.2813	0.22994652
19	4	4	2	5	3	0.3384	0.3281	0.10160428
20	4	5	3	1	4	0.2926	0.3854	0.0000000
21	5	1	5	4	3	1.0000	0.00000	0.57754011
22	5	2	1	5	4	0.7204	0.1302	0.47058824
23	5	3	2	1	5	0.5875	0.3854	0.22459893
24	5	4	3	2	1	0.4584	0.4167	0.17112299
25	5	5	4	3	2	0.3685	0.6146	0.13368984

Table 1: Normalized S/N Ratios for SS17-4 PH Using Electrode E_C

Exp No.	Process Parameters					Normalized S/N ratio		
	P on	P off	Wt	Wf	Wp	MRR	SR	KERF
1	1	1	1	1	1	0.260025	0.571429	1.000000
2	1	2	2	2	2	0.122807	0.612245	0.818681
3	1	3	3	3	3	0.072055	0.843537	0.236264
4	1	4	4	4	4	0.045739	0.952381	0.120879
5	1	5	5	5	5	0.000000	1.000000	0.076923
6	2	1	2	3	4	0.404762	0.197279	0.972527
7	2	2	3	4	5	0.278822	0.367347	0.785714
8	2	3	4	5	1	0.206767	0.469388	0.758242
9	2	4	5	1	2	0.130952	0.564626	0.648352
10	2	5	1	2	3	0.118421	0.816327	0.620879
11	3	1	3	5	2	0.619674	0.136054	0.791209
12	3	2	4	1	3	0.414160	0.340136	0.675824
13	3	3	5	2	4	0.312657	0.394558	0.538462
14	3	4	1	3	5	0.273810	0.448980	0.461538
15	3	5	2	4	1	0.206767	0.544218	0.115385
16	4	1	4	2	5	0.761278	0.047619	0.769231
17	4	2	5	3	1	0.582080	0.360544	0.489011
18	4	3	1	4	2	0.497494	0.272109	0.384615
19	4	4	2	5	3	0.395363	0.374150	0.362637
20	4	5	3	1	4	0.351504	0.442177	0.000000
21	5	1	5	4	3	1.000000	0.000000	0.390110
22	5	2	1	5	4	0.854637	0.115646	0.439560
23	5	3	2	1	5	0.614035	0.244898	0.450549
24	5	4	3	2	1	0.471805	0.183673	0.456044
25	5	5	4	3	2	0.399749	0.312925	0.181319

Table 3: SS17-4 PH Grey Relational Co-efficient and Grey Relational Grade for E_B

Exp No.	Process Parameters					Grey Relational Co-efficient			Grey grade
	P on	P off	Wt	Wf	Wp	MRR	SR	KERF	
1	1	1	1	1	1	0.067010	0.845304	0.86875	0.5919093
2	1	2	2	2	2	0.042096	0.955801	1.072595	0.5691591
3	1	3	3	3	3	0.024914	1.000000	0.4125	0.4871007
4	1	4	4	4	4	0.008591	0.878453	0.0750	0.4280348
5	1	5	5	5	5	0.000000	0.900552	0.1625	0.4493609
6	2	1	2	3	4	0.682131	0.712707	0.6250	0.6368338
7	2	2	3	4	5	0.573024	0.828729	0.7500	0.5646140
8	2	3	4	5	1	0.438144	0.878453	0.90625	0.5607570
9	2	4	5	1	2	0.359107	0.900552	0.6625	0.5981094
10	2	5	1	2	3	0.327320	0.883978	0.7000	**0.6578774**
11	3	1	3	5	2	0.719931	0.558011	0.14375	0.5371573
12	3	2	4	1	3	0.706186	0.403315	0.0375	0.4677346
13	3	3	5	2	4	0.604811	0.436464	0.20625	0.4500876
14	3	4	1	3	5	0.524313	0.646409	0.36875	0.4513811
15	3	5	2	4	1	0.448454	0.707182	0.24375	0.4697194
16	4	1	4	2	5	1.000000	0.215470	0.45625	0.6089725
17	4	2	5	3	1	0.621993	0.265193	0.44375	0.4820630
18	4	3	1	4	2	0.615979	0.337017	0.30625	0.4233142
19	4	4	2	5	3	0.596220	0.392265	0.35625	0.4048899
20	4	5	3	1	4	0.537801	0.000000	0.00000	0.3986803
21	5	1	5	4	3	0.365979	0.127072	0.4250	0.6251207
22	5	2	1	5	4	0.326460	0.281768	0.3375	0.4973618
23	5	3	2	1	5	0.310137	0.331492	0.4375	0.4628532
24	5	4	3	2	1	0.325601	0.403315	0.3625	0.4392702
25	5	5	4	3	2	0.352234	0.767956	1.0000	0.4575121

Table 4: SS17-4 PH Grey Relational Co-efficient and Grey Relational Grade for E_C

Exp No.	Process Parameters					Grey Relational Co-efficient			Grey grade
	P on	P off	Wt	Wf	Wp	MRR	SR	KERF	
1	1	1	1	1	1	0.348921	0.763713	1.169851	0.760828
2	1	2	2	2	2	0.342958	0.918782	0.459770	0.573837
3	1	3	3	3	3	0.338963	1.000000	0.350877	0.563280
4	1	4	4	4	4	0.335253	0.804444	0.373832	0.504510
5	1	5	5	5	5	0.333333	0.834101	0.571429	0.579621
6	2	1	2	3	4	0.611345	0.635088	0.666667	0.637700
7	2	2	3	4	5	0.539388	0.744856	0.842105	0.708783
8	2	3	4	5	1	0.470874	0.804444	0.597015	0.624111
9	2	4	5	1	2	0.438253	0.834101	0.625000	0.632451
10	2	5	1	2	3	0.426374	0.811659	0.368664	0.535565
11	3	1	3	5	2	0.640969	0.530792	0.341880	0.504547
12	3	2	4	1	3	0.629870	0.455919	0.386473	0.490754
13	3	3	5	2	4	0.558541	0.470130	0.441989	0.490220
14	3	4	1	3	5	0.512459	0.585761	0.398010	0.498743
15	3	5	2	4	1	0.475490	0.630662	0.479042	0.528398
16	4	1	4	2	5	1.000000	0.389247	0.473373	**0.635273**
17	4	2	5	3	1	0.569472	0.404922	0.418848	0.464414
18	4	3	1	4	2	0.565598	0.429929	0.437158	0.477562
19	4	4	2	5	3	0.553232	0.451372	0.333333	0.445979
20	4	5	3	1	4	0.519643	0.333333	0.465116	0.439364
21	5	1	5	4	3	0.440909	0.364185	0.430108	0.411734
22	5	2	1	5	4	0.426061	0.410431	0.470588	0.435694
23	5	3	2	1	5	0.420217	0.427896	0.439560	0.429224
24	5	4	3	2	1	0.425750	0.455919	1.000000	0.627223
25	5	5	4	3	2	0.435629	0.683019	1.000000	0.706216

APPENDIX III

Table 1: Normalized S/N Ratios for H13 Tool Steel Using Electrode E_B

Exp No.	Process Parameters					Normalized S/N ratio		
	P on	P off	Wt	Wf	Wp	MRR	SR	KERF
1	1	1	1	1	1	0.1986	0.5104	0.93582888
2	1	2	2	2	2	0.1123	0.6042	0.86631016
3	1	3	3	3	3	0.0672	0.6667	0.52406417
4	1	4	4	4	4	0.0298	0.6146	0.18181818
5	1	5	5	5	5	0.0000	0.7188	0.1657754
6	2	1	2	3	4	0.3751	0.4271	1.0000000
7	2	2	3	4	5	0.2452	0.8021	0.63636364
8	2	3	4	5	1	0.1673	0.8438	0.5828877
9	2	4	5	1	2	0.1390	0.9427	0.55614973
10	2	5	1	2	3	0.1008	1.0000	0.51336898
11	3	1	3	5	2	0.4431	0.2656	0.81818182
12	3	2	4	1	3	0.4293	0.3125	0.52941176
13	3	3	5	2	4	0.3247	0.4688	0.36363636
14	3	4	1	3	5	0.2506	0.5729	0.29411765
15	3	5	2	4	1	0.1742	0.7188	0.22459893
16	4	1	4	2	5	0.8930	0.1458	0.71122995
17	4	2	5	3	1	0.6272	0.2344	0.45454545
18	4	3	1	4	2	0.427	0.2813	0.22994652
19	4	4	2	5	3	0.3384	0.3281	0.10160428
20	4	5	3	1	4	0.2926	0.3854	0.0000000
21	5	1	5	4	3	1.0000	0.00000	0.57754011
22	5	2	1	5	4	0.7204	0.1302	0.47058824
23	5	3	2	1	5	0.5875	0.3854	0.22459893
24	5	4	3	2	1	0.4584	0.4167	0.17112299
25	5	5	4	3	2	0.3685	0.6146	0.13368984

Table 2: Normalized S/N Ratios for H13 Tool Steel Using Electrode E_C

Exp No.	Process Parameters					Normalized S/N ratio		
	P on	P off	Wt	Wf	Wp	MRR	SR	KERF
1	1	1	1	1	1	0.260025	0.571429	1.000000
2	1	2	2	2	2	0.122807	0.612245	0.818681
3	1	3	3	3	3	0.072055	0.843537	0.236264
4	1	4	4	4	4	0.045739	0.952381	0.120879
5	1	5	5	5	5	0.000000	1.000000	0.076923
6	2	1	2	3	4	0.404762	0.197279	0.972527
7	2	2	3	4	5	0.278822	0.367347	0.785714
8	2	3	4	5	1	0.206767	0.469388	0.758242
9	2	4	5	1	2	0.130952	0.564626	0.648352
10	2	5	1	2	3	0.118421	0.816327	0.620879
11	3	1	3	5	2	0.619674	0.136054	0.791209
12	3	2	4	1	3	0.414160	0.340136	0.675824
13	3	3	5	2	4	0.312657	0.394558	0.538462
14	3	4	1	3	5	0.273810	0.448980	0.461538
15	3	5	2	4	1	0.206767	0.544218	0.115385
16	4	1	4	2	5	0.761278	0.047619	0.769231
17	4	2	5	3	1	0.582080	0.360544	0.489011
18	4	3	1	4	2	0.497494	0.272109	0.384615
19	4	4	2	5	3	0.395363	0.374150	0.362637
20	4	5	3	1	4	0.351504	0.442177	0.000000
21	5	1	5	4	3	1.000000	0.000000	0.390110
22	5	2	1	5	4	0.854637	0.115646	0.439560
23	5	3	2	1	5	0.614035	0.244898	0.450549
24	5	4	3	2	1	0.471805	0.183673	0.456044
25	5	5	4	3	2	0.399749	0.312925	0.181319

Table 3: H13 Tool Steel Grey Relational Co-efficient and Grey Relational Grade for E_B

Exp No.	Process Parameters					Grey Relational Co-efficient			Grey grade
	P on	P off	Wt	Wf	Wp	MRR	SR	KERF	
1	1	1	1	1	1	0.067010	0.845304	0.86875	0.5919093
2	1	2	2	2	2	0.042096	0.955801	1.072595	0.5691591
3	1	3	3	3	3	0.024914	1.000000	0.4125	0.4871007
4	1	4	4	4	4	0.008591	0.878453	0.0750	0.4280348
5	1	5	5	5	5	0.000000	0.900552	0.1625	0.4493609
6	2	1	2	3	4	0.682131	0.712707	0.6250	0.6368338
7	2	2	3	4	5	0.573024	0.828729	0.7500	0.5646140
8	2	3	4	5	1	0.438144	0.878453	0.90625	0.5607570
9	2	4	5	1	2	0.359107	0.900552	0.6625	0.5981094
10	2	5	1	2	3	0.327320	0.883978	0.7000	**0.6586774**
11	3	1	3	5	2	0.719931	0.558011	0.14375	0.5371573
12	3	2	4	1	3	0.706186	0.403315	0.0375	0.4677346
13	3	3	5	2	4	0.604811	0.436464	0.20625	0.4500876
14	3	4	1	3	5	0.524313	0.646409	0.36875	0.4513811
15	3	5	2	4	1	0.448454	0.707182	0.24375	0.4697194
16	4	1	4	2	5	1.000000	0.215470	0.45625	0.6089725
17	4	2	5	3	1	0.621993	0.265193	0.44375	0.4820630
18	4	3	1	4	2	0.615979	0.337017	0.30625	0.4233142
19	4	4	2	5	3	0.596220	0.392265	0.35625	0.4048899
20	4	5	3	1	4	0.537801	0.000000	0.00000	0.3986803
21	5	1	5	4	3	0.365979	0.127072	0.4250	0.6251207
22	5	2	1	5	4	0.326460	0.281768	0.3375	0.4973618
23	5	3	2	1	5	0.310137	0.331492	0.4375	0.4628532
24	5	4	3	2	1	0.325601	0.403315	0.3625	0.4392702
25	5	5	4	3	2	0.352234	0.767956	1.0000	0.4575121

Table 4: H13 Tool Steel Grey Relational Co-efficient and Grey Relational Grade for E_C

Exp No.	Process Parameters					Grey Relational Co-efficient			Grey grade
	P on	P off	Wt	Wf	Wp	MRR	SR	KERF	
1	1	1	1	1	1	0.348921	0.763713	1.169851	**0.682628**
2	1	2	2	2	2	0.342958	0.918782	0.459770	0.573837
3	1	3	3	3	3	0.338963	1.000000	0.350877	0.563280
4	1	4	4	4	4	0.335253	0.804444	0.373832	0.504510
5	1	5	5	5	5	0.333333	0.834101	0.571429	0.579621
6	2	1	2	3	4	0.611345	0.635088	0.666667	0.637700
7	2	2	3	4	5	0.539388	0.744856	0.842105	0.608783
8	2	3	4	5	1	0.470874	0.804444	0.597015	0.624111
9	2	4	5	1	2	0.438253	0.834101	0.625000	0.632451
10	2	5	1	2	3	0.426374	0.811659	0.368664	0.535565
11	3	1	3	5	2	0.640969	0.530792	0.341880	0.504547
12	3	2	4	1	3	0.629870	0.455919	0.386473	0.490754
13	3	3	5	2	4	0.558541	0.470130	0.441989	0.490220
14	3	4	1	3	5	0.512459	0.585761	0.398010	0.498743
15	3	5	2	4	1	0.475490	0.630662	0.479042	0.528398
16	4	1	4	2	5	1.000000	0.389247	0.473373	0.620873
17	4	2	5	3	1	0.569472	0.404922	0.418848	0.464414
18	4	3	1	4	2	0.565598	0.429929	0.437158	0.477562
19	4	4	2	5	3	0.553232	0.451372	0.333333	0.445979
20	4	5	3	1	4	0.519643	0.333333	0.465116	0.439364
21	5	1	5	4	3	0.440909	0.364185	0.430108	0.411734
22	5	2	1	5	4	0.426061	0.410431	0.470588	0.435694
23	5	3	2	1	5	0.420217	0.427896	0.439560	0.429224
24	5	4	3	2	1	0.425750	0.455919	1.000000	0.627223
25	5	5	4	3	2	0.435629	0.683019	1.000000	0.606216

References

1. Altpeter, F. and Roberto, P. (2004), "Relevant topics in wire electrical discharge machining control", Journal of Materials Processing Technology, 149, 147–151.
2. Barker, T.B. (1986), "Quality engineering by design: Taguchi's Philosophy", Quality Progress, December, 33-42.
3. Barker, T.B. (1990), "Engineering quality by design", Marcel Dekker, Inc., New York.
4. Byrne, D.M. and Taguchi, S. (1987), "The Taguchi approach to parameter design", Quality Progress, 19-26.
5. Characteristics", Journal of Materials Processing Technology, 28, 127-138.
6. Chiang, K.T., Chang, F.P. (2006), "Optimization of the WEDM process of particle reinforced material with multiple performance characteristics using grey relational analysis", Journal of Materials Processing Technology, 180, 96-101.
7. D. Scott, S. Boyina, K.P. Rajurkar, "Analysis and optimization of parameter combination in wire electrical discharge machining", Int.J. Prod. Res. 29 (11) (1991) 2189–2207.
8. Danial Ghodsiyeh, Abolfazl Golshan, Jamal Azimi Shirvanehdeh , "Review on Current Research Trends in Wire Electrical Discharge Machining (WEDM)" Indian Journal of Science and Technology Vol: 6 Issue: 2 February 2013 ISSN:0974-6846.
9. Ebeid, S., Fahmy, R., Habib, S. (2003), "An operating and diagnostic knowledge-based system for wire EDM", Springer Berlin/Heidelberg Publisher, 2773, 16113349.
10. Goswami Amitesh, Kumar Jatinder, "An investigation into the machining characteristics of NIMONIC 80A using CNC WIRE EDM", International Journal of Advanced Engineering Technology E-ISSN 0976-3945 (2013).
11. H. Ding, R. Ibrahim, K. Cheng, S.J. Chen, "Experimental study on machinability improvement of hardened tool steel using two dimensional vibration-assisted micro-end milling", International Journal of Machine Tools and Manufacture 50 (2010) 1115–1118.

12. Han, F., Jiang, J., Dingwen, Yu. (2007), “Influence of machining parameters on surface roughness in finish cut of WEDM”, International Journal of Advanced Manufacturing Technology, 34, 538–546.
13. Hargrove, S. K., Ding, D. (2007), “Determining cutting parameters in wire EDM based on workpiece surface temperature distribution”, International Journal of Advanced Manufacturing Technology, 34, 295-299.
14. Ho, K.H., Newman, S.T., Rahimifard, S., Allen, R.D. (2004), “State of art in wire electrical discharge machining (WEDM)”, International Journal of Machine Tools and Manufacture, 44, 1247-1259.
15. Hsue, W.J., Liao, Y.S., Lu, S.S. (1999), “Fundamental geometry analysis of wire electrical discharge machining in corner cutting”, International Journal of Machine Tools & Manufacture, 39, 651–667
16. Huang, J.T., Liao, Y.S., Hsue, W.J. (1999), “Determination of finish-cutting operation number and machining parameter settings in wire electrical discharge machining”, Journal of Materials Processing Technology, 87, 69–81.
17. J Leunda, V. Garcia Navas, C. Soriano, C. Sanz, “Improvement of laser deposited high alloyed powder metallurgical tool steel by a post tempering treatment”, Physics Procedia 39 (2012) 392–400.
18. J. T. Huang & Y. S. Liao, “Optimization of machining parameters of Wire-EDM based on Grey relational and statistical analyses”, International Journal of Production Research, 41:8, (2003), 1707-1720.
19. Kumar, P. (1993), “Optimization of process variables affecting the quality of Al11%Si alloy castings produced by V-process”, Ph.D. Thesis, University of Roorkee, Roorkee.
20. Kuriakose, S., Shunmugam, M.S. (2005), “Multi-objective optimization of wire electro discharge machining process by non-dominated sorting genetic algorithm”, Journal of Materials Processing Technology, 170,133-141.

21. Kuriakose. S, Shunmugam, M.S. (2004), "Characteristics of wire-electro discharge machined Ti6Al4V surface", Materials Letters, 58, 2231– 2237.
22. L. Li, Y.B. Guo, X.T. Wei, W. Li, "Surface integrity characteristics in wire-EDM of Inconel 718 at different discharge energy", Procedia CIRP 6 (2013) 220 – 225.
23. Lautre, N.K., Manna, A. (2006), "A study on fault diagnosis and maintenance of CNC-Wire EDM based on binary relational analysis and expert system", International Journal of Advanced Manufacturing Technology, 29, 490–498.
24. Liao, Y.S. and Woo, J.C. (1997) "The effects of machining setting on the behaviour of pulse trains in the WEDM process" Journal of Materials Processing Technology, 71, 434-440.
25. Liao, Y.S. and Yu, Y.P. (2004), "The energy aspect of material property in WEDM and its application", Journal of Materials Processing Technology, 149, 77–82
26. Liao, Y.S., Huang, J.T., Chen, Y.H. (2004), "A study to achieve a fine surface finish in Wire-EDM", Journal of Materials Processing Technology, 149,165–171
27. Liao, Y.S., Huang, J.T., Su, H.C. (1997), "A Study of machining-parameters Optimization of wire electrical discharge machining", Journal of Material Processing Technology, 71, 487-493
28. Liao, Y.S., Yub, Y.P. (2004), "Study of specific discharge energy in WEDM and its application", International Journal of Machine Tools & Manufacture, 44, 1373–1380.
29. Lin, C.T., Chung, I.F., Huang, S.Y. (2001), "Improvement of machining accuracy by fuzzy logic at corner parts for wire-EDM", Fuzzy Sets and Systems, 122, 499–511.
30. Lin, H.C.,Lin, K.M., Chen, Y.S., Chu, C.L. (2005) ,"The wire electro-discharge machining characteristics of Fe–30Mn–6Si and Fe–30Mn–6Si–5Cr shape memory alloys", Journal of Materials Processing Technology, 161, 435–439.
31. Lin, J.L., Lin, C.L. (2005), "The use of grey-fuzzy logic for the optimization of the manufacturing process", Journal of Materials Processing Technology, 160, 9–14.

32. Lok, Y.K. and Lee, T.C. (1997), "Processing of advanced ceramics using the wire EDM process", Journal of Materials Processing Technology, 63 (1-3), 839-843.
33. Manna, A. and Bhattacharyya, B. (2006), "Taguchi and Gauss elimination method: A dual response approach for parametric optimization of CNC wire cut EDM of PRAlSiCMMC", International Journal of Advanced Manufacturing Technology, 28, 67–75.
34. Miller, S. F., Chen, C.K., Shih, A. J., Qu, J. (2005), "Investigation of wire electrical discharge machining of thin cross-sections and compliant mechanisms", International Journal of Machine Tools & Manufacture, 45, 1717–1725
35. Mr. Ballal Yuvaraj P., Dr. Inamdar K.H., Mr. Patil P.V., "application of taguchi method for design of experiments in turning gray cast iron" , International Journal of Engineering Research and Applications (IJERA),2012, ISSN: 2248-9622
36. Murphy, K.D. and Lin, Z. (2000), "The influence of spatially no uniform temperature fields on the vibration and stability characteristics of EDM wires", International Journal of Mechanical Sciences, 42, 1369-1390
37. Muthu Kumar V, Suresh Babu A, Venkatasamy R and Raajenthiren M , "Optimization of the WEDM Parameters on Machining Incoloy800 Super alloy with Multiple Quality Characteristics" International Journal of Engineering Science and Technology Vol. 2(6), 2010, 1538-1547.
38. Peace, G.S. (1993), Taguchi Methods: A hands on approach, Addison Wesley, New York.
39. Puri, A.B and Bhattacharyya, B. (2005), "Modelling and analysis of white layer depth in a wire-cut EDM process through response surface methodology", International Journal of Advanced Manufacturing Technology, 25, 301–307.
40. Puri, A.B. and Bhattacharyya, B. (2003), "An analysis and optimization of the geometrical inaccuracy due to wire lag phenomenon in WEDM", International Journal of Machine Tools & Manufacture, 43, 151–159

41. Puri, A.B. and Bhattacharyya, B. (2003), "Modelling and analysis of the wire-tool vibration in wire-cut EDM", Journal of Materials Processing Technology, 141, 295–301.
42. Ramakrishnan, R. and Karunamoorthy, L. (2006), "Multi response optimization of wire EDM operations using robust design of experiments", International Journal of Advanced Manufacturing Technology, 29, 105–112.
43. Ross, P.J. (1988), "Taguchi techniques for quality engineering", McGraw-Hill Book Company, New York
44. Roy, R.K. (1990), "A primer on Taguchi method", Van Nostrand Reinhold, New York.
45. S. R. Nithin Aravind, S. Sowmyi, K. P. Yuvara , "Optimization of metal removal rate and surface roughness on wire EDM using Taguchi method", IEEE-International Conference On Advances In Engineering, Science And Management (ICAESM - 2012) March 30, 31, 2012.
46. Sarkar, S., Mitra, S., Bhattacharyya, B. (2005), "Parametric analysis and optimization of wire electrical discharge machining of γ-titanium aluminide alloy", Journal of Materials Processing Technology, 159, 286–294.
47. Sarkar, S., Mitra, S., Bhattacharyya, B. (2006), "Parametric optimisation of wire electrical discharge machining of γ titanium aluminide alloy through an artificial neural network model", International Journal of Advanced Manufacturing Technology, 27, 501–508.
48. Sarkar, S., Sekh, M., Mitra, S., Bhattacharyya, B. (2007), "Modeling and optimization of wire electrical discharge machining of γ-TiAl in trim cutting operation", Journal of Material Processing Technology, 205, 376-387.
49. Scott, D., Boyina, S., Rajurkar, K.P. (1991), "Analysis and optimization of Parameter Combination in Wire Electrical Discharge Machining", International Journal of Production Research, 29, 2189-2207

50. Spedding, T. A., Wang, Z.Q. (1997), "Parametric optimization and surface characterization of wire electrical discharge machining process", Precision Engineering, 20(1), 5-15.
51. Sreenivasa Rao M, Venkaiah N, "Review on Wire-Cut EDM Process" International Journal of Advanced Trends in Computer Science and Engineering, Vol.2, No.6, Pages: 12-17(2013).
52. Tarng, Y. S., Ma, S. C., Chung, L. K. (1995), "Determination Of optimal cutting parameters in wire electrical discharge machining", International Journal of Machine Tools and Manufacture, 35, 1693-170
53. Tosun, N., Cogun, C. and Pihtili, H.(2003), "The effect of cutting parameters on wire crater sizes in wire EDM", International Journal of Advanced Manufacturing Technology,21,857-865.
54. Tosun, N., Cogun, C. and Tosun, G. (2004), "A study on kerf and material removal rate in wire electrical discharge machining based on Taguchi method", Journal of Materials Processing Technology, 152, 316-322
55. Tzeng, Y.F. and Chiu, N.H. (2003), "Electrical-discharge machining process using a Taguchi dynamic experiment", International Journal of Advanced Manufacturing Technology,
56. Wil Gaffga, Lori Turner & Mike O'Neill, WIRE EDM Gibbs CAM 2006
57. Williams, R. E. and Rajurkar, K. P. (1991), "Study of wire electrical discharge machined surface
58. Yan, M.T., Liao, Y.S., Chang, C.C. (2001), "On-line estimation of work piece height by using neural networks and hierarchical adaptive control of WEDM", International Journal of Advanced Manufacturing Technology, 18, 884–891.

PUBLICATIONS

1. "Optimization of WEDM Process Parameters on SS316 Using Taguchi Method" International Journal of Modern Engineering Research Vol. 3, Issue. 4, Jul. - Aug. 2013 pp-2281-2286.

2. Effect of Process Parameters in Wire Electrical Discharge Machining of H13 Using Taguchi Method (International Journal of Engineering and Technology, Accepted)

3. Influence of Process Parameters on Wire Electrical Discharge Machining of SS17-4 PH using Grey Relational Analysis (Journal of Manufacturing Technology Research, Accepted).

4. Prediction of Surface Roughness and Kerf for SS316 in Wire Electrical Discharge Machining using GRA (Journal of Manufacturing Technology Research, Accepted)

5. Effect of Process Parameters in Wire Electrical Discharge Machining of SS321 Using Taguchi Method (Journal of Scientific and Industrial Research, Accepted)

6. Optimization of Wire EDM Process Parameters on SS17-4 PH using Grey-Taguchi analysis (Frontiers of Mechanical Engineering, under review)

7. Influence of Process Parameters on Kerf and Surface roughness using Wire Electrical Discharge Machining of SS17-4 PH (International Journal of Advance Manufacturing Technology, communicated)

8. Prediction of Surface Roughness and Kerf for SS316 in Wire Electrical Discharge Machining using GRA (Journal of Manufacturing Technology Research, under review)

9. Effect of Process Parameters in Wire Electrical Discharge Machining of SS321 Using Grey-Taguchi Method (Journal of Scientific and Industrial Research, under review)

BIO-DATA

Name	Lokeswara Rao Thatuku
Date of birth	13-04-1985
Marital Status	Single
Present Position	Research Scholar
	Department of Mechanical Engineering
	National Institute of Technology
	Warangal-506004
	Andhra Pradesh, India.
Qualification	M. Tech (Product Design and Development)
Permanent Address	S/O T. Penchalaiah,
	L.A Sagaram,
	Naidupeta,
	Nellore District,
	Andhra Pradesh- 517644. India.
E-mail	tlrao777@gmail.com
	tlrao@nitw.ac.in

ACKNOWLEDGEMENTS

It is beyond my capacity to express deep sense of gratitude to my beloved and respected **Prof. N. Selvaraj** for his meticulous guidance, constant encouragement and time throughout the course of this research work. I express my gratitude and heartfelt thanks to **Prof. C.S.P. Rao**, Senior Professor and Head, Mechanical Engineering Department, National Institute of Technology, Warangal for his guidance and suggestions during the research work.

I express my sincere thanks to **Prof. T. Srinivasa Rao**, Director, NIT, and Warangal for providing the necessary help in completing the research work at the institute. I am very much thankful to **Dr. P.S.C. Bose**, Assistant Professor, Department of Mechanical Engineering and **Dr. N. Srikanth**, Associate Professor, Department of Electrical and Electronics Engineering, the members of the DSC for giving directions and suitable suggestions during the course of study.

I am thankful to **Prof. P. Bangaru babu**, Senior Professor, Department of Mechanical Engineering, National Institute of Technology Warangal, for his timely guidance, support and encouragement during my research work.

I express my sincere thanks to the faculty members in Mechanical Engineering Department, **Prof. A. Venugopal, G. Ventakateswara Rao, Prof. A.Nelakanteswara Rao, Dr. K.V. Sai Srinadth, Prof. Madhu Murthy** and **Prof. L. Krishnanand** for their encouragement and support during my research work

I express my sincere thanks to my co-scholars, **N.Vishnu Murthy, V. Jeevan** and **D. Vinay Kumar** for their help to carry out experiments, endless hours of discussions and arguments for the completion of the thesis.

The services of the staff of **Mr.Ilaiah, Mr. Raju** and **Mr. Rangilal**, Production Engineering Section, Mechanical Engineering Department, National Institute of Technology Warangal are acknowledged with sincere thanks.

I wish to extend my sincere thanks to my family for their understanding and continual support during the period of this research work.

Finally, I thank everyone who contributed either directly or indirectly in the successful completion of this research work.

Above all, I express my indebtedness to the "**ALMIGHTY**" for all His blessing and kindness.

(T. Lokeswara Rao)